ISSN 2355-5058 e-ISSN 2622-4852

# JURNAL Floatronic Control Toloromyunication Informati

Electronic, Control, Telecommunication, Information, and Power Engineering

https://ecotipe.ubb.ac.id/

Volume 12, Issue 2, October 2025



ISSN 2355-5058 e-ISSN 2622-4852

# 

Electronic, Control, Telecommunication, Information, and Power Engineering

https://ecotipe.ubb.ac.id/

Volume 12, Issue 2, October 2025







#### ISSN 2355-5068 e-ISSN 2622-4852

Volume 12, Issue 2, October 2025 DOI: 10.33019/jurnalecotipe.v12i2

#### **Editorial Board**

#### **Publisher**

Electrical Engineering Dept., Bangka Belitung University

#### **Editor-in-Chief**

Ir. Rudy Kurniawan, S.T., M.T.

#### **Managing Editor**

Nurhaeka Tou, S.Kom., M.Kom.

#### **Associate Editors**

Prof. Ir. Anton Yudhana, S.T., M.T., Ph.D. I Made Andik Setiawan, S.S.T., M.Eng. Ph.D. Munirul Ula, S.T., M.Eng., Ph.D. Esa Prakarsa, M.T., Ph.D.

**Reviewers Board** Prof. Ir. Refdinal Nazir, M.S., Ph.D. Prof. P. Chandra Sekhar Prof. Chuan-Kai Yang Ihwan Ghazali, M.Eng. Ph.D. Rishabh Das, Ph.D. Dr. Mawarni Mohamed Yunus Prof. Dr. Azriyenni Azhari Zakri, S.T., M.Eng. Dr. Triwahju Hardianto, S.T., M.T. Dr. Eng. Helmy Fitriawan, S.T., M.Sc. Dr. Bhakti Yudho Suprapto, S.T., M.T. Ir. Wahri Sunanda, S.T., M.Eng., IPM., ASEAN Eng. I Made Andik Setiawan, S.S.T., M.Eng., Ph.D. Dr. Yuli Asmi Rahman, S.T., M.Eng. Dr. Prajna Deshanta Ibnugraha, S.T., M.T. Dr. Riko Arlando Saragih, S.T., M.T. Dr. Sabhan Kanata, S.T., M.Eng. Dr. Tedy Juliandhy, S.T., M.Eng. Hanalde Andre, S.T., M.T. Ir. Rika Favoria Gusa, S.T., M.Eng. Dr. Ir. Ardi Pujiyanta, M.T. Indra Gunawan, S.Kom., M.Kom. Angga Wahyu Aditya, S.S.T., M.T. Muhammad Rifqi Ma'arif, S.T., M.Eng. Alwendi, S.Kom., M.Kom Riyana Prima Dewi, S.T., M.T. Novita Astin, S.T., M.T. Dr. Dian Mursyitah, S.T., M.T.

#### **Editors Board**

Fadhillah Azmi, M. Kom. Lathifah Alfat, S.T., M.T.

Sri Hartanto, S.T., M.T.

Putri Mentari Endraswari, S.Tr.Kom., M.Kom. Andri Ashfahani, S.T., M.Sc., Ph.D. Ir. Nur Hudha Wijaya, S.T., M.Eng. Ir. Wahri Sunanda, S.T., M.Eng., IPM., ASEAN Eng. Mohamad Abdul Hady, S.T., M.T. Asmar, S.T., M.Eng. Ghiri Basuki Putra, S.T., M.T.

Oktavia Citra Resmi Rachmawati, S.Tr.Kom., M.Tr.Kom

#### **Layout Editor**

Ridwan Andrian, S.T.

#### **Website Admin**

Hendy, S.T.

#### Preface

Jurnal Ecotipe (Electronics, Control, Telecommunication, Information, and Power Engineering) published by the Department of Electrical Engineering, University of Bangka Belitung, starting from Volume 7 Number 2, October 2020 to Volume 12 Number 1, April 2025 is still accredited by the Ministry of Education, Culture, Research, and Technology of the Republic of Indonesia based on Decree No. 158 / E / KPT / 2021 with a ranking of 3 (SINTA 3) but starting from Volume 12 Issue 2 and onwards, is still waiting for the results of the Accreditation assessment. Currently, the Ecotipe Journal is undergoing a re-Accreditation assessment to improve the Accreditation rating.

Currently, Jurnal Ecotipe volume 12, issue 2, October 2025, has been published. In this edition, the journal articles are entirely in English and consist of 15 articles by authors from outside the institution, numbered from pages 120-274. Hopefully, in the future, articles included in the journal's next edition will come from outside academia, both domestically and internationally.

Our highest appreciation goes to the Reviewers, Editorial Board, Authors, and all parties involved in the preparation and publication of the Jurnal Ecotipe volume 12 issue 2 October 2025. Hopefully, this journal can provide benefits and add scientific insight into the field of Electrical Engineering in particular and engineering in general. Therefore, we still hope for suggestions and constructive criticism for improvements and improvements for the progress of this journal.

#### **Editor-in-Chief**

#### Indexed journal on:



#### **Publisher Address:**

Electrical Engineering Department
Faculty of Science and Engineering - Bangka Belitung University
Balunijuk, Bangka Regency, Bangka Belitung Islands Province, Indonesia
Phone (0717) 4260033 ext. 2125, 2128
Website: https://journal.ubb.ac.id/index.php/ecotipe
E-mail: jurnal.ecotipe@yahoo.com / jurnalecotipe@ubb.ac.id



ISSN 2355-5068 e-ISSN 2622-4852

Volume 12, Issue 2, October 2025 DOI: 10.33019/jurnalecotipe.v12i2

### **Table of Content**

Editorial Board & Preface	
Table of Content	i
A New MPPT Scheme Based on Komodo Mlipir Algorithm for Stand-Alone Solar PV Systemelon Quality Sorting Prototype Based on Skin Texture Using Local Binary Pattern Histogram Fathurrahman, Khairun Saddami, Rika Sri Utami, Malahayati, Akhyar	120-128
Development of a Mental Health Consultation Website Using the Waterfall Method (Case Study of Biro Psikologi Putra Tunggal)  Muhammad Nur Hidayat, Yohani Setiya Rafika Nur	129-139
Prototype of Seaweed Dryer Operating in Manual and Automatic Mode Using Wi Fi Based Microcontroller Setiyono	140-150
Comparative Study of Sentiment Analysis for Interpreting the Customer Interest in Women Fashion Clothes Eka Legya Frannita, Alifia Revan Prananda, Marwanto	151-158
Design and Contruction of a Website for Garbage Sales in Sirau Village Using the Extreme Programming Method (Case Study of KSM Kudu Bisa)  Tegar Setio, Yohani Setiya Rafika Nur, Hari Widi Utomo	159-168
Solar Power Plant of Apartment Kertapati – A Design Study to Reduce Carbon Emission  Muhammad Abu Bakar Sidik, Muhammad Irfan Jambak, Rizda Fitri Kumia, Noer Fadzri Perdana Dinata, Muhammad Izman  Herdiansyah, Rian Alto Belly, Muhammad Alif Wicaksono, Rizki Aidil Fitrah, Muhammad Darmawan Fahreza	169-180
Development of a Library Information System for Data Processing at SMK N 1 Pangkalpinang Tri Ari Cahyono, Nursasono	181-189
Design and Simulations of 2x1 Rectangular Microstrip Array Antenna Using Inset and U-Slot Method at 3.5 Ghz for 5G Communication System  Lita Farahdiba, Indra Surjati, Syah Alam, Raden Deiny Mardian, Lydia Sari, Teguh Firmansyah, Zahriladha Zakaria	190-202
Integration of Al Models and Extreme Programming for Retail Price Prediction and Inventory Optimization Sapta Eka Putra, Yularni Putri, Faizal Burhani Ulil Fathan	203-214
Arduino-Based Capacitor Bank Automation for Power Factor Optimization  Hafidz Nindhom Zen, Ibrohim, Endryansyah, Subuh Isnur Haryudo	215-225
Optimization of Spot Welding Performance Through Microcontroller- Solenoid Drive and Ultrasonic Sensing Aldi Rahman, Surfa Yondri, Riza Widia, Muhardika, Yani Kamisa Putri, Dedi Erawadi, Tri Artono, Muhammad Rizal Syauqii	226-233
A Comparative Study of Traditional PID Tuning Techniques and Al-Based Algorithmic Approaches Utilizing the Python Control Library  Purwadi Joko Widodo, Heru Sukanto, Budi Santoso, Lullus Lambang Govinda Hidayat, Joko Triyono, Iwan Istanto, Rahman Wijaya Fitrian Imaduddin	234-244
A New 12-Phase Toroidal Transformer Design to Improve Efficiency and Power Quality in Electric Vehicle Fast Charging Systems  Partaonan Harahap, Muhammad Imran Hamid, Ariadi Hazmi	245-253
Adaptive PID–PD Hybrid Control for Precise Motion of ROVs in Dynamic Environments  Hendi Purnata, Hera Susanti, Dwi Sahidin, Galih Mustiko Aji, Nanda Pranandita	254-263
Least Square-Based Modelling of 0.5 HP Single-Phase Induction Motor  Abdul Hadi, Rindilla Antika, M. Farhan, Akmal Arif Ridhi Putra, Diva Ramadhan	264-274



Volume 12, Issue 2, October 2025, pp. 120-128 ISSN 2355-5068; e-ISSN 2622-4852

**DOI:** 10.33019/jurnalecotipe.v12i2.4557

### A New MPPT Scheme Based on Komodo Mlipir Algorithm for **Stand-Alone Solar PV System**

Fathurrahman<sup>1</sup>, Khairun Saddami<sup>2</sup>, Rika Sri Utami<sup>3</sup>, Malahayati<sup>4</sup> Akhyar<sup>5</sup>

1,2,3</sup> Universitas Syiah Kuala, Darussalam, Banda Aceh, Aceh, 23111, Indonesia.

1 Electrical Engineering Department, King Fahd University of Petroleum and Minerals, Saudi Arabia

4 Universitas Islam Negeri Ar-Raniry, Darussalam, Banda Aceh, 23111, Indonesia

5 Universiti Kebangsaan Malaysia, Bangi, Selangor, 43600, Malaysia.

#### ARTICLE INFO

#### **Article history:**

Received: 13/03/2025 Revised: 14/05/2025 Accepted: 30/10/2025

#### **Keywords:**

PV Module, Maximum Power Point Tracking, Komodo Mlipir Algorithm

#### **ABSTRACT**

The efficiency of PV modules remains relatively low, ranging from 15% to 35%, depending on the type of silicon technology used, including crystalline, polycrystalline, and thin-film. Then, the energy extraction efficiency from Solar Power Generation could be a lot higher (below 70%), especially in Solar Power Generation systems that still need to implement the Maximum Power Point Tracking (MPPT) algorithm. The MPPT algorithm is implemented in power electronic devices, such as boost converters, to optimise the power output of solar modules under various operating conditions, particularly during partial shading conditions. Various MPPT algorithms have been developed, each with its strengths and weaknesses. To enhance the efficiency of Solar Power Generation, this research will use a more effective state-of-the-art algorithm, namely the "Komodo Mlipir Algorithm" (KMA). KMA exhibits low system exploitation characteristics, utilising high exploration strategies, which align with the hunting behaviour of the Komodo dragon. This algorithm is expected to increase Solar Power Generation efficiency to above 90%.



This work is licensed under a Creative Commons Attribution 4.0 International License

#### **Corresponding Author:**

Fathurrahman

Universitas Syiah Kuala, Darussalam, Banda Aceh, Aceh, 23111, Indonesia.

Email: fathurrahman@usk.ac.id.

#### INTRODUCTION 1.

The role of electricity remains the most effective and efficient method of mass-energy transfer directly utilised by humans, compared to other methods such as wind utilisation in sailboats and the use of petroleum for internal combustion engines. However, electrical energy is a secondary form derived from the manifestation of primary energy conversion processes, such as wind, water, geothermal heat, sunlight, petroleum, and nuclear processes. The World Bank reports that, as of January 2023, at least 91.3% of the global population had access to electricity [1].

Indonesia has a relatively high electrification ratio of 99.28%. However, it is regrettable that Indonesia still relies on 85.5% of its primary electricity sources on fossil energy. It is a highly polluting energy source and contributes significantly to environmental pollution. This situation presents a paradox, considering that Indonesia is located on the equator with an average solar irradiation of 4.8 kWh/m²/day, receiving 12 hours of sunlight per day [2-3]. Solar power generation is one primary energy source component with a relatively low percentage in Indonesia. In 2023, out of Indonesia's 8.64% renewable energy mix, PV contributed only 0.16% [4-5]. Based on Indonesia's Electricity Supply

Volume 12, Issue 1, April 2025, pp. 120-128 ISSN 2355-5068; e-ISSN 2622-4852 **DOI:** 10.33019/jurnalecotipe.v12i2.4557

Business Plan, the country aims for carbon neutrality by 2060, with an initial target of incorporating 23% new renewable energy into the energy mix by 2030.

One challenge in utilisation, however, is that the efficiency of PV modules is still relatively low, ranging from 15% to 35%, depending on the silicon technology used (crystalline, polycrystalline, or thin film). Furthermore, the energy extraction efficiency from Solar Power Generation could be higher, especially in PV systems that still require the implementation of the Maximum Power Point Tracking (MPPT) algorithm in the solar energy extraction process [6-7]. Many PV installations, especially rooftop (off-grid) PV sites, still need the implementation of the MPPT algorithm in their systems. Therefore, MPPT must be developed and disseminated to the public and the government. The primary contribution of this research is the development of an MPPT algorithm for PV systems, enabling the system to extract up to 95% of the solar energy converted by PV modules under various operating conditions.

#### 2. RESEARCH METHOD

#### 2.1. PV Modules and PV Systems

PV systems are power generation systems that comprise one or more solar modules connected in series or in parallel. PV systems typically includes power electronic devices that serve as interfaces between the PV modules and the load or battery. Based on the grid connection, PV systems can be categorised into two topologies: on-grid and off-grid systems [8]. PV cells are the primary components of PV modules, modelled as a diode connected to a resistor, as depicted in Figure 1. PV cells exhibit current and voltage characteristics expressed mathematically using Equation 1. [9-12]:

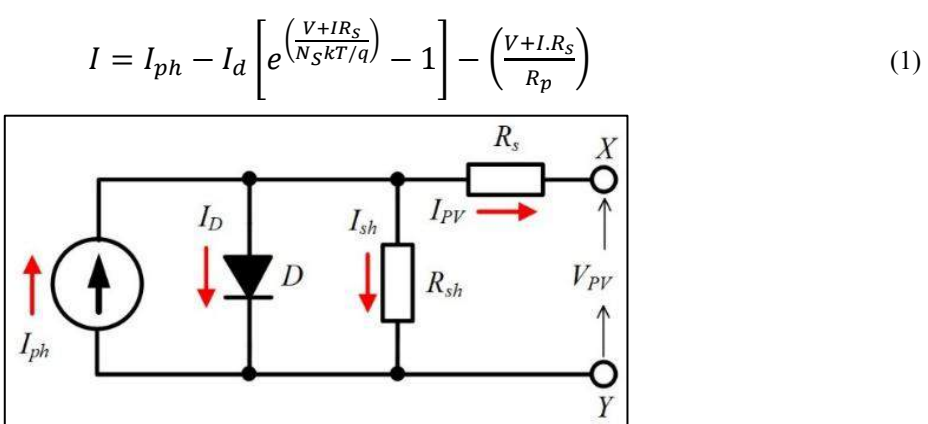


Figure 1. PV modules equivalent circuit

#### 2.2. Maximum Power Point Tracking (MPPT)

MPPT (Maximum Power Point Tracking) is the automatic load regulation in a PV system to track the maximum power point under various module operating conditions, allowing the system to extract optimal output power [13]. The MPPT circuit comprises control and DC-DC converter circuits, which can be implemented as a buck, boost, CUK, SEPIC, or buck-boost converter [14]. The DC-DC converter is driven by the controller, which utilises the MPPT algorithm to adjust parameters, thereby enabling the transfer of maximum power from the PV source under various environmental and load conditions. In simple terms, the MPPT system is shown in Figure 2.

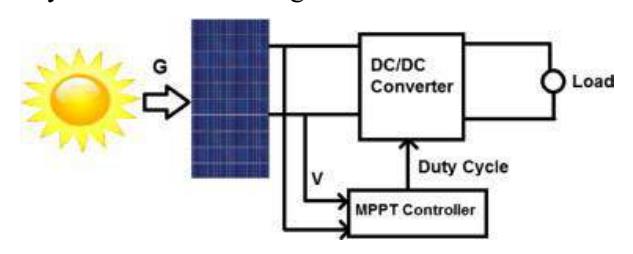


Figure 2. PV systems MPPT block diagram

Volume 12, Issue 2, October 2025, pp. 120-128 ISSN 2355-5068; e-ISSN 2622-4852 **DOI:** 10.33019/jurnalecotipe.v12i2.4557

#### 2.3. MPPT Using KMA

MPPT (Maximum Power Point Tracking) is the automatic load regulation in a PV system to track the maximum power point under various module operating conditions, allowing the system to extract optimal output power [13]. The MPPT circuit comprises control and DC-DC converter circuits, which can be configured as buck, boost, CUK, SEPIC, or buck-boost converters [14]. The DC-DC converter is driven by the controller, which utilises the MPPT algorithm to adjust parameters, thereby enabling maximum power transfer from the PV source under various environmental and load conditions. In simple terms, the MPPT system is depicted in Figure 3.

MPPT (Maximum Power Point Tracking) is the automatic load regulation in a PV system to track the maximum power point under various module operating conditions, allowing the system to extract optimal output power [13]. The MPPT circuit comprises control and DC-DC converter circuits, which can be configured as buck, boost, CUK, SEPIC, or buck-boost converters [14]. The DC-DC converter is driven by the controller, which utilises the MPPT algorithm to adjust parameters, thereby enabling maximum power transfer from the PV source under various environmental and load conditions. In simple terms, the MPPT system is depicted in Figure 3 [15-16].

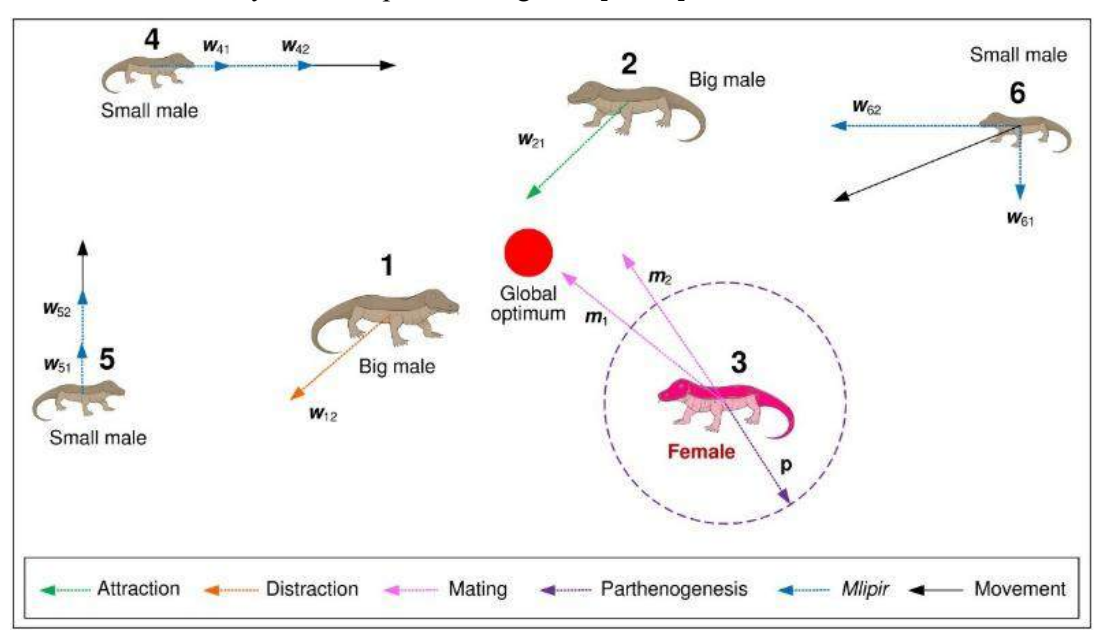


Figure 3. The representation of the KMA algorithm in searching for the optimal point

The utilisation of the KMA algorithm in the MPPT problem involves how the KMA algorithm attempts to reach the highest peak point of the P-V curve generated by MPPT, as illustrated in Figure 4.

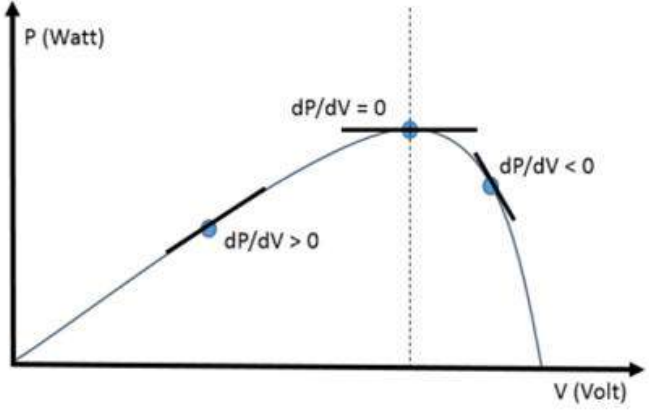


Figure 4. MPPT P\_V curve

Volume 12, Issue 1, April 2025, pp. 120-128 ISSN 2355-5068; e-ISSN 2622-4852 **DOI:** 10.33019/jurnalecotipe.v12i2.4557

#### 2.4. Research Design

This research begins with a literature review from various sources. It is a quantitative study based on laboratory experiments. In this study, a prototype power electronic device in the form of a boost converter is constructed and controlled using the Komodo Mlipir Algorithm (KMA)[15-16]. The following steps involve data collection and the selection of parameter values for each component of the PV system and load, which are then simulated using computer programs such as PSIM or MATLAB. Subsequently, the controller for the boost converter power electronic device is designed, considering the calculated component values based on the technical data of the solar panels and the load. The constructed model is simulated, and power values are chosen as the main observed variables. After a successful simulation, the final steps involve building and testing the prototype. The entire research draws conclusions based on the results obtained from simulation and hardware testing.

The design, assembly, and measurement of the MPPT KMA experimental circuit were carried out in the Power Electronics Laboratory of the Electrical Engineering Department at USK. The data collection and analysis stages involve obtaining data by testing the equipment in the field. Once the data is obtained, it is analysed to determine whether the prototype can function appropriately according to the intended goals by examining the power output characteristics produced by the solar panel with and without MPPT.

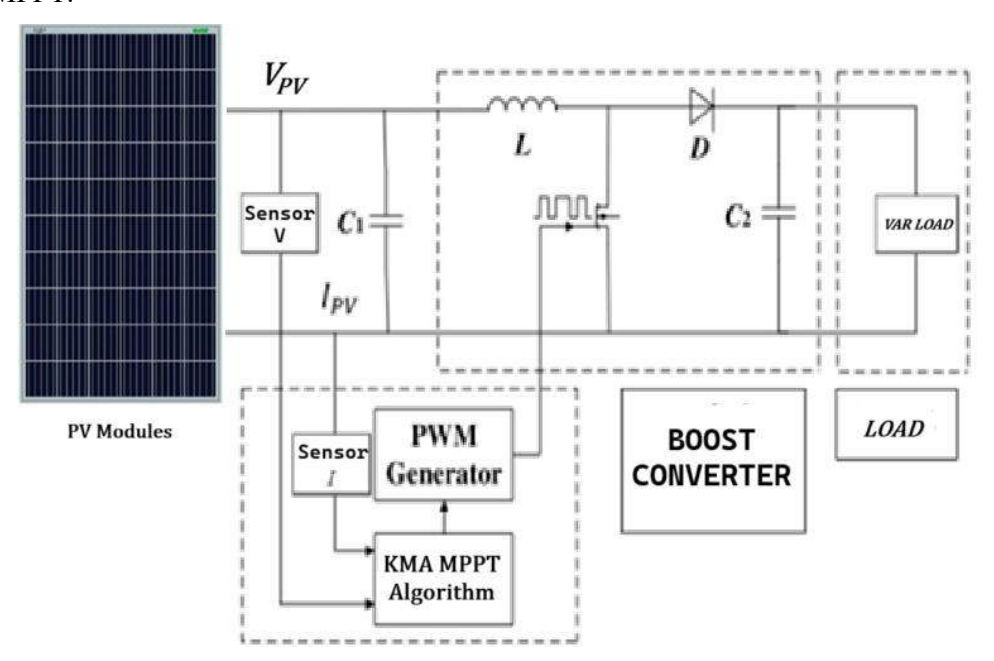


Figure 5. Block diagram of the MPPT KMA system design

The partial shading condition is based on research done in [17], where three stages of solar irradiance are simulated. The first shading configuration is set up so that two modules (partially shaded) receive solar irradiance at 0.6 kW/m², while the remaining two receive 1 kW/m² of solar irradiance. This configuration is Partial Shading Conditions (PSC) Pattern 1. The second configuration is set to a Uniform Insolation Condition (UIC), where all modules receive 1 kW/m² of solar irradiation (under no shading condition). The third shading configuration is set up where one modules (partially shaded) receive the solar irradiance at 0.7 kW/m², two modules (partially shaded) receive the solar irradiance at 0.9 kW/m², and the last module receives 1 kW/m². This configuration is Partial Shading Conditions (PSC) Pattern 2. Every shading condition stage is simulated for 4 seconds. Figure 6 illustrates the PV three-shading condition scenario.

Volume 12, Issue 2, October 2025, pp. 120-128 ISSN 2355-5068; e-ISSN 2622-4852 **DOI:** 10.33019/jurnalecotipe.v12i2.4557

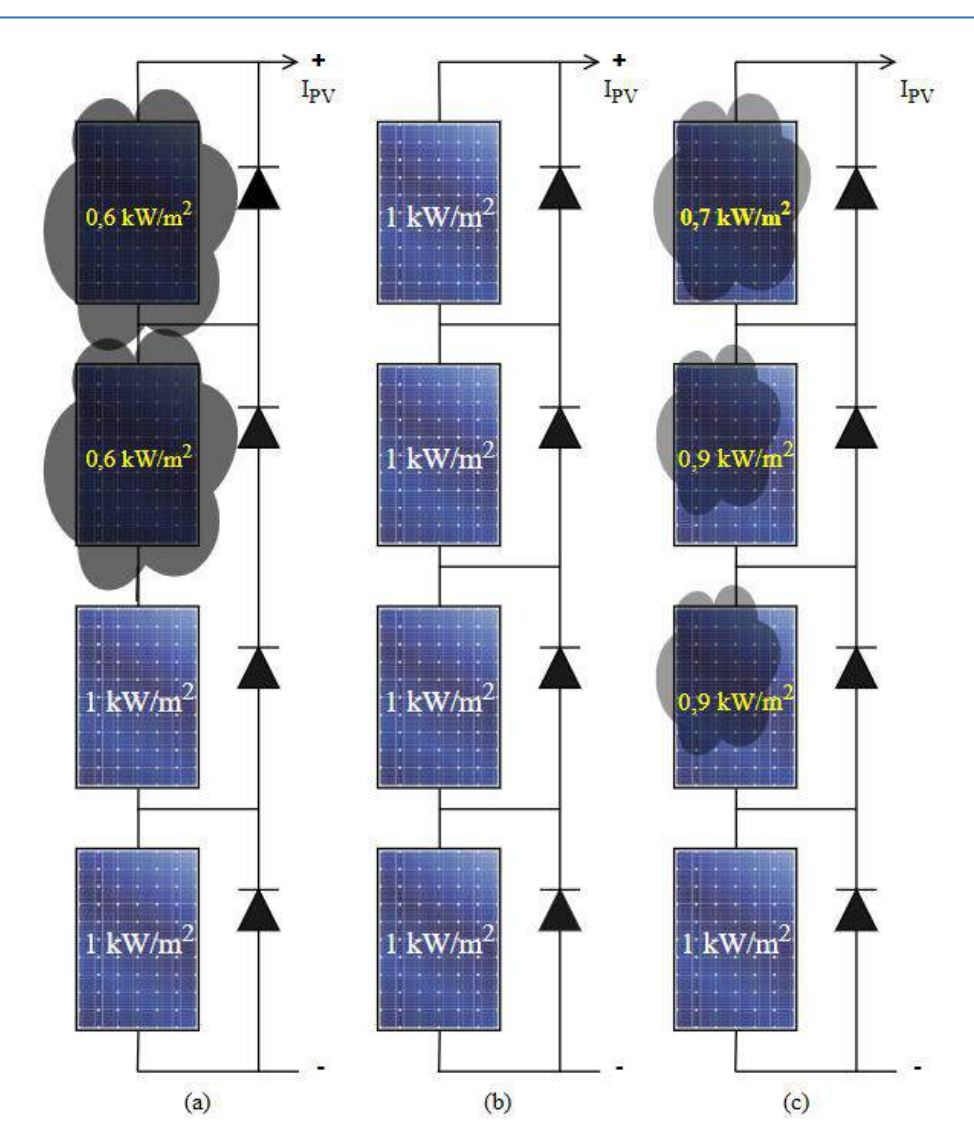


Figure 6. Scenario of PV Arrays Shading Condition (a) PSC Pattern 1; (b) UIC; (c) PSC Pattern 2

In this data analysis, efficiency will also be considered, both when using a conventional method and when using an MPPT. The prototype is functioning correctly if the obtained data aligns with the data in Table 1.

Table 1. Shading condition scenario

No.	Shading Condition	Efficiency
1.	Partial Shading Condition Schema 1	> 90 %
2.	No partial Shading Condition	> 90 %
3.	Partial Shading Condition Schema 1	> 90 %

#### 3. RESULTS AND DISCUSSION

The Experimental setup is shown in Figure 7. The PV system and load are then simulated using MATLAB. The simulation uses 4 x 100 Wp or 400 Wp PV Modules with a variable load. The change in solar irradiance occurs every 4 seconds. Based on the shading scenarios developed in Figure 6, the maximum possible power that can be extracted from the PV arrays is calculated and plotted as the set point value. The computed maximum power value is shown in Figure 7 and Table 2.

Volume 12, Issue 1, April 2025, pp. 120-128 ISSN 2355-5068; e-ISSN 2622-4852 **DOI:** 10.33019/jurnalecotipe.v12i2.4557

**Table 2**. Maximum power output from every shading scenario

No.	Shading Condition	Max Output Power (W)
1.	PSC Pattern 1	640
2.	No partial Shading Condition (UIC)	1000
3.	PSC Pattern 1	760

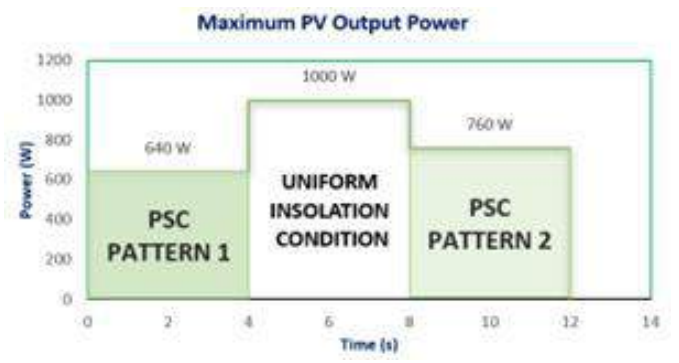


**Figure 7.** Maximum output PV array power for every given shading scenario

The simulation of the proposed MPPT Algorithm is computed using MATLAB/SIMULINK software. The MATLAB simulation set-up (block diagrams) is shown in Figure 6. The KMA Algorithm is employed in the Boost converter by controlling the MOSFET PWM drive, where the MOSFET operates based on the algorithm to vary the voltage accordingly, thereby producing a power value as close as possible to the set point value, as specified in Table 2 and Figure 7.

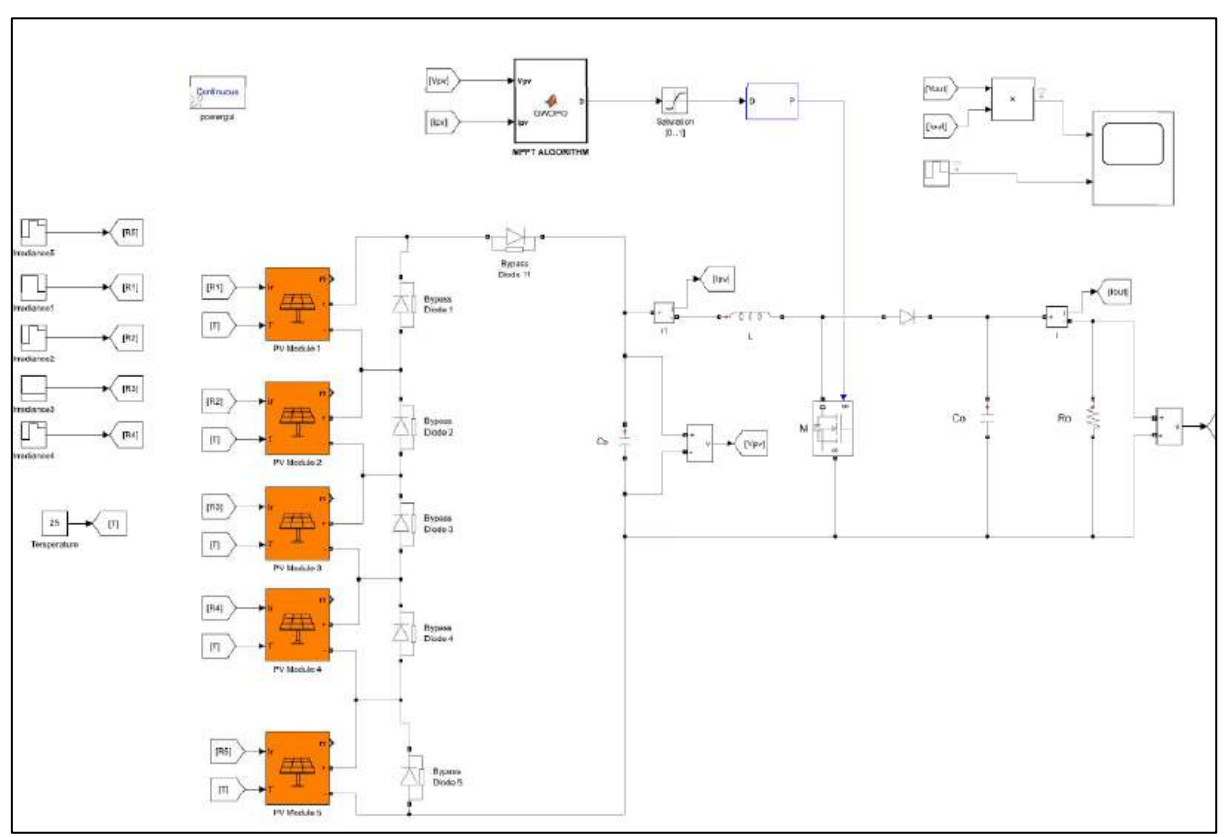


Figure 6. Simulation diagram setup

The power and output voltage of the solar module, as determined by the KMA MPPT algorithm, are shown in Figure 10. The green line represents the maximum power output from the solar module based on solar irradiance, and the yellow line represents the actual power produced by the solar module.

Volume 12, Issue 2, October 2025, pp. 120-128 ISSN 2355-5068; e-ISSN 2622-4852 **DOI:** 10.33019/jurnalecotipe.v12i2.4557

1 kW/m²; 1 kW/m²; 1 kW/m²; 1 kW/m² watt Peaks at 640 W

Watt Peaks at 640 W

Watt Peaks at 760 W

Watt Peaks at 760 W

MA Power Algorithm

Figure 7. Maximum power based on Solar Irradiance versus true PV Array Power Output using KMA

6 Time (s)

The performance of the solar module, specifically its output power and voltage as regulated by the KMA (Komodo Movement Algorithm) Maximum Power Point Tracking (MPPT) strategy, is illustrated in Figure 10. In the figure, the green line signifies the theoretical maximum power that the solar module is capable of generating under given solar irradiance conditions. This represents the ideal or reference power output. In contrast, the yellow line indicates the actual power generated by the solar module when operated using the current implementation of the KMA algorithm.

As shown in the figure, the KMA algorithm strives to track the maximum power point (MPP) under varying irradiance conditions. While it demonstrates a general tendency to track the MPP trajectory, a noticeable deviation remains between the ideal and actual power output curves. Specifically, the system efficiency remains below 90%, indicating a suboptimal energy harvesting performance at this simulation stage.

This reduced efficiency is attributed to the fact that the current KMA algorithm is still in its initial development phase, referred to as Stage One of the simulation. At this stage, only a portion of the entire algorithm has been implemented, and not all the behavioural dynamics of the Komodo-inspired search strategy have been integrated. The complete KMA algorithm comprises three distinct stages, each modelled after the characteristic movements of different members of a Komodo dragon group: large males, females, and petite males, as illustrated in Figure 3. Stage One corresponds to the basic search behaviour inspired by the movement of large male Komodo dragons, which typically involves broader, exploratory searching with less precision. As the simulation progresses into Stage Two and Stage Three, incorporating the more refined and convergent movements of females and petite males, the algorithm is expected to achieve significantly better convergence towards the actual maximum power point. This

Volume 12, Issue 1, April 2025, pp. 120-128 ISSN 2355-5068; e-ISSN 2622-4852 **DOI:** 10.33019/jurnalecotipe.v12i2.4557

progression is expected to enhance tracking accuracy and increase the overall efficiency of the MPPT process.

Therefore, while the current results are promising in showcasing the initial tracking capabilities of the KMA algorithm, further improvements are expected once all behavioural stages are integrated. The full implementation of the algorithm is likely to yield a more precise and responsive MPPT strategy, thereby reducing power losses and enhancing the reliability of solar energy conversion under dynamic environmental conditions.

#### 4. CONCLUSION

In conclusion, the preliminary simulation results demonstrate that the KMA (Komodo Movement Algorithm) exhibits a fundamental ability to track the maximum power point (MPP) of the photovoltaic (PV) system under varying irradiance conditions. Despite this, the observed tracking efficiency currently remains below 90%. This limitation is primarily due to the algorithm being in its early stage of development, specifically Stage One of the three-stage simulation framework. At this initial stage, only movement patterns inspired by adult male Komodo dragons have been implemented, focusing on broad and exploratory search behaviour.

The full potential of the KMA algorithm is expected to emerge as the subsequent stages are incorporated. Stages Two and Three will simulate the more adaptive and convergent behaviours inspired by female and juvenile Komodo dragons, respectively. These stages are designed to refine the search process, enhance local exploitation, and improve the overall convergence towards the global maximum power point. Once all three behavioural stages are fully integrated, the algorithm is anticipated to significantly enhance its MPPT accuracy and operational efficiency, ultimately ensuring more effective energy harvesting from the solar module across a broader range of environmental conditions.

Future work will focus on implementing and validating these additional stages, as well as benchmarking the complete KMA algorithm against other established MPPT techniques to quantify its advantages in real-world scenarios.

#### Acknowledgments

Thanks to the Institute for Research and Community Service of Universitas Syiah Kuala (LPPM USK), the research is funded by LPPM USK under the Research Grant Scheme Penelitian Asisten Ahli, Grant No. 382/UN11.2.1/PT.01.03/PNBP/2023.

#### **REFERENCES**

- [1] World Bank Group, World Development Indicators, (2022) "Access to electricity (% of population)", [Online]. Available: https://data.worldbank.org/indicator/EG.ELC.ACCS.ZS?end=2022&start=2019.
- [2] N. Winanti, A. Purwadi, B. Halimi and N. Heryana, "Study and Design of Energy-Saving Solar Lamp for Small Island in Indonesia: Matakus Island," (2018) Conference on Power Engineering and Renewable Energy (ICPERE), Solo, Indonesia, 2018, pp. 1-5, doi: 10.1109/ICPERE.2018.8739672.
- [3] T. Tarmizi, S. Syahrial and F. Fathurrahman, "Design of PV System with DC distribution for Rural Electricity," 2021 International Conference on Computer System, Information Technology, and Electrical Engineering (COSITE), Banda Aceh, Indonesia, (2021), pp. 46-50, doi: 10.1109/COSITE52651.2021.9649537.
- [4] Handbook of Energy & Economic Statistics of Indonesia 2023, The Ministry of Energy and Mineral Resources, Jakarta, Indonesia, 2023. Accessed: February 25, (2025) [Online]. Available: https://esdm.go.id/assets/media/content/content-handbook-of-energy-and-economic-statistics-of-indonesia-2023.pdf.

Volume 12, Issue 2, October 2025, pp. 120-128 ISSN 2355-5068 ; e-ISSN 2622-4852

**DOI:** 10.33019/jurnalecotipe.v12i2.4557

- [5] Indonesia Energy Transition Outlook 2024: Peaking Indonesia's Energy Sector Emission by 2030: The Beginning or The End of Energy Transition Promise, Institute for Essential Services Reform, Jakarta, Indonesia (2023). Accessed: March 05, 2025 [Online]. Available: https://iesr.or.id/wp-content/uploads/2024/03/Indonesia-Energy-Transition-Outlook-2024-1.pdf
- [6] N. S. Lubis, "Efisiensi Daya Keluaran Generator Photovoltaic (GPV) Menggunakan Maximum Power Point Tracking (MPPT) Dengan Algoritma Perturb and Observe (P&O) dan MPPT Standard Reference," B.S Thesis, Dept. of Physics, Universitas Sumatera Utara, Medan, Indonesia, 2019.
- [7] M. Effendy, N. A. Mardiyah, K. Hidayat, (2017) "Implementasi Maximum Power Point Tracking pada Photovoltaic Berbasis P&O-Fuzzy," Jurnal Nasional Teknik Elektro dan Teknologi Informatika, vol. 6, no. 1, pp. 2–7, 2017.
- [8] Guidelines for the Feasibility Study of a Solar Power Plant (PLTS)," Ditjen EBTKE KESDM in collaboration with USAID Indonesia Clean Energy Development II, Jakarta, Indonesia, pp. 30-31, 2018.
- [9] T. Le, H. Colin, F. A. Shakarchi and T. T. Quoc, (2018) "Improved Matlab Simulink Two-diode Model of PV Module and Method of Fast Large-Scale PV System Simulation,"7th International Conference on Renewable Energy Research and Applications (ICRERA), pp. 982-985, doi: 10.1109/ICRERA.2018.8566792.
- [10] K. Basaran, N. Sabit, and S. Borekci, (2016) "Energy management for on-grid and off-grid wind/PV and battery hybrid systems," Journal of IET Renewable Power Generation vol. 148, pp. 148–162.
- [11] M. N. Dehedkar and S. Vitthalrao Murkute, (2018) "Optimization of PV System using Distributed MPPT Control," 2018 International Conference on System Modeling & Advancement in Research Trends (SMART), pp. 216-220, doi: 10.1109/SYSMART.2018.8746931.
- [12] Chouder, S. Silvestre, B. Taghezouit, E. Karatepe, (2013) "Monitoring, modelling and simulation of PV systems using LabVIEW," Solar Energy, Volume 91, pp 337-349, ISSN 0038-092X.
- [13] Attou, A. Massoum, and M. Saidi, (2014) "Photovoltaic Power Control Using 40 MPPT and Boost Converter," Balk. J. Electr. Comput. Eng., vol. 2, no. 1, pp. 23–27.
- [14] N. Nguyen, V. T. Nguyen, M. Q. Duong, K. H. Le, H. H. Nguyen, and A. T. Doan, (2020) "Propose a MPPT Algorithm Based on Thevenin Equivalent Circuit for Improving Photovoltaic System Operation," Front. Energy Res., vol. 8.
- [15] Suyanto, S., Ariyanto, A. A., & Ariyanto, A. F. (2022). Komodo Mlipir Algorithm. *Applied Soft Computing*, vol. 114, pp. 10804.
- [16] Q. Liu, & X. Zhang, (2022). Improved Adaptive Komodo Mlipir Algorithm. *IEEE Access*, vol. 10, pp. 67883-67897.
- [17] Muyassar, M. et al. 2022. A GWO-P&O Algorithm MPPT for PV Systems Under UIC and PSC. Jurnal Nasional Teknik Elektro. 11, 3 (Nov. 2022).



Volume 12, Issue 2, October 2025, pp. 129-139 ISSN 2355-5068; e-ISSN 2622-4852 **DOI:** 10.33019/jurnalecotipe.v12i2.4548

## Development of a Mental Health Consultation Website Using the Waterfall Method (Case Study of Biro Psikologi Putra Tunggal)

Muhammad Nur Hidayat<sup>1</sup>, Yohani Setiya Rafika Nur <sup>2</sup>

1.2 Informatic Engineering Study Program, Telkom University, Purwokerto, Indonesia

#### **ARTICLE INFO**

#### Article historys:

Received: 12/02/2025 Revised: 20/05/2025 Accepted: 30/10/2025

#### **Keywords:**

Blackbox Testing; Mental Health Consultation System; System Usability Scale; Waterfall; Website Development

#### **ABSTRACT**

Mental health is an important issue that requires improved accessibility and efficiency in psychological services. Klinik Biro Psikologi Putra Tunggal, which serves various communities in Banyumas Regency, has a website as an information platform but does not yet support online consultation features. Therefore, this study aims to develop a web-based mental health consultation system to enhance the accessibility and effectiveness of psychological services. The system development follows the Waterfall method, consisting of analysis, design, implementation, testing, and maintenance stages, ensuring each phase is evaluated before progressing. The developed website includes user, service, and article management features for administrators; online and offline consultations by psychologists; as well as service booking and communication via chat rooms for patients. The system was tested using Blackbox Testing with descriptive analysis, vielding a feasibility score of 100%. Thus, the system is considered to be functioning properly and ready for deployment. The System Usability Scale (SUS) test showed that the new website scored 77.16, higher than the previous version, which only reached 69.5. With more comprehensive features, this website is deemed feasible and effective in improving the accessibility and efficiency of mental health services.



This work is licensed under a Creative Commons Attribution 4.0 International License

#### Corresponding Author:

Yohani Setiya Rafika Nur Informatic Engineering Study Program, Telkom University Purwokerto Campus, Jl. DI Panjaitan No.128, Purwokerto 53147, Central Java, Indonesia Email: yohanin@telkomuniversity.ac.id

#### 1. INTRODUCTION

Mental health is a crucial aspect of human life that significantly impacts quality of life and productivity. However, compared to physical health, mental health is often overlooked [1]. The World Federation for Mental Health states that understanding mental health should be expanded from an individual approach to a broader societal perspective [2]. The World Health Organization (WHO) defines health as physical, mental, and social well-being rather than merely the absence of disease, making mental health an essential component that cannot be ignored [3].

In Indonesia, the prevalence of mental disorders continues to rise. The 2018 Basic Health Research (Riskesdas) reported that over 6% of the population experiences emotional mental disorders [4]. Meanwhile, the 2021 Indonesia-National Adolescent Mental Health Survey (I-NAMHS) found that 34.9% of adolescents aged 10–17 exhibit symptoms of mental disorders [5]. Unfortunately, access to mental health services remains limited due to stigma, a shortage of professionals, and geographical

Volume 12, Issue 2, October 2025, pp. 129-139 ISSN 2355-5068 ; e-ISSN 2622-4852

**DOI:** 10.33019/jurnalecotipe.v12i2.4548

constraints [6]. Therefore, leveraging digital technology is a viable solution to improve accessibility to mental health services.

Biro Psikologi Putra Tunggal Clinic in Banyumas Regency currently relies on face-to-face consultations despite having a website that only serves as an informational platform. Interviews with the clinic owner and patients revealed that time and distance limitations are the primary barriers to accessing services. Out of 15 interviewed patients, 13 reported difficulties in receiving in-person consultations.

To address these challenges, developing a web-based consultation system is necessary to provide more flexible services and reach more patients. Digital transformation in mental health services offers various benefits, such as improved accessibility, flexible scheduling, and increased service efficiency [7]. One approach to developing an online consultation system is the Waterfall method, which enables systematic development through stages of analysis, design, implementation, testing, and maintenance. This structured approach ensures a well-defined system architecture while minimizing errors during development [8].

Previous studies on mental health consultation through websites have shown that digital technology can effectively enhance the accessibility of mental health services [9]. Furthermore, the results of other research indicate that the developed applications are successful in raising public awareness about the importance of mental health and enabling users to easily access help anytime and anywhere [10]. Both studies emphasize the importance of utilizing technology to broaden the reach of mental health services and overcome the access challenges often faced by many individuals.

This study focuses on developing a web-based mental health consultation system for Biro Psikologi Putra Tunggal using the Waterfall method. This approach was chosen to facilitate structured and systematic system development through sequential stages. The resulting system allows patients to consult online, enhancing service accessibility and supporting digital innovation in mental health care.

#### 2. RESEARCH METHOD

This research involves several stages that must be undertaken. The research flowchart below illustrates the research process in the preparation of this report, as shown in Figure 2.1.

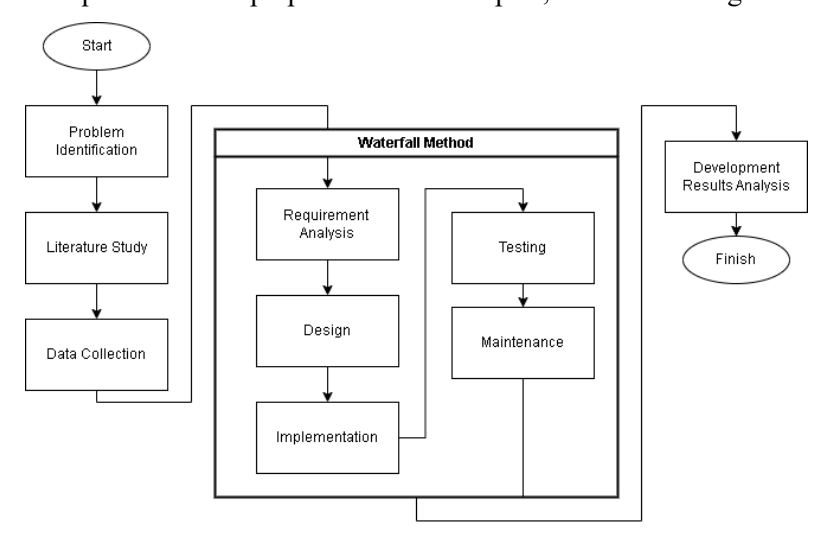


Figure 1. Research flowchart

#### 2.1 Problem Identification

This stage is the problem identification phase, aimed at recognizing obstacles in the consultation services at Biro Psikologi Putra Tunggal Clinic. This process involves an in-depth analysis of existing issues to ensure that the proposed solutions effectively enhance the clinic's consultation services.

#### 2.2 Literature Study

This stage involves gathering theoretical foundations and references related to the design of information systems from various sources, including books and previous journals. The purpose of this literature study is to enhance the understanding of the concepts and theories required for this research.

Volume 12, Issue 2, October 2025, pp. 129-139 ISSN 2355-5068; e-ISSN 2622-4852 **DOI:** 10.33019/jurnalecotipe.v12i2.4548

#### 2.3 Data Collection

This study employs data collection techniques, including interviews with the clinic owner, psychologists, and patients at Biro Psikologi Putra Tunggal Clinic, as well as usability testing results from the previous website using the System Usability Scale (SUS) method.

#### 2.4 Requirements Analysis

Requirements analysis is conducted to identify and evaluate the existing issues at Biro Psikologi Putra Tunggal Clinic. This process includes determining user requirements and system requirements, covering both functional and non-functional aspects.

#### 2.5 Design

The design phase aims to create a website according to the findings from the requirements analysis. The elements designed include Use Case Diagrams, Activity Diagrams, Sequence Diagrams, Class Diagrams, and basic User Interface (UI) designs to ensure user functionality is met.

#### 2.6 Implementation

The implementation phase, the application is coded using Next.js and PostgreSQL. This process involves writing the program code to develop the mental health consultation website for Biro Psikologi Putra Tunggal Clinic, based on the previous design results.

#### 2.7 Testing

The testing phase is carried out after implementation using Blackbox Testing to test functionality and System Usability Scale (SUS) to assess usability. The results of these tests are then analyzed to determine the feasibility of the website.

#### 2.8 Maintenance

The maintenance phase is the final step in the Waterfall method. Maintenance is carried out to prevent errors and adapt the system to changes and feature additions over time.

#### 2.9 Development Results Analysis

This stage is intended to identify the results of the development by comparing the SUS score of the previous website with the newly developed one.

#### 3. RESULTS AND DISCUSSION

#### 3.1 Data Collection

In the data collection phase, the researcher used data from interviews with clinic staff and patients, as well as the results of the System Usability Scale (SUS) method to evaluate the usability of the previous website. The data collection results are as follows:

#### Interviews and Observations

The interviews and observations at Biro Psikologi Putra Tunggal indicated that consultations are still conducted conventionally, which limits patient access due to time and distance constraints. Furthermore, the available facilities do not support online consultations, highlighting the need for a digital solution to enhance service reach and efficiency.

#### b. Usability Data from the Old Website

The System Usability Scale (SUS) testing on the old website was conducted to evaluate ease of use and user experience in accessing mental health consultation services at Biro Psikologi Putra Tunggal Clinic. The testing involved 30 respondents who filled out a questionnaire via Google Form. The total SUS score obtained was 2.085 from 30 respondents. The average SUS score was calculated using the following formula:

Average SUS Score: 
$$\frac{2085}{30}$$
 = 69,5

Thus, the average SUS score for the old website was 69.5. This score serves as baseline data before further development is carried out.

Volume 12, Issue 2, October 2025, pp. 129-139 ISSN 2355-5068; e-ISSN 2622-4852

**DOI:** 10.33019/jurnalecotipe.v12i2.4548

#### 3.2 Requirements Analysis

The requirements analysis phase includes several important elements, such as user requirements and functional requirements, all of which are part of the problem identification and investigation process.

#### a. User Requirement

Here are some user requirements based on the provided background:

Table 1. User requierment

Actor	Requirements		
	1. Patients must be able to create an account and easily access		
	consultation services.		
D-4:4	2. Patients want to easily choose consultation schedules with		
Patient	available psychologists.		
	3. Patients expect a safe, comfortable, and private consultation		
	experience.		
	4. Patients should have access to articles related to mental health.		
	1. Psychologists must be able to monitor offline consultation		
	schedules.		
Psychologist	Psychologists should be able to conduct online consultations		
1 Sychologist	with patients easily.		
	3. Psychologists should be able to access consultation history,		
	both online and offline.		
	1. Admin must have access to manage user data, including		
	patients and psychologists.		
	2. dmin can manage website articles.		
Admin	3. Admin can view all user activities (patients and		
	psychologists).		
	4. Admin dapat melihat kegiatan layanan dari semua pengguna		
	(pasien dan psikolog).		

Table 1 presents a detailed overview of the system requirements from the standpoint of users or stakeholders who will engage with the system. Each user group is granted specific access rights and functionalities based on their respective roles within the system.

#### b. System Requirement

Below are the system requirements based on the provided background:

Table 1. System requierement

System	Requirement		
Functional	1. Authentication and Authorization		
	2. Database Management		
	3. Online Chat		
	4. Scheduling		
	5. User Interface		
	6. Education and Resources		
Non-Functional	1. Security		
	Maintainability		
	3. Reliability		
	4. Scalability		
	5. Performance		

Table 2 outlines the technical specifications that must be fulfilled to develop a system aligned with user requirements, ensuring optimal system performance and functionality. These requirements are categorized into functional and non-functional aspects to provide a clear structure for implementation. Functional requirements define the core features that the system must support, while non-functional requirements ensure the system's quality attributes, such as security, scalability, and performance, are maintained throughout its operation.

Volume 12, Issue 2, October 2025, pp. 129-139 ISSN 2355-5068; e-ISSN 2622-4852 **DOI:** 10.33019/jurnalecotipe.v12i2.4548

#### 3.3 Design

The website design phase for mental health consultation at Klinik Biro Psikologi Putra Tunggal includes the creation of UML diagrams, such as Use Case and Activity Diagrams, and wireframes. These designs represent system functionality and the website's visual structure.

#### a. UML

In this study, UML is used to illustrate user interactions, processes, and system structure in the design and implementation of the mental health consultation website, with Use Case and Activity diagrams depicting workflows and system behavior in a clear and systematic manner.

#### 1. Use Case

The Use Case Diagram illustrates the interactions among three primary actors: patients, psychologists, and administrators. It provides a comprehensive overview of the system's functional scope by depicting the various actions that each actor can perform within the website. As shown in Figure 2, the diagram presents the available features and accessible menus for each actor, serving as a foundational representation of system behavior and user roles.

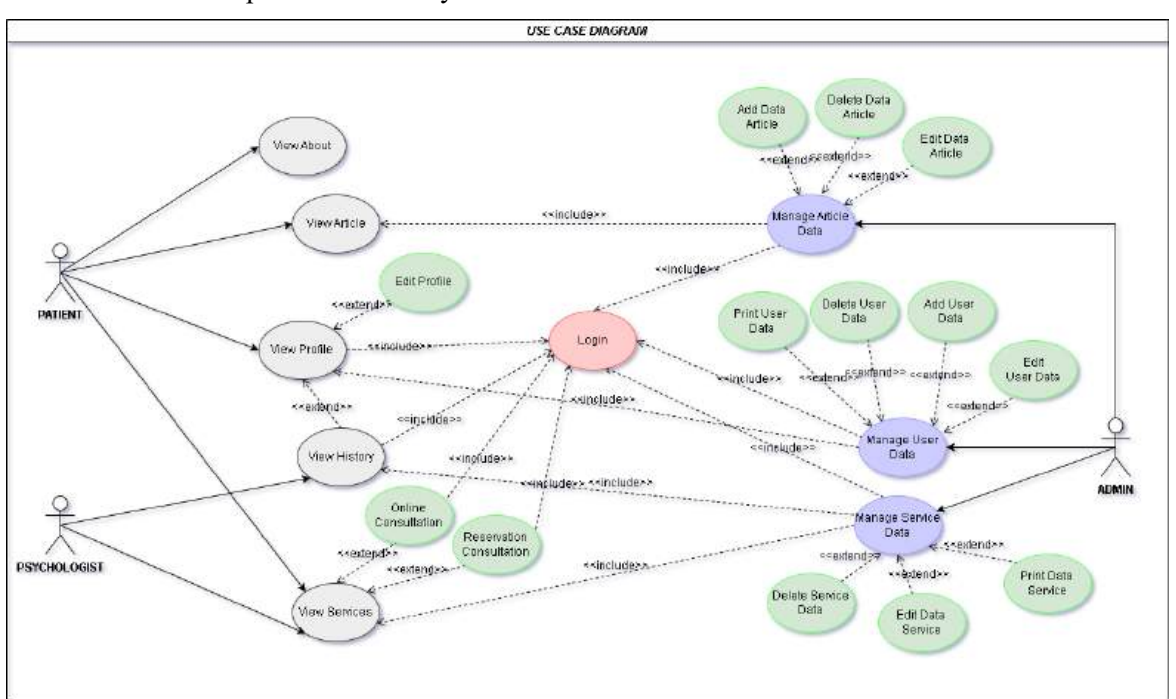


Figure 2. Use case diagram

#### 2. Activity Diagram

This diagram illustrates the interactions between the three primary actors: patients, psychologists, and administrators. Each actor holds a vital role in ensuring the system operates effectively and efficiently.

#### a) Patient Activity

The following figure illustrates the activity diagram of a patient when accessing the service page and initiating a consultation service, either online or offline.

Volume 12, Issue 2, October 2025, pp. 129-139 ISSN 2355-5068; e-ISSN 2622-4852

**DOI:** 10.33019/jurnalecotipe.v12i2.4548

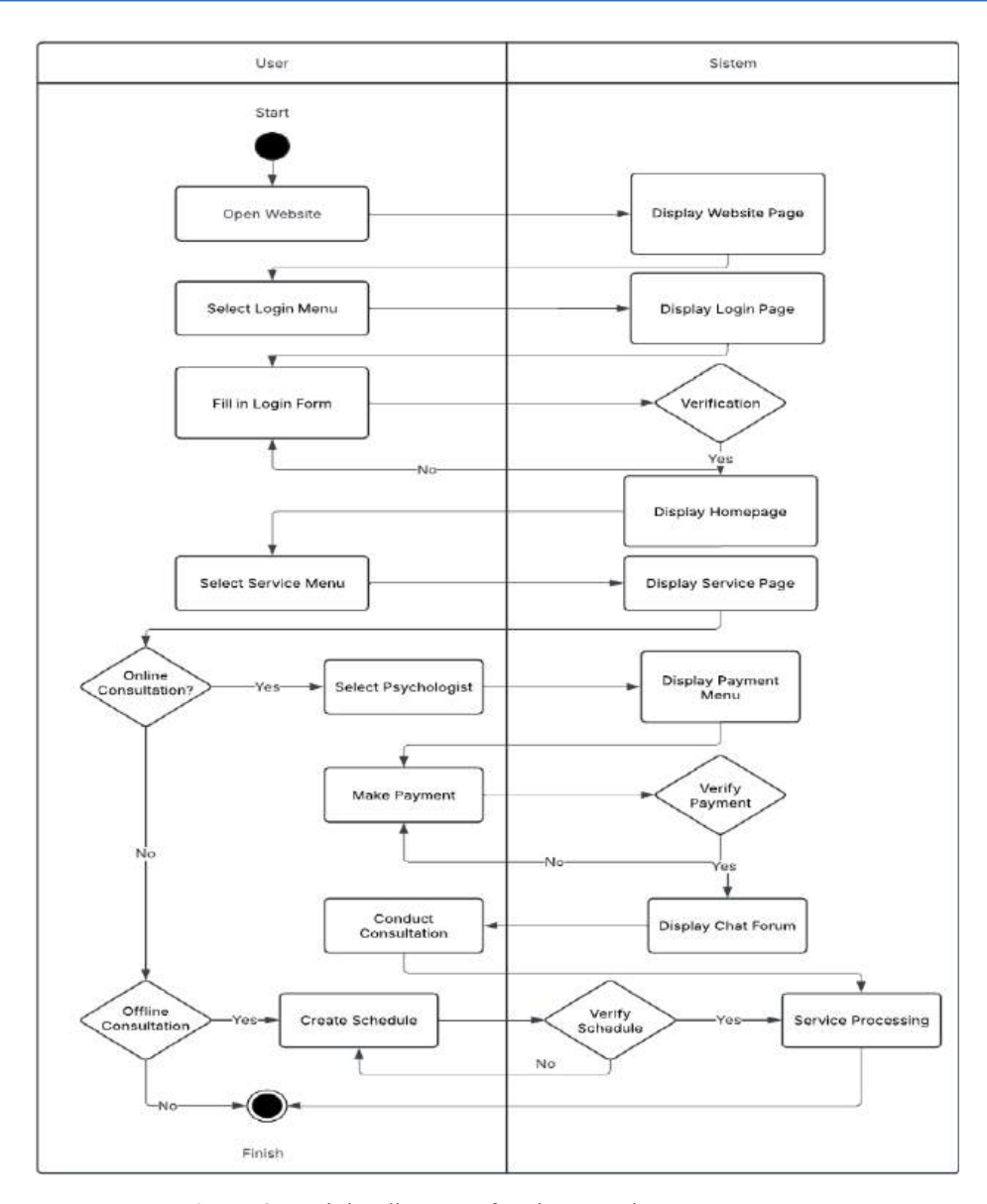


Figure 3. Activity diagram of Patient Service Page

Figure 3 illustrates the patient's activity flow in accessing consultation services, either online or offline. The process begins when the user opens the website and logs in through the login menu. After successful verification, the user navigates to the service menu to choose between online or offline consultation. For online consultation, the user selects a psychologist, makes a payment, and upon verification, accesses the chat forum for consultation. For offline consultation, the user creates a schedule, which the system verifies before processing the service.

#### b) Pyschologist Activity

The following is a diagram of the activities of psychologists and admins when they want to manage the service page.

Volume 12, Issue 2, October 2025, pp. 129-139 ISSN 2355-5068; e-ISSN 2622-4852 **DOI:** 10.33019/jurnalecotipe.v12i2.4548

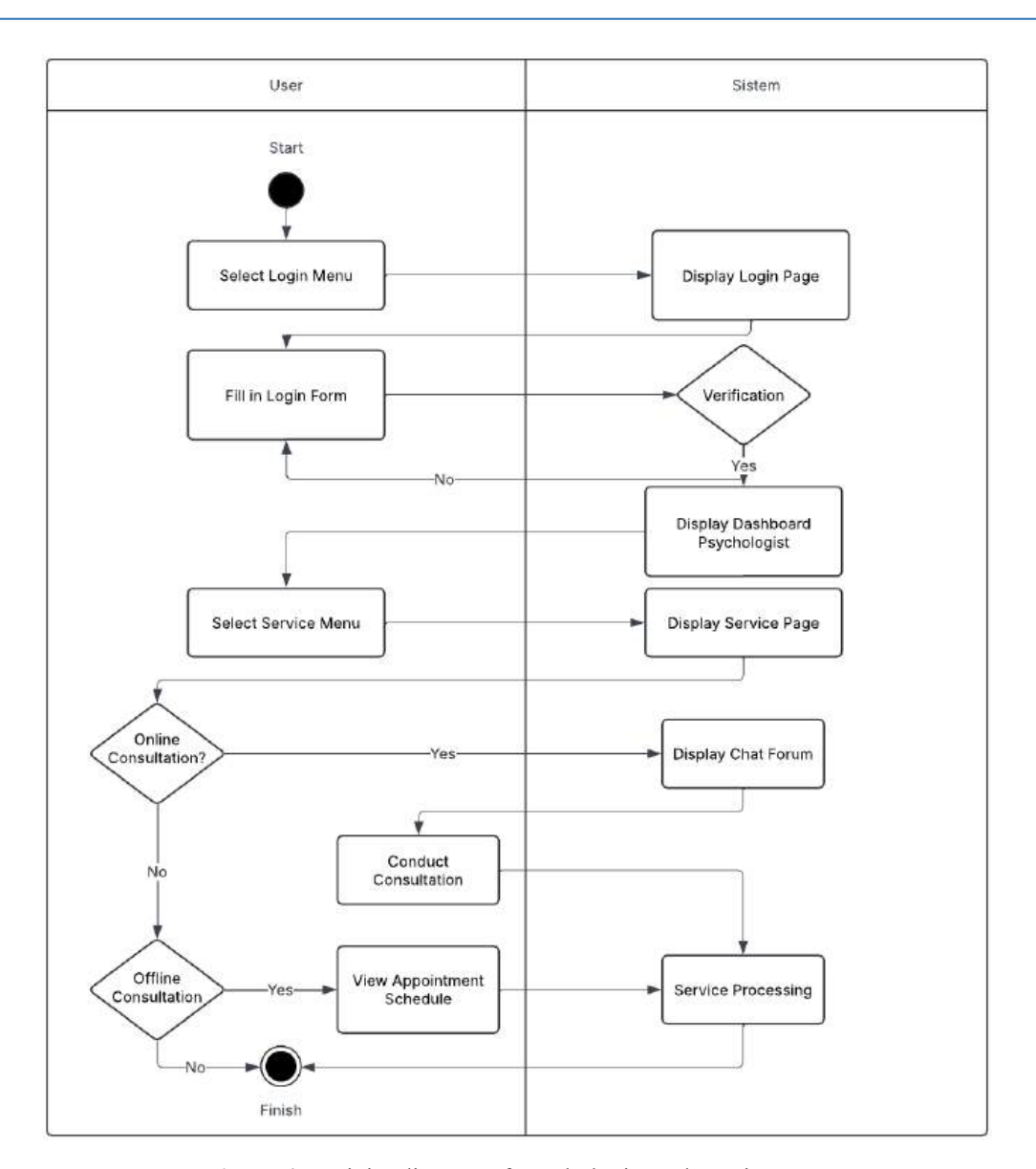


Figure 4. Activity diagram of Psychologist and Service Page

Figure 4 illustrates the flow of Psychologist and system activities in managing consultation services. The process begins with the user logging into the system and selecting the service menu. Users can choose between online or offline consultation services. If online consultation is selected, the system will display a chat forum to conduct the consultation. If offline consultation is chosen, users can view the appointment schedule, and the system will process the service accordingly. This activity flow supports the smooth operation and accessibility of psychological services within the system.

# c) Administrator Activity The following is a diagram of the activities of psychologists and admins when they want to manage the service page.

Volume 12, Issue 2, October 2025, pp. 129-139 ISSN 2355-5068 ; e-ISSN 2622-4852

**DOI:** 10.33019/jurnalecotipe.v12i2.4548

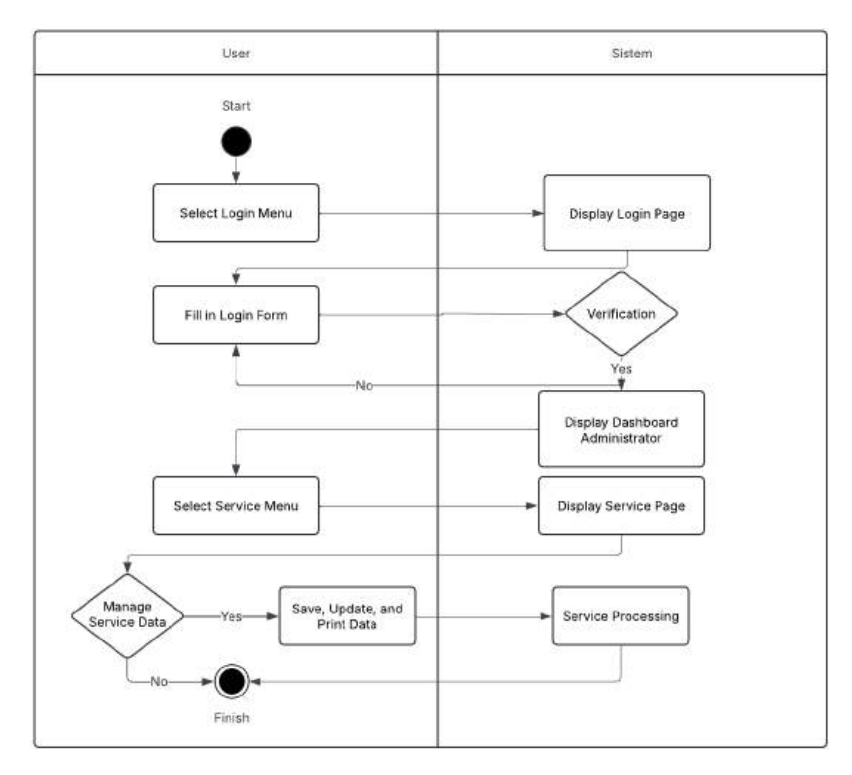


Figure 5. Activity diagram of Admin Managing Data

Figure 5 illustrates the administrator's workflow in managing service data within the system. The process begins when the administrator selects the login menu and fills in the login form. Upon successful verification, the system displays the administrator dashboard, providing access to various service-related features. The administrator then navigates to the service menu to manage service data. If data management is required, the administrator can perform actions such as saving, updating, and printing service data. These activities are processed by the system to ensure data accuracy and service efficiency. This workflow enables the administrator to maintain and control service information effectively, supporting the overall functionality and performance of the system.

#### b. Wireframe

Wireframes were created based on use case and activity diagrams. The user-friendly UI design ensures an effective interaction between users. The wireframes for each menu are presented below:

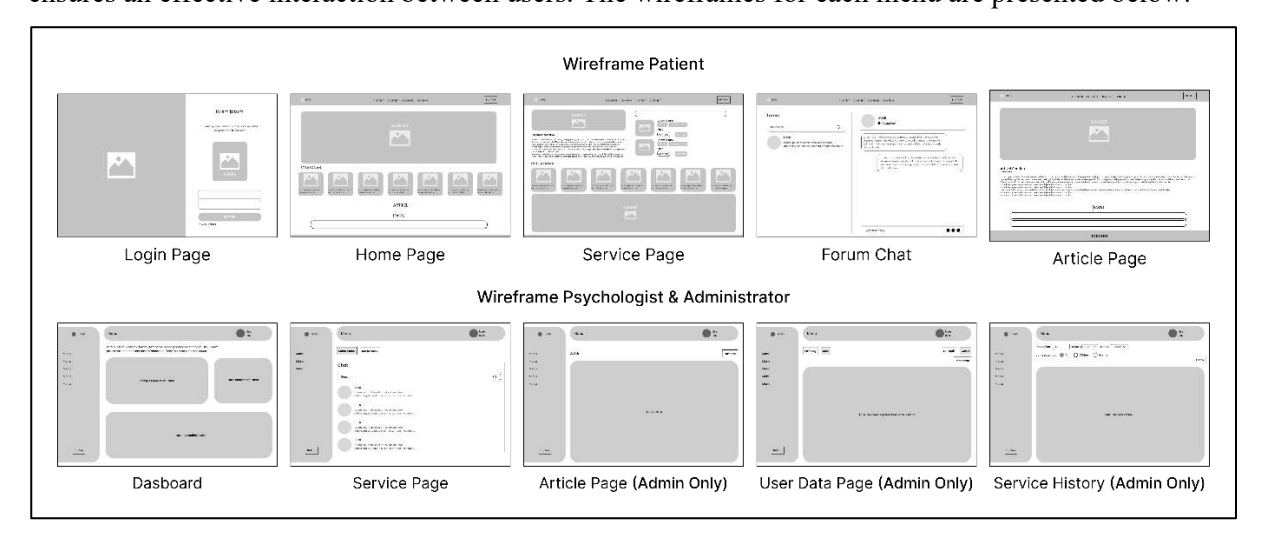


Figure 6. Wireframing

Volume 12, Issue 2, October 2025, pp. 129-139 ISSN 2355-5068; e-ISSN 2622-4852 **DOI:** 10.33019/jurnalecotipe.v12i2.4548

Figure 6 illustrates the wireframes designed for both patients and administrators/psychologists, covering key pages such as login, home, services, forum chat, and data management. These wireframes serve as the foundation for the system's user interface, ensuring intuitive navigation and efficient interaction for all user roles.

#### 3.4 Implementasi

The implementation phase resulted in the following developments:

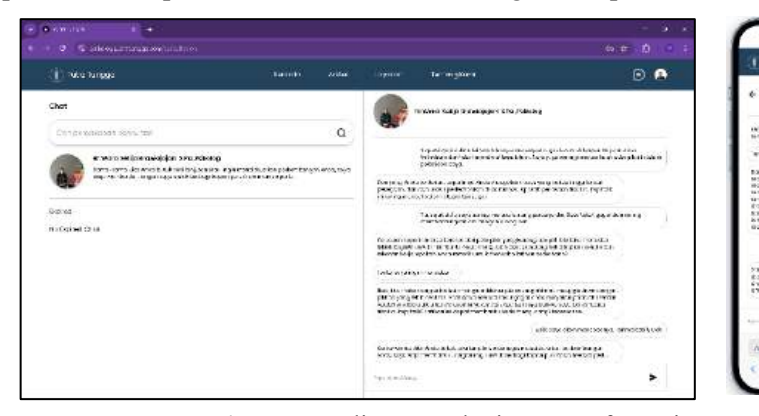


Figure 7. Online consultation menu for patients

Figure 7 shows the online consultation menu, which requires users to log in and complete payment before accessing consultation services. Patients can select a psychologist, make payments, and gain chat access for one hour with their chosen psychologist upon successful payment validation.

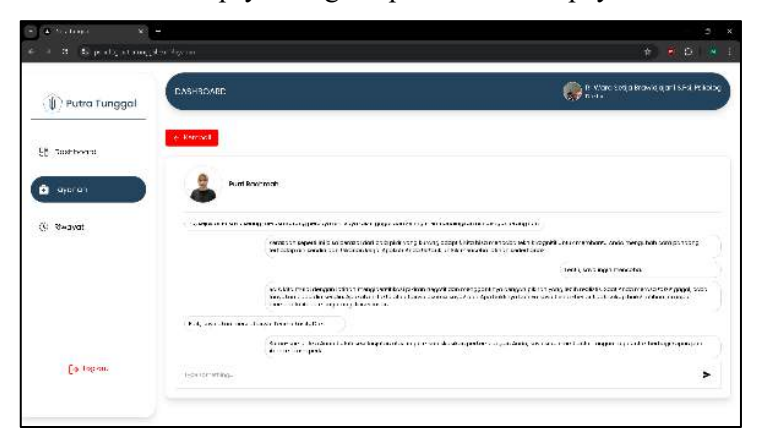


Figure 8. Consultation management menu for psychologist

Figure 8 shows the page where psychologists can conduct online consultations with patients who have completed payment and also view the schedule of offline consultations booked by patients.

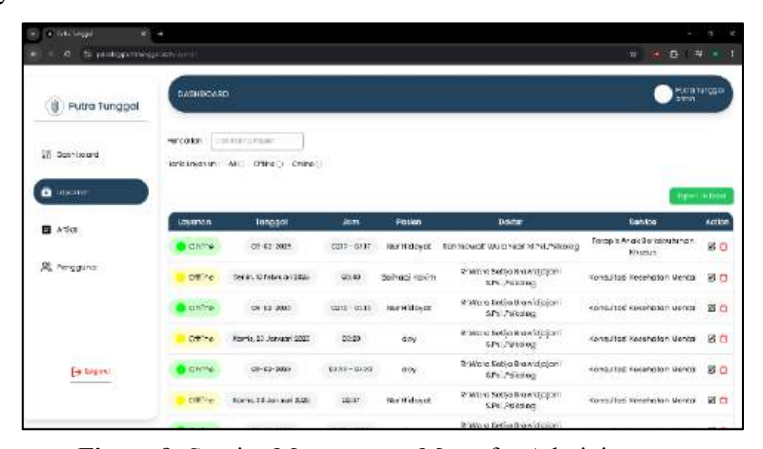


Figure 9. Service Management Menu for Administrators

Volume 12, Issue 2, October 2025, pp. 129-139 ISSN 2355-5068; e-ISSN 2622-4852

**DOI:** 10.33019/jurnalecotipe.v12i2.4548

Figure 9 shows the admin page where administrators manage consultation services by editing, deleting, and generating reports, allowing efficient control and monitoring of service activities.

#### 3.5 Testing

The website underwent two testing methodologies: Blackbox Testing for functionality and System Usability Scale (SUS) for usability evaluation:

#### a. Blackbox Testing

Table 3.3 presents the results of Blackbox testing conducted on five main pages of the system: Admin, Psychologist, Patient, Login, and Registration. All tests were successful with no failures, resulting in a total of 105 successful tests. These results indicate that the system operates reliably and stably according to its intended functions.

**Test Results** No **Test Scenario** Successful **Failed Tests Tests** Admin Page 0 1 18 2 Psychologist Page 0 11 Patient Page 3 62 0 4 Login Page 0 6 5 Registration Page 8 0 **Total Test Results** 0 105

Table 3. Blackbox Testing Results

Success Rate Calculation:

Successful Tests: 
$$\frac{105}{105} \times 100\% = 100\%$$
$$Failed Tests: \frac{0}{105} \times 100\% = 0\%$$

Base on black box testing result, with a 100% success rate, the mental health consultation website at Klinik Biro Psikologi Putra Tunggal is highly functional and fully operational.

#### b. System Usability Scale (SUS)

This study employs the stratified sampling method by dividing respondents into two groups: clinic staff and the Banyumas community, with a total of 30 respondents. The distribution is based on population proportions to ensure more accurate and representative results. The test results indicate that the total System Usability Scale (SUS) score obtained is 2,315. The average SUS score is calculated using the following formula:

Average SUS score: 
$$\frac{2315}{30} = 77,16$$

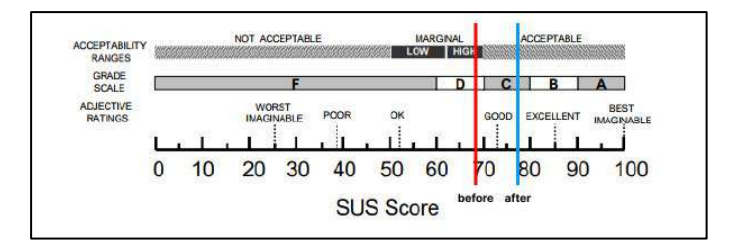


Figure 10. SUS testing results

Based on this calculation, the average SUS score of 77.16 falls within the **Acceptability Ranges** category as Acceptable. According to the **Grade Scale**, the system is classified as **Grade C**, while based on the **Adjective Rating**, it is categorized as **Good**. These results demonstrate that the website

Volume 12, Issue 2, October 2025, pp. 129-139 ISSN 2355-5068; e-ISSN 2622-4852 **DOI:** 10.33019/jurnalecotipe.v12i2.4548

development has successfully improved the system's quality compared to the previous version, which had a SUS score of only 69.5.

#### 4. CONCLUSION

The existing website primarily functions as an informational platform without online consultation features, limiting service flexibility and hindering clinical expansion, which still relies on face-to-face consultations. The development of a digital mental health consultation system through the Klinik Biro Psikologi Putra Tunggal website addresses these limitations by enhancing service accessibility and efficiency.

Developed using the Waterfall method, the new website goes beyond information dissemination by integrating an online consultation service, improving patient engagement and convenience. Blackbox Testing, conducted with 105 test scenarios, achieved a 100% success rate, Thus, the system is considered to be functioning properly and ready for deployment. Additionally, System Usability Scale (SUS) testing with 30 respondents showed an increase in the usability score from 69.5 to 77.16, indicating a significant improvement in user experience.

These results demonstrate that the digital transformation of the mental health consultation system successfully enhances patient access, optimizes consultation processes, and improves overall service quality at Klinik Biro Psikologi Putra Tunggal.

#### REFERENCES

- [1] A. Rahmadhani, F. Fauziah, and A. Aningsih, "Sistem Pakar Deteksi Dini Kesehatan Mental Menggunakan Metode Dempster-Shafer," *Sisfotenika*, vol. 10, no. 1, p. 37, 2020, doi: 10.30700/jst.v10i1.747.
- [2] Y. A. Rozali, N. W. Sitasari, and A. Lenggogeni, "Meningkatkan Kesehatan Mental Di Masa Pandemic," *J. Pengabdi. Masy. AbdiMas*, vol. 7, no. 2, 2021, doi: 10.47007/abd.v7i2.3958.
- [3] D. Novianti, "Isu Kesehatan Mental (Mental Health) dan Peranan Pelayanan Konseling Pastoral Kristen," *J. Kadesi*, vol. 5, no. 1, pp. 137–162, 2023.
- [4] S. Diah Puspita, "Kesehatan Mental Dan Penanganan Gangguannya Secara Islami Di Masa Kini," *J. Forum Kesehat. Media Publ. Kesehat. Ilm.*, vol. 12, pp. 2–3, 2022, [Online]. Available: http://e-journal.poltekkes-palangkaraya.ac.id/jfk/
- [5] A. E. Wahdi, S. A. Wilopo, and H. E. Erskine, "122. The Prevalence of Adolescent Mental Disorders in Indonesia: An Analysis of Indonesia National Mental Health Survey (I-NAMHS)," *J. Adolesc. Heal.*, vol. 72, no. 3, p. S70, 2023, doi: 10.1016/j.jadohealth.2022.11.143.
- [6] R. A. Listiyandini, "Layanan kesehatan mental digital: Urgensi riset dan penerapannya di Indonesia," *J. Psikol. Ulayat*, vol. 10, no. 1, pp. 1–4, 2023, doi: 10.24854/jpu789.
- [7] R. Arjadi, S. J. Kusumawardhani, N. Purnomo, and C. L. Bockting, "Benefits and challenges in implementing online mental health consultation in Indonesia: Survey in practitioners," *J. Psikol. Ulayat*, vol. 10, pp. 284–299, 2023, doi: 10.24854/jpu726.
- [8] U. S. Senarath, "Waterfall methodology, prototyping and agile development," *Tech. Rep.*, no. June, pp. 1–16, 2021, doi: 10.13140/RG.2.2.17918.72001.
- [9] B. R. Faturizky and R. Komalasari, "Sistem Informasi Layanan Konsultasi Kesehatan Mental Berbasis Website," *J. Teknol. Sist. Inf.*, vol. 5, no. 1, pp. 133–144, 2024, doi: 10.35957/jtsi.v5i1.7793.
- [10] M. P. Aji and U. G. Aeman, "Rancang Bangun Website Kesehatan Mental Mindland," *J. Media Pratama*, vol. 17, no. 1, pp. 61–73, 2023.



Volume 12, Issue 2, October 2025, pp. 140-150 ISSN 2355-5068; e-ISSN 2622-4852

**DOI:** 10.33019/jurnalecotipe.v12i2.4560

## Prototype of Seaweed Dryer Operating in Manual and Automatic Mode Using Wi Fi Based Microcontroller

#### Setiyono

Department of Electrical Engineering, Gunadarma University, Indonesia

#### **ARTICLE INFO**

#### Article historys:

Received: 14/04/2025 Revised: 18/04/2025 Accepted: 30/10/2025

#### Keywords:

Seaweed Dryer, Internet of Things, Microcontroller Platform, Telegram Application

#### **ABSTRACT**

This study discusses the development of a seaweed dryer prototype that can operate automatically or manually using a IoT (Internet of Things) based Nodemcu ESP826 microcontroller and Telegram application. The operation of the tool can choose automatic mode, where the system regulates the temperature independently, or manual mode via telegram to control the drying parameters directly. The drying process can be carried out by operating an incandescent lamp (50 W) as a heat generator and a fan to generate air flow in the seaweed drying area. The method of testing the tool with automatic mode is by installing a rainwater sensor that will provide a signal for the microcontroller to order the motor to rotate to open or close the roof and turn on the lights and fan, while in manual mode the roof opening and closing operation is carried out by changing the use of automatic mode to manual on the telegram command. The test results are in the form of voltage measurements on several tool components that are in accordance with the working parameters of each part and this tool can operate in automatic or manual mode. When the drying process takes place, the incandescent lamp and fan will be active or ON, and when the water sensor receives rainwater, the drive motor will immediately be active to close the roof. When the water sensor does not receive rainwater, all systems will automatically be OFF. This prototype is worthy to be implemented into a real tool to help seaweed farmers in the seaweed drying process to be more efficient, easier to control, and can improve the quality of the final seaweed product.



This work is licensed under a Creative Commons Attribution 4.0 International License

#### **Corresponding Author:**

Setiyono

Department of Electrical Engineering, Gunadarma University, Jl Margonda Raya 100 Pondokcina Depok 16424, Indonesia Email : setiyono@staff.gunadarma.ac.id

#### 1. INTRODUCTION

Indonesia is recorded as one of the largest seaweed producing countries, with production reaching 10.25 million tons in 2021 according to data from the Ministry of Maritime Affairs and Fisheries (KKP) [1]. Seaweed is one of the leading commodities in the fisheries sector which has high economic value, especially in the West Nusa Tenggara region which is the seaweed production center [2]. The characteristic of seaweed lies in the type of pigment it contains, which is the basis for grouping it into several divisions, namely Rhodophyta (red algae), Chlorophyta (green algae), Phaeophyta (brown algae), and Chrysophyta (golden/blond algae) [3]. Processed seaweed products are widely used in the food and non food [4], cosmetics (face mask) [5,6], pharmaceutical [7] and other sectors [8]. One of the important stages in seaweed processing is the drying process, which has a direct effect on the quality



Volume 12, Issue 2, October 2025, pp. 140-150 ISSN 2355-5068; e-ISSN 2622-4852

**DOI:** 10.33019/jurnalecotipe.v12i2.4560

and durability of the final product. Conventional (open) drying requires large areas of land and relies on sunlight, often facing various obstacles, such as dependence on weather, long drying times, and the risk of contamination, so this method is not recommended in the seaweed processing industry [9]. Therefore, innovative solutions are needed to improve the efficiency and quality of seaweed drying. As technology develops, Internet of Things (IoT) based systems can be applied to automate remote monitoring processes, evaluate performance and control drying [10]. Nodemcu ESP8266 is NodeMCU is an open source IoT platform that includes hardware a microcontroller [11] that can be used to develop automatic drying systems for remote monitoring and control [12,13]. The ESP8266 is an ultra-low cost module with advanced features, making it an ideal choice for smart home applications with the Internet of Things (IoT) [14]. By integrating temperature and humidity sensors, this system is able to adjust drying conditions in real-time. In addition, using the Telegram application allows users to monitor and control the dryer both automatically and manually remotely. Until now, innovation and research on seaweed drying equipment continues to be carried out. Some previous research includes: G.B. Pradana discusses the process of drying seaweed using a tray dryer equipped with an air dehumidification system to increase energy efficiency and product quality. Seaweed was dried using a tray dryer at temperatures of 40°C, 50°C, 60°C, and 70°C for 2, 3, and 4 hours. Water content was measured every 30 minutes to monitor the drying process. The research results showed that water content in accordance with Indonesian National Standards (SNI) was achieved after drying for 4 hours at 50°C, 4 hours at 60°C, and 2, 3, and 4 hours at 70°C. The increase in drying temperature is directly proportional to the drying rate, but over time, the drying rate decreases. The highest energy efficiency was achieved in drying for 4 hours at 50°C, namely 91.50% [15]. A. Culaba and his colleagues discussed mathematical modeling of the seaweed drying process using sequential statistical criteria analysis to determine the best drying model. Drying modeling is important to understand drying behavior and optimize the process [16]. Sarah Dewi discussed the development of a seaweed dryer that uses an Arduino Uno microcontroller equipped with an OLED LCD screen to monitor and display temperature and humidity during the drying process. This dryer prototype is equipped with a temperature sensor to detect temperature and humidity, a heater to dry seaweed, a fan to distribute heat evenly in the drying chamber, and an OLED LCD screen to display real-time temperature and humidity information. Tests show that this tool is capable of drying 4 kg of seaweed within 4-5 hours until it reaches the desired dryness level [17]. Apart from the many benefits obtained from seaweed processing, there is also waste from processing and it needs to be handled properly before being disposed of into the environment, namely through a neutralization process [18].

#### 2. RESEARCH METHOD

This research aims to develop a prototype seaweed dryer based on the Internet of Things (IoT) using Nodemcu ESP8266 and the Telegram application. This tool is designed to work in manual or automatic mode, so users can control and monitor the drying process remotely. By utilizing temperature and humidity sensors, this system can adjust drying parameters automatically to increase efficiency and quality of drying results. To achieve this goal, this research uses an experimental method with a prototype development approach. The research steps carried out were the first: System Design, several things discussed included, determining the specifications of the seaweed dryer, designing a control system based on the NodeMCU ESP8266, determining the type of temperature and humidity sensor used (DHT22/SHT11) and designing the Telegram application interface for control and monitoring. Prototype Development, assembling hardware components, such as heaters (Bulb Lamp 50W) as a simulator to generate heat and increase room temperature), fans (to generate air flow in the dryer tools) , temperature and humidity sensors, as well as the Nodemcu ESP8266, developing software for control tool via Telegram, implementing manual and automatic control modes. Testing and Evaluation, testing the system in various environmental conditions, evaluating the effectiveness of the automation system in maintaining temperature and humidity according to optimal parameters, testing is carried out by measuring the voltage parameters produced in each important part of the tool being tested. Data analysis, evaluating measurement results and preparing recommendations for further development. The results of Volume 12, Issue 2, October 2025, pp. 140-150 ISSN 2355-5068 ; e-ISSN 2622-4852

**DOI:** 10.33019/jurnalecotipe.v12i2.4560

this research are expected to provide innovative solutions in the seaweed drying process by utilizing IoT technology which can be controlled manually or automatically via the Telegram application.

#### 2.1. Design System

Figure 1. is a depiction of the overall design made on the prototype that was built. Includes input blocks, process blocks and output blocks as well as functions that will be described in each component contained in each block. The input block consists of a rain sensor, LDR sensor and also the Telegram application. These components are the initial trigger for the operation of this seaweed dryer. The triggers created by the input block components will be processed and processed by the process block consisting of the ESP8266 Nodemcu which is connected to the internet, where the data obtained will be processed by the ESP8266 NodeMCU which will then run the other components contained in the output block. Figure 2 is a prototype of the resulting seaweed dryer.

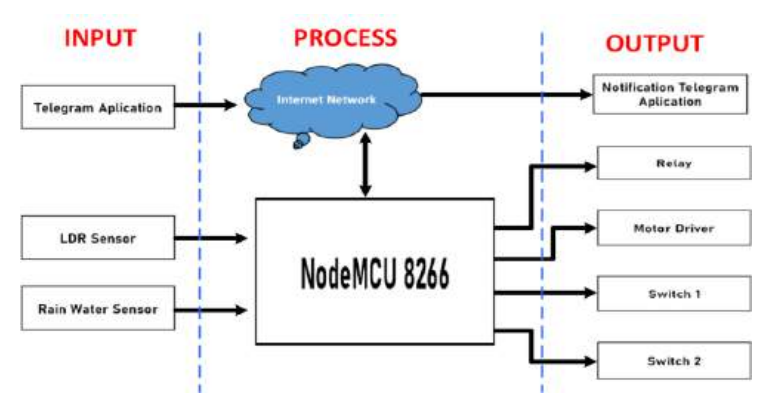


Figure 1. Overall system design diagram

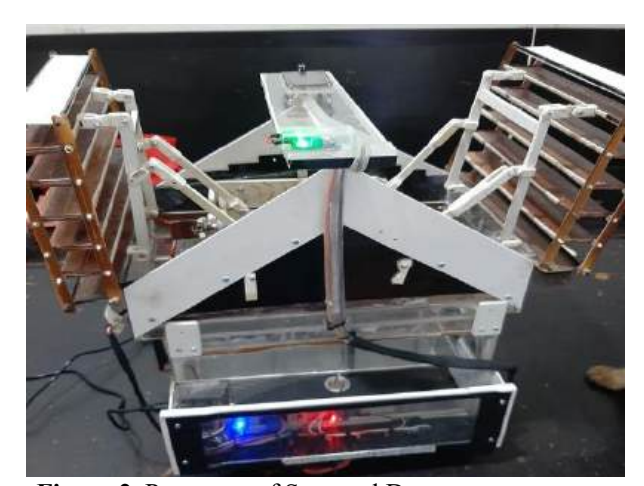


Figure 2. Prototype of Seaweed Dryer

#### 2.2. Input Block

This In this input block there are two components, namely the rain sensor and the LDR sensor as triggers for this tool to run. This sensor works in a way that if the rain sensor is exposed to water, the sensor will detect it. Likewise with the LDR sensor, if the LDR sensor is not exposed to enough light or is dark, the sensor will detect it. Then there is the Telegram application which is used to change manual or automatic methods on tools via bots, which then trigger the triggers which will be processed later in the process block. In the Telegram application you can also find out the current state of the device with the "status" command to find out whether the device is in manual or automatic mode and whether the roof is open or closed. In the automatic method the initial trigger comes from the rain sensor and LDR sensor only and in the manual method the initial trigger comes from Telegram, where the user will give the command to change the tool method in the Telegram application and give the command to open and close the roof from telegram.



Volume 12, Issue 2, October 2025, pp. 140-150 ISSN 2355-5068; e-ISSN 2622-4852 **DOI:** 10.33019/jurnalecotipe.v12i2.4560

#### 2.3. Process Block

In the process block, the trigger signal given from the input block will be received by the Nodemcu ESP8266 as a microcontroller on the device and process it according to the program that has been designed in the Arduino IDE application. In the automatic method the input block trigger comes from the rain sensor and LDR sensor and in the manual method the trigger comes from the Telegram application which commands the manual method and opens or closes the roof. Then, after the triggers have been processed by the , they are forwarded to the output block and run the components in the output block. Figure 3 is the lead info for the Nodemcu 8266 pin. Table 1 is the relationship between the Nodemcu ESP8266 PIN and the input and output units.

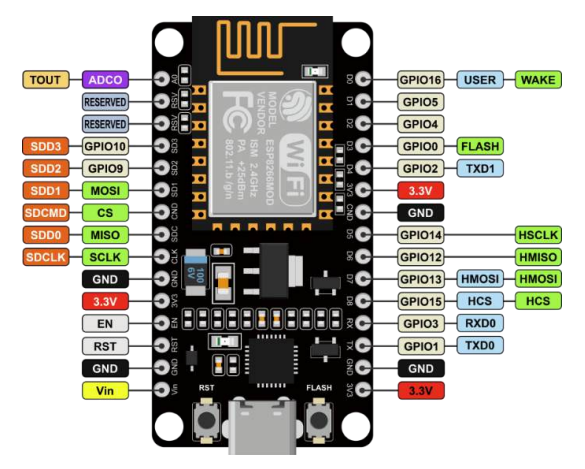


Figure 3. Nodemcu ESP8266 Pin [19]

Table 1. Relationship between Nodemcu Pins and Output Devices

PIN	Terhubung ke		
D1	Pin D0 sensor LDR		
D2	Pin D0 sensor hujan		
D3	Pin IN1 Relay		
D4	Pin A-IB motor driver		
3V3	Pin VCC motor driver		
GND	Pin GND motor driver		
D5	Pin tengah limit switch 1		
D6	Pin tengah limit switch 2		
GND	Pin bawah limit switch 1 dan 2		
D7	Pin A-IA motor driver		
GND	Pin GND sensor hujan dan sensor LDR		
3V3	Pin VCC sensor hujan dan sensor LDR		
GND	Pin GND Relay		

#### 1. Telegram

Telegram is a cloud-based messaging application that focuses on speed and security and is designed to make it easier for users to send text, audio, video, image and sticker messages to each other safely [20]. By default, all content transferred to Telegram will be encrypted to international standards. Therefore, messages sent are completely safe from third parties, even from Telegram. The Telegram application can not only send text, images or videos, but Telegram can also be a place to send documents, music, zip files, real-time locations and also saved contacts to other people's devices. Because Telegram is a cloud-based application, it makes it easier for users to access one Telegram account from different devices simultaneously. Telegram was pioneered by two brothers from Russia, namely Nikolai Durov and Pavel Durov. The two brothers shared tasks, Nikolah focused on application development by creating the MTPtoro protocol which became the motor for Telegram. Meanwhile, Pavel is responsible for funding and infrastructure through digital fortless funding.

Volume 12, Issue 2, October 2025, pp. 140-150 ISSN 2355-5068; e-ISSN 2622-4852

**DOI:** 10.33019/jurnalecotipe.v12i2.4560

#### 2. Arduino

Arduino IDE (Integrated Development Environment) is a software that has a very important role in programming, compiling binaries and downloading microcontroller memory. Apart from many supporting modules such as sensors, monitors, readers and others, Arduino itself has become the choice for many professionals. One of the reasons Arduino attracts many people is because of its open source nature, both in hardware and software. Schematics on arduino are also free for everyone, free to download images buy components, make pcb and assemble it yourself without paying arduino maker. Likewise, the Arduino IDE can be downloaded for free and installed on a computer.

#### 2.4. Output Block

In the output block, there are relay components, motor drivers, switches, DC motors, fans, LEDs and telegram applications. After the process block, whether you use manual or automatic methods, the work on the output block components remains the same. After the data is processed by the NodeMCU, when the roof must be closed or opened, the relay and motor driver are active to move the DC motor where the DC motor makes the roof move to open or close. After the roof is opened or closed, the roof will press the switch on each side according to the condition of the roof at that time, then when the roof is closed and pressing the switch it will turn on the fan component and LED, likewise when the roof is open and pressing the switch it will turn the fan component and LED off. Then for the Telegram application in the output block as a notification or notification on Telegram, the notification displays data such as method transfer, equipment status at that time, notification when the roof is closed or notification when the roof is open.

#### 3. RESULTS AND DISCUSSION

The test results are in the form of voltage observations on each part where the working voltage is obtained according to the specifications of each component. Shown in Figure 5 is one of the voltage observations on the LDR sensor, rainwater sensor and relay while table 2 is the result of voltage observations for each component. This prototype is designed to work in two modes, namely automatic and manual, to increase the efficiency of the drying process. Tests were carried out to evaluate the system's reliability in controlling temperature, humidity, and the device's responsiveness to commands sent via the Telegram application. Apart from that, the test results were also compared with conventional drying methods to see the effectiveness of the equipment in speeding up the drying process and maintaining the quality of seaweed. Figure 4 is the workflow of the prototype tool that was built. is a flow diagram that explains the process and how it works from the design and construction of a seaweed dryer using manual and automatic methods using the Nodemcu ESP826 based telegram application. Starting from activating the tool using a 12V - 5A power supply, then initializing the Nodemcu, there are two methods for running this seaweed dryer. The first method is the automatic method, where this automatic method uses readings from the LDR sensor and rain sensor to run this tool. If the LDR sensor detects a lack of light or darkness and the rain sensor detects water hitting the sensor, the Nodemcu will automatically process the data.

The explanation of Figure 4 is as follows, the rain sensor detects water that is hit by the detector board. The rain sensor moves the DC motor to close the roof. When the roof moves, the telegram will send a notification "Roof Closed Automatically" and after the roof is closed and pressing the switch, the fan and LED turn on, then a notification will appear on the telegram, namely, "Weather is Raining - Close the Roof, Turn on the Fan and LED". And if the rain sensor does not detect water that has hit the sensor body or the rain has stopped, the NodeMCU will process the data get this and then move the motor to open the roof, when the roof moves to open the telegram it will send a notification "Roof Opened Automatically" and after the roof opens and presses the switch, the fan and LED will also turn off, then a notification will appear on the telegram "Sunlight Detected - Opening the roof, Turning off the Fan and LED". "Roof Closes Automatically" and after the roof is closed and pressing the switch, the fan and LED turn on, which then a notification will appear on the telegram, namely, "Dark Weather / Night - Closing the Roof, Turning on the Fan and LED". And when the LDR sensor detects light, it works the same as if the rain sensor does not detect water. The second method is the manual method, where this manual method will run if the user uses a command on the Telegram application, to change

Volume 12, Issue 2, October 2025, pp. 140-150 ISSN 2355-5068; e-ISSN 2622-4852 **DOI:** 10.33019/jurnalecotipe.v12i2.4560

the method that will be used, they will use the "manual method" command on the Telegram application. If the device is in manual mode then you have to use the command "close the roof" or "open the roof", if you use the command "close the roof" the command will then be received by the NodeMCU and the data will be processed and a notification will appear on the Telegram application, namely "The roof is closed manually" and move the motor to close the roof until pressing switch 2. Then a notification will appear on the Telegram application that says "The roof is closed" then the fan and LED turn on. Likewise, if you use the command "open the roof", the command will be received by the NodeMCU and the data will be processed and a notification will appear on the telegram application, namely "Roof opened manually" and moving the motorbike to open the roof after it is open and pressing switch 1, a notification will appear on the telegram "Roof is Open". To find out whether the system design works well, testing is needed at certain points to measure the voltage parameters that occur at that point. Table 2 is the measurement results at each point of the equipment where the measurement results are within the tolerance value of the recommended voltage for each component.

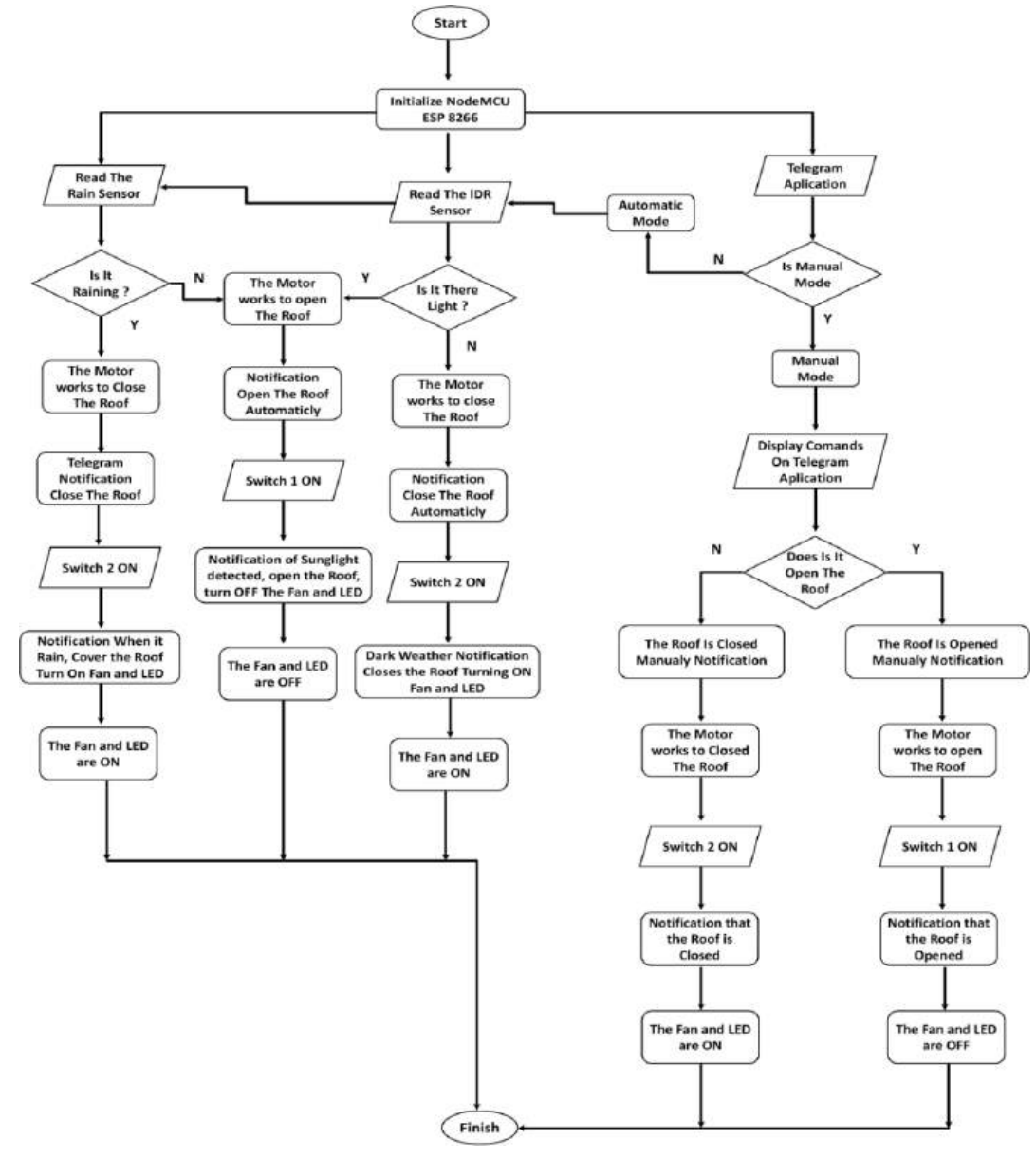
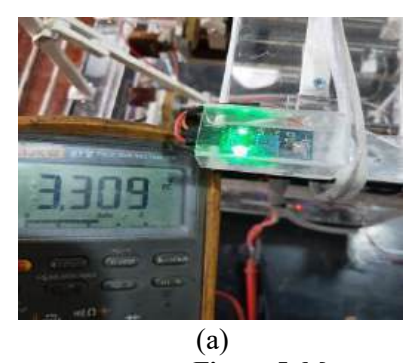


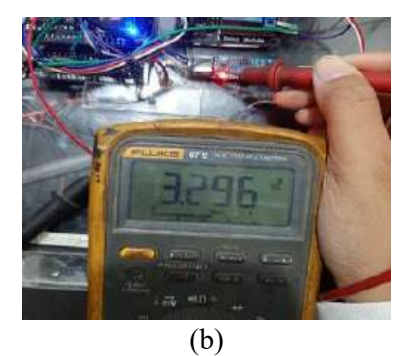
Figure 4. Working step of seaweed dryer research method

Volume 12, Issue 2, October 2025, pp. 140-150 ISSN 2355-5068; e-ISSN 2622-4852 **DOI:** 10.33019/jurnalecotipe.v12i2.4560

Table 2. Measurement of tool operating voltage on each unit

Unit Test Point	Voltage measurement results	Recommended Operating Voltage Range
LDR Sensor	3.309 V	3.3 – 5 V
Rain water sensor	3.29 V	3.3 – 5 V
Relay	4.992 V	5 – 24 V
NodeMCU ESP8266	4.991 V	3 – 12 V
Motor driver	4.983 V	3.2 – 40 V





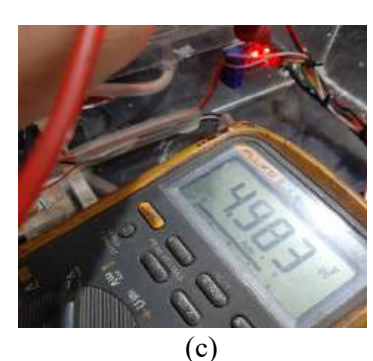


Figure 5. Measurement results (a) LDR sensor (b) Rainwater sensor (c) Relay

Figure 5a Display of measurements on the light sensor using LDR, Figure 5b Measurement results on the rainwater sensor and Figure 5c Is a relay voltage measurement. The development of this system is an innovation in seaweed drying equipment that can work automatically or manually so that it can reduce the workload of seaweed farmers.

#### 3.1. Obeservation Data

In collecting this observational data, it was obtained from the results of testing the seaweed dryer in accordance with the workings of the tool that has been designed and implemented, then the results of this seaweed dryer will be data and described for each component.

#### LDR Sensor Testing

The LDR sensor works by detecting light caught on the sensor. This test was carried out with the aim of determining the sensitivity of the LDR sensor. In this seaweed dryer, the LDR sensor is the input to run the tool automatically, therefore the LDR sensor is tested by providing light which is measured using a lux reader application, the light provided comes from the lamp light and flashlight light. In each experiment you will also see the notification that appears on the Telegram application and also the response from the LDR sensor detecting light until finally the roof runs. In this experiment, the condition of the rain sensor was dry so it only used the LDR sensor as input for this tool. Table 3 is the result of observations on the light sensor unit when it was in several different light conditions.

Table 3. LDR sensor test results

**Testing** State of Light Respon time (s) **Roof State Telegram Notification** Dark / Night Weather 1 1 - close the roof, turn on the fan and Dark Closed Sunlight detected A Litle light - open the roof, turn off the fan 2 1 Opened and LEDs Dark Weather / Night – closingatap, 3 1 Closed Dark turn ON Fan and LEDs Sunlight detected – opens roof, turns 1 4 **Bright** Opened off fan and LEDs

Prototype of Seaweed Dryer Operating in Manual ... (Setiyono)

Volume 12, Issue 2, October 2025, pp. 140-150 ISSN 2355-5068 ; e-ISSN 2622-4852

**DOI:** 10.33019/jurnalecotipe.v12i2.4560

Table 3 shows that the LDR sensor is very sensitive to detecting light. If there is a little light, the LDR sensor immediately detects it and the motor immediately moves to open the roof. Likewise, when it is dark, it takes a really dark situation to make the light sensor detect it and make the motor move to close the roof. The responsive time of the LDR sensor has an average time of 1 second, where the LDR sensor detects the motor's light immediately moving without a long delay. In the telegram notification, in the dark and the rain sensor is dry, the notification says "Dark Weather / Night - close the roof, turn on the fan and LED" so the roof is closed due to lack of light or darkness. When it detects light and the rain sensor is dry, the notification says "Sunlight detected - open roof, turn off fan and LED".

#### 2. Rain Water Sensor Testing

In the Rain sensor test, the sensor will only be observed when it is wet and dry. This test was carried out with the aim of determining the sensitivity of the rain sensor. In this seaweed dryer, a rain sensor is used as input to run the tool automatically. Where the rain sensor will detect water that is hit by the detector board on the rain sensor. The experiment was carried out by giving water to the sensor and drying it, then for each experiment you will also see the notification that appears on the Telegram application and also the response from the rain sensor detecting water until finally the roof runs.

Testing	Sensor State	Time Respon Sensor (s)	Roof State	Telegram Notification
1	Wet	0.46	Closed	The weather is raining – close the roof, turn off the fan and LED
2	Dry	0,47	Opened	Sunlight detected – open the roof, turn off the fan and LED
3	Wet	0,47	Closed	It was raining – closed the roof, turned off fan and LED
4	Dry	0,47	Opened	Sunlight detected – open the roof, turn off the fan and LED

Table 4. Rain sensor test results

Table 4 is the result of experiments carried out on the rain sensor. It can be said that the rain sensor has high sensitivity, the sensor can quickly read when the sensor is exposed to water and is also dry. Even though it's only a little water, the rain sensor immediately detects it quickly and the motor moves to close the roof. Likewise, when the sensor is dry, the motor immediately moves to open the roof. The rain sensor has an average detection speed of 1.87 seconds. In the rain sensor notification, when the rain sensor detects water, the text in the notification is "The weather is raining - close the roof, turn off the fan and LED" whereas when the rain sensor is dry, the notification that looks the same as the notification when the light sensor detects it is "Sunlight detected - open the roof, turn off the fan and LED".

#### 3. Roof Door Open and Close Testing

In this roof test, you will observe how long the roof takes to open or close in automatic or manual conditions. You will calculate with a stopwatch how long it takes for the roof to move, with different equipment conditions.

Testing	Operation Mode	Tools State	Roof State	Time (s)
1	Automatic	Dark	Closed	4.15
2	Automatic	A litle Light	Opened	4.18
3	Automatic	Bright	Opened	4.20
4	Automatic	Rain	Closed	4.17
5	Manual	Closed Roof	Closed	4.18
6	Manual	Opened Roof	Opened	4.20

Table 5. Roof door open and close test results

Volume 12, Issue 2, October 2025, pp. 140-150 ISSN 2355-5068; e-ISSN 2622-4852

**DOI:** 10.33019/jurnalecotipe.v12i2.4560

Table 5 with different conditions and with different methods for the roof to move to open and close, the roof takes about 4 minutes to open and close with the valve. To be precise, the average time to open or close the roof is 4 minutes 18 seconds.

#### 4. Testing Responsiveness in the Bot Menu on Telegram

In testing the bot menu on Telegram, only one of the menus was tried several times to compare the response time of the Telegram bot. This test is carried out in the "/status" menu, which is a menu to see the status of the roof condition, where the test will be carried out for 10 trials by opening and closing the roof as well as changing the methods used. This menu/status is very important to see the condition of the roof at that time, therefore the experiments were carried out alternately by opening and closing the roof. After opening the roof then pressing the /status menu and after closing the roof pressing the /status menu, this experiment was also carried out by changing the method used on this tool.

Testing	Telegram Menu	Respon Time (s)	Telegram Menu Reply
1	/state	3	Open Roof Condition Mode: Automatic
2	/state	3	Closed Roof Condition Mode: Automatic
3	/state	3	Closed Roof Condition Mode: Automatic
4	/state	5	Open Roof Condition Mode: Automatic
5	/state	4	Closed Roof Condition Mode: Manual
6	/state	4	Closed Roof Condition Mode: Manual
7	/state	5	Opened Roof Condition Mode: Manual
8	/state	4	Closed Roof Condition Mode: Otomatic
9	/state	4	Closed Roof Condition Mode: Automatic
10	/state	3	Open Roof Condition Mode: Automatic

Table 6. Bot menu test results on Telegram

Table 6 explains the response time after clicking the /status menu, namely 3.4 seconds. This experiment was carried out by alternating with other menus to see whether the response time in this menu/status was faster or slower. To use the menu on Telegram or notifications usually also depends on the data network or WiFi signal at that time. The response time for the Telegram menu can be long because the data network or WiFi is slow and the response time for the Telegram menu can also be very fast because the data network or WiFi is also fast.

#### 4. CONCLUSION

After designing, testing and data observations were carried out on the seaweed dryer using manual and automatic methods using the Nodemcu ESP826 based telegram application. This tool consists of a rain sensor and LDR sensor, Nodemcu ESP826, limit switch, motor driver, DC motor, relay, DC fan and LED. This tool has a way of working that starts with a rain sensor that detects water or an LDR sensor that detects light. Then the input is processed on the nodeMCU and sends a program to the motor driver then moves the DC motor to open or close the roof until the roof presses the limit switch and the fan and LED turn on or off. This seaweed dryer can dry seaweed in rainy or hot conditions, day or night. The seaweed dryer can operate automatically with an LDR sensor and rain sensor as the main input and this seaweed dryer can also operate manually using the Telegram application as the input. Then when the roof opens and closes it also successfully displays a notification on the Telegram application, then also a notification when the roof has successfully opened and closed. From the results of data observations, it is known that the LDR sensor works with an average time of 1 second to process from the sensor detecting light until the roof moves, as well as the rain sensor which takes an average of 1.87 seconds to detect water until the roof moves. The process of opening and closing the roof takes an average of 4 minutes 18 seconds to open and close completely. Then the Telegram menu also has an average responsiveness of 3.4 seconds. This prototype is very suitable to be realized into a real tool to help seaweed farmers in processing their harvest, where the benefits of grass packaged in dry form include making it last longer, being practical for consumption, maintaining nutritional content, being a



Volume 12, Issue 2, October 2025, pp. 140-150 ISSN 2355-5068; e-ISSN 2622-4852 **DOI:** 10.33019/jurnalecotipe.v12i2.4560

natural and sustainable product, and being able to be processed into other forms, such as cosmetic products or animal feed.

#### Acknowledgments

We would like to express our deepest gratitude to the Chancellor of Gunadarma University for her moral and material support so that this research can be successful and this prototype can easily be implemented in the future as a real tool to help seaweed farmers.

#### REFERENCES

- [1] W. Rizkaprilisa *et al.*, "3 (2) Science, Technology and Management Journal PEMANFAATAN RUMPUT LAUT SEBAGAI PANGAN FUNGSIONAL: SYSTEMATIC REVIEW Info Artikel," *Sci. Technol. Manag. J.*, vol. 3, no. 182, pp. 28–33, 2023, doi: http://dx.doi.org/10.26623/jtphp.v13i1.1845.kodeartike.
- [2] A. Hidayat and P. Safitri, "SEAWEED' S GLOBAL VALUE CHAIN AND," *jesp* | *J. Ekon. Stud. Pembang. Artic.*, vol. 20, no. 1, pp. 49–62, 2019, doi: 10.18196/jesp.20.1.5013.
- [3] Yasin, "Pengolahan Rumput Laut (Eucheuma Cottoni) Menjadi Dawet Rumput Laut," *SINAU J. Ilmu Pendidik. dan Hum.*, vol. 7, no. 1, pp. 27–36, 2020, doi: 10.37842/sinau.v7i1.22.
- [4] N. Maghfuroh, "Potensi Bubuk Rumput Laut (Eucheuma cottonii) Sebagai Body Lotion Anti Radikal Bebas Sinar Ultra Violet," *J. Mar. Res.*, vol. 13, no. 4, pp. 753–764, 2024, doi: 10.14710/jmr.v13i4.44343.
- [5] N. Sari, B. Bakhtiar, and N. Azmin, "Pemanfaatan Rumput Laut (Eucheuma cottonii) Sebagai Bahan Dasar Masker Wajah Alami," *JUSTER J. Sains dan Terap.*, vol. 1, no. 1, pp. 28–35, 2022, doi: 10.55784/juster.vol1.iss1.15.
- [6] T. H. Perikanan et al., "PEMANFAATAN RUMPUT LAUT Caulerpa racemosa SEBAGAI BAHAN BAKU MASKER WASH-OFF DENGAN PENAMBAHAN PEPTIDA SIPUT GONGGONG Utilization Seaweed Caulerpa racemosa as Wash-Off Mask Raw Material with Addition of Gonggong Snail Peptides," J. Pengolah. Has. Perikan. Indones., vol. 27, pp. 917–931, 2024, doi: https://doi.org/10.17844/jphpi.v27i10.45866.
- [7] P. Agustina, D. P. Valentina, I. Kurniawati, S. Mudrikah, and T. Amelia, "Potensi Bahan Alam Bawah Laut Sebagai Obat Alami untuk Pengobatan Diabetes," *J. Pharm. Tiara Bunda*, vol. 2, pp. 1–5, 2024, doi: https://doi.org/xx.xxxxx/jptb.v1i1.1.
- [8] E. Science, "The development of Indonesian seaweed based on innovation cluster model The development of Indonesian seaweed based on innovation cluster model," *IOP Conf. Ser. Earth Environ. Sci.*, vol. 763, pp. 1–8, 2020, doi: 10.1088/1755-1315/763/1/012016.
- [9] H. Phang, C. Chu, S. Kumaresan, M. Rahman, and S. Yasir, "PRELIMINARY STUDY OF SEAWEED DRYING UNDER A SHADE AND IN A International Journal of Science and Engineering (IJSE) Preliminary Study of Seaweed Drying under A Shade and in A Natural Draft Solar Dryer," *Int. J. Sci. Eng.*, vol. 8, no. April 2015, pp. 10–14, 2014, doi: 10.12777/ijse.8.1.10-14.
- [10] W. Agustiono, F. M. Wahyu, and W. Findiastuti, "An internet of things-based solar dryer: A conceptual design for seaweed cultivation in Madura," vol. 01032, pp. 1–7, 2024.
- [11] A. A. Rismayadi, A. Sobri, F. Khoirunnisa, and A. Dedy, "Perancangan Alat Monitoring Ketinggian Air Bak Berbasis IoT Menggunakan Mikrokontroler Node MCU ESP8266," *Jl. Antapani, Jl. Terusan Sekol.*, vol. 7, no. 4, p. 7100124, 2024.
- [12] E. Kasmi, "A patient' s temperature remote control system based on NODEMCU ESP8266," *E3S Web Conf.*, 01053 ICCSRE, vol. 01053, no. 297, pp. 1–6, 2021, doi: 10.1051/e3sconf/202129701053.
- [13] T. Sutikno, H. S. Purnama, A. Pamungkas, and A. Fadlil, "Internet of things-based photovoltaics parameter monitoring system using NodeMCU ESP8266," *Int. J. Electr. Comput. Eng.*, vol. 11, no. 6, pp. 5578–5587, 2021, doi: 10.11591/ijece.v11i6.pp5578-5587.
- [14] A. Rathee, Y. Ahuja, K. K. Singh, A. Chand, and Y. Diwan, "IOT BASED HOME AUTOMATION



Volume 12, Issue 2, October 2025, pp. 140-150 ISSN 2355-5068; e-ISSN 2622-4852 **DOI:** 10.33019/jurnalecotipe.v12i2.4560

- SYSTEM USING ESP8266 BASED MODULE," *Int. Res. J. Mod. Eng. Technol. Sci.* (, vol. 7, no. 01, pp. 3178–3184, 2025, doi: /10.56726/IRJMETS66481.
- [15] E. Science, "Seaweed Drying Process Using Tray Dryer with Dehumidified Air System to Increase Efficiency of Energy and Quality Product Seaweed Drying Process Using Tray Dryer with Dehumidified Air System to Increase Efficiency of Energy and Quality Product," *IOP Conf. Ser. Earth Environ. Sci.*, pp. 1–7, 2019, doi: 10.1088/1755-1315/292/1/012070.
- [16] H. C. I. Che, "Seaweed drying characterization via serial statistical criteria analysis Seaweed drying characterization via serial statistical criteria analysis," *IOP Conf. Ser. Mater. Sci. Eng.*, pp. 1–10, 2021, doi: 10.1088/1757-899X/1109/1/012051.
- [17] A. Info, "DEVELOPMENT OF A SEAWEED DRYER USING ARDUINO UNO EQUIPPED WITH AN OLED," *J. Electr. Eng. Informatics e-ISSN 3025-213X*, vol. 2, no. 1, pp. 1–11, 2024, doi: 10.59562/jeeni.v2i1.4538.
- [18] W. T. Handoyo, B. B. Sedayu, S. K. Wirawan, and A. R. Hakim, "Kandungan Limbah Pengolahan Rumput Laut Dan Potensi Pemanfaatannya (Review)," *J. Trunojoyo*, vol. 5, no. 2, pp. 183–195, 2024.
- [19] I. Sulistiyowati and M. I. Muhyiddin, "Disinfectant Spraying Robot to Prevent the Transmission of the Covid-19 Virus Based on the Internet of Things (IoT)," *J. Electr. Technol. UMY*, vol. 5, no. 2, pp. 61–67, 2021, doi: 10.18196/jet.v5i2.12363.
- [20] C. U. Nkanu, J. E. Imoke, and A. E. Bisong, "Integrating Telegram Messenger Application for Effective Instructional Content Delivery in Post COVID-19 Era," *SIASAT J. Soc. Cult. Polit. Stud.*, vol. 8, no. 2, pp. 103–110, 2022, doi: 10.33258/siasat.v8i2.150 103.



Volume 12, Issue 2, October 2025, pp. 151-158 ISSN 2355-5068; e-ISSN 2622-4852

**DOI:** 10.33019/jurnalecotipe.v12i2.4561

## Comparative Study of Sentiment Analysis for Interpreting the **Customer Interest in Women Fashion Clothes**

Eka Legya Frannita<sup>1</sup>, Alifia Revan Prananda<sup>2</sup>, Marwanto<sup>3</sup>
<sup>1</sup>Departement of Leather Product Processing Technology, Politeknik ATK Yogyakarta, Indonesia
<sup>2</sup>Departement of Information Technology, Faculty of Engineering, Universitas Tidar, Magelang, Indonesia <sup>3</sup>Departement of Dance Education, Faculty of Language and Arts, Universitas Negeri Yogyakarta, Yogayakrta, Indonesia

#### ARTICLE INFO

#### Article historys:

Received: 28/04/2025 Revised: 04/06/2025 Accepted: 30/10/2025

#### **Keywords:**

Comparative Study; Customer Review; E-Commerce; Machine Learning; Sentiment Analysis

#### ABSTRACT

Public sentiment is widely recognized as a key factor influencing fluctuations in stock prices, product sales, and emerging trends. Since the user interest analysis played an essential role in representing the trend of the market and it is also extremely useful for generating the strategy and decision of trading, analyzing the public sentiment is quite important. In the contemporary era, virtual space has been perpetually evolving and used in plenteous applications including analyzing customer interest. This research work aimed to conduct comparative study in analyzing customer interest about women fashion clothes using sentiment analysis methodbased machine learning approach. The proposed study was initiated by conducting data acquisition process. It was then continued with labelling and predicting the user sentiment by comparing eleven machine learning approaches. According to comparison result, Naïve Bayes successfully obtained the best performance with accuracy of 94%, precision of 87%, recall of 82%, f1-score of 84%. It can be inferred that Naïve Bayes was viable approach for predicting the user sentiment.



This work is licensed under a Creative Commons Attribution 4.0 International License

#### **Corresponding Author:**

Eka Legya Frannita

Department of Leather Product Processing Technology, Politeknik ATK Yogyakarta, Yogyakarta, Indonesia

Email: eka.legya@atk.ac.id

#### INTRODUCTION

The contemporary era has introduced how almost all human activities have been occurred in the virtual space [1]. In the current decade, it has been proven that online services, such as online discussion, e-commerce, e-learning, social media, etc., have become an effective way for almost all purposes [2–4]. It has accelerated significantly due to the frequent entrance of information that has giving effect to the development of innovation technology [5]. Thanks to the rapid growth of technology as a fresh wave of digitalization that has been fundamentally assisted human work and inspired to develop the improved technologies or even multifunction of technologies that offer wide range of uses [6].

E-commerce is one of the online services offering several facilities for encouraging and supporting customer needs [5]. In the last two years, the pace of e-commerce transaction has increased tremendously due to a high user population during the COVID-19 pandemic. In that situation, ecommerce has successfully assisted the customers for providing all needs such as foods, clothes, shoes, medicines, or other daily needs. It was then giving impact to the increasing of company profit [7].



Regardless that the e-commerce traffic was significantly increased in the last two years, a company who has employee the e-commerce still needs to analyse how does the market trend. It was needed to support the selling process [7]. In the new era, company also can use e-commerce to analysis the customers perspective about their products by using sentiment analysis. It was performed by analysing the customers opinion or review in market place or social media which was significantly useful for their selling process [8]. Sentiment analysis not only can give the companies customers perspective, but it also can give the companies some advises regarding to the customer needs or even somethings that make them feel satisfy or disappointed. This advice was extremely useful to create the selling strategies. Sentiment analysis results also can be used as a database for creating a prediction about what the future market trends [9–12].

Sentiment analysis offers several benefits across various domains due to its ability to analyse and interpret the emotional tone and opinions expressed in text. Businesses can utilize customers sentiment for analysing customer responses, comments, and feedback. By understanding customer sentiments, companies can recognize areas needing enhancement, respond to customer feedback, and elevate overall service quality. Sentiment analysis helps companies monitor and manage their brand reputation online. By analysing social media mentions, reviews, and news articles, organizations can gain insights into how their brand is perceived and take corrective actions if needed. Understanding customer sentiments about products or services can guide product development and service improvements. Positive sentiments can be reinforced, and negative sentiments can be addressed to enhance the overall quality and satisfaction levels. Sentiment analysis is valuable in market research to gain public response about new products, advertising campaigns, or industry trends. This information aids companies in making informed business decisions and staying competitive in the market. Sentiment analysis is widely used for monitoring social media platforms to understand public opinions, trends, and discussions. This is crucial for social media managers, public relations teams, and marketing professionals to engage with the audience effectively [10]. In the financial industry, sentiment analysis is used to analyse news articles, financial reports, and social media discussions related to stocks and investments. This information can help investors make more informed decisions by considering market sentiment. Sentiment analysis can be integrated into customer support systems to automatically categorize and prioritize customer queries based on sentiment. This enables companies to provide timely and appropriate responses, enhancing customer support and engagement. Sentiment analysis is applied to analyse public opinions and sentiments regarding political candidates, parties, or policies. This can be useful for political campaigns and strategists to understand the public mood and tailor their messaging accordingly. In the healthcare industry, sentiment analysis can be applied to patient feedback, reviews of healthcare providers, and discussions on social media. This information can be valuable for improving healthcare services and patient experiences. Sentiment analysis can be used internally to analyse employee feedback, surveys, and sentiments expressed in communication channels. This information can be instrumental in improving workplace satisfaction and addressing employee concerns. Overall, sentiment analysis provides actionable insights by automating the analysis of vast amounts of text data, allowing organizations to make data-driven decisions, enhance user experiences, and respond effectively to changing sentiments in various contexts [13].

Sentiment analysis can be classified into different types based on the scope of analysis, the nature of sentiment, and the desired outcomes. Binary sentiment analysis aimed to determine whether the sentiment expressed in the text is positive or negative. Binary sentiment analysis is commonly used for applications where a simple positive/negative classification is sufficient, such as product reviews or social media sentiment. Multi-class sentiment analysis classified sentiment into multiple classes, such as positive, negative, neutral, and sometimes more fine-grained categories. It useful in scenarios where a more nuanced understanding of sentiment is required, such as customer feedback analysis with multiple sentiment categories. Aspect-based sentiment analysis analysed sentiment at a more granular level by identifying sentiments associated with specific aspects or features mentioned in the text. It was valuable for product reviews, where sentiment is analysed not only at an overall level but also for specific product features or aspects. Fine-grained sentiment analysis provided a more detailed sentiment analysis by categorizing sentiments into multiple fine-grained categories, such as very positive, neutral, negative, very negative. It was useful when a more nuanced understanding of sentiment intensity

is required, allowing for a more detailed analysis of the sentiment expressed. Emotion detection goes beyond basic sentiment analysis to identify specific emotions conveyed in the text, such as joy, anger, sadness, or surprise. It was applied in scenarios where understanding the emotional tone of the text is crucial, such as social media monitoring for brand sentiment during a marketing campaign. Intent analysis determined the intent behind a piece of text, such as whether it expresses a desire, request, complaint, or appreciation. It was helpful in understanding the underlying intentions of users, which can be valuable for customer support and interaction with chatbots. Temporal sentiment analysis analysed the changes in sentiment over time, tracking how sentiments evolve or fluctuate. It was useful for monitoring public opinion during events, product launches, or marketing campaigns to understand the impact over time. Cross-domain sentiment analysis involved training sentiment analysis models on data from one domain and applying them to another domain. It was enabled sentiment analysis models to adapt to different industries or domains, even when labelled data for the specific domain is limited. Domain-Specific Sentiment Analysis focused on sentiment analysis within a specific industry or domain, considering domain-specific language and context. It customized sentiment analysis models for industries like healthcare, finance, or technology where language and sentiments may be unique [14].

Generally, the sentiment analysis process can be conducted using two famous methods which were lexicon approach and supervised learning based. Both of them had almost similar procedure to analyse the customer perspective. However, in the lexicon approach we have to provide the emotional words expressing the customers satisfaction about the products or the services which was difficult enough if we used the unstructured data like review or social media data. On the other hand, supervised learning approach worked by learning the customers expression and grouped the data that have similar meaning to analyse and interpret them. Hence, for the advanced analysis, supervised learning approach is more effective than lexicon approach [5].

This research work aims to develop sentiment analysis method for interpreting the women interest in fashion clothes. Customers opinion and reviews completed with rating score were employed and analysed to produce the customers sentiments. The analysis process had occurred by performing the following contributions.

- 1. Conducting comparison study of several classifier for interpreting the women interest in fashion clothes through their opinion, review or even the customer rate in the e-commerce.
- 2. Generating the rank of customers' interest in fashion clothes by considering the customers impression through their opinion, review or even the customer rate which was important for the companies to create a suitable selling strategy.

The rest of this article was structured as follow: section 2 defines the previous related research, section 3 describes about the data, methodology and evaluation method, section 4 illustrates the result and discussion, and section 5 presents the conclusion that was generated regarding to the results.

#### 2. DATA AND RESEARCH METHOD

# 2.1. Brief Information about Dataset

This study used online e-commerce user review proposed by Agarap [15]. The dataset contained of 23,486 customer response completed with 10 features illustrated the data. The ten features were clothing ID, age, title, review text, rating (1 to 5), recommended IND, positive feedback count, division name, department name and class name. Example dataset is illustrated in following table.

**Table 1.** Example of data

No.	Review Text	•••	Class Name
1	I had such high hopes for this dress and	• • •	Dress
2	Love this dress! it's sooo pretty. I happened		Dress
3	I love, love, love this jumpsuit. it's fun, fl		Pants
4	I love tracy reese dresses, but this one is not for		Dress
	the very petite. i am just under 5 feet tall and		
23486	This shirt is very flattering to all due		Blouse

Volume 12, Issue 2, October 2025, pp. 151-158 ISSN 2355-5068 ; e-ISSN 2622-4852

**DOI:** 10.33019/jurnalecotipe.v12i2.4561

## 2.2. Scenario of Experiments

The experiment was started by preparing the dataset. In the beginning process, we conducted data acquisition aimed to remove unnecessary data. As illustrated in Table 1, there are several data that are not valid (illustrated by "Nan"). Those data existed in the title column. Furthermore, several features were not necessary in the analysis process, hence we have to remove those several features. The remained features that were used in the analysis process were review text, rating, class name, and age. Then, we conducted word count process to calculate the number of words in every review and to calculate how many those words were used. Hence, we got the new combination of data with the following features: review text, rating, class name, age and word count.

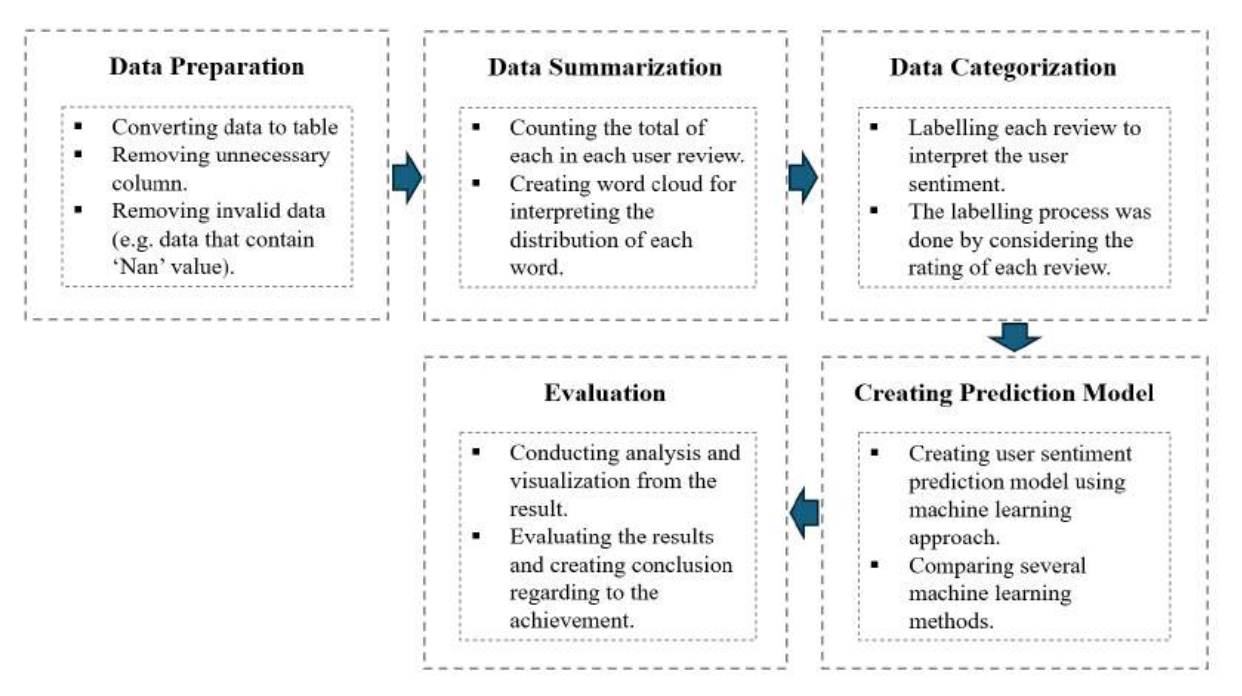


Figure 1. Block diagram of experiment

After preparing the data, we continued the process by labelling each review in three categories (positive, neutral and negative). The review which had 5 or 4 rating were labelled as positive sentiment. Review contained of 3 rating were labelled as neutral sentiment. While, review that contained 1 or 2 rating were labelled as negative sentiment. Then, the process was continued by conducting classification process. In this process, we used eleven classifiers in order to find the best machine learning method for predicting the user sentiment. Overall processes can be seen in the Figure 1.

#### 3. RESULTS AND DISCUSSION

In the first process, we conducted data accusation process to remove some unnecessary features and created the word count to calculate the number of words. The result of this process can be defined in Table 2. In this process, we also calculated the number of each interesting word and created the word cloud to illustrate how the distribution of user interest. The illustration of word cloud and the calculated word are depicted in Figure 2.

Figure 2 illustrates the distribution of total user mention in every product. There are several women fashion clothes mentioned in the user review such as blouse, casual bottom, chemises, dress, jacket, jeans, knit, layering, legwear, outerwear, pant, short, skirt, sleepwear, sweater, swimming wear, and other fashion clothes. This distribution of total user mention in every product was then used to determine the most popular product and to create word cloud in order to visualize how the popularity of each product.

	Table	2.	Result of v	word count	process
--	-------	----	-------------	------------	---------

ID.	Review Text	Rating	Class Name
1	I had such high hopes for this	3	{'and': 3, 'be': 1, 'bottom':
	dress		1, 'but': 2, 'ch
2	Love this dress! it's sooo pretty. I	5	{'am': 1, 'and': 2, 'bc': 2,
	happened		'be': 1, 'below':
3	I love, love, love this jumpsuit. it's	5	{'and': 1, 'but': 1,
	fun, fl		'compliments': 1, 'every'
23486	This shirt is very flattering to all	5	{'adjustable': 1, 'all': 1,
	due		'and': 1, 'any': 1

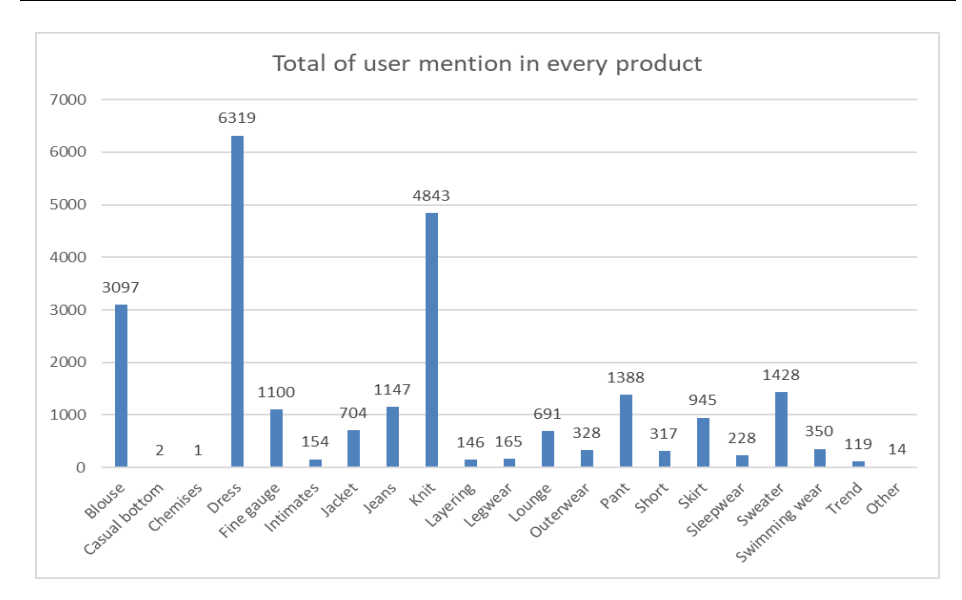


Figure 2. Distribution of user mention in each women fashion clothes

In this step, we not only counted the total of user mention in every product, but we also counted the total of each term that illustrated the satisfaction of the customers. The example words were 'love'. 'pretty', 'great', 'super', 'happy', 'disappointed', etc. This process was used to evaluate the satisfaction of the customer. Result of this step is depicted in Figure 3(a). This figure illustrates the top mentioned words which illustrates how was the user satisfaction about each product.



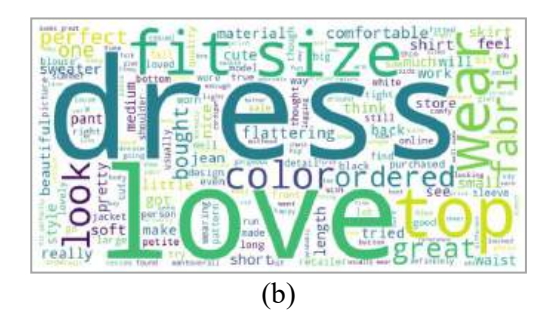


Figure 3. Data acquisition results: (a) the number of each word and (b) word cloud

Result in Table 3 illustrates how every word in every user review was counted. This process was conducted to analyze the most interesting women fashion clothes and how did the satisfaction of each user. After conducting word counting in each user review. We evaluated the counted result as depicted in Figure 3. In the Figure 3(a), we can analyze the most popular women fashion clothes and how did their opinion about the products. According to Figure 3(a), we found that there are five the most type of

Volume 12, Issue 2, October 2025, pp. 151-158 ISSN 2355-5068; e-ISSN 2622-4852

**DOI:** 10.33019/jurnalecotipe.v12i2.4561

women fashion clothes which are dresses, knits, blouses, sweaters, and pants. Dresses became the most mentioned women fashion clothes with the total mention of this type of clothes of 6319 mentions. Knits wear was in the second position with the total mention of 4843 mentions. Blouses was in the third position with the total mention of 3097 mentions. Sweaters was in the fourth position with the total mention of 1428 mentions. The last type of clothes, pants, was in the fifth position with the total mention of 1388 mentions. Figure 3(a) also illustrates the total of each word mentioned in the user review. In this process, we found five the most words that have been mentioned in the user review. The term 'love' became the most mentioned word that was mentioning by the user with the total mention of 8951 words. The term 'great' was in the second position with the mention of 6117 words. The term 'super' was in the third position with the mention of 1726 words. The term 'happy' was in the fourth position with the mention of 705 words. The term 'glad' was in the fifth position with the mention of 614 words. According to Figure 3(a) we can concluded that the users were satisfy about almost all product that were reviewed. It was indicated by the word counting result which the five most mentioned word were referred to the positive review. Based on the Figure 3(a) we also can concluded that most loved women fashion clothes were dresses. It was indicated by the total mention in the review data in which the term 'dress' was mentioned more than 6000 times. In the second position, there was knit wear that became the most mentioned clothes type after dresses. In the third position, there was blouses followed by sweaters and pants.

Figure 3(b) illustrates the word cloud as the visualization of results in Figure 3(a). Word cloud was used to illustrate the distribution of total mention of each word. For example, in the term of 'dress', in Figure 3(b) the term of 'dress' becomes the biggest word compared with other which means that the term 'dress' obtained the most mentioned word. Finally, according to Figure 3(a) and 3(b), we can summarize that the most interesting women fashion clothes based on the customer review is dress wear.

In the next process, we labelled the data into three categories which were positive, neutral and negative. Then, we predicted the user sentiment in several classifier. In this study, we performed 11 classifiers. This process was used to predict how are the customer sentiment regarding to their review. By classifying each customer review in three categories (positive, neutral and negative) we can understand what the customer perspective to the product. According to labelled process, we found that 18,208 review indicated positive sentiment, 2,871 reviews indicated neutral sentiment, and 2,407 reviews indicated negative sentiment. Those data were then trained to create prediction model. The following table illustrates the comparison result of all classifier.

Method	Accuracy	Precision	Recall	F1-score
Logistic regression	94%	87%	81%	83%
Naïve Bayes	94%	87%	82%	84%
SVM	93%	88%	72%	77%
Neural Network	93%	85%	80%	82%
Stochastic Gradient Descent	92%	79%	80%	79%
K-Nearest Neighbors	89%	81%	51%	49%
Decision Tree	90%	76%	62%	66%
Random Forest	90%	76%	61%	64%
SVM (Linear Kernel)	94%	88%	78%	81%
SVM (Polynomial Kernel)	89%	44%	50%	47%
SVM (RBF Kernel)	89%	44%	50%	47%

Table 3. Result of word count process

Table 3 illustrates the comparison results between eleven classifiers in predicting the user sentiment. According to Table 2, Naïve Bayes achieved the best performance with accuracy of 94%, precision of 87%, recall of 82%, f1-score of 84%. Hence, it can be concluded that Naïve Bayes was suitable for classifying customer review in three classes which are positive sentiment, neutral sentiment and negative sentiment. This result indicated that Naïve Bayes was significant for interpreting and predicting the user interest in the cases of women fashion clothes reviews.

## 4. CONCLUSION

This research work aimed to conduct comparison study in development of sentiment analysis method-based machine learning approach which was performed in the online user review of women fashion clothes. The proposed study was started by conducting data acquisition process. It was then continued with labelling and predicting the user sentiment by comparing eleven machine learning approach. According to comparison result, Naïve Bayes successfully obtained the best performance with accuracy of 94%, precision of 87%, recall of 82%, f1-score of 84%. It can be inferred that Naïve Bayes was viable approach for predicting the user sentiment.

#### REFERENCES

- [1] J. An and W. M. N. Wan Zainon, "Integrating color cues to improve multimodal sentiment analysis in social media," *Eng. Appl. Artif. Intell.*, vol. 126, p. 106874, 2023, doi: https://doi.org/10.1016/j.engappai.2023.106874.
- [2] H. Wang and M. Hou, "Quantum-like implicit sentiment analysis with sememes knowledge," *Expert Syst. Appl.*, vol. 232, p. 120720, 2023, doi: https://doi.org/10.1016/j.eswa.2023.120720.
- [3] P. Hajek, L. Hikkerova, and J.-M. Sahut, "Fake review detection in e-Commerce platforms using aspect-based sentiment analysis," *J. Bus. Res.*, vol. 167, p. 114143, 2023, doi: https://doi.org/10.1016/j.jbusres.2023.114143.
- [4] P. Savci and B. Das, "Prediction of the customers' interests using sentiment analysis in ecommerce data for comparison of Arabic, English, and Turkish languages," *J. King Saud Univ. Comput. Inf. Sci.*, vol. 35, no. 3, pp. 227–237, 2023, doi: https://doi.org/10.1016/j.jksuci.2023.02.017.
- [5] M. Demircan, A. Seller, F. Abut, and M. F. Akay, "Developing Turkish sentiment analysis models using machine learning and e-commerce data," *Int. J. Cogn. Comput. Eng.*, vol. 2, pp. 202–207, 2021, doi: https://doi.org/10.1016/j.ijcce.2021.11.003.
- [6] J. Wang and J.-J. Lee, "Predicting and analyzing technology convergence for exploring technological opportunities in the smart health industry," *Comput. Ind. Eng.*, vol. 182, p. 109352, 2023, doi: https://doi.org/10.1016/j.cie.2023.109352.
- [7] R. K. Das, M. Islam, M. M. Hasan, S. Razia, M. Hassan, and S. A. Khushbu, "Sentiment analysis in multilingual context: Comparative analysis of machine learning and hybrid deep learning models," *Heliyon*, vol. 9, no. 9, p. e20281, 2023, doi: https://doi.org/10.1016/j.heliyon.2023.e20281.
- [8] R. V Karthik and S. Ganapathy, "A fuzzy recommendation system for predicting the customers interests using sentiment analysis and ontology in e-commerce," *Appl. Soft Comput.*, vol. 108, p. 107396, 2021, doi: https://doi.org/10.1016/j.asoc.2021.107396.
- [9] F. Xu, Z. Pan, and R. Xia, "E-commerce product review sentiment classification based on a naïve Bayes continuous learning framework," *Inf. Process. Manag.*, vol. 57, no. 5, p. 102221, 2020, doi: https://doi.org/10.1016/j.ipm.2020.102221.
- [10] P. Atandoh, F. Zhang, D. Adu-Gyamfi, P. H. Atandoh, and R. E. Nuhoho, "Integrated deep learning paradigm for document-based sentiment analysis," *J. King Saud Univ. Comput. Inf. Sci.*, vol. 35, no. 7, p. 101578, 2023, doi: https://doi.org/10.1016/j.jksuci.2023.101578.
- [11] M. Nakayama and Y. Wan, "The cultural impact on social commerce: A sentiment analysis on Yelp ethnic restaurant reviews," *Inf. Manag.*, vol. 56, no. 2, pp. 271–279, 2019, doi: https://doi.org/10.1016/j.im.2018.09.004.
- [12] N. Ramshankar and J. P. P.M., "Automated sentimental analysis using heuristic-based CNN-BiLSTM for E-commerce dataset," *Data Knowl. Eng.*, vol. 146, p. 102194, 2023, doi: https://doi.org/10.1016/j.datak.2023.102194.



- [13] P. Kathuria, P. Sethi, and R. Negi, "Sentiment analysis on E-commerce reviews and ratings using ML & NLP models to understand consumer behavior," in 2022 International Conference on Recent Trends in Microelectronics, Automation, Computing and Communications Systems (ICMACC), 2022, pp. 1–5. doi: 10.1109/ICMACC54824.2022.10093674.
- [14] S. S. Sohail, J. Siddiqui, and R. Ali, "Feature extraction and analysis of online reviews for the recommendation of books using opinion mining technique," *Perspect. Sci.*, vol. 8, pp. 754–756, 2016, doi: https://doi.org/10.1016/j.pisc.2016.06.079.
- [15] A. F. Agarap, "Women's E-Commerce Clothing Reviews," *Kaggle Dataset*, 2017. https://www.kaggle.com/datasets/nicapotato/womens-ecommerce-clothing-reviews



# Design and Contruction of a Website for Garbage Sales in Sirau Village Using the Extreme Programming Method (Case Study of KSM Kudu Bisa)

Tegar Setio<sup>1</sup>, Yohani Setiya Rafika Nur<sup>2</sup>, Hari Widi Utomo<sup>3</sup>

1.2.3 Informatic Engineering Study Program, Telkom University, Purwokerto, Indonesia

#### ARTICLE INFO

#### **Article historys:**

Received :12/02/2025 Revised :14/07/2025 Accepted :30/10/2025

#### **Keywords:**

Garbage Sales Website; Extreme Programming; Black box; User Experience Questionnaire

#### **ABSTRACT**

Waste management remains a critical issue in Indonesia, including in Banyumas Regency, where increasing volumes are driven by population growth, urbanization, and low public awareness in waste sorting. In Sirau Village, the KSM KuduBisa waste management group faces various operational challenges, including the absence of real-time waste data, manual transaction records, and high operational costs. This study aims to design and develop a digital waste sales platform using the Extreme Programming (XP) method, chosen for its adaptability and emphasis on continuous testing. The system was built using the full-stack Next.js framework, allowing integrated front-end and back-end development, and was evaluated through Blackbox Testing and the User Experience Questionnaire (UEQ). The results showed a functional success rate of 98.96% and excellent usability scores across all UEQ dimensions. The novelty of this research lies in the integration of digital waste transaction features with educational content within a role-based, modern web architecture—an approach that not only enhances operational efficiency but also promotes public awareness and engagement in sustainable waste practices.



This work is licensed under a Creative Commons Attribution 4.0 International License

# Corresponding Author:

Yohani Setiya Rafika Nur Informatic Engineering Study Program, Telkom University, Purwokerto Campus Jl. DI Panjaitan No.128, Purwokerto 53147, Central Java, Indonesia Email: yohanin@telkomuniversity.ac.id

#### 1. INTRODUCTION

Waste management is a significant global challenge, especially in developing countries, including Indonesia. Population growth, urbanization, and lifestyle changes have drastically increased the volume of waste [1]. In Indonesia, the waste management system still faces various obstacles, such as inadequate infrastructure, lack of public awareness, and limited technology [2].

At the local level, Sirau Village, Kemranjen District, Banyumas Regency, faces specific problems in waste management. The KuduBisa Community Empowerment Group (KSM) experiences operational difficulties, including high costs for waste collection and sorting, manual transaction recording, and lack of real-time data on waste collection points. This results in low operational efficiency and the risk of data loss [3].

To overcome these problems, digital solutions are needed that can increase efficiency and transparency in waste management [4]. The application of technologies such as the Internet of Things (IoT) and Artificial Intelligence (AI) have proven effective in optimizing waste collection and

Volume 12, Issue 2, October 2025, pp. 159-168 ISSN 2355-5068; e-ISSN 2622-4852

**DOI:** 10.33019/jurnalecotipe.v12i2.4549

processing systems in various countries [5]. In Indonesia, studies on the circular economy show that digitalization plays an important role in increasing management efficiency and strengthening community involvement [6]. In addition, the digital approach is also able to encourage changes in community behavior towards more responsible waste management [7].

The Extreme Programming (XP) methodology was chosen in the development of this system because of its ability to adapt to changing user needs and focus on continuous testing [8]. XP has been widely used in web application development because of its emphasis on continuous interaction between developers and users [9].

Based on this background, this study aims to design and develop a web-based waste management and sales system that is tailored to the needs of KSM KuduBisa in Sirau Village. This system will be built using the Next.js full-stack framework and evaluated through Blackbox Testing and User Experience Questionnaire (UEQ) to assess efficiency, effectiveness, and user satisfaction. It is hoped that the implementation of this system can optimize waste management and increase public awareness of sustainable waste management practices.

#### 2. RESEARCH METHOD

The development process of the waste sales website in Sirau Village follows the Extreme Programming (XP) methodology, which emphasizes continuous feedback, iterative development, and direct user involvement. The research framework consists of several interconnected stages, as illustrated in Figure 1. Each stage is designed to systematically address the research objectives while ensuring that the system is developed effectively and efficiently.

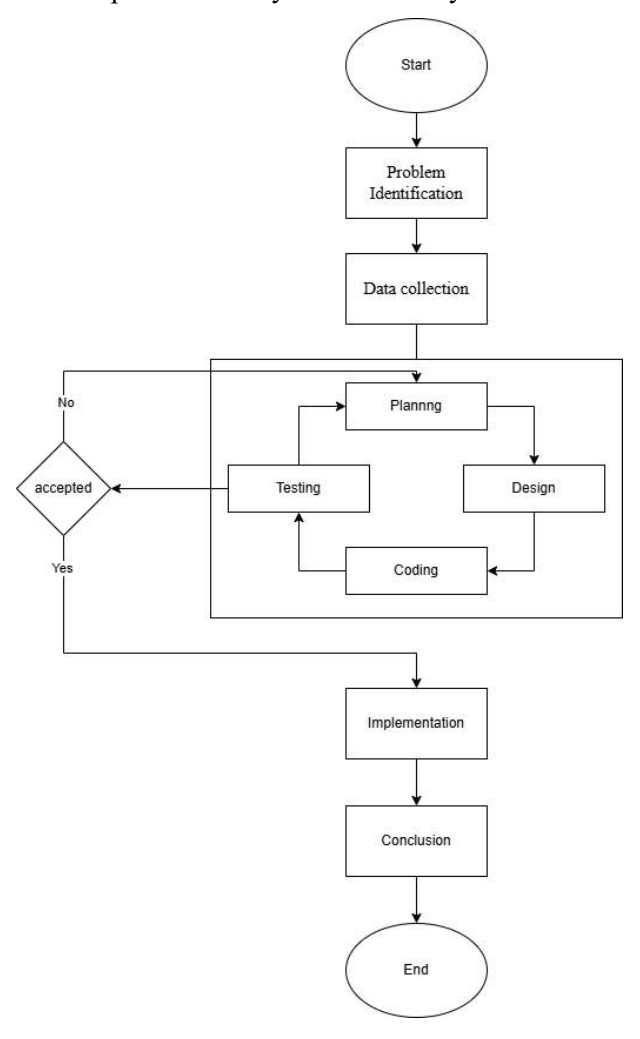


Figure 1. Research flow chart



The following is an explanation of Figure 1, regarding the stages of the research method used, which are explained in each of the following sub-chapters:

#### 2.1. Problem Identification

This initial stage focuses on identifying the core problems faced by KSM KuduBisa in managing waste transactions. Through preliminary observations and stakeholder analysis, the research highlights issues such as manual transaction records, high operational costs, and a lack of access to timely waste collection information.

#### 2.2. Data collection

Data were collected through field surveys, in-depth interviews with KSM KuduBisa staff, and a review of relevant literature. The survey aimed to understand current operational workflows and technological limitations, while interviews captured specific user needs and pain points. Literature reviews helped identify best practices in digital waste management and previous implementations of XP in similar domains.

#### 2.3. Planning

In this phase, user requirements were translated into system goals. Functional and non-functional specifications were defined. Planning also involved setting project milestones, identifying potential risks, and preparing use case scenarios for the next phases. User stories were drafted to align development with actual stakeholder needs.

# 2.4. Design

System design was carried out using UML (Unified Modeling Language), which includes use case diagrams, activity diagrams, and system architecture design. The aim was to visualize how users (public, agents, collectors, and admins) would interact with the system and how system components would communicate internally.

# 2.5. Coding

The development stage implemented the previously designed system using Next.js as a full-stack JavaScript framework, integrating both frontend and backend components. Server-side rendering (SSR) and static site generation (SSG) were used to optimize performance. MySQL was chosen as the database for its robustness and compatibility with Next.js. Features developed included: homepage, educational content, services, about page, login, and registration modules.

# 2.6. Testing

The testing phase aims to evaluate both the functionality and usability of the developed system to ensure it meets the requirements of each user role. Functional testing was conducted using the Blackbox Testing method, which focuses on validating system outputs based on specific inputs without examining the internal structure of the code. This approach allows each feature and module—ranging from community transactions to admin dashboards—to be tested independently and thoroughly. In addition to functional validation, usability testing was carried out using the User Experience Questionnaire (UEQ), which measures various dimensions such as attractiveness, efficiency, dependability, and novelty. Feedback was collected from users representing the community, agents, collectors, and administrators to assess the overall user experience. Only after all evaluation results met the predefined acceptance criteria did the system proceed to the implementation phase.

#### 2.7. Implementation

After successful testing, the system was deployed and implemented at KSM KuduBisa. This involved user training and monitoring to ensure proper system adoption. Feedback was gathered to evaluate real-world usability and suggest future improvements.

## 2.8. Conslusion

This final phase summarizes findings across all research stages and draws conclusions based on system performance and user feedback. It evaluates whether the proposed solution met the original objectives and discusses its potential for future scaling or enhancement.

Volume 12, Issue 2, October 2025, pp. 159-168 ISSN 2355-5068; e-ISSN 2622-4852

**DOI:** 10.33019/jurnalecotipe.v12i2.4549

#### 3. RESULTS AND DISCUSSION

4.

#### 3.1. Planning

In the planning stage, the system is analyzed to identify needs, problems, and determine goals, limitations, and alternative solutions. This analysis is done to understand the system workflow and the activities that will be involved.

In this study, the research variables are defined to guide the development and evaluation of the system. The first variable is \*\*Functional Suitability\*\*, which refers to the system's ability to perform its intended operations accurately and reliably. This variable is assessed using the Blackbox Testing method. The second variable is \*\*User Experience\*\*, which reflects user perceptions of the system in terms of attractiveness, efficiency, perspicuity, dependability, stimulation, and novelty. This variable is measured through the User Experience Questionnaire (UEQ).

These variables were selected because they align with the study's goal to develop a functional, efficient, and user-friendly web-based waste sales system for community use.

Furthermore, User Requirements are determined in Table 1 and Software Requirements in Table 2 according to research needs.

**User Categories System Requirements** Access the homepage, information, educational materials, and waste price list Public without logging in. Register and log in. Sell waste by filling out the transaction form. 3. View sales transaction history. Login to access agent features. Agent 1. 2. Manage Community sales transactions (view, add, update, and delete). View Community transaction history. 3. Collector 1. Login to access Collector features. Manage Agent sales transactions (view, add, update, and delete). View Agent transaction history. Admin Login to access admin features. Manage sales transactions for all users. Add, update, and delete educational content, product data, types of waste, and 3.

Table 1. User requirement

Table 1 is a breakdown of system requirements from the perspective of users or stakeholders who will interact with the system. Each user category has different access and features according to their role in the system.

Manage user data (community, agents, collectors).

View transaction history for all users.

Table 2. Software requirement

Category	<b>Technical Specifications</b>
Functional	1. The system must provide authentication and authorization for various types of users
	(agents, community, collectors, admins).
	2. Use a relational database to store user data, transactions, and reports.
	3. The interface must be user-friendly and support access across multiple devices.
	4. The system must record and manage waste sales transactions.
Non-Functional	1. The system must be able to handle the growth of users and data efficiently.
	2. Responsive in processing user requests.
	3. Have security mechanisms to protect data and transactions.
	4. Must be reliable with minimal downtime.
	5. The source code must be easy to maintain and further develop.

Table 2 defines the technical specifications that must be met, to build a system according to User requirements, so that the system can run properly.

Volume 12, Issue 2, October 2025, pp. 159-168 ISSN 2355-5068 ; e-ISSN 2622-4852

**DOI:** 10.33019/jurnalecotipe.v12i2.4549

#### 3.2. Design

At the design stage, the system workflow design is carried out using UML, the structure and component design through the Design System, and the visualization of the interface layout through wireframes. This process is carried out based on the analysis of system requirements to ensure that the design of the Website system for selling waste in Surau Village can function optimally according to its purpose.

# a. Unified Modelling Language (UML)

In this study, UML is used to describe the system workflow, structure, and component interactions in the design of the waste sales website in Sirau Village.

#### 1. Used case

A used case diagram illustrates the actions that actors or users can perform within a system. It is developed based on system requirement analysis during the requirement-gathering phase. The application is designed for four types of users: the public (customers), agents, collectors, and the waste bank administrator. Each user has different access rights, as depicted in Figure 2.

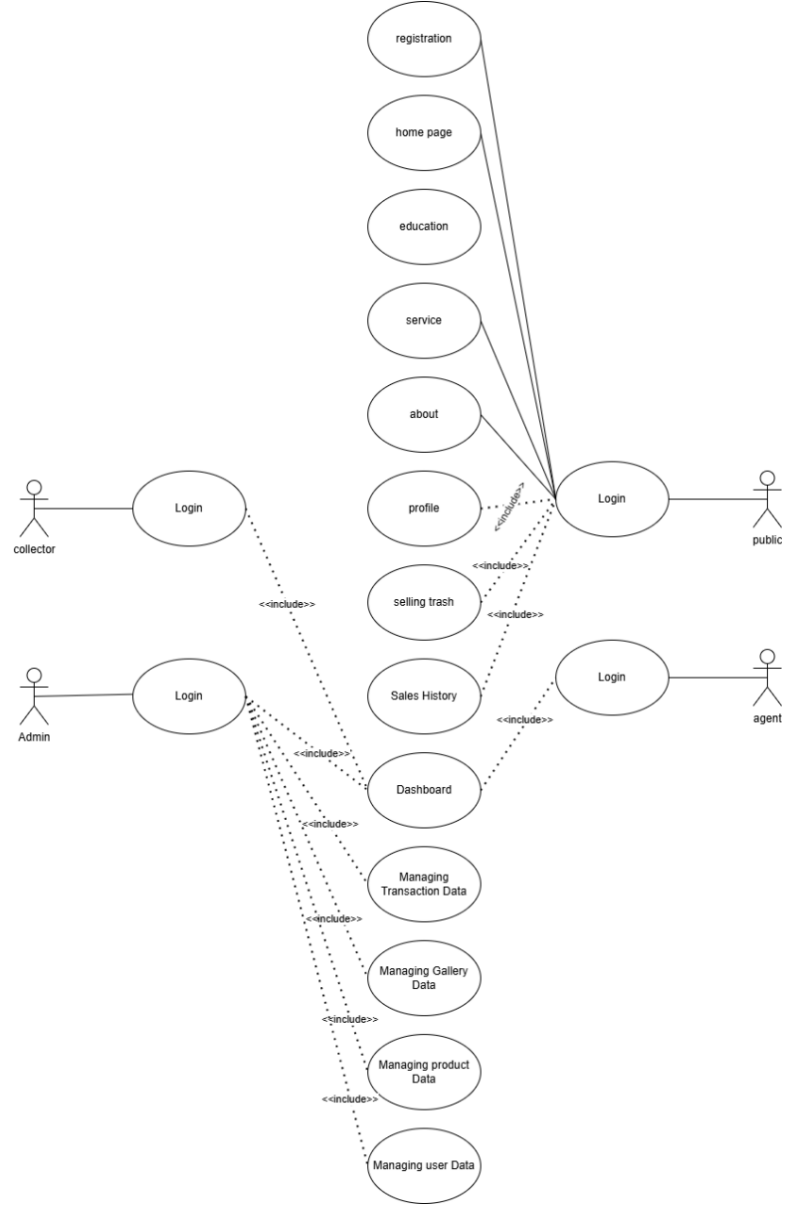


Figure 2. Used case diagram website Garbage Sales

#### 2. Activity Diagram

Volume 12, Issue 2, October 2025, pp. 159-168 ISSN 2355-5068; e-ISSN 2622-4852

**DOI:** 10.33019/jurnalecotipe.v12i2.4549

This diagram visualizes the interaction between three main actors: Community, Agent, Collector and admin. Each actor plays an important role in ensuring the system functions properly.

a) The following is a picture of the Community Activity diagram when they want to open the service page and want to make a waste sales transaction.

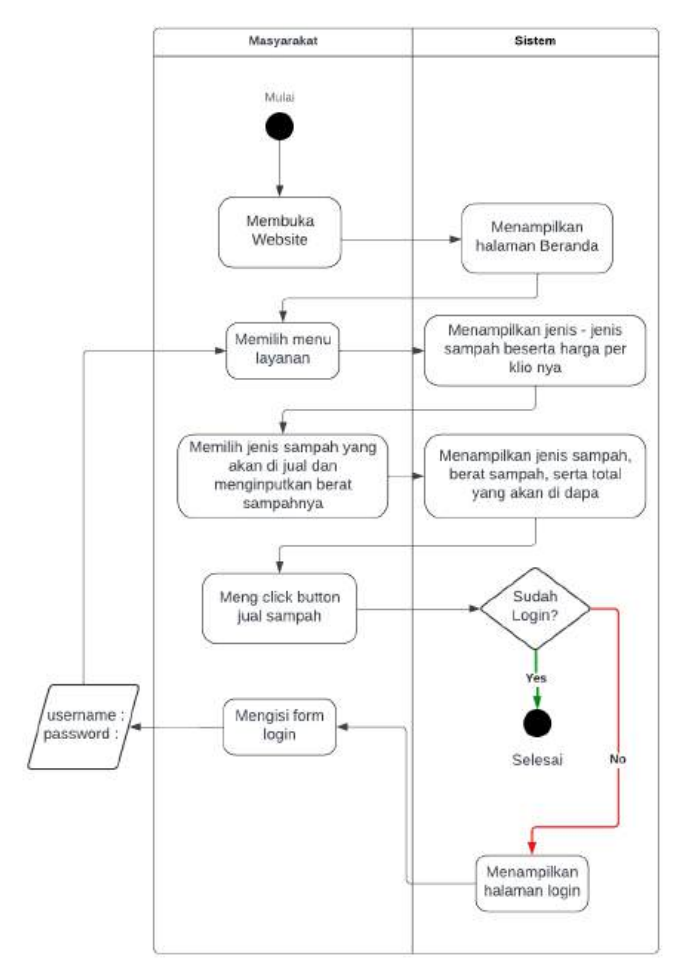


Figure 3. Activity Diagram Halaman Layanan

Figure 3 illustrates the user's activity flow when accessing the service page and selling waste. Upon reaching the website's homepage, users can navigate to the "Services" menu to view the types of waste that can be sold along with their respective prices. If a user wishes to sell waste but does not have an account, they must first register. However, registered users can simply log in. After logging in, users can select the waste type and input its weight to calculate the total earnings they will receive.

b) Activity diagram Viewing Agent, Collector and Admin Transaction Pages
The following is a picture of the Activity diagram of Agents, Collectors, and Admins when
they want to open the transaction page.



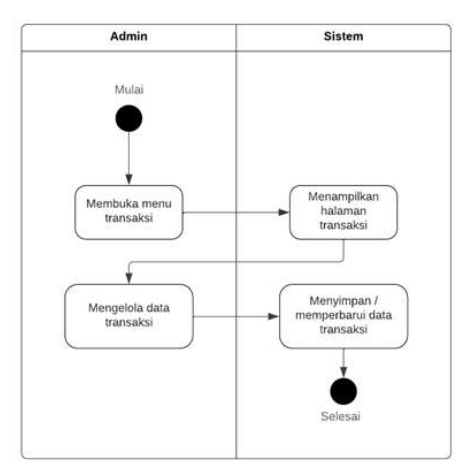


Figure 4. Activity Diagram Managing Agent, Collector, Admin Transactions

Figure 4 shows the process of agent, collector and admin activities when managing Transaction data according to each Role. This process occurs when you are on the home page, then select the Transaction menu to display Transaction data. There is a detail and delete menu, which is useful for managing Transaction data, an export button to export data to excel, filter data based on status and month, and there is also a search feature based on the name of the User who made the transaction.

#### B. Wireframe

Wireframe is an initial framework of interface design used to visualize the layout of elements on a website, such as navigation, buttons, and forms. Wireframe Design helps researchers design user interaction flows efficiently before the development stage. Figure 5 is a Low Fidelity Design of the User page.

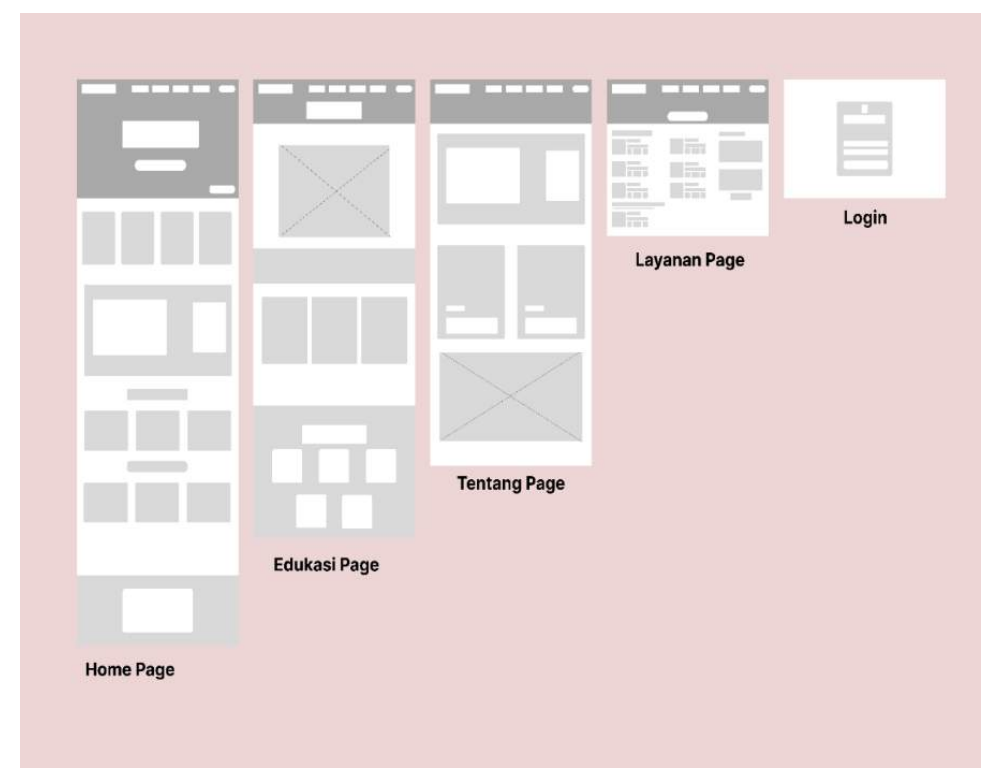


Figure 5. Wireframe User Page

There are 5 pages on the User page including the home page, education, about, services, and Login. Each page has a different size to suit the information needs that will be displayed on the page.

Volume 12, Issue 2, October 2025, pp. 159-168 ISSN 2355-5068 ; e-ISSN 2622-4852

**DOI:** 10.33019/jurnalecotipe.v12i2.4549

Previous studies have demonstrated the practical benefits of incorporating UML modeling and wireframe design to facilitate clarity and stakeholder alignment in system development [10].

#### 3.3. Coding

After completing the design stage, the research continues to the coding stage. At this stage, system development is carried out thoroughly, starting from the user interface to the backend process. Coding includes creating display designs, functionality, and integration with existing systems.

#### 3.4. Testing

At the Testing stage, it is done to ensure that the Website functions as needed, has optimal performance, and provides a good user experience. Testing includes the Blackbox Testing method and the User Experience Questionnaire (UEQ).

# Blackbox Testing

Table 3. Recapitulation of blackbox testing results

No	Pola Situasi	Hasil Pengujian Berhasil	Hasil Pengujian Tidak Berhasil
1	Halaman <i>User</i>	28	1
2	Halaman Admin	37	0
3	Halaman Agen	8	0
4	Halaman Pengepul	8	0
5	Halaman Login	6	0
6	Halaman Register	8	0
	Total Hasil Pengujian	96	0

The recapitulation data is then calculated using descriptive analysis techniques, namely:

Testing Successful = 
$$\frac{95}{96} x 100\% = 98.96\%$$
  
Test Failed =  $\frac{1}{96} x 100\% = 1.04\%$ 

Based on calculations using descriptive analysis, the results of Blackbox Testing show a success rate of 98.96% and a failure rate of 1.04%. With these results, the KSM KuduBisa Website is declared very feasible and can be used well.

The Blackbox Testing method is widely recognized for validating web application functionality from the user's perspective, as it verifies the behavior of the system without accessing internal code [11].

#### 2. User Experience Questionnaire

Table 4. UEQ user questionnaire results

Scale	Mean	Comparisson to banchmark
Attractiveness	2,89	Excellent
Perspicuity	2,83	Excellent
Efficiency	2,89	Excellent
Dependability	2,83	Excellent
Stimulation	2,89	Excellent
Novelty	2,71	Excellent

Based on the results of the UEQ questionnaire, the system received an excellent category in every aspect of the assessment. Attractiveness received a score of 2.89, indicating an attractive and user-friendly system display. Perspicuity received a score of 2.83, indicating ease of understanding the system. Efficiency also received a score of 2.89, proving that the system is efficient in helping the waste sales process. Stimulation with a score of 2.89 indicates an attractive and beneficial system. Meanwhile, Novelty received a score of 2.71, indicating that the system has elements of novelty and creativity.

The User Experience Questionnaire (UEQ) is a reliable and benchmarked tool for measuring UX in interactive systems, with metrics that include attractiveness, dependability, and novelty [12].

# 3.5. Implementation

The following are the results of the implementation that has been carried out



Figure 6. Login menu results

Figure 6 is the Login page containing the Username and password. This display is presented in 2 models for access using a PC or gadget. On this page there is also a registration feature for community actors who do not have an account.

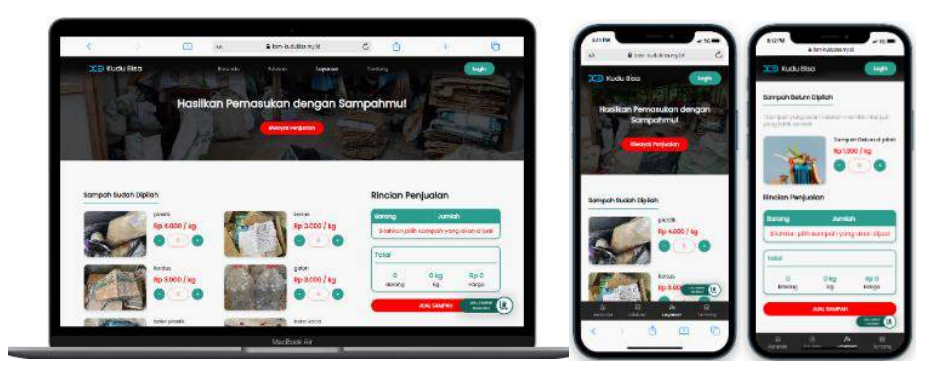


Figure 7. User service page

Figure 7 is a service page for users whose function is for the public to make waste sales transactions. This display is presented in 2 models for access using a PC or gadget.

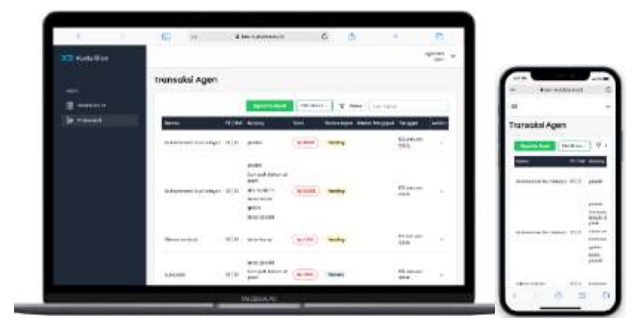


Figure 8. Agent, Collector, Admin transaction dashboard page

Figure 8 is the admin transaction dashboard page. The purpose of this page is to manage waste sales data. There are also export features to excel and data filtering to make it easier for admins to manage it. This display is presented in 2 models for access using a PC or gadget.

#### 4. CONCLUSION

Based on the research conducted, the development of the KSM KuduBisa Website using the Extreme Programming method has been successfully implemented. The development process begins

Volume 12, Issue 2, October 2025, pp. 159-168 ISSN 2355-5068 ; e-ISSN 2622-4852

**DOI:** 10.33019/jurnalecotipe.v12i2.4549

with the planning stage to determine user needs, then continues with the design stage to ensure the flow and appearance of the website are in accordance with needs. The resulting website is able to facilitate users in accessing educational information about waste management and conducting digital waste sales transactions. Testing using the Blackbox Testing method showed a system feasibility level of 98.96% with the category "Very Feasible". In addition, usability evaluation through the User Experience Questionnaire (UEQ) involving 32 respondents showed that this system had an average score above 2.50 in all aspects, so it is included in the "Excellent" category. Thus, the system developed can be well accepted by the community and functions optimally in supporting digital waste management and sales.

# REFERENCES

- [1] O. Ainun Syifa Salsabila, A. Sekarkirana Pramesti Kameswara, and F. Hidayanto, "Industry 4.0 Technology Impact On Environement: A Systematic Literature Review," *Jurnal Ilmiah Hospitality*, vol. 11, no. 2, 2022, [Online]. Available: <a href="http://stp-mataram.e-journal.id/JIH">http://stp-mataram.e-journal.id/JIH</a>.
- [2] D. Mangindaan, A. Adib, H. Febrianta, and D. J. C. Hutabarat, "Systematic Literature Review and Bibliometric Study of Waste Management in Indonesia in the COVID-19 Pandemic Era," Mar. 01, 2022, MDPI. doi: 10.3390/su14052556.
- [3] D. A. Kristiyanti *et al.*, "Digital transformation in waste management: Enhancing financial transaction efficiency at a waste bank," *Abdimas: Jurnal Pengabdian Masyarakat Universitas Merdeka Malang*, vol. 9, no. 3, pp. 459–471, Oct. 2024, doi: 10.26905/abdimas.v9i3.12937.
- [4] M. Ghahramani, M. Zhou, A. Molter, and F. Pilla, "IoT-based Route Recommendation for an Intelligent Waste Management System," Jan. 2022, doi: 10.1109/JIOT.2021.3132126.
- [5] R. Saeed Al Qurashi *et al.*, "Smart Waste Management System for Makkah City using Artificial Intelligence and Internet of Things," 2025. [Online]. Available: <a href="https://orcid.org/0000-0003-0539-7361">https://orcid.org/0000-0003-0539-7361</a>.
- [6] M. M. Gitau, A. Farkas, V. Ördög, and G. Maróti, "Evaluation of the biostimulant effects of two Chlorophyta microalgae on tomato (Solanum lycopersicum)," *J Clean Prod*, vol. 364, Sep. 2022, doi: 10.1016/j.jclepro.2022.132689.
- [7] A. A. Hs, P. M. Sunusi, A. Nurwahyuni, D. Reskita, N. Mustari, and M. L. M. Sonni, "Analisis Bibliometrik: Penerapan Mobile Application 'Bank Sampah' sebagai Layanan Pengelolaan Sampah di Era Digital," vol. 5, no. 2, pp. 137–147, 2025, doi: 10.51135/kambotivol5issue2p.
- [8] A. Maalouf and P. Agamuthu, "Waste management evolution in the last five decades in developing countries A review," Sep. 01, 2023, SAGE Publications Ltd. doi: 10.1177/0734242X231160099.
- [9] S. Dewi Andriana, D. Al-Muntazhim Lubis, and A. Prastiko Juned, "Pengelolaan Sampah Di Era Revolusi Industri 4.0 Berbasis Startup Digital," 2019.
- [10] H. Koç, A. M. Erdoğan, Y. Barjakly, and S. Peker, "UML Diagrams in Software Engineering Research: A Systematic Literature Review," MDPI AG, Mar. 2021, p. 13. doi: 10.3390/proceedings2021074013.
- [11] Y. Salih and R. Saefullah, "Black Box Testing on Website-Based Guestbook Registration Applications," *International Journal of Mathematics, Statistics, and Computing*, vol. 2, no. 2, pp. 44–49, 2024.
- [12] Martin Schrepp, "User Experience Questionnaire Handbook," Dec. 2023. [Online]. Available: www.ueq-online.org



Volume 12, Issue 2, October 2025, pp. 169-180 ISSN 2355-5068 ; e-ISSN 2622-4852

**DOI:** 10.33019/jurnalecotipe.v12i2.4566

# Solar Power Plant of Apartment Kertapati – A Design Study to Reduce Carbon Emission

Muhammad Abu Bakar Sidik<sup>1</sup>, Muhammad Irfan Jambak<sup>2</sup>, Rizda Fitri Kurnia<sup>3</sup>, Noer Fadzri Perdana Dinata<sup>4</sup>, Muhammad Izman Herdiansyah<sup>5</sup>, Rian Alto Belly<sup>6</sup>, Muhammad Alif Wicaksono<sup>7</sup>, Rizki Aidil Fitrah<sup>8</sup>, Muhammad Darmawan Fahreza<sup>9</sup>

1.2,3,4,7,8,9 Department of Electrical Engineering, Faculty of Engineering, Universitas Sriwijaya, Sumatera Selatan, Indonesia
4.5 Department of Electrical Engineering, Faculty of Science and Engineering, Universitas Bina Darma, Sumatera Selatan, Indonesia
6 PT. PLN (Persero) Unit Induk Distribusi, Kalimantan Selatan dan Kalimantan Tengah Indonesia

#### **ARTICLE INFO**

#### **Article historys:**

Received: 09/07/2025 Revised: 15/08/2025 Accepted: 30/10/2025

#### **Keywords:**

Apartment; Solar Power Plant; Carbon Emission

#### **ABSTRACT**

Energy demand in residential and housing areas in Indonesia is still predominantly reliant on fossil fuels. This dependency grows, triggering various environmental issues such as air pollution and global warming. Furthermore, energy costs in these areas are relatively high, partly due to increasing tariffs from PLN (Indonesia's state electricity company). One residential area in Palembang City with the potential for developing a Solar Power Plant (Solar PV System) is the Kertapati Rental Apartment Complex (Apartment Kertapati), located in Karya Jaya Sub-district, Kertapati District, Palembang City, South Sumatra. This area spans approximately 7 hectares and consists of a total of 300 units. Energy demand in this area is significant, particularly to support public and social facilities such as lighting, cooling systems, and various other needs. This study utilises PVsyst software, which is designed for the planning, simulation, and analysis of solar power systems. With the identified energy needs and favourable environmental conditions, this project has significant potential to deliver both economic and environmental benefits. However, this study focuses exclusively on on-grid systems for analysis and data processing.



This work is licensed under a Creative Commons Attribution 4.0 International License

#### **Corresponding Author:**

Muhammad Abu Bakar Sidik Department of Electrical Engineering, Faculty of Engineering Universitas Sriwijaya, Indralaya, Sumatera Selatan, Indonesia Email: abubakar@unsri.ac.id

#### 1. INTRODUCTION

#### 1.1. Background

The development of Solar Power Plants (PV power plants) represents a significant effort to reduce dependence on fossil fuels, which are becoming increasingly scarce and contribute to serious environmental issues [1], [2]. As a renewable and environmentally friendly energy source, PV power plant offers a promising alternative to help meet the growing energy demands of the future [3], [4].

To address climate change and promote environmental sustainability, the Indonesian government has set a target to reduce greenhouse gas emissions by 29% by 2030 [5], [6]. One of the primary strategies to achieve this goal is the increased adoption of renewable energy sources, including the construction and use of PV power plants [7].

Volume 12, Issue 2, October 2025, pp. 169-180 ISSN 2355-5068; e-ISSN 2622-4852

**DOI:** 10.33019/jurnalecotipe.v12i2.4566

#### 1.2. Problem Statement

In Indonesia, the development of PV power plants has been gaining momentum, supported by both government initiatives and private sector investment. Residential and settlement areas have become key targets for solar energy deployment due to their high electricity consumption, particularly for lighting, cooling, and various household needs [8], [9], [10].

However, energy use in residential areas across the country continues to be dominated by fossil fuels. This reliance not only contributes to environmental degradation, such as air pollution and global warming, but also results in relatively high energy costs, especially as electricity prices from the state utility company, PLN, continue to rise [11].

#### 1.3. Research Objective

This study explores the potential for solar energy development in Palembang, the capital of South Sumatra Province, which covers approximately 352.52 km² and is home to nearly 1.7 million residents. With a tropical climate, an average annual rainfall of 2,500 mm, and solar radiation averaging 4.67 kWh/m²/day, Palembang presents a strategic opportunity for integrating renewable energy, particularly solar photovoltaic systems. The research focuses on the Kertapati Apartments in Karya Jaya Village, Kertapati District, assessing the feasibility of installing a PV power plant to meet local energy needs. The complex spans around 7 hectares and includes 300 residential units with significant electricity demands, especially for public lighting, communal facilities, and cooling systems. By evaluating solar potential, energy consumption, and installation capacity, the study aims to provide a practical, scalable model for deploying solar energy in densely populated urban residential areas of Palembang.

#### 1.4. Contributions

This study contributes valuable, up-to-date data and insights into the potential for solar energy utilization at the Kertapati Apartments in Palembang. It identifies strategic opportunities for solar panel installation and assesses both the technical and economic feasibility of implementing a PV power plant within the residential complex. Beyond the technical evaluation, the research offers practical policy recommendations and development strategies aimed at supporting the sustainable integration of solar energy into the apartment's infrastructure. These contributions are expected to serve as a reference for future renewable energy initiatives in similar urban residential settings.

# 2. METHOD

To achieve the objectives of the study, the scope of work for the PV power plant Feasibility Study at the Kertapati Apartments includes several key activities. First, it involves reviewing relevant materials to support the study process and compiling a list of necessary primary and secondary data [12], [13], [14]. Second, the study includes the preparation of data collection and preparation required for further analysis. Third, it entails the collection of data related to the potential implementation of solar panels. The main outcome of this activity is a set of technical recommendations, including components, proposed locations, and the appropriate panel capacity for the Kertapati Apartments. The study employs PVsyst software, for simulation and analysis of solar power systems.

#### 2.1. Solar Energy Potential

Indonesia holds significant potential for solar energy due to its geographical location near the equator, which allows the country to receive abundant sunlight throughout the year. While solar energy potential varies across different regions and islands, overall, it remains highly promising [15], [16], [17]. As an archipelagic nation, Indonesia experiences average daily solar radiation ranging from 4.5 to 6.5 kWh/m² in most areas, including South Sumatra.

With a growing population, the demand for electricity in Indonesia continues to rise. In response, the government has introduced various policies and incentives to promote the adoption of PV power plants. This transition not only supports efforts to meet the increasing energy demand but also helps reduce dependence on fossil fuels and contributes to lowering greenhouse gas emissions [18], [19], [20].

#### 2.2. Components of PV Power Plant

The capacity of photovoltaic modules, inverters, transformers, switchgear, AC cables, and DC cables are components that must be considered in designing a solar power plant. Figure 1 shows a typical diagram of an off-grid and on-grid PV power plant system.

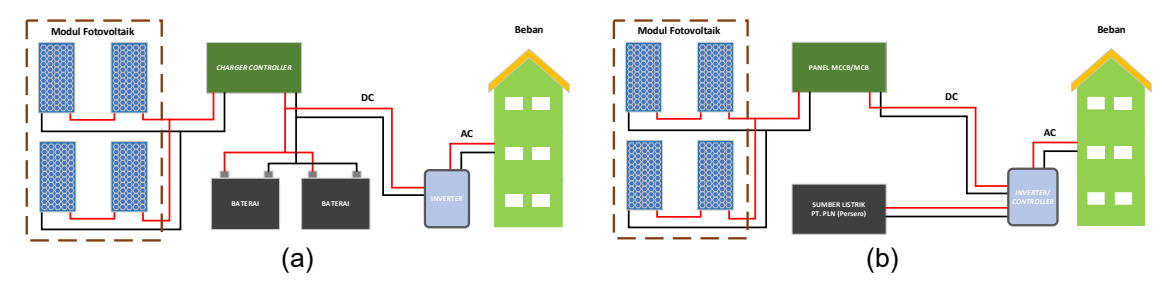


Figure 1. Block Diagram of Solar PV System (a) on-grid, and (b) off-grid

A photovoltaic power plant uses interconnected modules made of silicon-based solar cells to convert sunlight into direct current (DC) electricity. The size and layout of the array depend on available space and energy needs, with installation possible on rooftops, open land, or integrated into buildings. Support structures secure the modules and optimize their orientation for maximum sunlight. An inverter converts the DC output into alternating current (AC), sized according to the plant's capacity and load. Relays and circuit breakers are included to protect the system, ensure reliability, and maintain safety.

# 2.3. South Sumatra Solar Radiation Profile and Technical Feasibility

South Sumatra Province receives abundant sunlight year-round, with about 300 sunny days annually. Average daily solar radiation ranges from 4.6 kWh/m² in the west to around 5 kWh/m² in the central region, totaling 1,300–1,900 kWh/m² per year. Figure 2a illustrates the solar radiation distribution across the province, while Figure 2b highlights local weather conditions and sunlight exposure at the site, along with detailed mapping that supports the efficiency of solar PV system.

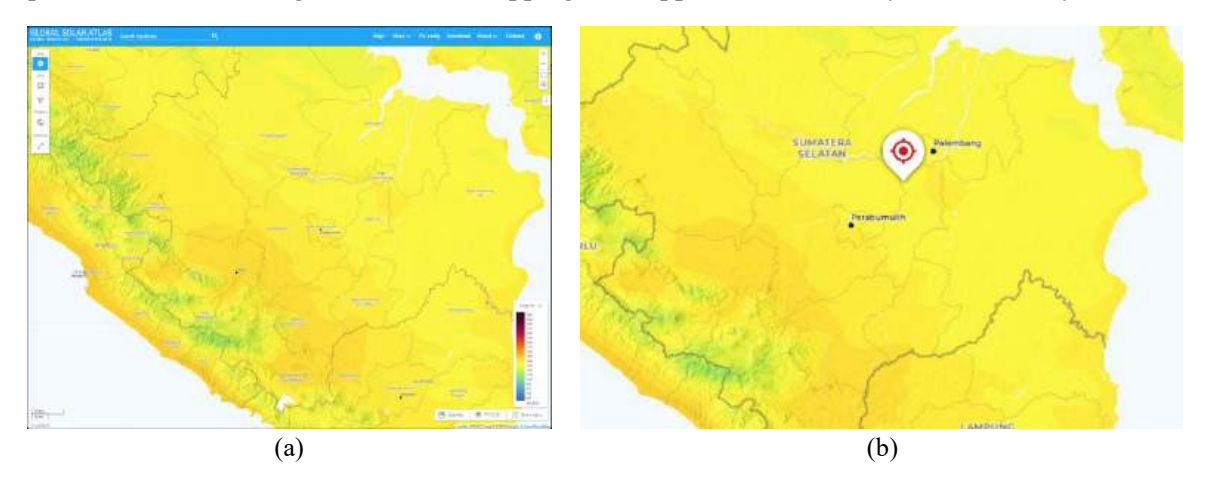


Figure 2. (a) Map of solar radiation in South Sumatra Province, (b) Solar Profile at the Apartment Kertapati

#### 2.4. Location Analysis and Power Requirement

Site analysis confirms that the Kertapati Apartment complex in Palembang is well-suited for a solar power plant, with sufficient solar exposure and flexible installation options on rooftops or open land. Local mapping and surveys reveal the site's structural suitability, as illustrated in Figure 3a and 3b, which show the general layout and available space, while Figure 3c highlights rooftop areas ideal for panel placement. The apartment's power needs are divided between public facilities (Fasus and Fasum) and residential units. For the three buildings, the total power requirement for Fasus and Fasum is 49.5 kVA (16.5 kVA per building), based on the installed PLN meter, as shown in Figure 3d.

Volume 12, Issue 2, October 2025, pp. 169-180 ISSN 2355-5068 ; e-ISSN 2622-4852

**DOI:** 10.33019/jurnalecotipe.v12i2.4566



**Figure 3.** Site visit, (a) and (b) show the placement options for the PV panels in open fields available at the location. (c) Shows the placement options for the PV panels at the rooftop location. (d) A 3-phase meter

Based on billing data from the past two months and PLN's government office tariff of Rp. 1,699.53/kWh for 6.6–200 kVA, the estimated monthly energy consumption for Block A is 2,350 kWh, or about 78.33 kWh per day. This indicates substantial electricity use that must be factored into the solar power plant design. Buildings B and C each require approximately 26.67 kWh per day, and while their consumption is lower than Block A's, these figures are essential for designing a system that effectively meets the daily energy needs of all three buildings [21], [22], [23], [24].

The total power requirement for the Kertapati Apartment housing units is estimated at 390 kVA, based on 1,300 VA meters installed in each of the 300 residential units (1,300 VA  $\times$  300). This figure represents the overall capacity needed to support the daily operations and energy demands of all households, as indicated by the installed PLN meters.

#### 2.5. Solar Profile

The solar profile describes the sunlight patterns at a specific location over time, showing how solar intensity varies daily, seasonally, and annually. This data is crucial for designing and optimising solar power systems. Key parameters of the solar profile are presented in Table 1.

**Table 1.** Main parameters for characterization of solar energy profiles

Parameter	Description
Sunlight Irradiance	It is a measure of the intensity of sunlight reaching an area in a given
	unit of time, to measure how much solar energy can be absorbed.
Daily Variations	A solar profile provides insight into how sunlight intensity varies in a
	day It involves changes in light intensity from sunrise to sunset.
Seasonal Variations	Shows how sunlight intensity changes throughout the year in relation
	to seasonal changes.
Shadow and Barrier Effects	Solar profiles also help identify potential shadows or obstructions that
	can affect the efficiency of solar panels.
Optimal Orientation and Tilt of	Based on the solar profile, the optimal orientation and tilt of the solar
Solar Panels	panels can be calculated to capture as much sunlight as possible.
Utilization of Energy	This information is important in understanding how efficiently a solar
	PV system can utilize the solar energy available at a particular location.

# 2.6. Horizon, Sunpath, and Climate Profile

Following a site survey and location visit, historical climate data for the Kertapati Apartment area was analysed using the GlobalAtlas tool, with results shown in Table 2. Located on the equator, the area has a tropical climate with warm temperatures year-round, ranging from 24 °C to 32 °C. It experiences high humidity, distinct wet and dry seasons, and lush vegetation. The rainy season runs from October to April, with December being the wettest month (312 mm), while the dry season lasts from May to September, with August being the driest (84 mm). A summary of the region's climate is presented in Figure 4. For optimal solar panel performance, the ideal tilt angle, based on latitude, maximises annual solar radiation, though adjustments must consider factors like dust accumulation and potential shading between panels.

**Table 2.** Location map results information.

Item	Acronym	Mark
PV Specific Power Output	PVOUT	1324.5 kWh / kWp
Normal Irradiation	DNI	874.1 kwH / m <sup>2</sup>
Global Horizontal Irradiation	GHI	1669.3 kWh / m <sup>2</sup>
Diffuse Horizontal Irradiation	DIF	986.1 kWh / m <sup>2</sup>
Global tilted irradiation	GTI Opta	1677.3 kWh / m <sup>2</sup>
Optimum tilt angles	OPTA	70
Water temperature	TEMP	27.1 °C
Elevation	ELE	2 m

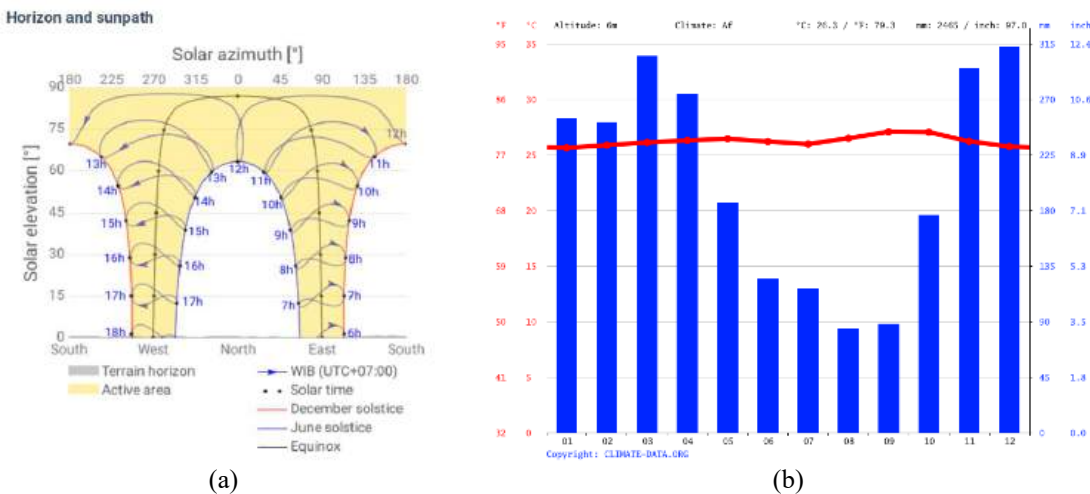


**Figure 4.** (a) Shows a picture of the solar irradiance path at the location, (b) Average annual climate conditions in the Apartment Kertapati area

Volume 12, Issue 2, October 2025, pp. 169-180 ISSN 2355-5068 ; e-ISSN 2622-4852

**DOI:** 10.33019/jurnalecotipe.v12i2.4566

The solar profile provides insight into how sunlight intensity varies over the course of a day. It involves changes in light intensity from sunrise to sunset, as seen in Figure 5a. Furthermore, Figure 5b shows how sunlight intensity changes throughout the year in relation to seasonal changes.

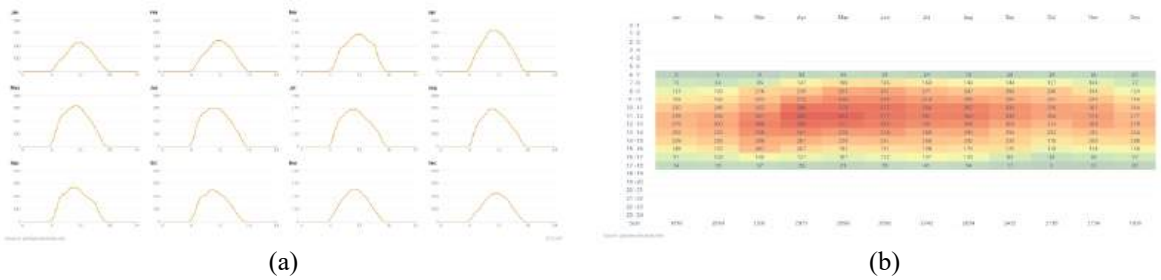


**Figure 5.** (a) Profile of average daily solar radiation values in Apartment Kertapati.(b) Profile of monthly average solar radiation values Apartment Kertapati

#### 3. RESULTS AND DISCUSSION

# 3.1. Selection of PV Power Plant Components

At the beginning of the design process, it is very important to choose the technology that will be used in the 3 x 16.5 kWp solar power plant. A simulation was carried out using PVsyst software by utilizing the solar radiation profile at the location. In this simulation environment, monocrystalline solar panels were selected, resulting in a total system production of an average of 90 MWh/year. The details of the generation can be seen in Figure 6.

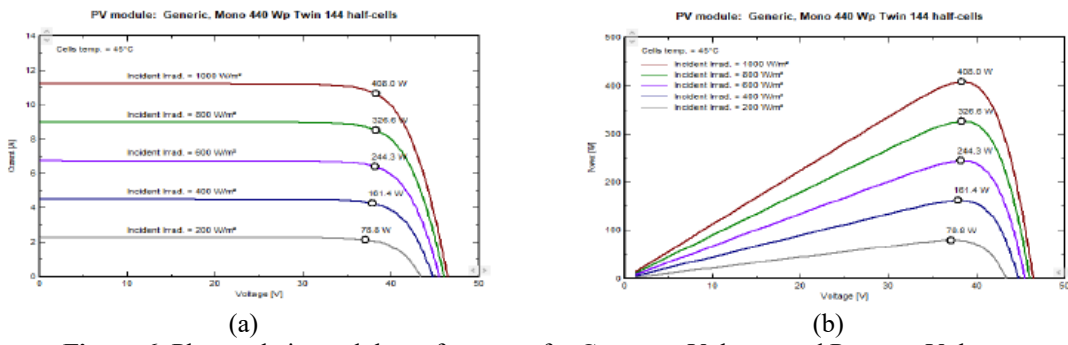


Figure 6. Photovoltaic module performance for Current – Voltage, and Power – Voltage

Choosing the right photovoltaic modules is essential for system efficiency and should consider factors like module performance, climate suitability, and compatibility with other components. Higher-efficiency modules offer more output but come at a higher cost, requiring a balance with budget and project goals. Table 3 lists the specifications for the selected module.

**Table 3.** Minimum characteristics required for photovoltaic modules

Commercial Data			
Nominal Power	≥ 400 Wp	Technology	Si-mono (minimum)
Module size	Est. 1.05 x 2.12 m2	Rough module area	Est. 2.23 m2
Rough Specifications			
Ref.temp	25 – 60oC	Ref. irradiance	1000 W/m2
Open Circuit Voltage	49.7 V	short circuit current	11.10 A
Vmpp	41.6 V	Impp	10.70 A
Pmpp	440.6 W	Isc temp. coefficient	6.3 mA/oC
One-diode Model Parai	neter		
Rshunt	600Ω	Io Ref	0.01 nA
Rseries	$0.22\Omega$	Gamma	0.978

#### 3.2. Number of Arrays and Modules

The total number of photovoltaic modules required in the system, as well as the space required for the implementation of the PV system, will vary based on the module technology chosen for the PV system. Equation (1) is used to calculate the number of photovoltaic modules required (NPV):

$$N_{PV} = \frac{P_{design} \times 10^6}{P_m STC} \tag{1}$$

Where, is the design capacity of the power plant in MW and is the power rating of the photovoltaic modules. The number of photovoltaic modules calculated is only an estimate based on the design capacity of the power plant.

#### 3.3. Inverter Selection

Selecting the right inverter for a solar power plant is a crucial decision that can have a significant impact on system performance and efficiency. To summarise the minimum inverter characteristic requirements, Table 4 presents important considerations for inverter selection.

**Commercial Data** Technology 16 kHz-IGBT Width x Height Est. 468 mm x 613 mm **IP65** Est. 242 mm Protection Depth **Input Characteristic** DC Phonograph **MPPT** 10 kW Operating mode MPP VMax 750 V Pmax DC 12 kW Absolute PV Volt 900 V Max PV Current 38 A **Output Characteristics** Grid Voltage 400 VAC 3-Phase 9 kVA AC Air Conditioning Pnom Grid Frequency 50Hz 10 kVA AC Pmax AC AC Inom 13 A Imax AC 20 A **Minimum Technical Features** 

Table 4. Minimum characteristics for the required Inverter

The required efficiency is shown in Figure 7. The efficiency  $(\eta)$  of a power converter is defined as the ratio of the useful output power  $(P_{\text{out}})$  to the total input power  $(P_{\text{in}})$ , commonly expressed as a percentage. Equation (2) shows that efficiency as a complement of the ratio of losses to input power.

Array isolation monitoring; Internal DC and AC Switch; Output Voltage Disconnect Adjustment

$$\eta = \left(1 - \frac{P_{loss}}{P_{in}}\right) \times 100\% \tag{2}$$

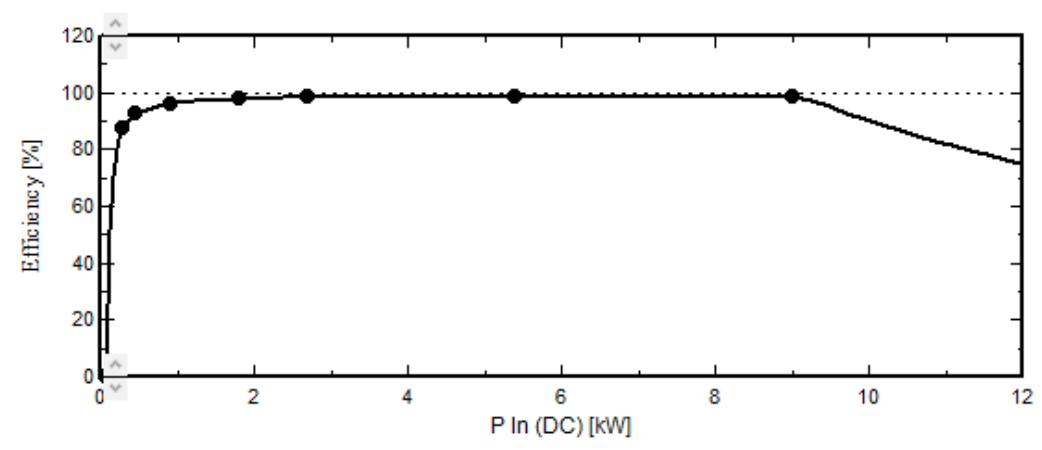


Figure 7. Required inverter efficiency curve

Volume 12, Issue 2, October 2025, pp. 169-180 ISSN 2355-5068 ; e-ISSN 2622-4852

**DOI:** 10.33019/jurnalecotipe.v12i2.4566

At low power region, 0 kW to  $\approx$  1 kW, the efficiency rises very rapidly from 0%. At extremely low input power, the fixed losses ( $P_{\rm fixed}$ ) represent a significant proportion of the total input power. As  $P_{\rm in}$  increases,  $P_{\rm out}$  also increases, and the fixed losses become a smaller percentage of the overall power. This leads to a steep increase in efficiency from the very low value towards the peak. Equation (3) clearly illustrates this, as  $P_{\rm in}$  increases, the  $P_{\rm fixed}/P_{\rm in}$  decreases significantly, driving up efficiency.

$$\eta = \left(1 - \frac{P_{fixed} + P_{variable}}{Pin}\right) \tag{3}$$

At mid to high power region the efficiency plateaus at its highest level approaching 98 - 99%. The device operates under conditions where the ratio of total losses to input power is minimized. Eventually, at high power region, above 9 kW, the efficiency begins to decline. This drop is attributable to the quadratic increase in conduction losses,  $I^2R$ , as the current levels rise with higher input power.

#### 3.4. Technical Feasibility Study Results

The simulation results are divided into two parts, namely: (a) simulation for Public Facilities and Public Facilities, and (b) simulation for houses. Table 5 shows the results of the PVsyst software simulation.

Public Facilities and Facilities

Project Reacons Karlaged Gold Connected

Votor She smallers with

Project Reacons Managed Gold Connected

Votor She smallers with

Project Reacons Managed Gold Connected

Votor She smallers with

Project Reacons Managed Gold Connected

Votor She smallers with

Project Reacons Managed Gold Connected

Votor She smallers with

Project Reacons Managed Gold Connected

Votor She smallers with

Project Reacons Managed Gold Connected

Votor She smallers

Project Reacons Managed Gold Connected

Project Reacons Manag

Table 5. Simulation results



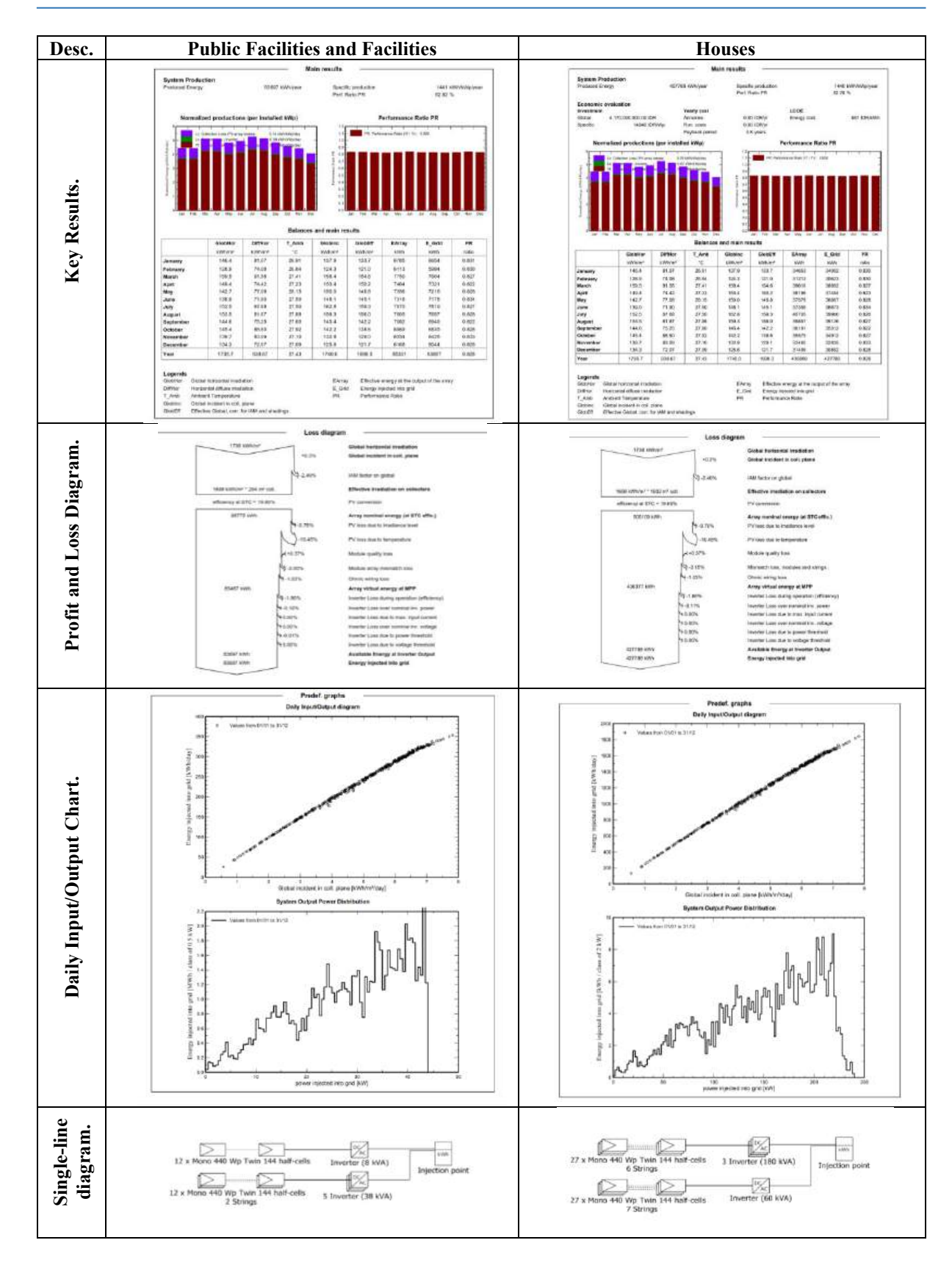


Figure 8 illustrates the projected reduction in CO2 emissions over time for the Kertapati Apartment solar project, showing a steady annual increase in savings throughout the PV system's 30-year lifespan. Table 6 compares CO2 emission reductions, with total savings estimated at around 1,559.6 tCO2 for public facilities and 7,629.6 tCO2 for residential units. These reductions result from replacing fossil

Volume 12, Issue 2, October 2025, pp. 169-180 ISSN 2355-5068 ; e-ISSN 2622-4852

**DOI:** 10.33019/jurnalecotipe.v12i2.4566

fuel-generated electricity with clean solar energy, highlighting the long-term environmental benefits of the system.

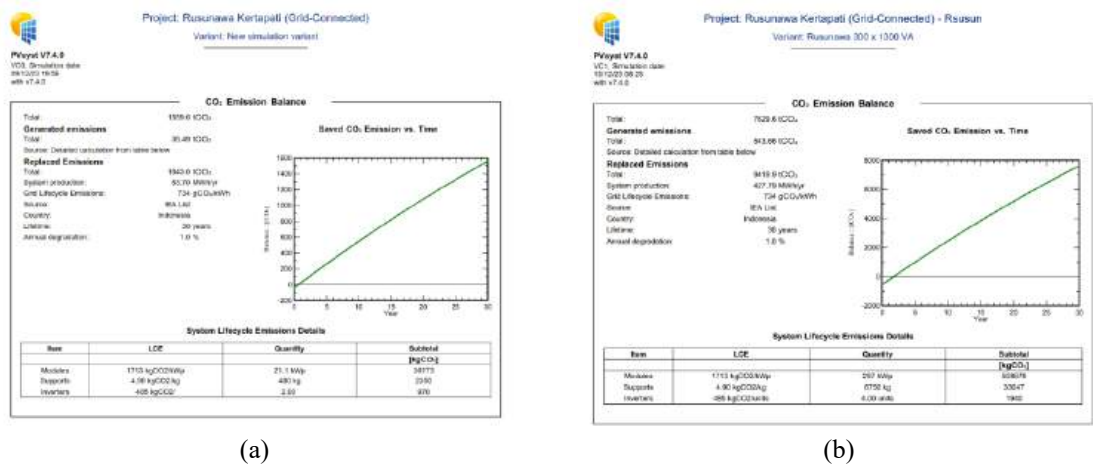


Figure 8. (a) CO2 emissions for public facilities and infrastructure, and (b) CO2 Emissions from Houses

Table 6. Comparison of CO2 equilibrium for Public Facilities and Public Facilities and Houses.

Description	Unit	Public Facilities and Facilities	Houses
Total emission savings	tCO <sub>2</sub>	1559.6	7629.6
Emissions generated during the life cycle of a solar power plant consisting of modules, supports, and inverters	tCO <sub>2</sub>	39.49	543.66
Total emissions displaced	tCO <sub>2</sub>	1843.0	9419.9
PV System Results	MWh/year	83.70	427.79
Replaced emissions	gCO <sub>2</sub> /kWh	734	734

# 4. CONCLUSION

Based on the results of the study conducted, it was concluded that the location of Apartment Kertapati in Palembang has good potential to be a location for the placement of PV power plant. With the identified power needs and supportive environmental conditions, this project has the potential to provide significant economic and environmental benefits. However, this study only considers the ongrid system as data and analysis material. The need for off-grid analysis results requires analysis of energy storage systems such as batteries which tend to affect the price and initial investment as well as higher maintenance costs. So that the on-grid system is a more efficient and effective choice for Apartment Kertapati with the target of saving daily electricity usage costs at the location.

#### **Acknowledgments**

This publication is funded by the DIPA Budget of the Sriwijaya University Public Service Agency for the 2024 Fiscal Year. SP DIPA-23.17.2.677515/2024, dated November 24, 2023, in accordance with the Rector's Decree Number: 0011/UN9/SK.LP2M.PM/2024 dated July 10, 2024.

#### **REFERENCES**

- [1] International Renewable Energy Agency, "Renewable Power Generation Costs In 2024", 2025.

  Accessed: Jul. 27, 2025. [Online]. Available: <a href="https://www.irena.org/Publications/2025/Jun/Renewable-Power-Generation-Costs-in-2024">https://www.irena.org/Publications/2025/Jun/Renewable-Power-Generation-Costs-in-2024</a>
- [2] M. Sujai, R. Wahyudi, and N. A. Sakina, "Transition from Coals to Renewable Energy: Evidence from Indonesia," Oct. 2023, doi: 10.56506/DMQN4483.

- [3] N. F. P. Dinata, M. A. M. Ramli, M. I. Jambak, M. A. B. Sidik, and M. M. Alqahtani, "Designing an optimal microgrid control system using deep reinforcement learning: A systematic review," *Engineering Science and Technology, an International Journal*, vol. 51, 2024, doi: 10.1016/j.jestch.2024.101651.
- [4] M. A. Syahbani *et al.*, "Performance enhancement of grid-forming inverter-controlled PV systems: A comparative study with and without battery energy storage under intermittent and unbalanced load conditions," *Results in Engineering*, vol. 27, p. 105980, Sep. 2025, doi: 10.1016/J.RINENG.2025.105980.
- [5] PT. PLN (Persero), "Indonesia PLN's Statistics 2024," 2024. Accessed: Jul. 27, 2025. [Online]. Available: <a href="https://web.pln.co.id/statics/uploads/2025/07/Statistik-PLN-2024-Audited-Indo-Eng-Final-Compressed-update-sheet.pdf">https://web.pln.co.id/statics/uploads/2025/07/Statistik-PLN-2024-Audited-Indo-Eng-Final-Compressed-update-sheet.pdf</a>
- [6] PT. PLN Persero, "RENCANA USAHA PENYEDIAAN TENAGA LISTRIK (RUPTL)," 2025. Accessed: Jul. 27, 2025. [Online]. Available: <a href="https://web.pln.co.id/stakeholder/ruptl">https://web.pln.co.id/stakeholder/ruptl</a>
- [7] M. L. Tuballa and M. L. Abundo, "A review of the development of Smart Grid technologies," *Renewable and Sustainable Energy Reviews*, vol. 59, pp. 710–725, 2016, doi: 10.1016/j.rser.2016.01.011.
- [8] A. Rofik and T. Y. R. Syah, "The effect of fuel mix, moderated by Indonesia crude price and foreign exchange, and power losses on profitability of PT PLN (PERSERO)," *International Journal of Energy Economics and Policy*, vol. 10, no. 4, 2020, doi: 10.32479/ijeep.9575.
- [9] Z. Qin, D. Liu, H. Hua, and J. Cao, "Privacy Preserving Load Control of Residential Microgrid via Deep Reinforcement Learning," *IEEE Trans Smart Grid*, vol. 12, no. 5, pp. 4079–4089, 2021, doi: 10.1109/TSG.2021.3088290.
- [10] M. C. Argyrou, C. C. Marouchos, S. A. Kalogirou, and P. Christodoulides, "Modeling a residential grid-connected PV system with battery–supercapacitor storage: Control design and stability analysis," *Energy Reports*, vol. 7, 2021, doi: 10.1016/j.egyr.2021.08.001.
- [11] N. A. Pambudi *et al.*, "Renewable Energy in Indonesia: Current Status, Potential, and Future Development," 2023. doi: 10.3390/su15032342.
- [12] A. Shrivastava, R. Sharma, M. Kumar Saxena, V. Shanmugasundaram, M. Lal Rinawa, and Ankit, "Solar energy capacity assessment and performance evaluation of a standalone PV system using PVSYST," *Mater Today Proc*, vol. 80, 2023, doi: 10.1016/j.matpr.2021.07.258.
- [13] S. A. D. Mohammadi and C. Gezegin, "Design and Simulation of Grid-Connected Solar PV System Using PVSYST, PVGIS and HOMER Software," *International Journal of Pioneering Technology and Engineering*, vol. 1, no. 01, 2022, doi: 10.56158/jpte.2022.24.1.01.
- [14] International Telecommunication Union (ITU), Measuring digital development: Facts and figures. 2021.
- [15] A. El Hammoumi, S. Chtita, S. Motahhir, and A. El Ghzizal, "Solar PV energy: From material to use, and the most commonly used techniques to maximize the power output of PV systems: A focus on solar trackers and floating solar panels," 2022. doi: 10.1016/j.egyr.2022.09.054.
- [16] V. Benda and L. Černá, "PV cells and modules State of the art, limits and trends," 2020. doi: 10.1016/j.heliyon.2020.e05666.
- [17] The Performance of Photovoltaic (PV) Systems. 2017. doi: 10.1016/c2014-0-02701-3.
- [18] R. Satpathy and V. Pamuru, *Solar PV Power: Design, Manufacturing and Applications from Sand to Systems*. 2020. doi: 10.1016/B978-0-12-817626-9.09990-1.
- [19] S. Weckend, A. Wade, and G. Heath, End of Life Management Solar PV Panels. 2016.



Volume 12, Issue 2, October 2025, pp. 169-180 ISSN 2355-5068 ; e-ISSN 2622-4852

**DOI:** 10.33019/jurnalecotipe.v12i2.4566

- [20] K. Komoto, J. S. Lee, Z. J.S., and R. J., *End-of-Life Management of Photovoltaic Panels: Trends in PV Module Recycling Technologies*, vol. 10, no. January. 2018.
- [21] H. M. Shertukde, *Power Systems Analysis Illustrated with MATLAB® and ETAP®*. 2019. doi: 10.1201/9780429436925.
- [22] D. Mondal, A. Chakrabarti, and A. Sengupta, *Power System Small Signal Stability Analysis and Control*. 2020. doi: 10.1016/C2018-0-02439-1.
- [23] K. O. Papailiou, Springer Handbook of Power Systems. 2021.
- [24] F. Milano, Advances in power system modelling, control and stability analysis. 2016. doi: 10.1049/PBPO086E.



# **Development of a Library Information System** for Data Processing at SMK N 1 Pangkalpinang

Tri Ari Cahyono<sup>1</sup>, Nursasono<sup>2</sup>

<sup>1</sup>Information Technology Study Program, University of Bangka Belitung, Indonesia

<sup>2</sup>Visual Communication Design Study Program, SMK N 1 Pangkalpinang, Indonesia

#### ARTICLE INFO

#### Article historys:

Received: 26/06/2025 Revised: 06/08/2025 Accepted: 30/10/2025

#### **Keywords:**

Information System; Library; Object-Oriented Methodology; UML

#### ABSTRACT

SMK N 1 Pangkalpinang is one of the schools in Pangkalpinang City that has a library playing an important role in supporting the learning process. However, the current library data processing system is still manual, relying on Microsoft Office applications, and lacks an integrated information system. This condition leads to various challenges in library management. such as difficulty in book searches, recording errors in borrowings and returns, and limitations in report generation. Therefore, this study aims to develop a more effective and efficient library data processing information system. Data collection methods used in this research include direct observation of library activities and interviews with related parties to identify system requirements. The system analysis and design were carried out using an object-oriented approach, with the Unified Modeling Language (UML) used as a modeling tool. Diagrams used include use case diagrams, class diagrams, sequence diagrams, and activity diagrams to illustrate business processes, data structures, and system logic to be built. The result of this research is a desktop-based library information system application featuring member and book data management, automated borrowing and returning transaction records, and computerized report generation. With this system, administrative processes become faster and more accurate, facilitating data management and search. The system also supports more systematic and real-time reporting, providing a positive impact on the overall quality of library services. Moreover, the use of object-oriented methodology and UML modeling allows the system to be more flexible and easily developed in the future.



This work is licensed under a Creative Commons Attribution 4.0 International License

#### **Corresponding Author:**

Tri Ari Cahyono<sup>1</sup>

<sup>1</sup>Information Technology Study Program, University of Bangka Belitung

Email: triari@ubb.ac.id.

# INTRODUCTION

The school library is one of the essential facilities that supports the teaching and learning process [1]. Its existence helps students and educators access various sources of information to improve the quality of learning. However, inefficient library management can hinder the optimal utilization of this facility. Currently, SMK N 1 Pangkalpinang does not yet implement an integrated information system and still uses a manual system for processing library data, aided by Microsoft Office applications such as Microsoft Excel and Microsoft Word. This system has various limitations, such as difficulties in searching for books, inaccuracies in recording borrowings and returns, and time-consuming report generation. These issues reduce the efficiency of library administrative processes and may decrease the quality of service for users.

Volume 12, Issue 1, April 2025, pp. 181-189 ISSN 2355-5068 ; e-ISSN 2622-4852

**DOI:** 10.33019/jurnalecotipe.v12i2.4564

The use of a manual system in library management often results in recording errors, data duplication, and delays in managing borrowing and returning transactions. Additionally, data entry processes using Microsoft Office do not allow for optimal automation, thus requiring more time in data management. Therefore, a library information system is needed to improve efficiency and accuracy in data processing.

This study aims to develop a library data processing information system at SMK N 1 Pangkalpinang using an object-oriented methodology. The object-oriented approach was chosen because it enables a more structured, flexible, and scalable system model, using the Unified Modeling Language (UML). UML is used as a design tool to visualize various aspects of the system through diagrams such as use case diagrams, class diagrams, sequence diagrams, and activity diagrams. The object-oriented approach in software development allows for more accurate modeling of system requirements and increases efficiency in implementation and maintenance [2].

With the implementation of this information system, it is expected that library management at SMK N 1 Pangkalpinang will improve user satisfaction by accelerating services and reducing potential errors in data recording. This solution is intended to address the administrative challenges in the library and contribute to the development of a more modern and integrated school library information system.

#### 2. RESEARCH METHOD

This study adopts a systematic approach encompassing two main methods: data collection methods and system engineering methods.

#### 2.1 Data Collection Methods

To obtain accurate information regarding the requirements of the library data processing information system at SMK N 1 Pangkalpinang, this research employed two primary data collection techniques :

- **a. Interview Method :** Conducted with librarians, teachers, and students as library users to understand the processes of book borrowing and returning, the challenges encountered in data management, and the required features in the information system to be developed.
- b. Observation Method: Direct observation was carried out on administrative activities within the library, including manual recording of borrowing and returning transactions using Microsoft Office. This method aims to identify weaknesses in the manual system and the need for a more efficient one.

# 2.2 System Engineering Method

After collecting the data, the next step is system engineering using the waterfall methodology to develop a solution that meets user requirements. The stages of this method include:

- a. Requirement Analysis: Based on data from interviews and observations, this stage identifies issues in the manual system and determines the functional and non-functional requirements needed for the new system.
- b. Design: This stage follows requirement analysis and involves modeling the system using the Unified Modeling Language (UML), which serves as a visual notation to model and communicate the system through various diagrams and supporting texts. The modeling includes use case diagrams, activity diagrams, sequence diagrams, and class diagrams.
- c. Development and Implementation: The system is developed by creating the user interface and coding based on the design. The application is built as a desktop-based program. Implementation includes installing the software, migrating data from the old system, and conducting initial trials to ensure the system operates properly.
- d. Testing: The testing phase uses black-box testing, which focuses on evaluating the system's functionality without examining the source code. The results of this testing are used to assess whether the system performs according to specifications. If errors are found, corrections are made before the system is fully deployed.

#### 3. RESULTS AND DISCUSSION

The development of this library information system was carried out through several main stages to ensure that the data processing at the SMK N 1 Pangkalpinang library could be developed systematically.

#### 3.1 Data Collection

In developing the library information system, data collection was conducted to understand the system requirements and ensure that the proposed solution addresses the identified issues. Interviews were conducted with librarians, teachers, and students as library users to gather information regarding the procedures of borrowing and returning books, the challenges in recording and managing book data, expected features of the new system, and the required access control and security. Observations were made by directly monitoring library activities to gain a real understanding of the manual system workflow. Observed aspects included how librarians recorded borrowings and returns, the use of Microsoft Office or other tools in data management, and the time required for book searching and logging. The data collected was used as the basis for the requirement analysis and system design to ensure that the developed information system would improve the library's efficiency.

#### 3.2 Requirement Analysis

Requirement analysis is a crucial stage in developing the library information system, aiming to identify problems in the current manual system and determine the necessary features and functionalities for the new system.

#### a. Identified Issues in the Manual System

Based on interviews and direct observations, several problems were identified in the manual library system that relies on Microsoft Office tools. One of the main issues is the manual process of recording borrowings and returns, which increases the risk of errors and data loss. Moreover, the book search process in the library catalog takes a long time due to the absence of a structured and automated search system. Report generation related to borrowing and returning activities is also still performed manually, which makes it inefficient and time-consuming. Additionally, the absence of an automatic reminder system for due dates causes users to return books late, potentially disrupting the circulation of collections in the library.

# b. Functional Requirements

Functional requirements are the core features the system must provide to replace the current manual processes. Key functional requirements include:

- 1. Book data processing: allows librarians to add, edit, delete, and view book information.
- 2. Borrowing and returning management: enables automated recording of book transactions.
- 3. Book search: allows users to search for books by title, author, or category.
- 4. Library member data management: stores member data and their borrowing history.
- 5. Report generation: produces automated reports on borrowing, returns, and book inventories.

# c. Non-Functional Requirements

In addition to the core features, the system must fulfill several non-functional aspects, such as:

- 1. Data security: ensuring access control based on user roles.
- 2. System performance: the ability to handle large datasets with fast response times.
- 3. Usability: the interface should be user-friendly and easy to use.

# 3.3 Design

This design phase creates a technical blueprint based on the requirement analysis to describe how the library information system will function before implementation.

# a. Conceptual Design

This initial design phase defines the system's structure and workflow using an object-oriented approach with Unified Modeling Language (UML). The diagrams used include:

1. Use Case Diagram: illustrates interactions between users and the system, showing the main functions.

Volume 12, Issue 1, April 2025, pp. 181-189 ISSN 2355-5068; e-ISSN 2622-4852

**DOI:** 10.33019/jurnalecotipe.v12i2.4564

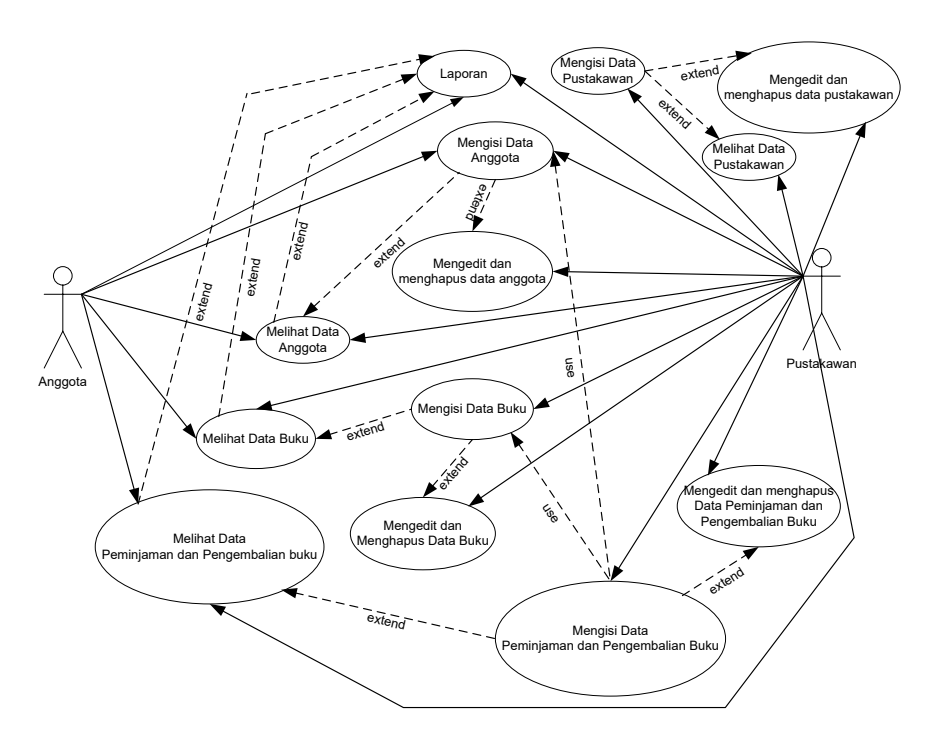


Figure 1. Use Case Diagram

Class Diagram: shows the data structure within the system, including classes, attributes, and object relationships, and supports database design with entities like Book, Member, and Transaction.

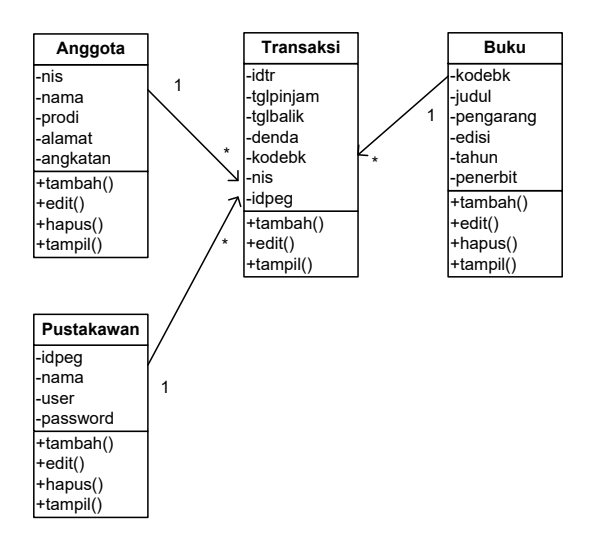


Figure 2. Class Diagram

Sequence Diagram: describes the sequence of interactions between system objects over time and ensures proper communication between users and the system.

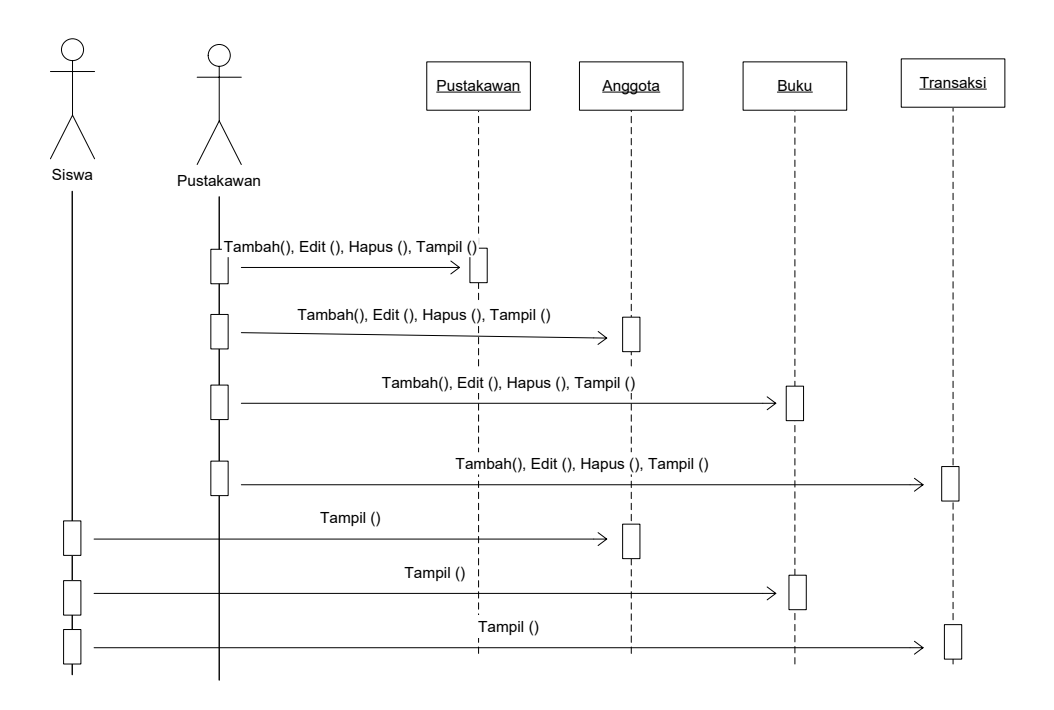


Figure 2. Sequence Diagram

4. Activity Diagram : visualizes workflows such as borrowing and returning processes, helping to understand each step of the operations.

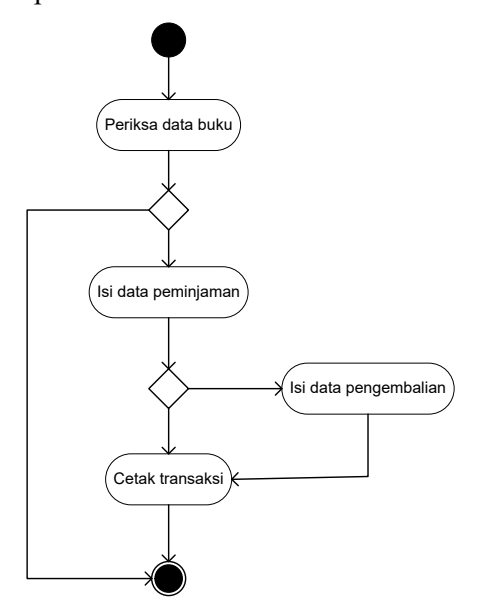


Figure 3. Activity diagram of book borrowing and returning data entry

b. Interface Design

The interface design aims to create a user-friendly system interface that allows users to interact with the system efficiently. Key elements include forms for book data input.



PENGISI	AN DATA	BUKU		
Kode Buku			_	
	1		_*	
Judul	*		*	
Pengarang	*		×	
Edisi	¥		×	
Tahun	*		×	
Penerbit	*		×	
× tambah	× edit	*		
× hapus	× seles	ai 🐰		
^ IIapus	1 301031	al î		

Figure 4. Book data entry interface

# c. Development and Implementation

System development involved creating the user interface and programming based on the design. The application was built as a desktop-based system. Implementation included software installation, data migration from the old system, and initial trials to ensure functionality.

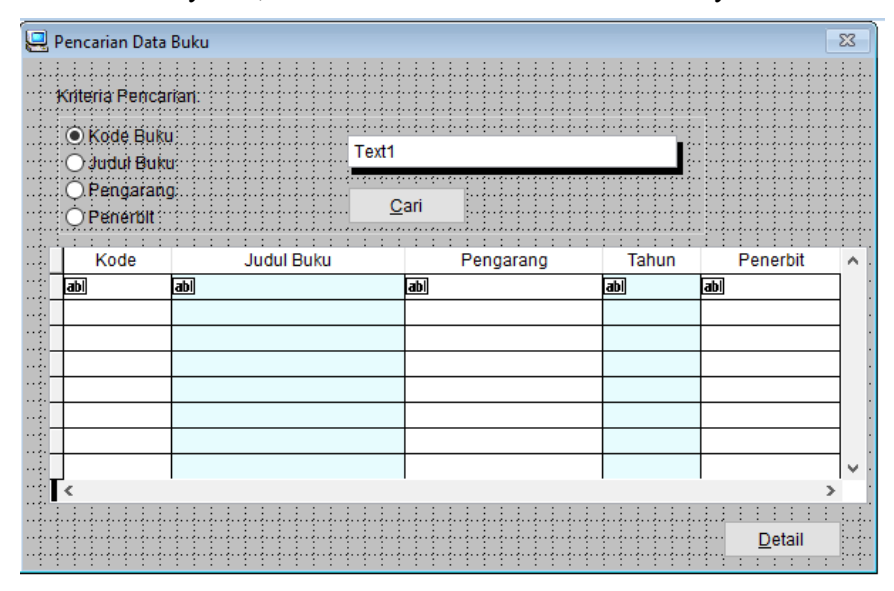


Figure 5. Book data search display

# d. Testing and User Response Evaluation

Testing was performed using black-box testing, which focuses on system functionality without inspecting the source code. The tests involved librarians and prospective users (teachers and students). The results helped determine whether the system met the expected specifications. Any identified bugs were fixed before full deployment.

Table 1. Black Box testing results

No.	<b>Tested Feature</b>	Test Scenario	Input	<b>Expected Output</b>	Test Result	Notes
1	Member Data Entry Form	Admin inputs new member data completely	Name, Student ID (NIS), class, address, etc.	Member data is successfully saved and displayed in the member list	Passed	Validation and saving work well
2	Member Data Entry Form	Admin inputs member data with missing/incomplete fields	Empty fields	Error message appears and data is not saved	Passed	Input validation is active
3	Book Data Entry Form	Admin adds a new book with complete information	Title, author, publisher, year, quantity, etc.	Book data is successfully added to the system	Passed	Data saved correctly
4	Borrowing and Returning Transaction Entry Form	Admin fills in transaction form with member ID and book ID	Member ID, Book ID, borrow date, return date	Transaction is saved; book stock decreases on borrow and increases on return	Passed	Borrowing flow functions properly
5	Book Search Form	User searches for a book by title	Title keyword	Relevant books appear in the search results	Passed	Accurate search results
6	Member Search Form	Admin searches member data by name or Student ID (NIS)	Name/NIS keyword	Matching members are displayed	Passed	Search function is active
7	Transaction Search Form	Admin searches transactions by member name or date	Name/NIS or transaction date	Relevant transaction data appears	Passed	Search meets criteria
8	Member Report	Admin prints or views a report of all members	-	Report appears in table or PDF format	Passed	Neat report format
9	Book Report	Admin views a report of available books	-	Complete book report displayed according to existing data	Passed	Output matches the data content
10	Borrowing and Returning Transaction Report	Admin prints a report of transactions based on a specific date range	Date range	Transactions for the selected period are displayed completely	Passed	Date filter functions properly

User testing was conducted at SMK N 1 Pangkalpinang's library for one week, involving 2 staff and 10 students. Overall average score = 4.48 (Effective category). Based on observation and interviews, the average score was as follows:

Table 2. User response evaluation

1							
No	Evaluated Aspect	Average Score (1-5)	Description				
1	Ease of Use	4.6	Very Good				
2	Data Access Speed	4.5	Very Good				
3	Recording Accuracy	4.4	Good				
4	Interface Appearance	4.2	Good				
5	Report Generation	4.7	Very Good				

Volume 12, Issue 1, April 2025, pp. 181-189 ISSN 2355-5068; e-ISSN 2622-4852 **DOI:** 10.33019/jurnalecotipe.v12i2.4564

#### 4. CONCLUSION

Based on the research and development that have been carried out, the developed library information system has been successfully implemented and tested. This system is designed to replace the previous manual method that relied on Microsoft Office applications, which tended to be inefficient and prone to human error. With the new system, the processes of recording book data, library members, as well as borrowing and returning transactions can now be done automatically. This automation not only improves data accuracy but also accelerates workflows and reduces the administrative burden that was previously performed manually.

The implemented features in the system provide various practical benefits. The book search process becomes faster and more structured, making it easier for users to find the information they need. In addition, the system is capable of systematically recording borrowing and returning transactions, supported by a due-date reminder feature that helps prevent late returns. Librarians can also manage transaction histories more easily and efficiently, and generate reports on borrowing, returns, and book stock automatically. This greatly saves time and effort, especially in routine reporting and documentation tasks.

From a software development perspective, the use of object-oriented methodology and modeling with Unified Modeling Language (UML) makes the system more structured and easier to understand. This approach assists the development team in designing and building the system, while also providing opportunities for future expansion. The system is designed to be flexible and adaptable, allowing for adjustments in response to policy changes or improvements in library services. Thus, the system not only meets current needs but is also ready to face future library management challenges.

The main contributions of this development lie in increasing operational efficiency, reducing errors in manual recording, and providing easier access to and retrieval of data. Furthermore, the system supports more systematic and professional data management, and provides a strong foundation for future development if needed. The implementation of this information system is expected not only to assist librarians in their daily tasks but also to serve as a digital library solution model for other schools with similar needs.

#### REFERENCES

- [1] A. Suryanto and H. Yuliyanto, "Implementation of Web-Based Library Information System to Improve Data Management Efficiency," *Journal of Information Technology and Computer*, vol. 5, no. 1, pp. 45–52, 2021.
- [2] R. Pressman and B. Maxim, *Software Engineering: A Practitioner's Approach*, 8th ed., New York: McGraw-Hill, 2014.
- [3] I. Sommerville, *Software Engineering*, 10th ed., Boston: Pearson, 2016.
- [4] G. Booch, J. Rumbaugh, and I. Jacobson, *The Unified Modeling Language User Guide*, 2nd ed., Boston: Addison-Wesley, 2005.
- [5] A. Nugroho, Software Engineering Using UML and Java, Yogyakarta: Andi, 2017.
- [6] D. Nur, "Analysis and Design of Desktop-Based Library Information System," *Journal of Computer and Informatics Science (KOMPUTA)*, vol. 6, no. 2, pp. 12–19, 2020.
- [7] S. Sutarman, *Introduction to Information Technology*, Jakarta: Bumi Aksara, 2012.
- [8] D. Oktavianti, E. Fatmawati, and R. Permana, "Development of a Web-Based Library Information System at SMK Negeri 4 Pontianak," *Journal of Information Technology and Science Research*, vol. 1, no. 4, 2024.
- [9] N. A. Saputro and S. Wahyuni, "Design of a Library Information System Using PHP & MySQL at SMK Negeri 1 Jakarta," *Journal of Mandalika Literature*, vol. 5, no. 1, pp. 9–19, Mar. 2024.



Volume 12, Issue 1, April 2025, pp. 181-189 ISSN 2355-5068; e-ISSN 2622-4852 **DOI:** 10.33019/jurnalecotipe.v12i2.4564

- [10] S. M. Simanjorang et al., "Design and Development of a School Library Information System as a Medium to Improve Student Literacy," *Journal of Community Service Nusantara*, vol. 5, no. 3, pp. 3304–3310, Jul. 2024.
- [11] S. AM Sulasminarti, I. Kurnia, and F. Ardhy, "Web-Based Library Book Borrowing and Returning Information System at SMK Negeri 1 Negerikaton," *Journal of Software and Network Informatics*, 2023.
- [12] D. Ayu Namira, A. Amroni, and Y. Hartiwi, "Design of a Web-Based Library Information System at SMK Swasta Harapan Bangsa Kota Jambi," *Journal of Informatics and Computer Engineering (JAKAKOM)*, 2023.



Volume 12, Issue 2, October 2025, pp. 190-202

ISSN 2355-5068; e-ISSN 2622-4852 **DOI:** 10.33019/jurnalecotipe.v12i2.4563

## Design and Simulations of 2x1 Rectangular Microstrip Array Antenna Using Inset and U-Slot Method at 3.5 GHz for 5G Communication System

Lita Farahdiba<sup>1</sup>, Indra Surjati<sup>2</sup>, Syah Alam<sup>3</sup>, Raden Deiny Mardian<sup>4</sup>, Lydia Sari<sup>5</sup>, Teguh Firmansyah<sup>6</sup>, Zahriladha Zakaria<sup>7</sup>

1.2,3,4,5 Department of Electrical Engineering, Universitas Trisakti, West Jakarta, Indonesia, 11440
 6 Department of Electrical Engineering, Universitas Sultan Ageng Tirtayasa, Banten, Indonesia, 42117
 7 Faculty of Electronic and Computer Engineering and Technology, Universiti Teknikal Malaysia Melaka, Malaysia, 76100

#### **ARTICLE INFO**

#### **Article historys:**

Received: 24/06/2025 Revised: 15/08/2025 Accepted: 30/10/2025

#### **Keywords:**

2×1 Array, 5G Communication, Microstrip Antenna, Inset Feed, U-

#### **ABSTRACT**

This paper presents the design and realization of a 2×1 rectangular microstrip array antenna operating at 3.5 GHz for 5G communication systems. The design incorporates inset feed and U-slot techniques to improve antenna performance in terms of return loss, gain, and bandwidth. AWR Microwave Office 2009 was used for simulation, and iterative optimization was conducted on parameters such as feed position and slot dimensions. The final prototype achieves a return loss of –36.75 dB, a gain of 9.246 dB, a VSWR of 1.115, and a bandwidth of 169 MHz. These results demonstrate the effectiveness of combining array configuration, inset feed, and U-slot techniques for enhanced antenna characteristics.



This work is licensed under a Creative Commons Attribution 4.0 International License

#### Corresponding Author:

Syah Alam

Department of Electrical Engineering, Universitas Trisakti, West Jakarta, Indonesia, 11440

Email: syah.alam@trisakti.ac.id

#### 1. INTRODUCTION

The Fifth Generation (5G) of communication systems has marked a significant technological evolution since its introduction in 2017, offering extremely high data transfer speeds and much broader bandwidth compared to previous generations [1]. 5G technology enables the development of more advanced applications and enhances user experience across various sectors, including telecommunications, transportation, healthcare, and others. This generation of communication utilizes a wide range of frequency bands, such as the high band (28 GHz), mid band (15 GHz), and low band (3.5 GHz), as regulated by international standards [2].

In wireless communication systems, antennas play a vital role in transmitting and receiving signals, which are converted into electrical waves for voice and data communication [3]. One widely used antenna type in wireless systems is the microstrip antenna [4], known for its compact design, low fabrication cost, and capability to operate at high frequencies [5]. However, microstrip antennas also have limitations, such as low gain and directivity [6]. Despite these drawbacks, their compact form makes them suitable as receiving antennas in wireless communication systems. For reliable connectivity between transmitter and receiver, an antenna with optimal directionality and gain is required.

To address the gain limitation, this study focuses on enhancing microstrip antenna performance at 3.5 GHz using an array method, along with the application of inset and U-slot techniques. The array configuration increases the number of radiating elements, thereby enhancing gain and narrowing the



Volume 12, Issue 2, October 2025, pp. 190-202 ISSN 2355-5068; e-ISSN 2622-4852 **DOI:** 10.33019/jurnalecotipe.v12i2.4563

beamwidth for better signal direction. In addition, the inset feed and U-slot methods are employed to improve impedance matching, expand bandwidth, and reduce return loss and radiation pattern distortion. The combination of these techniques is expected to optimize antenna performance at 3.5 GHz in terms of gain and directional accuracy.

Previous studies [7] have attempted to design a 2x1 rectangular patch array antenna at 3.5 GHz but did not achieve satisfactory results in return loss, gain, or bandwidth. Another research [8] successfully designed a 1x2 rectangular patch array antenna for 5G communication at 3.5 GHz, but its parameters were still suboptimal. A different approach was presented in [9] using a 2x1 MIMO patch array with slit and inset-feed at 10 GHz, yet challenges remained in achieving the desired return loss, bandwidth, and gain. Therefore, the combination of U-slot and inset-feed techniques with a 2x1 array configuration is proposed to overcome these limitations and improve overall antenna performance [10].

This research aims to design a microstrip antenna operating at  $3.5 \, \text{GHz}$ , optimized using a 2x1 array to achieve high gain. Furthermore, the inset feed and U-slot methods are applied to reduce return loss to  $\leq$  -10 dB. As highlighted, 5G communication systems require microstrip antennas with optimal gain and directionality to ensure stable and effective connectivity. Therefore, improving microstrip antenna performance through these methods is the primary focus of this work, with the goal of meeting performance standards for 5G applications and enhancing efficiency and effectiveness at  $3.5 \, \text{GHz}$ .

#### 2. RESEARCH METHOD

This section describes the techniques and stages involved in designing the proposed microstrip antenna, including inset feed, U-slot, and 2×1 array methods. The entire research was conducted using full-wave electromagnetic simulation in AWR Microwave Office 2009 without physical fabrication. All performance parameters, including return loss, VSWR, gain, and bandwidth, were derived solely from simulation results.

#### 2.1. Inset Feed Technique

Inset feeding is a method used to connect the RF source to a microstrip patch antenna by introducing a notch into the patch, positioned away from the outer edge. [11] This approach is primarily employed to adjust the input impedance of the antenna so it aligns with the characteristic impedance of the feed line—typically 50  $\Omega$ —thereby minimizing return loss and enhancing feeding efficiency.

Determining the appropriate inset dimensions involves analyzing the variation of input impedance along the patch width, which tends to be highest at the edges and lowest at the center. The optimal inset position is selected at the point where the antenna's input impedance matches the feed line impedance. This location is identified through a combination of theoretical calculations, simulation results, and empirical models presented in relevant literature. Typically, the inset width equals the feed line width, while the inset length (Li) is fine-tuned through simulation.

#### 2.2. U-Slot Method

The U-slot technique modifies the patch by introducing a U-shaped slot into its surface. This approach is employed to enhance bandwidth and, in some cases, to adjust the radiation pattern or impedance matching. The slot dimensions and placement are optimized via simulation to avoid interference with the patch's fundamental resonant mode. The slot's width (W\_slot) and length (L\_slot) directly affect the resonance frequency and bandwidth, requiring precise tuning through iterative simulation.

#### 2.3. Antenna Design Stages

Figure 1 presents the design evolution of the proposed microstrip antenna, comprising the following stages: (a) a basic rectangular patch,(b) a patch with inset feed, and(c) a patch incorporating both inset feed and a U-slot modification.

- 1. Patch Dimension Calculation: The patch width (W) and length (L) were calculated using standard equations for a 3.5 GHz resonance frequency.
- 2. Antenna Modeling and Simulation: AWR Microwave Office 2009 was used to model and simulate the antenna, aiming for return loss values below –10 dB.

Volume 12, Issue 2, October 2025, pp. 190-202 ISSN 2355-5068; e-ISSN 2622-4852 **DOI:** 10.33019/jurnalecotipe.v12i2.4563

- 3. Inset Feed Implementation: This technique was applied to improve impedance matching and polarization, targeting an axial ratio below 3 dB.
- 4. 2×1 Array Configuration: The antenna was extended to a 2×1 array to enhance gain, with careful spacing between elements and preserved feeding structure.
- 5. Performance Evaluation: Key performance metrics—return loss, bandwidth, VSWR, and gain were evaluated for each configuration: rectangular, inset-fed, U-slot, and array.

To ensure simulation efficiency while maintaining result accuracy, the number of optimization iterations for key parameters (such as inset length and slot dimensions) was limited to three per configuration. This limitation was based on observed convergence trends, where performance metrics began stabilizing after the third iteration. Additional iterations were deemed unnecessary due to marginal expected improvements.

Through the systematic application of inset feeding and U-slot techniques, and careful simulation-based optimization, this study demonstrates the potential of the proposed 2×1 array antenna to fulfill the performance requirements of 5G communication systems.

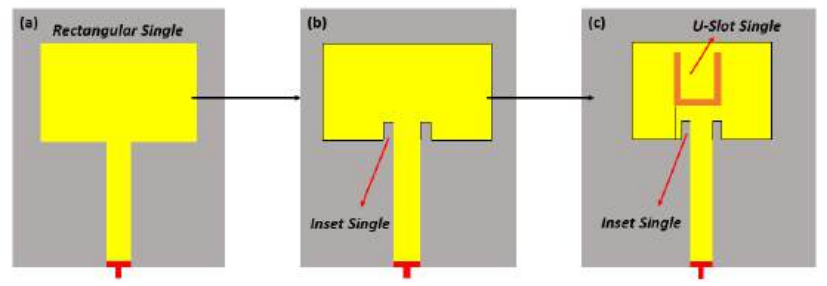


**Figure 1**. Microstrip antenna design development: (a) Rectangular Single, (b) Inset Single, (c) Inset Single with U-Slot

The simulated antenna was analyzed to evaluate its return loss, VSWR, gain, and bandwidth. The antenna uses an FR-4 substrate with a dielectric constant of 4.3, a thickness of 1.6 mm, and a loss tangent of 0.0265. The design is optimized to operate at a center frequency of 3.5 GHz.

#### 3. RESULTS AND DISCUSSION

#### 3.1 Antenna Design Parameters

In this study, the proposed microstrip antenna was designed to operate at a center frequency of 3.5 GHz, using the following substrate characteristics [12]:

Substrate type : FR4 Epoxy
 Substrate thickness : 1.6 mm
 Dielectric constant (ε<sub>r</sub>) : 4.3
 Loss tangent : 0.0265
 Operating frequency : 3.5 GHz

Based on the substrate parameters and the target resonant frequency, the dimensions of the initial rectangular single patch antenna were calculated using standard microstrip antenna design equations. The resulting patch width (W) and length (L) were 26.3 mm and 20.2 mm, respectively. These values served as the baseline for further design development.

The design process continued through a series of structural modifications—namely the implementation of inset feed, U-slot, and a 2×1 array configuration. These were introduced to overcome typical performance limitations found in single-element microstrip antennas, such as low gain, narrow bandwidth, and suboptimal return loss. While performance improvements were clearly observed in simulation results after each modification, this study does not delve into the detailed electromagnetic mechanisms that cause such improvements. The focus remains on the practical optimization of antenna design for 5G operation, rather than advancing new theoretical foundations.

Additionally, although inset feeding techniques can influence polarization characteristics, this study does not provide polarimetric results—such as axial ratio plots or polarization purity analysis—to

Volume 12, Issue 2, October 2025, pp. 190-202 ISSN 2355-5068; e-ISSN 2622-4852 **DOI:** 10.33019/jurnalecotipe.v12i2.4563

substantiate any claims related to polarization behavior. Therefore, statements regarding polarization improvement are qualitative in nature.

This research is centered on design optimization and simulated performance enhancement tailored for a specific application—namely 5G operation at 3.5 GHz—rather than on foundational scientific discovery or the introduction of novel concepts in electrical engineering.

#### 1. Patch Antenna Dimensions

The proposed microstrip antenna consists of a rectangular patch whose dimensions are calculated using the following standard formulas [13]:

$$W = \frac{C}{2f\sqrt{\frac{\varepsilon_r + 1}{2}}}\tag{1}$$

$$L = L_{eff} - 2\Delta L \tag{2}$$

$$L_{eff} = \frac{C}{2f\sqrt{\varepsilon_{eff}}} \tag{3}$$

$$\varepsilon_{eff} = \frac{\varepsilon_r + 1}{2} + \frac{\varepsilon_r - 1}{2} \left[ 1 + 12 \frac{h}{W} \right]^{-\frac{1}{2}} \tag{4}$$

$$\Delta L = 0.412h \frac{\left(\varepsilon_{eff} + 0.3\right) \left(\frac{W}{h} + 0.264\right)}{\left(\varepsilon_{eff} - 0.258\right) \left(\frac{W}{h} + 0.8\right)}$$

$$(5)$$

Where

C = Speed of light in vacuum  $(3 \times 10^8 \text{ m/s})$ 

h = Thickness of dielectric substrate (1.6 mm)

W = Patch width (mm)

L = Patch length (mm)

 $\varepsilon_r$  = Relative permittivity of the substrat

f = Resonant frequency (3.5 GHz)

#### 2. Inset Single Antenna Design

After calculating the patch dimensions, the feed line width was determined using transmission line theory to achieve impedance matching with a 50  $\Omega$  input. The equations used are [14]:

$$W = \frac{2h}{\pi} \left\{ B - 1 - \ln(2B - 1) + \frac{\varepsilon_r - 1}{2\varepsilon_r} \left[ \ln(B - 1) + 0.39 - \frac{0.61}{\varepsilon_r} \right] \right\}$$
 (6)

$$B = \frac{60\pi^2}{Z_0 \sqrt{\varepsilon_{eff}}} \tag{7}$$

Where:

B = Impedance constant

 $Z_0$  = Desired impedance (typically 50  $\Omega$ )

h = Substrate thickness (1.6 mm)

#### 3. Spacing Between Antenna Elements

To implement the  $2\times1$  array configuration and enhance the gain, the spacing between the two antenna elements (d) was calculated based on the following [10]:

$$\lambda = \frac{C}{f} \tag{8}$$

**DOI:** 10.33019/jurnalecotipe.v12i2.4563

$$d = \frac{\lambda}{2} \tag{9}$$

Where:

 $\lambda$  = Wavelength at 3.5 GHz

C =Speed of light (3 × 10 $^8$  m/s)

d = Spacing between patch elements (mm)

#### 3.2 Antenna Simulation and Optimization Process

The antenna design process was carried out through several systematic stages using electromagnetic simulation software AWR Microwave Office 2009. Each stage involved parameter optimization to enhance performance at the operating frequency of 3.5 GHz. All results presented are based exclusively on simulation data; no physical fabrication or measurement was conducted.

#### 1. Process Rectangular Single Microstrip Antenna Design

The initial design began with a conventional rectangular microstrip patch antenna as a baseline. The physical structure is illustrated in Figure 2(a), with key dimensions listed in Table 1. The antenna was designed using standard formulas for width (W) and length (L) of the patch, based on the chosen substrate (FR-4,  $\varepsilon r = 4.3$ , h = 1.6 mm).

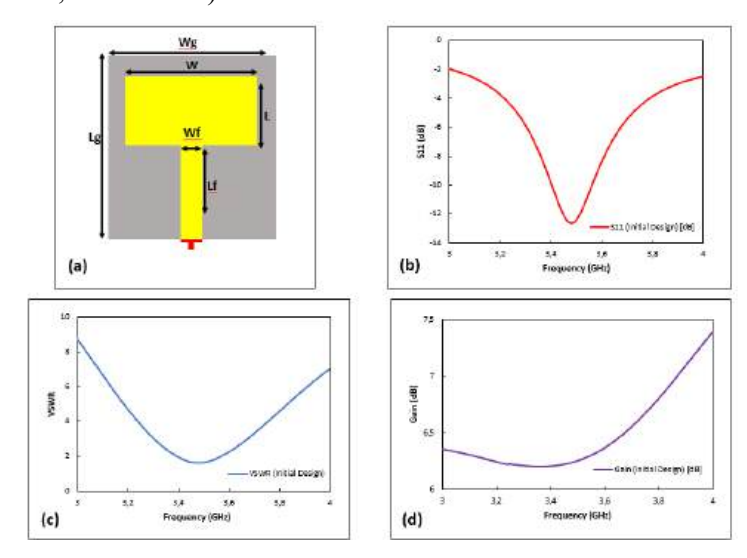


**Figure 2**. (a) Structure of the Rectangular Single Microstrip Antenna, (b) Return Loss Simulation Result, (c) VSWR Simulation Result, (d) Gain Simulation Result.

 Table 1. Dimensions of the Rectangular Single Microstrip Antenna

Parameter	Description	Dimension (mm)
Wg	Enclosure width	50
Lg	Enclosure length	50
W	Patch width	26,3
L	Patch length	20,2
Wf	Feed line width 3,1	
Lf	Feed line length	20

Simulation results in Figures 2(b)-(d) show that the antenna operates at 3.5 GHz with a return loss of -12.67 dB, a bandwidth of 160 MHz, a VSWR of 1.626, and a gain of 5.702 dB.

Volume 12, Issue 2, October 2025, pp. 190-202 ISSN 2355-5068; e-ISSN 2622-4852 **DOI:** 10.33019/jurnalecotipe.v12i2.4563

2. Inset-Fed Single Microstrip Antenna Design

To improve impedance matching and reduce return loss, an inset notch was introduced to the rectangular patch. The key variable optimized in this stage was the inset length ( $\Delta Y$ ). Three simulations were conducted with  $\Delta Y$  values of 4 mm, 5 mm, and 6 mm. Table 2 and Figures 3(b)-(d) present the results:

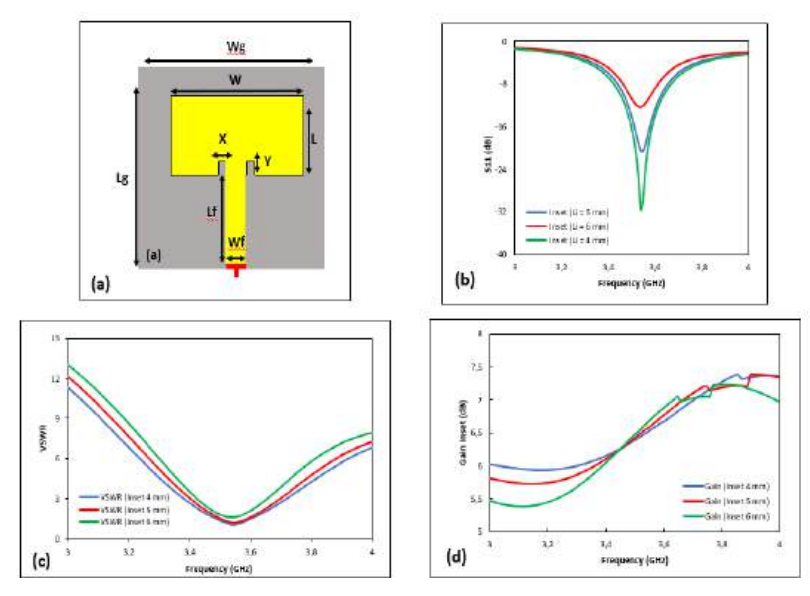


**Figure 3.** (a) Structure of the Inset-Fed Single Microstrip Antenna, (b) Return Loss Simulation Result, (c) VSWR Simulation Result, (d) Gain Simulation Result

Iteration **Parameter**  $\Delta Y$ Return Loss (dB) Bandwidth (MHz) Gain (dB) **VSWR** *Y*₁ Iteration -31,61 190 6,383 1,367 Y<sub>2</sub> Iteration -20,65 161 6,422 1,485 5  $Y_3$  Iteration -12,3595 6,48 1,87

Table 2. Simulation Results for Inset-Fed Single Microstrip Antenna

• The best performance was achieved at  $\Delta Y = 4$  mm, with return loss = -31.61 dB, bandwidth = 190 MHz, gain = 6.383 dB, and VSWR = 1.367.

This demonstrates that adding an inset feed can significantly enhance the impedance match and widen the bandwidth.

#### 3. Inset-Fed Single Microstrip Antenna with U-Slot

To further improve gain and bandwidth, a U-slot was introduced at the center of the patch. The slot dimensions were optimized through three iterations ( $\Delta C = 4$  mm, 5 mm, 6 mm). This slot serves to perturb the surface current, enhancing radiation efficiency.

The optimal result was found at  $\Delta C = 6$  mm with:

- Return loss = -14.01 dB
- Bandwidth = 132 MHz
- VSWR = 1.494

6

• Gain = 6.123 dB

Figures 4(b)-(d) and Table 4 show how the U-slot improves performance compared to the plain inset-fed design.

**DOI:** 10.33019/jurnalecotipe.v12i2.4563

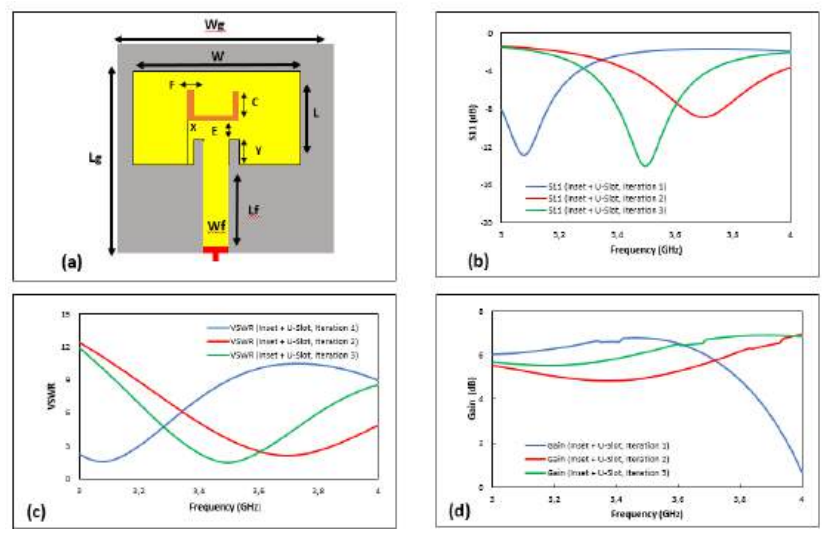


**Figure 4.** (a) Structure and Dimensions of the Inset-Fed and U-Slot Single Microstrip Antenna, (b) Return Loss Simulation Result, (c) VSWR Simulation Result, (d) Gain Simulation Result

Table 4. Simulation Results of the Inset-Fed and U-Slot Single Microstrip Antenna

	Parameter										
Iteration ∆C	Return Loss (dB)	Bandwidth (MHz)	VSWR	Gain (dB)							
Iteration 8	-12,76	104	9	6,673							
Iteration 5	-5,78	-	3,544	4,961							
Iteration 6	-14,01	132	1,494	6,123							

As presented in Table 4, the integration of inset feed and U-slot techniques in the microstrip antenna design resulted in notable enhancements in return loss, VSWR, and gain. The optimal performance was recorded at  $\Delta C = 6$  mm, where the antenna operating at 3.5 GHz achieved a return loss of –14.01 dB, a bandwidth of 132 MHz, a VSWR of 1.494, and a gain of 6.123 dB.

#### 4. 2×1 Inset-Fed Microstrip Antenna Array Design

To boost gain further, a  $2\times1$  antenna array configuration was developed. Two identical inset-fed patches were arranged with a spacing of  $\lambda/2$ . The patch dimensions were reduced to maintain resonance at 3.5 GHz.

The simulation results show:

- Return loss = -18.49 dB
- Bandwidth = 186 MHz
- VSWR = 1.268
- Gain = 8.627 dB

As seen in Table 5 and Figures 5(b)-(d), the array design improves gain compared to single-element antennas.

**DOI:** 10.33019/jurnalecotipe.v12i2.4563

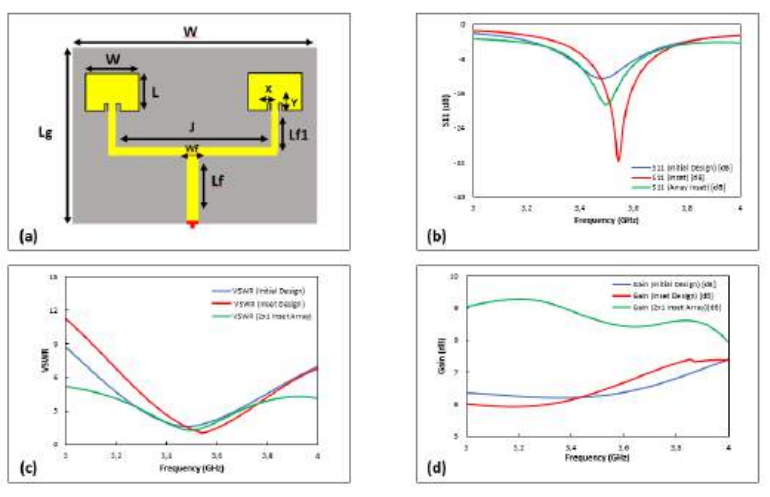


Figure 5. (a) Structure and Dimensions of the 2×1 Inset-Fed Microstrip Antenna Array, (b) Return Loss Simulation Result, (c) VSWR Simulation Result, (d) Gain Simulation Result

Table 5. Simulation Results for the 2×1 Inset-Fed Microstrip Antenna Array

Design Type	Parameter										
Design Type	Return Loss (dB)	Bandwidth (MHz)	VSWR	Gain (dB)							
Rectangular Single	-12,67dB	160	1,626	5,702							
Inset Single	-31,61	190	1,367	6,383							
Array Inset	-18,49	186	1,268	8.627							

Table 5 demonstrates that the 2×1 inset-fed array antenna design successfully improves the gain, while the addition of slits contributes to reducing return loss and axial ratio. The best performance is observed at an inset length of X = 3 mm, achieving a return loss of -18.49 dB, bandwidth of 186 MHz, VSWR of 1.268, and gain of 8.627 dB at 3.5 GHz.

#### 2×1 Inset-Fed Microstrip Antenna Array with U-Slot

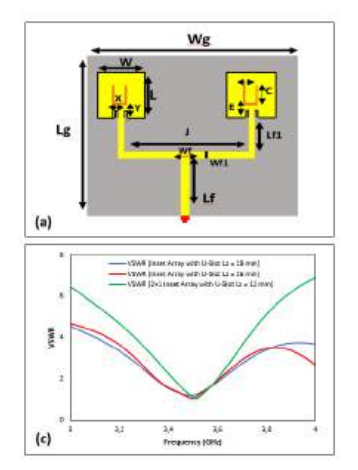
The final configuration combines the 2×1 array structure with U-slot on each patch. Patch and slot dimensions were optimized across three iterations ( $\Delta E = 1 \text{ mm}, 2 \text{ mm}, 3 \text{ mm}$ ).

The optimal performance was achieved at  $\Delta E = 3$  mm:

- Return loss = -36.75 dB
- Bandwidth = 169 MHz
- VSWR = 1.115
- Gain = 9.246 dB

These results, summarized in Table 6 and Figures 6(b)-(d), confirm that combining array configuration and U-slot modification yields significant improvement in gain and return loss.

**DOI:** 10.33019/jurnalecotipe.v12i2.4563



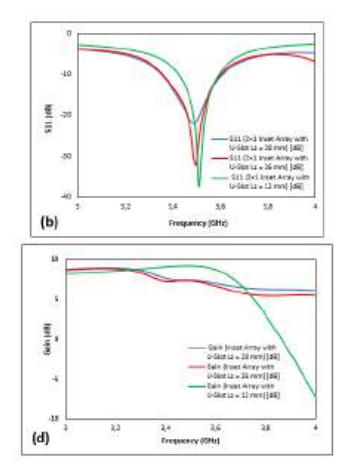


**Figure 6.** (a) Structure and Dimensions of the 2×1 Inset-Fed and U-Slot Microstrip Antenna Array, (b) Return Loss Simulation Result, (c) VSWR Simulation Result, (d) Gain Simulation Result

Iteration	Parameter									
$\Delta \mathbf{E}$	Return Loss (dB)	Bandwidth (MHz)	VSWR	Gain (dB)						
Iteration 1	-21,57	259	1,186	7,420						
Iteration 2	-32,12	245	1,05	7,392						
Iteration 3	-36,75	169	1,115	9,246						

Table 6. Simulation Results for the 2×1 Inset-Fed and U-Slot Microstrip Antenna Array

As shown in Table 6, the implementation of a  $2\times1$  microstrip antenna array with inset feed and U-slot integration significantly improves the antenna's gain performance. Furthermore, the addition of the U-slot contributes to a reduction in return loss and VSWR. The optimal performance was recorded in the third iteration ( $\Delta E = 3$  mm), achieving a return loss of -36.75 dB, a bandwidth of 169 MHz, a VSWR of 1.115, and a gain of 9.246 dB at the operating frequency of 3.5 GHz.

#### 3.3 Antenna Simulation Analysis

Upon completion of all design and simulation phases, the analysis of key performance parameters—including return loss, VSWR, gain, and bandwidth—demonstrates that the integration of inset feeding, U-slot modification, and a  $2\times1$  array configuration substantially enhances the overall performance of the microstrip antenna.

#### 1. Inset Length Determination Process

Figure 7 and Table 7 provide a comparative overview of the return loss simulation results across the different antenna designs evaluated in this study.

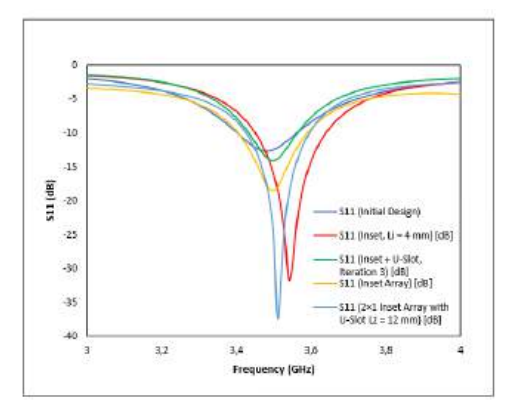


Figure 7. Comparison of Return Loss Simulation Results for Antenna Designs

Volume 12, Issue 2, October 2025, pp. 190-202 ISSN 2355-5068; e-ISSN 2622-4852 **DOI:** 10.33019/jurnalecotipe.v12i2.4563

Table 7. Comparison of Return Loss and Bandwidth Simulation Results

Antenna Design	Return loss (dB)	Bandwidth (MHz)
Rectangular Patch Single	-12,67	160
Inset Single	-31,61	190
Inset dan U-Slot Single	-14,01	132
Array 2x1 Inset	-18,49	186
Array 2x1 Inset dan U-Slot	-36,75	169

The integration of the inset feed and U-slot techniques in the 2×1 array configuration significantly reduces return loss and enhances bandwidth. The improvement in return loss is likely due to better impedance matching and increased surface current path introduced by the U-slot structure, which minimizes reflection. Meanwhile, the bandwidth enhancement can be attributed to the multiple resonant modes enabled by the slot, which broadens the frequency response [15].

Return Loss Reduction = 
$$\frac{-36,75 - (-12,76)}{-12,76} \times 100\% = 188\%$$

Bandwidth Improvement 
$$=\frac{169-(160)}{160} \times 100\% = 5,625\%$$

#### 2. VSWR Analysis

Figure 8 and Table 8 compare the VSWR simulation results of the designed antennas.

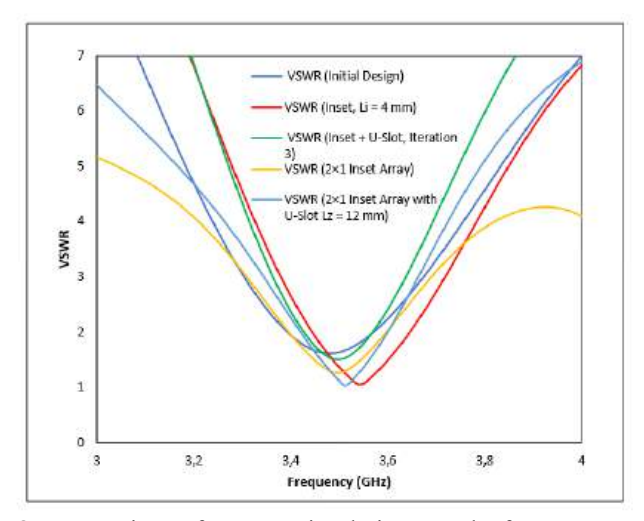


Figure 8. Comparison of VSWR Simulation Results for Antenna Designs

Table 8. Comparison of VSWR Simulation Results

Antenna Desgin	VSWR
Rectangular Patch Single	1,626
Inset Single	1,367
Inset dan U-Slot Single	1,494
Array 2x1 Inset	1,268
Array 2x1 Inset dan U-Slot	1,115

The 2×1 Inset and U-Slot Array achieves the lowest VSWR value of 1.115. This result indicates excellent impedance matching between the feed line and the antenna, which contributes to higher transmission efficiency and minimal signal reflection [16][17].

Volume 12, Issue 2, October 2025, pp. 190-202 ISSN 2355-5068; e-ISSN 2622-4852 **DOI:** 10.33019/jurnalecotipe.v12i2.4563

VSWR Reduction = 
$$\frac{1,115 - (1,626)}{1,626} \times 100\% = -31.42\%$$

#### 3. Gain Analysis

Figure 9 and Table 9 present a comparison of gain simulation results from the antenna designs.

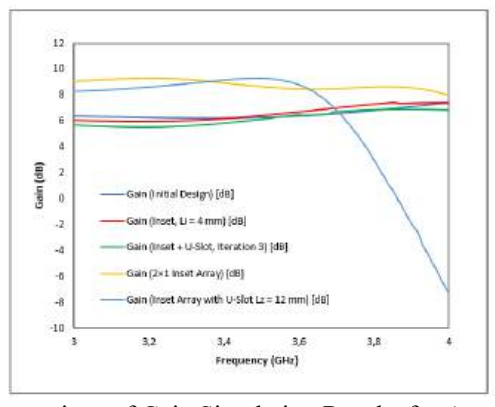


Figure 9. Comparison of Gain Simulation Results for Antenna Designs

Table 9. Comparison of Antenna Gain

Antenna Design	Gain (dB)
Rectangular Patch Single	5,702
Inset Single	6,383
Inset dan U-Slot Single	6,123
Array 2x1 Inset	8,627
Array 2x1 Inset dan U-Slot	9,246

The 2×1 Inset and U-Slot Array provides the highest gain of 9.246 dB. This enhancement in gain is attributed to the array configuration that increases the effective aperture, as well as the U-slot that contributes to better radiation efficiency by shaping current distribution on the patch [18],[19],[20].

Gain Improvement = 
$$\frac{9,246 - (5,702)}{5,702} \times 100\% = 62,15\%$$

#### 4. Comparison with Previous Research

Table 10 presents a comparative analysis between the results obtained in this study and those reported in previous research works.

Table 10. Comparison with Previous Research

Reference	Method	Resonant Frequency	S11 (dB)	VSWR	Bandwidth (MHz)	Gain (dB)	Polarization	Patch Dimensions (mm)
[7]	Rectangular Patch Array 2x1 with Inset & Slit (2)	3.5 GHz	-24	<2	360	10	Unknown	28.3 x 35
[8]	Rectangular Patch Array 1x2 for 5G Communicatio n (1)	3.5 GHz	-12.54	1.6	66.5	5.5	Vertical or Unidirectional	19.5 x 26.5
[9]	MIMO Patch Array 2x1 with Slit & Inset	3.5 GHz	-25	≤2	220	≥6	Directional	35 x 28.3
This Research	Rectangular Patch 2x1 with Inset & U-Slot	3.5 GHz	-36.75	1.115	169	9.246	Unidirectio-nal	18.2 x 22.3

Volume 12, Issue 2, October 2025, pp. 190-202 ISSN 2355-5068; e-ISSN 2622-4852 **DOI:** 10.33019/jurnalecotipe.v12i2.4563

This comparison reveals that the proposed 2×1 array antenna using inset feed and U-slot techniques achieves a significantly better return loss and gain compared to the references, with competitive VSWR and bandwidth. However, it is important to note that polarization characteristics (such as axial ratio or polarization purity) were not simulated. Although the gain improvement may suggest improved radiation behaviour, future research should include explicit polarization analysis to validate this claim.

#### 4. CONCLUSION

The determination of the inset length and the progressive optimization of the microstrip antenna design across multiple stages have demonstrated substantial performance enhancements. Simulation outcomes validate the adoption of the inset feed, U-slot, and 2×1 array configuration as effective strategies for achieving optimal values in return loss, VSWR, gain, and bandwidth, while also contributing positively to radiation behavior.

The finalized 2×1 microstrip antenna array, operating at 3.5 GHz with inset feed and U-slot integration, achieved a return loss of –36.75 dB, a gain of 9.246 dB, a VSWR of 1.115, and a bandwidth of 169 MHz. These results confirm the antenna's suitability for 5G communication systems, offering improved gain and directivity in line with modern microstrip antenna requirements.

#### References Acknowledgement

This research was funded by the Research and Community Services Institute of Universitas Trisakti in collaboration with the Ministry of Research, Technology, and Higher Education of the Republic of Indonesia, through a competitive research grant under the Postgraduate Research Scheme for the 2025 fiscal year, under contract numbers 124/C3/DT.05.00/PL/2025 and 1014/LL3/AL.04/2025.

#### REFERENCES

- [1] M. Höyhtyä, O. Apilo, dan M. Lasanen, "Review of latest advances in 3GPP standardization: D2D communication in 5G systems and its energy consumption models," Futur. Internet, vol. 10, no. 1, 2018, doi: 10.3390/fi10010003.
- [2] A. Hikmaturokhman, K. Ramli, dan M. Suryanegara, "Spectrum considerations for 5G in Indonesia," Proceeding 2018 Int. Conf. ICT Rural Dev. Rural Dev. through ICT Concept, Des. Implic. IC- ICTRuDEv 2018, 2018, hlm. 23–28, doi: 10.1109/ICICTR.2018.8706874.
- [3] S. Alam dan I. Wibisono, Pengantar Antena dan Propagasi: Konsep Dasar dan Teori, vol. 45. DKI Jakarta: UTA 45 Jakarta Press, 2017.
- [4] I. Surjati, Antena Mikrostrip: Konsep dan Aplikasinya. DKI Jakarta: Universitas Trisakti, 2010.
- [5] M. Alaydrus, "Riset antena State of the art," J. Telekomun. dan Komput., vol. 6, no. 1, hlm. 1, 2017. doi: 10.22441/incomtech.v6i1.1146.
- [6] D.-G. Fang, Antenna Theory and Microstrip Antennas. CRC Press, 2017.
- [7] A. Anindito, A. Putranto, I. Surjati, S. Alam, L. Sari, and R. Vaswani, "Desain Antena Mikrostrip Array 2x1 Elemen dengan Teknik Inset dan Slit untuk Sistem Komunikasi 5G," J. Telemat., vol. 16, no. 1, pp. 18–24, 2021.
- [8] Fahrul Solehudin1), Zikra Aulia 2), Syah Alam 3)\*, Lydia Sari 4) & Indra Surjati 5), ''Design of 2x1 MIMO Microstrip Antenna Using Slit and Inset Technique For 5G Communication,''
  JITE (Journal of Informatics and Telecommunication Engineering), 2021.
- [9] Rissa Rahmania 1, Heroe Wijanto 2, Pamungkas Daud, "PERANCANGAN DAN REALISASI ANTENA MIKROSTRIP ARRAY INSET-FED REKTANGULAR DENGAN U-SLOT UNTUK APLIKASI RADIO OVER FIBER PADA FREKUENSI 10 GHZ," e-Proceeding of Engineering: Vol.2, No.3, Desember 2015.
- [10] N. Aulia and Elisma, "Desain Antena Mikrostrip Array 2x4 dengan Teknik Pencatuan Proximity

**DOI:** 10.33019/jurnalecotipe.v12i2.4563

- Coupled untuk Aplikasi 5G pada Frekuensi 2, 6 GHz," *Pros. 12th Ind. Res. Work. Natl. Semin.*, pp. 717–723, 2021.
- [11] R. B. Putra, S. Alam, and I. Surjati, "Perancangan Antena Mikrostrip Segiempat Peripheral Slit untuk Aplikasi 2,4Ghz dengan Metode Pencatuan Proximity Coupled," *J. Nas. Tek. Elektro*, vol. 7, no. 1, p. 38, 2018, doi: 10.25077/jnte.v7n1.520.2018.
- [12] S. Alam, N. Media Rizka, I. Surjati, P. Dewi Marlina, and G. Tjahjadi, "Desain Antena Mikrostrip dengan Multi Band Frekuensi Menggunakan Metode Parasitik," *J. Tek. Media Pengemb. Ilmu dan Apl. Tek.*, vol. 19, no. 01, pp. 18–23, 2020.
- [13] C. Andrieyani, B. Sumajudin, and T. Yunita, "Perbandingan Antena Mikrostrip Array Dual Band Dengan Pencatuan Microstrip Line Dan Electromagnetically Coupled (Emc)," *TEKTRIKA J. Penelit. dan Pengemb. Telekomun. Kendali, Komputer, Elektr. dan Elektron.*, vol. 5, no. 1, p. 19, 2020, doi: 10.25124/tektrika.v5i1.3241.
- [14] W. Kristanto *et al.*, "Perancangan Antena Microstrip Patch Multi Band," *J. Kajain Tek. Elektro*, vol. 3, no. 1, pp. 72–82, 2019.
- [15] K. L. Wong, Compact and Broadband Microstrip Antennas, John Wiley & Sons, 2002.
- [16] J. D. Kraus and R. J. Marhefka, Antennas for All Applications, 3rd ed., McGraw-Hill, 2002.
- [17] M. R. Ahsan, M. I. Hossain, M. T. Islam, dan M. R. I. Faruque, "Compact U-Slot Microstrip Patch Antenna for 5G Application," Wireless Personal Communications, vol. 102, no. 1, pp. 229–243, 2018. doi: 10.1007/s11277-017-4916-2
- [18] N. M. Din, M. F. Ain, dan N. H. Osman, "Design and Analysis of a 2x1 MIMO Microstrip Patch Antenna Array for 5G Applications," International Journal of Microwave and Wireless Technologies, vol. 13, no. 6, pp. 601–608, 2021.
- [19] A. Ullah, M. S. Sharawi, dan R. Mittra, "A Review of MIMO Antennas for 5G mmWave Communications," Micromachines, vol. 10, no. 11, p. 1530, 2019. doi: 10.3390/mi10101530
- [20] S. M. Moghaddam, M. K. A. Rahim, dan M. F. Ain, "2×1 Patch Antenna Array with High Gain for 5G Applications," IEEE Access, vol. 7, pp. 19000–19008, 2019.

**DOI:** 10.33019/jurnalecotipe.v12i2.4576

### **Integration of AI Models and Extreme Programming for Retail Price Prediction and Inventory Optimization**

Sapta Eka Putra<sup>1</sup>, Yularni Putri<sup>2</sup>, Faizal Burhani Ulil Fathan<sup>3</sup>

1,2 Retail Management, Universitas Tamansiswa, Jl. Taman Siswa No.9, Padang, 25171, Indonesia

Biomedical Engineering, Telkom University, Jl. DI Panjaitan No.128, Purwokerto, 53147, Indonesia

#### ARTICLE INFO

#### Article historys:

Received: 14/08/2025 Revised: 01/09/2025 Accepted: 30/10/2025

#### **Keywords:**

Artificial Intelligence; Extreme Programming; Price Forecasting, Retail Management; Stock Optimization

#### **ABSTRACT**

Food prices in modern retail are highly volatile and complex inventory management is often an obstacle to maintaining operational efficiency. The research developed Smart Retail AI, an artificial intelligence-based application that integrates Long Short-Term Memory (LSTM) for price prediction and Extreme Gradient Boosting (XGBoost) for stock optimization. The software development method uses the Agile Extreme Programming (XP) approach, which emphasizes rapid iteration, user engagement, and continuous testing. The test results showed that all application features worked according to the specifications through Black Box Testing, while the usability test using the System Usability Scale (SUS) resulted in an average score of 87 (Excellent category). These findings confirm that the app has high reliability and an excellent level of ease of use. The novelty of the research lies in the direct integration of AIbased predictive models into real operational retail applications with the XP cycle, thus bridging the gap between algorithmic research and practical application. Overall, Smart Retail AI contributes to improving decisionmaking efficiency, operational responsiveness, and business sustainability in the modern retail ecosystem.



This work is licensed under a Creative Commons Attribution 4.0 International License

#### **Corresponding Author:**

Sapta Eka Putra

Retail Management, Universitas Tamansiswa, Jl. Taman Siswa No.9, Padang, 25171, Indonesia

Email: saptaeka54putra@gmail.com

#### **INTRODUCTION**

The rapid transformation in retail business models in the digital age has demanded profound changes in consumer behavior as well as in supply chain management strategies [1-3]. Modern retail, which relies on digital platform integration, real-time data analytics, and decision-making automation, needs systems that can provide accurate predictive information to maintain operational efficiency and maintain a competitive advantage [4-6]. On the other hand, the food sector is facing high challenges due to extreme commodity price volatility and complex inventory management. Price fluctuations are triggered by seasonal conditions, disruptions in supply chains, and sudden changes in demand patterns, resulting in difficulties in setting optimal stock levels without disrupting profit margins [7], [8]. This situation indicates the need for the application of artificial intelligence-based technology, which has the potential to support faster and more precise decision-making.

Artificial intelligence (AI) is increasingly recognized as a strategic solution to prediction and optimization challenges, including in the retail realm [9], [10]. Machine learning methods, such as Long Short-Term Memory (LSTM) and Extreme Gradient Boosting (XGBoost), have shown high

**DOI:** 10.33019/jurnalecotipe.v12i2.4576

performance in time series forecasting and predictive analytics in research contexts [11]. Nonetheless, some of the research has tended to focus on model development and evaluation of accuracy in offline scenarios, ignoring the move to the integration stage into an operational and ready-to-use application system in a real-world context.

Previous research has provided an important foundation for this study. The Long Short-Term Memory (LSTM) model shows superior ability to predict e-grocery demand compared to traditional methods, but it has not yet been integrated into daily operations. Decision tree-based methods such as XGBoost show excellent performance when tested on physical retail data, but they do not yet have an end-user accessible interface. The combination of LSTM and LightGBM, accompanied by pre-processing techniques, does result in higher precision, but all of that exploration is boxed into a simulated environment. Some studies compare standard-models with hybrid models such as Random Forest, XGBoost, and Linear Regression; Despite the high accuracy, the relationship between the findings and real use in retail applications has not been established. Finally, studies of the Extreme Programming (XP) methodology have shown a positive impact on improving software quality through rapid development cycles and continuous testing, but the application of this methodology to the development of AI-based systems in contemporary retail is still minimal.

From the overall review above, it can be seen that the gaps that need to be filled in further research:

- a. the development of AI models remains separate from integration in the operational environment,
- b. the application of the XP methodology to AI-based retail systems has not been expanded, and
- c. the evaluation of the system is holistic, measuring the accuracy of predictions, system performance, and user satisfaction levels in a single research frame, almost unfounded.

To answer this gap, this study proposes the development of price prediction and food stock optimization applications for modern retail, utilizing artificial intelligence and Agile software development methods based on Extreme Programming. The designed application will integrate Albased prediction models into a ready-to-operate system, through responsive development cycles, rapid prototyping, continuous testing, and active user participation at every stage. With this approach, this study aims to strengthen the application of artificial intelligence in modern retail, while improving operational efficiency, competitiveness, and corporate sustainability.

#### 2. RESEARCH METHOD

This study uses the Extreme Programming (XP) method, which is one of the approaches in the framework of Agile Software Development. The choice of the XP method is based on its characteristics that are able to speed up the development process through short iterations, active user engagement, rapid prototyping, and continuous testing. This approach is particularly suitable for the development of applications that require accurate predictions based on artificial intelligence as well as adaptability to changing user needs in the modern retail sector. This research stage is designed to ensure that the process runs systematically, starting from problem identification to evaluation of implementation results. In general, the stages of research include:

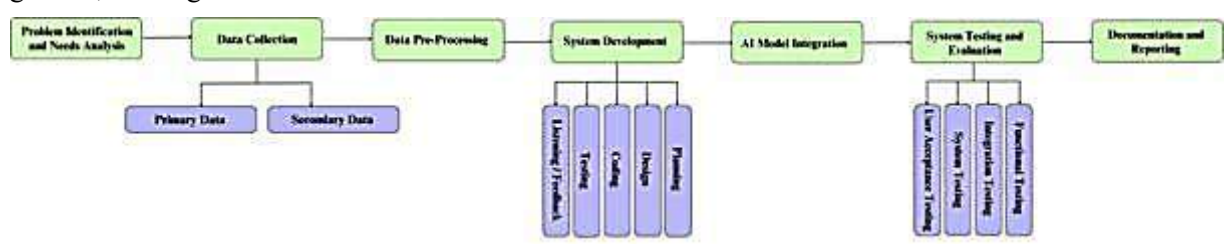


Figure 1. Research Methodology

#### 2.1. Problem Identification and Needs Analysis

This initial stage aims to understand the problems faced by modern retailers, especially related to food price fluctuations and stock management. The identification process is carried out through literature studies, interviews with stakeholders, and analysis of ongoing business processes. The resulthis is how

**DOI:** 10.33019/jurnalecotipe.v12i2.4576

to start a subsection of this stage is a list of core problems and opportunities for the development of artificial intelligence- based systems.

#### 2.2. Data Collection

Data collection techniques include interviews and documentation, so that the information obtained includes both practical perspectives from the field and measured historical data. The data used consisted of:

- 1. Primary data: collected through in-depth interviews with retail managers, warehouse managers, and operational staff to obtain information about system requirements, stock workflows, and pricing policies.
- 2. Secondary data: obtained from historical sales documents, inventory records, price fluctuation reports, as well as scientific literature and online sources relevant to the study.

#### 2.3. Pre-Processing Data

The data that has been collected is processed through the stages of data cleaning, normalization, and feature encoding. At this stage, datasets are also shared for AI model training and testing.

#### 2.4. System Development

Application development is carried out using the Agile Software Development method using the Extreme Programming (XP) approach. This approach was chosen because it is able to accommodate rapidly changing user needs, facilitate iterative prototyping, and implement continuous testing.

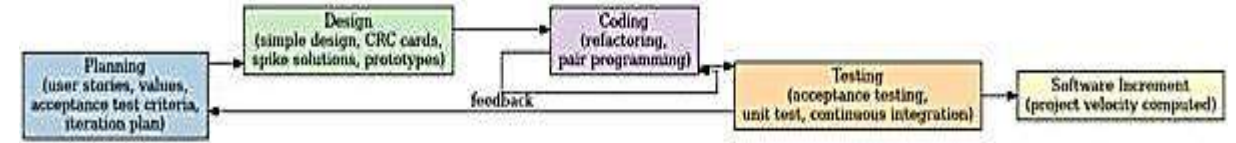


Figure 2. Extreme Programming

The XP stages applied include [19]:

- 1. Planning, identifying user stories, feature priorities, and iteration targets.
- 2. Design, designing system architecture and user interface.
- 3. Coding, code implementation with pair programming and code review.
- 4. Testing, unit testing, integration, and performance of AI models in each iteration.
- 5. Listening/Feedback, evaluation with users for feature improvements.

#### 2.5. AI Model Integration

The artificial intelligence model used combines Long Short-Term Memory (LSTM) algorithms for price forecasting and Extreme Gradient Boosting (XGBoost) for price factor analysis as well as stock optimization. The trained model is integrated into the application backend so that it can be accessed in real-time by the user.

#### 2.6. System Testing and Evaluation

Testing is carried out to ensure that the application developed is in accordance with the needs and specifications that have been set at the planning stage. Testing focuses on aspects of software development, which include:

- 1. Functional Testing ensuring that each app's feature works according to the agreed user stories.
- 2. Integration Testing verifies that all system components, including the user interface, backend, and database, are connected to each other and work without errors.
- 3. System Testing evaluates the overall performance of an application in a usage scenario that resembles real conditions in a modern retail environment.

User Acceptance Testing (UAT) – involves the end user to ensure that the application meets expectations and can be used effectively in day-to-day operations.

**DOI:** 10.33019/jurnalecotipe.v12i2.4576

#### 2.7. Documentation and Reporting

The final stage is the preparation of technical documentation and research reports, which include analysis of results, discussion of contributions, and recommendations for further development.

#### 3. RESULTS AND DISCUSSION

This section presents the results of the development of artificial intelligence-based applications for price prediction and optimization of modern retail food stocks. The methodology used is Agile Software Development with an Extreme Programming (XP) approach. This approach was chosen for its ability to respond quickly to changing user needs, maintain software quality through continuous testing, and accelerate release cycles with short iterations. The development stages follow the main cycle of XP: planning, design, coding, and testing with stakeholders directly involved in each step. The finish not only meets functional specifications, but also demonstrates a high level of usability in the context of modern retail operations.

#### 3.1 Planing

The planning stage is focused on identifying system needs through the creation of user stories from the perspective of the Operational Manager, Procurement/Purchasing Team, and Warehouse Manager. The activity was carried out through interviews and discussions with stakeholders to explore the workflow, problems faced, as well as priority features such as AI-based food price prediction, automated stock optimization, purchase request management, supplier data management, and critical stock notifications. In addition, acceptance test criteria are prepared as a reference for feature acceptance and an iteration plan that divides development into weekly cycles. The result of this stage is a planning document containing a list of user stories, development priorities, iteration schedules, and acceptance criteria for each feature.

#### 3.2 Design

At this stage, a use case diagram was designed to map the interaction between actors and system features, an activity diagram was created to describe the main process flow, a database table was compiled to support data management, and wireframe was created as an initial prototype of the user interface. This design ensures that all system components are well-structured and aligned with the user's needs. Figure 3 is a use case diagram that illustrates the relationship between the main actors and the system functions.

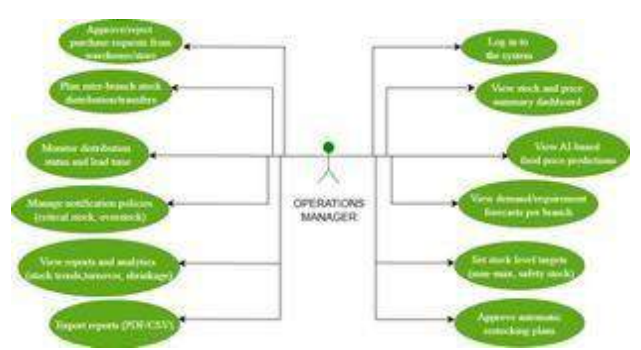


Figure 3. Use Case Diagram Operation Manager

Figure 3 is a use case diagram that shows the interaction between Operations Manager and the system. These actors have a critical role in monitoring and controlling retail operations, from the login process to strategic decision management. Accessible functions include viewing a stock and price summary dashboard, monitoring AI-based price predictions, viewing estimated needs per branch, setting target stock levels (minimum, maximum, and safety stock), and approving an automatic restocking plan. In addition, Operations Manager can set notification policies (e.g. critical stock or overstock), monitor distribution status and delivery times, plan distributions between branches, and generate reports in various formats such as PDF or CSV for further analysis. The next use case diagram is Procurement / Purchasing Team.

Volume 12, Issue 1, October 2025, pp. 203-214 ISSN 2355-5068; e-ISSN 2622-4852 **DOI:** 10.33019/jurnalecotipe.v12i2.4576

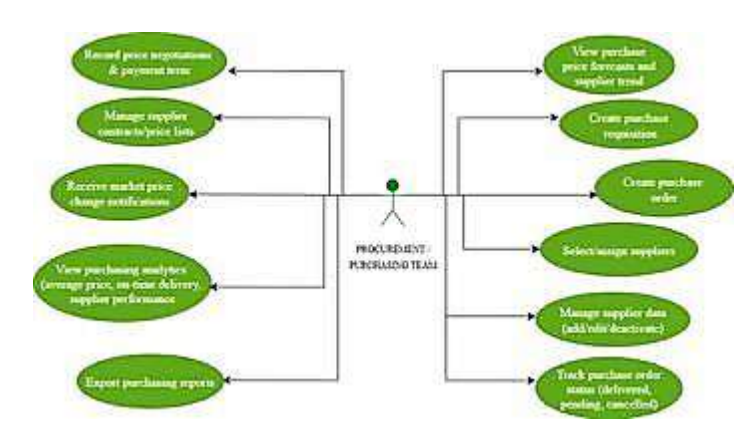


Figure 4. Use Case Diagram Procurement

The use case diagram above illustrates the role of the Procurement/Purchasing Team in managing the entire purchasing process, starting from looking at purchase price predictions and supplier trends, making purchase requisition and purchase orders, selecting and assigning suppliers, to managing supplier data. This team is also tasked with tracking the status of purchase orders (delivered, pending, cancelled), recording price negotiations and payment terms, managing contracts or supplier price lists, and receiving notifications of market price changes. Additionally, teams can view purchasing analytics such as average prices, delivery timeliness, and supplier performance, as well as export purchase reports for evaluation.

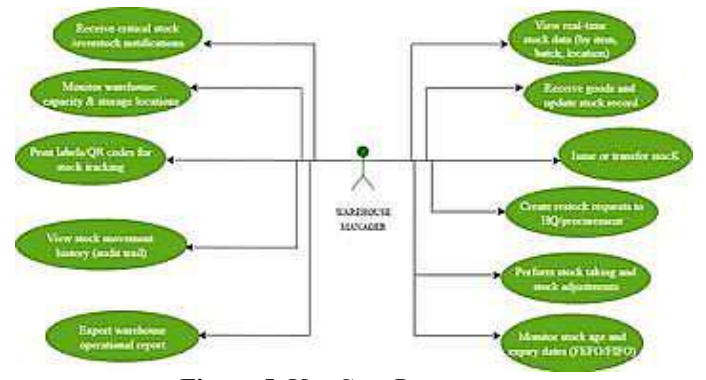


Figure 5. Use Case Procurement

The Warehouse Manager use case diagram shows all the key interactions for managing physical stock in the warehouse: from viewing real-time stock data (by item, batch, location), receiving goods and updating stock records, to issuing or transferring stock as per operational needs. This role can also make restock requests to the center/procurement, conduct stock taking and stock adjustments, and monitor stock age and expiration date (FEFO/FIFO) to prevent stockouts and accumulation of expired goods. To maintain efficiency, the Warehouse Manager monitors warehouse capacity and storage locations, receives critical stock notifications/overstock, prints labels/QR for tracking, reviews stock movement history (audit trail), and exports operational reports. Next, an activity diagram will be displayed.

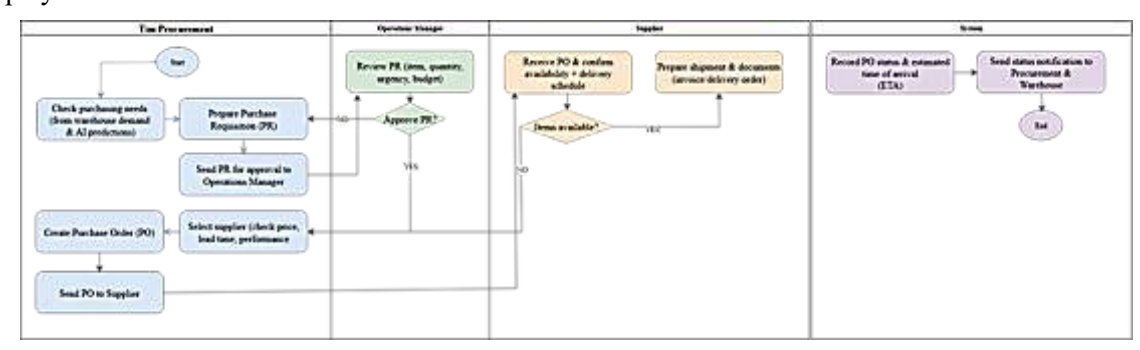


Figure 6. Activity Diagram of the Purchasing Process

**DOI:** 10.33019/jurnalecotipe.v12i2.4576

Figure 6 above shows the activity diagram of the goods purchase process involving four swimlanes, namely the Procurement Team, Operations Manager, Supplier, and System. This diagram illustrates the flow from checking purchase needs to sending order status notifications to Procurement and Warehouse. Next, an activity diagram of the Goods Purchase Process will be displayed.

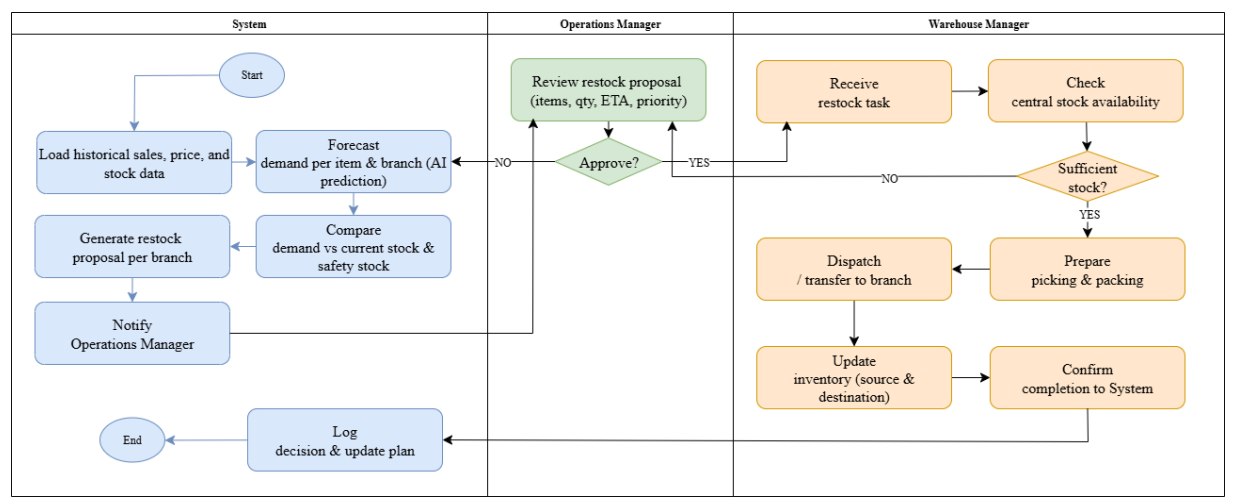


Figure 7. Activity diagram of the automatic restocking process

Figure 7 above is an activity diagram of the Automatic Restocking process involving three main swimlanes, namely System/AI, Operations Manager, and Warehouse Manager. This diagram shows the flow from the processing of historical data by the system, the creation of demand predictions, the approval of the restocking plan by the Operations Manager, to the execution of stock distribution by the Warehouse Manager and the update of the inventory record.



Figure 8. Wireframe System

#### 3.3 Coding

The coding stage in the Extreme Programming (XP) method focuses on translating the system design into program code that works according to the needs of the user. The implementation is carried out with the principle of pair programming to improve the quality and accuracy of the code, as well as the practice of continuous integration so that every change can be tested immediately. Artificial intelligence models for price prediction and stock optimization are integrated into the application backend at this stage, while the refactoring process is ongoing to ensure the code structure remains efficient, easy to maintain, and ready for the testing phase.



Volume 12, Issue 1, October 2025, pp. 203-214 ISSN 2355-5068; e-ISSN 2622-4852 **DOI:** 10.33019/jurnalecotipe.v12i2.4576



Figure 9. Login Page

The login page serves as an initial authentication gateway before the user accesses system features, ensuring secure access and proper role mapping. The interface is designed to be compact with the main elements in the form of Email/Username and Password fields, Login buttons, Forgot Password links, and List options (if allowed). Client-side and server-side validation are applied for email formats, password lengths, and clear error feedback; meanwhile, a "Remember me" mechanism and rate limiting/captcha (optional) are set up to improve the experience and security. Next the home page will be displayed in Figure 10.



Figure 10. Warehouse Manager Page

Figure 10 presents the Warehouse Manager interface in the mobile edition of the Smart Retail AI app, which is optimized for inventory management and goods receipt management. In this interface, essential components, including Stock Data, Goods Receipts, Daily Sales, and Statistics, are organized in bottom navigation tabs for easy access to the menu. Warehouse managers are also given access to check daily stock demands, so that they can monitor the details of the quantity and type of goods requested and also record the receipt of goods with regular and documented historical records. In addition, warehouse management has other pages, including Home (Dashboard), Stock Data, Receipt of Goods, Expenses or Stock Transfers, and Notifications. Next, the Data Analyst page will be presented.



Figure 11. Warehouse Manager Page

Figure 12 presents the Warehouse Manager interface in the mobile edition of the Smart Retail AI app, which is optimized for inventory management and goods receipt management. In this interface, essential components, including Stock Data, Goods Receipts, Daily Sales, and Statistics, are organized in bottom navigation tabs for easy access to the menu. Warehouse managers are also given access to

**DOI:** 10.33019/jurnalecotipe.v12i2.4576

check daily stock demands, so that they can monitor the details of the quantity and type of goods requested and also record the receipt of goods with regular and documented historical records. In addition, warehouse management has other pages, including Home (Dashboard), Stock Data, Receipt of Goods, Expenses or Stock Transfers, and Notifications. Next, the Data Analyst page will be presented.

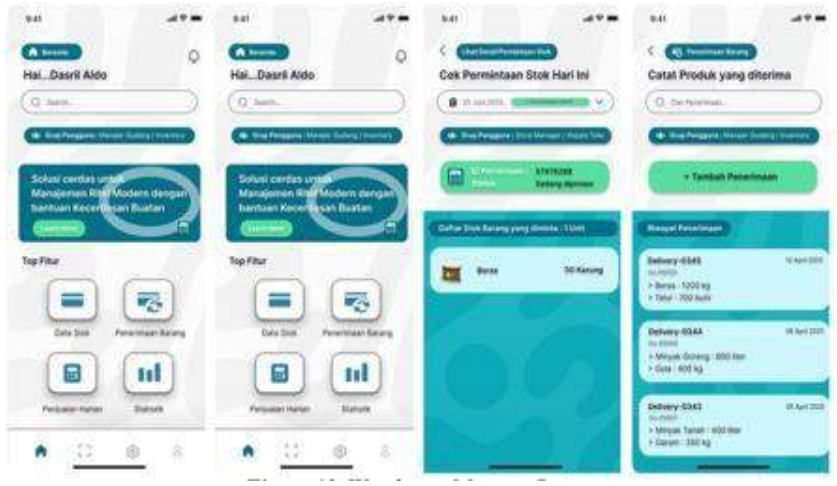


Figure 12. Warehouse Manager Page

Figure 12 presents the Warehouse Manager interface in the mobile edition of the Smart Retail AI app, which is optimized for inventory management and goods receipt management. In this interface, essential components, including Stock Data, Goods Receipts, Daily Sales, and Statistics, are organized in bottom navigation tabs for easy access to the menu. Warehouse managers are also given access to check daily stock demands, so that they can monitor the details of the quantity and type of goods requested and also record the receipt of goods with regular and documented historical records. In addition, warehouse management has other pages, including Home (Dashboard), Stock Data, Receipt of Goods, Expenses or Stock Transfers, and Notifications. Next, the Data Analyst page will be presented.



Figure 13. Data Analyst Page

Figure 13 shows the Dashboard & Main Menu page view for the Data Analyst/ AI Specialist role in the Smart Retail AI application. This interface displays the performance substance of the artificial intelligence model, starting from the predictive accuracy value, the distribution of the model performance categories differentiated into Good, Fair, and Poor labels, to the analysis of price trends for a specific product, in this example red chili. In addition, this page includes a feature importance graph that outlines the relative contribution of each variable to the final prediction, along with the option to insert notes and recommendations. The combination of these functions supports Data Analysts and AI Specialists in continuously monitoring, analyzing, and adjusting models to maintain the accuracy and

**DOI:** 10.33019/jurnalecotipe.v12i2.4576

relevance of predictions. In addition to these roles, this interface is also intended for Operations Managers, Procurement Teams, Inventory Controllers, Data Analysts, Store Managers, and Top Management.

#### 3.4 Testing

Testing in the Extreme Programming (XP) methodology is designed to guarantee that each feature released operates according to user expectations and meets the quality criteria that have been formulated. Test activities run on a recurring basis after the completion of each development iteration, so that any anomalies can be identified and corrected immediately. The method adopted is Black Box Testing, where attention is paid to the behavior of the system without conducting an inspection of the source code. Each feature is evaluated through a series of scenarios that assume a wide range of inputs, and the output obtained is compared to the results that have been formulated in the specification. In this way, the system is explored in a wide range of situations including legitimate inputs, condition-violating inputs, and exact scenarios being at the limits of specifications that collectively demonstrate that the developed functions are capable of meeting the needs of the user consistently.

ID Feature **Test Case** Precondition **Expected Output Status** Redirect to username=valid, Login with valid TC-01 Authentication dashboard; session Success credentials password=valid created Error message Login with invalid username=valid, TC-02 Authentication shown; stay on Success password password=wrong login page Overstock TC-21 Notifications Overstock alert stock >= max level notification Success displayed Export Access denied TC-23 Reports without user lacks role Success message permission

Table 1. Blackbox Testing

Black box testing of the Smart Retail AI application demonstrated that every function, from authentication to the final report generation phase, operated without deviation from the specified specifications. This finding indicates that the platform has achieved the level of reliability required for application in a contemporary retail context. Following this verification phase, the testing team then conducted an evaluation using the System Usability Scale (SUS) metrics to measure the system's usability dimensions.

Table 2. System Usability Scale (SUS) Testing													
Respond	1	2	3	4	5	6	7	8	9	10	Sum	Value (Total x 2.5)	
R1	5	2	5	2	4	2	5	2	5	1	35	87,5	
R2	5	1	5	2	5	2	5	1	5	2	34	85	
R3	5	2	5	2	5	2	4	2	5	2	34	85	
R4	5	1	5	1	5	1	5	1	5	1	37	92,5	
R5	4	2	5	2	5	2	5	2	5	1	34	85	
R6	5	1	5	2	4	1	5	1	5	1	35	87,5	
R7	5	1	5	1	5	1	5	1	5	1	37	92,5	
R8	5	1	5	1	5	2	5	1	5	2	36	90	
R9	4	2	4	2	5	2	5	2	5	2	33	82,5	
R10	5	1	5	1	5	1	5	1	5	1	37	92,5	
R11	5	2	5	2	5	2	5	2	5	1	35	87,5	
	Total number of scores												
				A	var	age					·	87	

Table 2. System Usability Scale (SUS) Testing

**DOI:** 10.33019/jurnalecotipe.v12i2.4576

Based on the analysis of the System Usability Scale (SUS) score shown in the table above, an average score of 87 was obtained, which in reference to the SUS standard is in the Excellent category. This score indicates that Smart Retail AI applications have a very high level of usability, adequate ease of use, and features that users consider relevant. Given that this value is well above its category threshold, which is 68 (Good category), it can be concluded that the application is feasible to implement and has the potential to be positively received by users in the modern retail operational environment.

The listening/feedback process in the development of the Smart Retail AI application is carried out after the initial release of the application in a staging environment and is used by users who act as Operations Managers, Procurement Team members, and Warehouse Managers. In this phase, users run all features related to their respective tasks, starting from logging in, accessing the dashboard, reviewing price predictions, compiling purchase requests, processing restocking, to recording the receipt of goods. Feedback was obtained through brief interviews, integrated online forms, and hands-on observation by the developer team. Analysis of this feedback led to several suggestions for improvement, including clarification of navigation menu labels, the addition of status indicators to the restocking process, and an increase in the loading speed of price prediction pages. All of these inputs are thoroughly vetted and implemented in subsequent iterations of development, with the goal of ensuring that the application is referenced, functions optimally, and is in line with operational needs in the field.

#### 4. CONCLUSION

This research successfully developed Smart Retail AI, an application that integrates artificial intelligence for price prediction and food stock optimization in modern retail chains. Development was conducted using an Agile Software Development approach using the Extreme Programming (XP) method. All phases of planning, design, coding, testing, and feedback were executed iteratively, involving three key stakeholders: the Operations Manager, the Procurement Team, and the Warehouse Manager. Black Box testing results showed that all core modules and key features, including user authentication, the dashboard, AI-based price prediction, automatic restocking, procurement management, stock receiving and distribution, and operational reports, performed according to specifications. Evaluation using the System Usability Scale (SUS) yielded an average score of 87, which falls within the Excellent category. This indicates that the application not only functions well but also has a high level of usability.

Furthermore, the listening and feedback phase provided important input, including improvements to navigation menu labels, the addition of status indicators for the restocking process, and optimization of load times in the price prediction module. This feedback was integrated into subsequent development iterations to improve the application's responsiveness, clarity, and suitability to operational needs. From a scientific perspective, this research contributes by integrating AI-based predictive models (LSTM and XGBoost) into a real-world retail system using the XP cycle, thus bridging the gap between algorithmic research previously limited to simulation and operational implementation. This contribution strengthens the understanding of how AI can be effectively operationalized in modern retail supply chain management, while providing a foundation for further research to explore the evaluation of prediction metrics (RMSE, MAE, MAPE), comparison with baseline models, and generalization to broader data scales and populations. Thus, Smart Retail AI is not only ready to be implemented as a practical tool that supports fast, accurate, and efficient decision-making, but also provides an academic contribution in the form of an AI integration framework and XP methods that can be used as a reference in research and implementation of intelligent systems in retail and similar domains.

#### Acknowledgments

The authors would like to express their gratitude to the Direktorat Penelitian dan Pengabdian kepada Masyarakat (DPPM), Lembaga Penelitian dan Pengabdian kepada Masyarakat (LPPM) Universitas Taman Siswa Padang, for the support and funding provided for this research project.

Volume 12, Issue 1, October 2025, pp. 203-214 ISSN 2355-5068; e-ISSN 2622-4852 **DOI:** 10.33019/jurnalecotipe.v12i2.4576

#### **REFERENCES**

- [1] St. Paul and M. Hao, 'Research on Business Model Transformation of Traditional Retail Enterprises under the Background of Digital Economy', *GHSS*, vol. 5, no. 9, pp. 352–357, Sep. 2024, doi: 10.61360/BoniGHSS242016930904.
- [2] D. V. Smerdova and D. S. Burtsev, 'Methodology for Assessing the Level of Readiness of Retail Trade in Russia for the Digital Transformation Process', *EPI*, no. 3, pp. 19–29, Sep. 2024, doi: 10.17586/2713-1874-2024-3-19-29.
- [3] Z. B. Akhmetova, J. T. Kozhamkulova, and I. A. Kim, 'Consumer behavior transformation in the digital economy on the basis of quantitative analysis', *jour*, no. 4, pp. 116–129, Dec. 2022, doi: 10.46914/1562-2959-2022-1-4-116-129.
- [4] Vivek Prasanna Prabu, 'Advanced Software Tools for Enhancing Retail Operations in the Digital Era', *IJSAT*, vol. 13, no. 3, p. 3382, Sep. 2022, doi: 10.71097/IJSAT.v13.i3.3382.
- [5] Lingareddy Alva, 'AI-augmented real-time retail analytics with spark and Databricks', *World J. Adv. Eng. Technol. Sci.*, vol. 15, no. 2, pp. 1024–1033, May 2025, doi: 10.30574/wjaets.2025.15.2.0631.
- [6] Venkata Krishna Pradeep Mattegunta, 'Integrated retail ecosystem: The convergence of predictive analytics and omnichannel strategies in modern merchandising', *World J. Adv. Eng. Technol. Sci.*, vol. 15, no. 2, pp. 168–176, May 2025, doi: 10.30574/wjaets.2025.15.2.0509.
- [7] Y. A. Davizon, J. M. Amillano-Cisneros, J. B. Leyva-Morales, E. D. Smith, J. Sanchez-Leal, and N. R. Smith, 'Mathematical Modeling of Dynamic Supply Chains Subject to Demand Fluctuations', *Eng. Technol. Appl. Sci. Res.*, vol. 13, no. 6, pp. 12360–12365, Dec. 2023, doi: 10.48084/etasr.6491.
- [8] R Shravya, 'Enhancing Supply Chain Resilience in Bengaluru's Restaurant Industry through Data Analytics and Strategic Vendor Management', *IJFMR*, vol. 6, no. 6, p. 31577, Dec. 2024, doi: 10.36948/ijfmr.2024.v06i06.31577.
- [9] R. Agarwal, 'AI-Driven Retail Analytics: Leveraging Predictive Models for Consumer Goods and Retail Optimization', *JAIGS*, vol. 2, no. 1, pp. 271–277, Feb. 2024, doi: 10.60087/jaigs.v2i1.235.
- [10] M. Sivasankari, 'Artificial Intelligence in Retail Marketing: Optimizing Product Recommendations and Customer Engagement', *jier*, vol. 5, no. 1, Jan. 2025, doi: 10.52783/jier.v5i1.2105.
- [11] H. Oukhouya, H. Kadiri, K. El Himdi, and R. Guerbaz, 'Forecasting International Stock Market Trends: XGBoost, LSTM, LSTM-XGBoost, and Backtesting XGBoost Models', *Stat., optim. inf. comput.*, vol. 12, no. 1, pp. 200–209, Nov. 2023, doi: 10.19139/soic-2310-5070-1822.
- [12] Vijaya Bhaskar.Reddypogu, Devi Prasad.U, 'Demand Forecasting in E-Commerce Fashion Retail: A Comparative Study of Generative AI, LSTM and ARIMA Models', *jisem*, vol. 10, no. 18s, pp. 23–28, Mar. 2025, doi: 10.52783/jisem.v10i18s.2876.
- [13] [13]H. Wijaya, D. P. Hostiadi, and E. Triandini, 'Optimization XGBoost Algorithm Using Parameter Tunning in Retail Sales Prediction', *j. nas. pendidik. teknik. inform.*, vol. 13, no. 3, Dec. 2024, doi: 10.23887/janapati.v13i3.82214.
- [14] [14]J. Ren, Z. Yu, G. Gao, G. Yu, and J. Yu, 'A CNN-LSTM-LightGBM based short-term wind power prediction method based on attention mechanism', *Energy Reports*, vol. 8, pp. 437–443, Aug. 2022, doi: 10.1016/j.egyr.2022.02.206.
- [15] [15]A. Mitra, A. Jain, A. Kishore, and P. Kumar, 'A Comparative Study of Demand Forecasting Models for a Multi-Channel Retail Company: A Novel Hybrid Machine Learning Approach', *Oper. Res. Forum*, vol. 3, no. 4, p. 58, Sep. 2022, doi: 10.1007/s43069-022-00166-4.

Volume 12, Issue 1, October 2025, pp. 203-214 ISSN 2355-5068; e-ISSN 2622-4852 **DOI:** 10.33019/jurnalecotipe.v12i2.4576

- [16] [16]Md Tanvir Islam *et al.*, 'Revolutionizing Retail: A Hybrid Machine Learning Approach for Precision Demand Forecasting and Strategic Decision-Making in Global Commerce', *JCSTS*, vol. 6, no. 1, pp. 33–39, Jan. 2024, doi: 10.32996/jcsts.2024.6.1.4.
- [17] [17]B. Pramudya, D. C. P. Ramadhani, H. N. Mujaddidah, and R. Siwi Pradini, 'Implementation of Extreme Programming (XP) in the Development of Dental Clinic Information Systems', *JESICA*, vol. 2, no. 1, pp. 20–28, Feb. 2025, doi: 10.47794/jesica.v2i1.22.
- [18] [18]A. Maulana, M. Mardiana, and R. A. Pradipta, 'DEVELOPMENT OF AN E-COMMERCE PLATFORM USING EXTREME PROGRAMMING METHODOLOGY', *FaktorExacta*, vol. 17, no. 3, p. 275, Oct. 2024, doi: 10.30998/faktorexacta.v17i3.23248.
- [19] [19]A. B. Semma, M. Saerozi, K. Kusrini, A. Syukur, and A. Maimun, 'An Extreme Programming Approach to Streamlining Thesis Writing', *Int. J. Adv. Sci. Eng. Inf. Technol.*, vol. 13, no. 6, pp. 2308–2313, Dec. 2023, doi: 10.18517/ijaseit.13.6.18701.

**DOI:** 10.33019/jurnalecotipe.v12i2.4577

# Arduino-Based Capacitor Bank Automation for Power Factor Optimization

Hafidz Nindhom Zen<sup>1</sup>, Ibrohim<sup>2</sup>, Endryansyah<sup>3</sup>, Subuh Isnur Haryudo<sup>4</sup>

1.2.3.4 Departement of Electrical Engineering State University of Surabaya, A5 Building Unesa 1 Campus, Surabaya, Indonesia

#### ARTICLE INFO

#### Article historys:

Received: 21/08/2025 Revised: 27/08/2025 Accepted: 02/09/2025

#### **Keywords:**

Automation; Capasitor Bank; Microcontroller; Power Factor Optimization

#### **ABSTRACT**

Electrical energy efficiency in PLN customers in the R1 category is a crucial issue due to the low value of the power factor ( $\cos \varphi$ ), which is caused by the dominance of the use of inductive equipment. This condition not only causes significant energy waste but also puts a strain on the power grid, where the urgency is amplified by various economic factors. This resaerch designed an automatic capacitor bank system to dynamically correct the power factor. By integrating the Arduino Nano microcontroller and the PZEM-004T sensor, the system monitors electrical parameters such as voltage, current, and  $\cos \varphi$  in real-time. Based on this data, the system autonomously activates the relay to connect capacitors with the most optimal capacitance value to compensate for reactive power precisely. Its main innovation is an adaptive automation mechanism that is able to respond to load fluctuations. The implementation aims to increase the cost value  $\varphi$  close to 1.0, so that it has great potential to reduce power losses, reduce electricity bills, and improve the overall efficiency of the electrical system.



This work is licensed under a Creative Commons Attribution 4.0 International License

#### **Corresponding Author:**

Hafidz Nindhom Zen Departement of Electrical Engineering State University of Surabaya, A5 Building Unesa 1 Campus, Ketintang Street, Surabaya 60231, Indonesia Email: hafidznindhom.22032@mhs.unesa.ac.id

#### 1. INTRODUCTION

Electrical energy efficiency is a critical concern for households, and the power factor ( $\cos \varphi$ ) serves as a key performance indicator [1]. A low power factor, typically below the 0.85 standard set by PLN (Perusahaan Listrik Negara), indicates a high consumption of reactive energy. This type of energy doesn't perform any useful work, such as powering an appliance, but it still puts a strain on the electrical grid and adds to a consumer's electricity bill.1 The main culprits are inductive appliances like air conditioners, water pumps, and refrigerators, which are common sources of wasted energy and inefficiency in residential electrical systems [2].

The most effective technical solution to this issue is the installation of a capacitor bank. A capacitor bank acts as a local source of reactive power, offsetting the inductive loads of household equipment.2 This reduces the amount of reactive power that the main grid needs to supply, leading to a decrease in the total current.3 As a result, power losses are minimized, and the power factor can be corrected to a value closer to the ideal of 1 [3]. Implementing this solution for R1 PLN customers, who represent a significant portion of the nation's energy consumers, has the potential to bring about widespread energy savings and system optimization.

The need to adopt this energy-saving solution is becoming more urgent due to increasing economic pressures on households. Several factors, such as the planned increase in the Value Added Tax (VAT)

**DOI:** 10.33019/jurnalecotipe.v12i2.4577

to 12% in 2025 [4], the significant weakening of the rupiah against the US dollar [5], and the downward trend of the Composite Stock Price Index (JCI), all signal a challenging national economic outlook. These conditions will directly and indirectly increase household expenses, making electricity consumption efficiency a highly relevant strategy for easing financial burdens.

While the concept of using capacitor banks is not new, existing research and systems have limitations. Previous solutions were often manual, requiring users to activate capacitors with static values that were only suited for a specific load. This method is impractical and ineffective for households, where electrical loads fluctuate significantly throughout the day [6].

This research introduces an innovative solution: an automatic and adaptive capacitor bank system. The system's core is an Arduino Nano microcontroller, which is integrated with a PZEM-004T sensor. This sensor continuously monitors crucial electrical parameters in real-time, including voltage, current, and the power factor.4 Based on this live data, the system intelligently controls relays to connect or disconnect capacitors with the most appropriate capacitance values to match the current load.

The primary objective of this research is to thoroughly analyze the impact of an automatic capacitor bank on power factor improvement and energy efficiency in R1 PLN customer installations. The research will compare electrical conditions before and after the system's installation to measure its effectiveness.

In addition to technical performance, the research will also evaluate the economic benefits. This includes quantifying the reduction in electricity bill costs that result from improved efficiency.

The findings of this research are expected to provide concrete evidence and a solid technical foundation for implementing a practical and affordable energy-saving solution for households. This will empower consumers to take control of their electricity usage and manage their household finances more effectively.

#### 2. RESEARCH METHOD

#### 2.1. System Design

The hardware structure of this system is built with a modular philosophy, which breaks down its functionality into three main parts that interact with each other: the sensor module, the central control unit, and the actuator device. This separation of functions aims to create a more structured and systematic workflow, thus simplifying the process of designing, developing, and maintaining the system in the future [7].

As a subsystem of data acquisition, the sensor module is in charge of collecting various electrical parameters in real-time. The data obtained becomes crucial input for the control algorithm run by the system. Therefore, these modules must have sensors with a high level of accuracy and the ability to respond to load fluctuations quickly and precisely [8].

To meet these needs, this research relies on the PZEM-004T sensor. This sensor was chosen because of its capable ability to measure voltage, current, power, energy, and power factors simultaneously. In addition, PZEM-004T is known for its high reliability, ease of integration with microcontrollers, and adequate accuracy for power factor optimization applications. The collected data is then sent to the main control unit for further processing.

The core of data processing and decision-making lies in the main control unit implemented using Arduino Nano. This device is responsible for executing a pre-programmed control algorithm, by processing the input data from the sensor module. The Arduino Nano is the top choice thanks to its compact size, power efficiency, and wide compatibility with a wide range of additional components.

The actuator device is the physical executor of this system, consisting of five DC relays that function as electronic switches. These relays dynamically connect capacitor banks of a certain capacity into the electrical system to perform power factor corrections. Each relay is independently controlled by Arduino Nano, based on the results of the data analysis that has been processed.

**DOI:** 10.33019/jurnalecotipe.v12i2.4577

For easy monitoring and configuration, the system is equipped with a 20x4 I2C LCD screen as a visual interface. This display presents important parameters such as voltage, current, power factor, total energy, instantaneous power, operating mode, and relay status in real-time. The functional relationships and workflows between these components are visualized in more detail through the system architecture diagram.

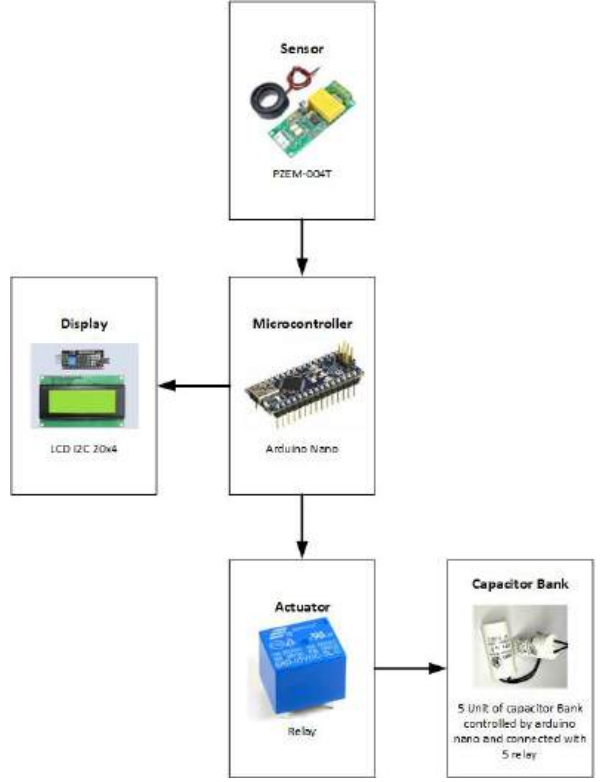


Figure 1. Work System Chart Design

#### 2.2. System Workflow

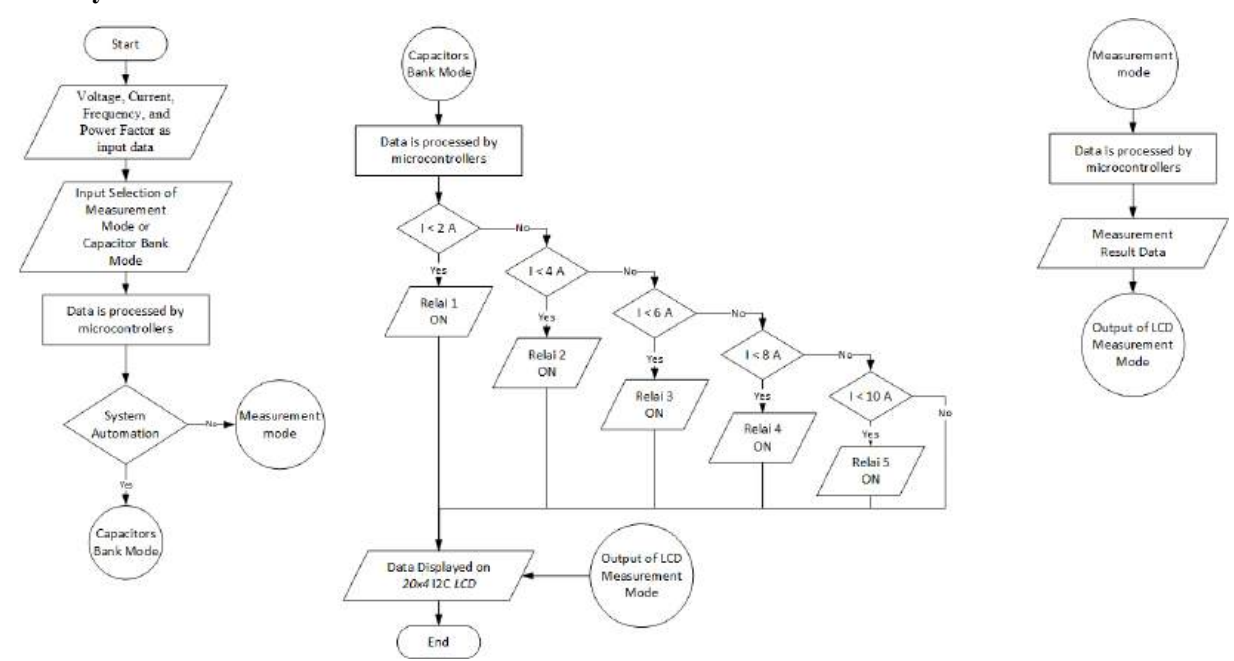


Figure 2. Flowchart diagram of the working system

**DOI:** 10.33019/jurnalecotipe.v12i2.4577

Based on the flowchart in Figure 2, the system workflow can be outlined as follows:

- 1. The process is initiated by a PZEM004T sensor that is in charge of measuring vital electrical parameters such as voltage, current, frequency, and power factors. All data from these measurements is then forwarded to the microcontroller for further processing.
- 2. Next, users can determine how the system will operate by selecting one of the two modes available through a switch. The options are "measurement mode" which is passive, or "capacitor bank mode" which is active and auto-corrects.
- 3. The two inputs, namely data from the sensor and the mode selection from the user, are received by the Arduino Nano. The way Arduino processes data is highly dependent on the mode it is on. In "capacitors bank mode", the load current data is the reference for automatically activating the capacitor. This activation occurs gradually whenever the load current increases in multiples of 2 Ampere. In contrast, in "measurement mode", the incoming data is only prepared for display without any further automation process.
- 4. As a final stage, the execution of the command and the appearance of the results will be different according to the mode. In "capacitors bank mode", after the Arduino Nano processes the current data, it will send a signal through the digital pin to activate the relay. This relay is in charge of connecting capacitors with the appropriate value to the consumer's electrical installation (PLN R1 household). Meanwhile, if the system is in "measurement mode", the processed data will be displayed immediately. In both modes, all information and process results are displayed to the user through the 20x4 I2C LCD screen.

#### 2.3. Calculation of the Capacitors Required to Fit the Needs.

In this research, the determination of the capacitance value needed for household electrical installations with PLN R1 customer calcification requires special calculations. This calculation is important so that the installed capacitor does not become excessive and instead becomes a new capacitive load [9]. For this reason, the calculation is carried out in several stages, starting from the first step:

1. Classify the load.

Classifies loads based on their current value. In this case, a current of 2 Amperes is used as a reference for load classification.

2. Calculating the tan value

Calculating the tan value of the power factor value ( $\cos \phi$ ), it can be done using the following formula:

$$\tan(\cos^{-1}\phi) \tag{1}$$

Description:

 $\tan = \text{Tan value}$   $\cos^{-1} \phi = \text{Phasa angle}$ 

3. Calculating reactive power

Calculating reactive power can be done with the following formula:

$$Q = V \times I \times \sin \phi \tag{2}$$

Description:

Q = Reactive power (VAR)

V = Voltage (Volt)
I = Current (Ampere)
sin φ = Reactive power angle

Calculating reactive power can also be done with the following formula:

$$Q = P x \tan \phi \tag{3}$$

Description:

Q = Reactive Power (VAR) P = Active power (Watt)

 $\tan \varphi = \text{The tan value of the change result of the } \varphi$ 

**DOI:** 10.33019/jurnalecotipe.v12i2.4577

#### 4. Calculate the required power compensation

The reactive power data that has been obtained can then be used to calculate the required power compensation. The calculation of this reactive power compensation ratio can be done using the following formula:

$$Qc = Q_0 - Q_1 \tag{4}$$

Description:

Qc = Reactive force compensation (VAR) Q<sub>0</sub> = Pre-intervention reactive power (VAR)

 $Q_1$  = Post-intervention reactive power (VAR)

#### 5. Calculating the current flowing through the capacitor (Ic)

Calculating the current flowing through the capacitor (Ic) can be done using the following formula:

$$I_{c} = \frac{Q_{c}}{V} \tag{5}$$

Description:

 $I_C$  = Current passing through the capacitor (Ampere)

 $Q_C$  = Reactive power compensation (VAR)

V = System nominal voltage (Volt)

#### 6. Capacitive reactance (Xc).

The capacitive reactance value (Xc) is used to determine the most appropriate capacitor size in power factor repair using a capacitor bank. The calculation of the value of capacitive reactance can be done using the following formula:

$$X_{C} = \frac{V}{I_{C}} \tag{7}$$

Description:

 $X_C$  = Capacitive reactance  $(\Omega)$ 

V = System voltage (Volt)

I<sub>C</sub> = Current passing through the capacitor (Ampere)

#### 7. Calculate the required capacitor value.

Once the capacitive reactance value is obtained, the next step is to calculate the required capacitor value. This calculation can be done using the following formula:

$$X_{C} = \frac{1}{2\pi FC} \tag{6}$$

Description:

 $X_C$  = Capacitive reactance  $(\Omega)$ 

F = Frequency (Hz)

C = Capacitor value (F)

#### 8. Converting the amount of capacitor value.

It is important to convert the calculated capacitor value into microfarad units ( $\mu$ F). This conversion is necessary because in the Indonesian market, capacitors are generally sold in these standard units. This conversion calculation can be done using the following formula:

$$C(\mu F) = C(F) \times 10^{-6}$$
 (8)

Description:

 $C (\mu F) = Capacitor Values (\mu F)$  C (F) = Capacitor Values (F) $10^6 = Multiplier factors$ 

## 2.4. Calculation of the Analysis of the Results obtained by the Capacitor bank Automation System

Analysis of the performance of the capacitor bank automation system that has been designed can be carried out through a series of careful calculation stages [10]. First, electrical data that has been collected in real-time—such as voltage, current, and power factors—is the main basis for evaluation. With this data, we can compare the conditions before and after the installation of the device to see the difference quantitatively. A variety of relevant mathematical formulas were applied to this data to

**DOI:** 10.33019/jurnalecotipe.v12i2.4577

measure the effectiveness of the system as a whole, including how far the power factor was successfully corrected close to the ideal value of 1 [11]. In addition, the calculation will also include the energy efficiency generated and the potential for electricity cost savings for consumers. Each of these calculation stages is designed to provide a clear and concrete picture of the positive impact of the system on household electrical installations. This whole process will generate powerful data to prove that this solution is not only technical, but also provides significant economic benefits. To analyze the work results of the capacitor bank automation system that has been made before, it can be done in several calculation stages using the following formula:

#### a. Improvement Results on Power Factor Testing

In calculating the improvement results of power factor testing, pre-intervention data and post-intervention data are needed. The data is obtained from direct measurements using a pre-built system. To analyze the results of improvements in the power factor test in percentage (%) by using the following formula:

Result Cos 
$$\varphi$$
 Repair (%) =  $\frac{\cos \varphi_1 - \cos \varphi_0}{\cos \varphi_0} \times 100\%$  (9)

#### Description:

 $Cos \phi_0$  = Power Factor pre-intervention  $Cos \phi_1$  = Power Factor post-intervention

From the results of the calculation, data on the percentage (%) of improvement that can be achieved in post-intervention data compared to pre-intervention data is obtained.

#### b. Improvement Results in Testing Electrical Power Consumption

In calculating the results of electrical power consumption test improvements, pre-intervention data and post-intervention data are needed. The data is obtained from direct measurements using a pre-built system. To analyze the results of improvements in the test of electrical power consumption in percentage (%) by using the following formula:

Improvement Result of electrical power comsumption(%) = 
$$\frac{P_1 - P_0}{P_0} \times 100\%$$
 (10)

#### Description:

 $P_0$  = Electrical Power Consumption pre-intervention

 $P_1$  = Electrical Power Consumption post-intervention

From the results of the calculation, data on the percentage (%) of improvement that can be achieved in post-intervention data compared to pre-intervention data is obtained.

#### c. Improvement Results in Customer issued electricity cost

In calculating the results of customer issued electricity cost test improvements, pre-intervention data and post-intervention data are needed. The data is obtained from electricity costs paid by customers every month. To analyze the results of customer issued electricity cost in percentage (%) by using the following formula:

Improvement Result of customer issued electricity cost(%) = 
$$\frac{IDR_1 - IDR_0}{IDR_0}$$
 x 100% (11)

#### Description:

 $IDR_0$  = Customer issued electricity cost pre-intervention

 $IDR_1$  = Customer issued electricity cost post-intervention

From the results of the calculation, data on the percentage (%) of improvement that can be achieved in post-intervention data compared to pre-intervention data is obtained.

#### 2.5. Data acquisition methodology

Direct measurement methods are also needed to collect data after the device is installed in the customer's household installation for PLN's R1 tariff. Both sets of data are required for analysis of the device's success rate. Each set of data is collected over a 2-month period, specifically 2 months before and 2 months after the installation of the capacitor bank. Data collection is done weekly to observe the effectiveness of the capacitor bank, which uses an automation system to optimize the power factor for each power group, as per the calculations and planning conducted before installation. Data is collected

Volume 12, Issue 2, October 2025, pp. 215-225 ISSN 2355-5068; e-ISSN 2622-4852 **DOI:** 10.33019/jurnalecotipe.v12i2.4577

from 2 kWh meters installed in 2 different PLN R1 power scopes where data collection is feasible: 900 VA and 1300 VA, simultaneously over a total effective period of 4 months. From these two power ratings, data on the power factor improvement and electrical energy usage are obtained. Using this data, a comparison between the two power ratings is necessary in the data analysis sub-section to confirm the degree of success and error in the research.

#### RESULTS AND DISCUSSION

Using formulas (1) to (8) and a nominal voltage of 220 Volts, the calculation results are presented in table 1 which contains the following calculation results:

	Table 1. Table of calculation results												
Current (Ampere)	Cos φ Pre- intervention	Tan φ Pre- intervention	Cos φ Post- intervention	Tan φ Post- intervention	Pre- intervention reactive power (VAR)	Post- intervention reactive power (VAR)	Reactive power compensatio n (VAR)	Current passing through the capacitor	Capacitive reactance (Ω)	Capacitor value (uF)			
2	0.85	0.62	0.95	0.33	231.78	137.39	94.39	0.43	512.74	6.2			
4	0.85	0.62	0.95	0.33	463.57	274.78	188.79	0.86	256.37	12.4			
6	0.85	0.62	0.95	0.33	695.35	412.17	283.18	1.29	170.91	18.6			
8	0.85	0.62	0.95	0.33	927.14	549.5598	377.578	1.72	128.19	24.85			
10	0.85	0.62	0.95	0.33	1158.922	689.9498	471.9721	2.145	102.55	31.06			

Table 1 Table of calculation results

This system is made based on the calculated value of the capacitor. The device operates according to a pre-established working method, using the number of capacitors that have been measured and detailed in the calculation result in table 1. The data collection process in this research began with the installation of a power factor correction system in household electrical installations. Once the system is installed, the electrical parameters are measured in real-time. The PZEM-004T sensor serves as the primary tool for collecting voltage, current, and power factor data. The data obtained is then sent to Arduino Nano, which is in charge of processing the information. The results of this data processing are displayed on a visual interface in the form of a 20x4 LCD screen. This data collection was carried out in two periods: before the intervention (before the system was installed) and after the intervention (after the system was operational). The comparison of data from these two periods aims to analyze the effectiveness of the system that has been installed.

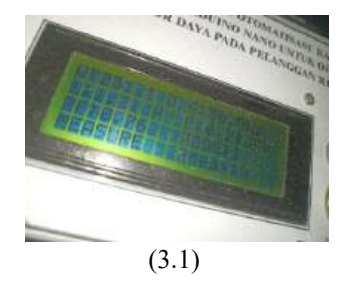




Figure 3.1. Result Pre-Intervention in device 1 and Figure 3.2. Result Pre-Intervention in device 2

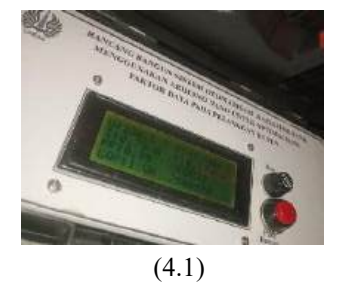




Figure 4.1. Result Post-Intervention in device 1 and Figure 4.2. Result Post-Intervention in device 2

In this research, electrical data was collected from two different conditions. Figures 3.1 and 3.2 present pre-intervention data, which show parameters such as actual power factor, usable power, and

**DOI:** 10.33019/jurnalecotipe.v12i2.4577

active relay status via the LCD interface. In contrast, Figures 4.1 and 4.2 show the same data in real time post-intervention has been performed. Regular measurement and recording of data from these two conditions is essential to ensure that the results of the study are valid and accurate. Data were collected through random weekly sampling, which was conducted for two months in the pre-intervention period and two months in the post-intervention period. The data obtained are then presented in Table 2, 3, and 4 below.

Table 2. System Measurement Results for power factor

			Devi	ice 1		Device 2				
Num	Weeks	Pre-Interv	vention	Post-Inter	vention	Pre-Interv	vention	Post-Intervention		
Num	Weeks	Current	Power	Current	Power	Current	Power	Current	Power	
		(Ampere)	Factor	(Ampere)	Factor	(Ampere)	Factor	(Ampere)	Factor	
1	First	2.89	0.83	2.43	0.99	1.68	0.81	1.38	0.98	
2	Second	2.85	0.83	2.39	0.99	2.67	0.8	2.2	0.96	
3	Third	1.17	0.77	0.95	0.95	0.98	0.79	0.73	0.95	
4	Fourth	3.12	0.82	2.61	0.98	1.28	0.78	1.03	0.9	
5	Fifth	0.96	0.82	0.8	0.98	1.57	0.79	1.4	0.95	
6	Sixth	2.75	0.75	2.22	0.93	1.08	0.8	0.87	0.94	
7	Seventh	3.22	0.81	2.66	0.98	1.35	0.81	1.12	0.97	
8	Eighth	2.99	0.82	2.48	0.99	1.32	0.79	1.05	0.91	

Table 3. System Measurement Results for Electrical Power Consumption

Num	Weeks	Device	1 (kWh)	Device 2 (kWh)		
Num	vveeks	Pre-Intervention Post-Interven		Pre-Intervention	Post-Intervention	
1	First	31.8	26.2985	78	72	
2	Second	29.6	24.4856	79	73	
3	Third	30.5	25.1267	65	62	
4	Fourth	29.2	24.2356	93	88	
5	Fifth	26.9	20.1534	80	74	
6	Sixth	27.9	22.4587	78	73	
7	Seventh	27.6	21.8675	75	70	
8	Eighth	27.4	21.6574	66	62	
Sum of kWh		230.9	186.2834	614	574	

Table 4. System Measurement Results for Customer-Issued Electricity Costs

Ī	Num	Months	Device 1		Device 2	
			Pre-Intervention	Post-Intervention	Pre-Intervention	Post-Intervention
			(Rp)	(Rp)	(Rp)	(Rp)
I	1	First	100000	75000	500.589	468.806
ĺ	2	Second	90000	65000	475.162	443.378

Using formulas (9), (10), and (11) for data analysis, it can be done and presented for each type of data in the following analysis results table 5 and 6 below:

Table 5. Results Analysis of power factors and electrical power consumption data

	Weeks	Result Cos φ Repair (%)		Improvement Result of Electrical Power Cosumption (%)	
Num					
		Device 1	Device 2	Device 1	Device 2
1	First	19.28	20.99	20.92	8.3333333
2	Second	19.28	20	20.89	8.2191781
3	Third	23.38	20.25	21.39	4.8387097
4	Fourth	19.51	15.39	20.48	5.6818182
5	Fifth	19.51	20.26	33.48	8.1081081
6	Sixth	24	17.5	24.23	6.8493151
7	Seventh	20.99	19.75	26.22	7.1428571
8	Eighth	20.73	15.1898	26.52	6.4516129

Volume 12, Issue 2, October 2025, pp. 215-225 ISSN 2355-5068; e-ISSN 2622-4852 **DOI:** 10.33019/jurnalecotipe.v12i2.4577

Table 6. Results Analysis of Customer Issued Electricity Cost

Ni	Months	Improvement Result of Customer Issued Electricity Cost (%)			
Num		Device 1	Device 2		
1	First	33.333333	6.7795634		
2.	Second	38.4615385	7.1686011		

The analysis was also strengthened by validation and reliability tests carried out with the help of SPSS software whose results were presented as follows:

Table 7. Results of Validation and Reliability Test Analysis using SPSS software

	Factor Test Results	Electrical Power Cosumption Validation Test Results		Customer-Issued Electricity Costs Validation Test Results	
Device 1	Device 2	Device 1	Device 2	Device 1	Device 2
0.986	0.849	0.976	0.995	1.000	1.000
Power	Factor	<b>Electrical Power Cosumption</b>		<b>Customer-Issued Electricity Costs</b>	
Reliability '	Test Results	Reliability Test Results		Reliability Test Results	
Device 1	Device 2	Device 1	Device 2	Device 1	Device 2
0.970	0.839	0.996	0.979	1.000	1.000

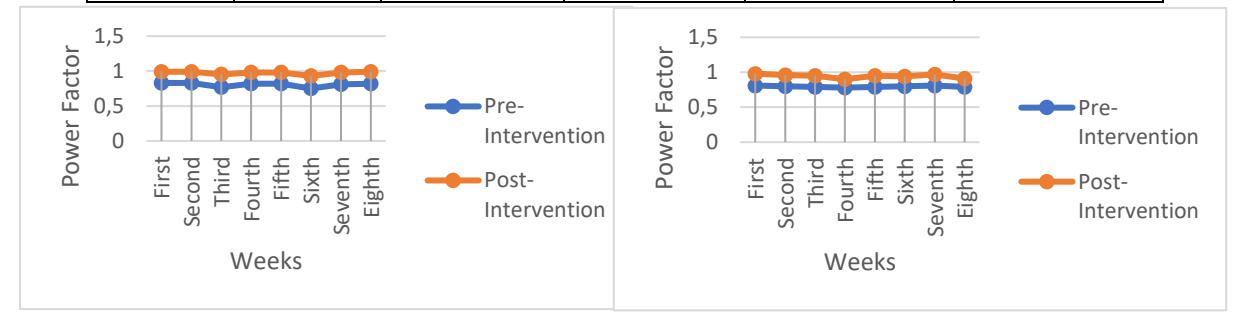


**Figure 5.** System Measurement Results for power factor in Device 1

**Figure 6.** System Measurement Results for power factor in Device 2

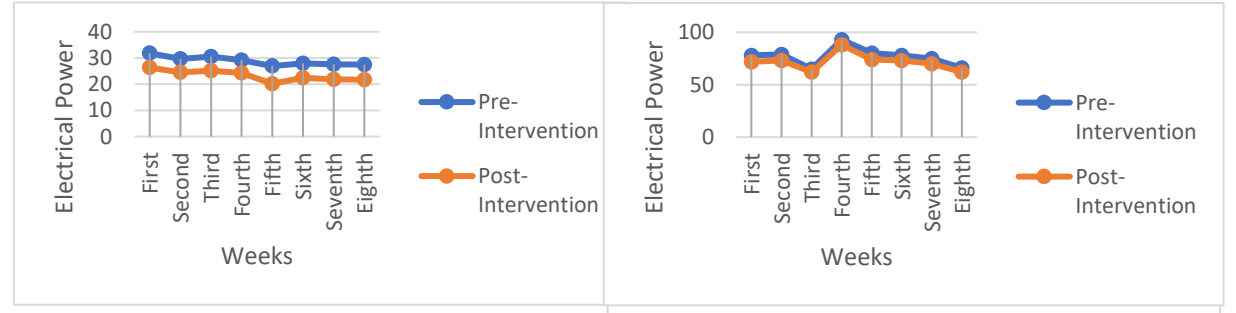


Figure 7. System Measurement Results for Electrical Power Consumption in Device 1 Power Consumption in Device 2



**Figure 9.** System Measurement Results for Customer-Issued Electricity Costs in Device 1

**Figure 10.** System Measurement Results for Customer-Issued Electricity Costs in Device 2

**DOI:** 10.33019/jurnalecotipe.v12i2.4577

# 4. CONCLUSION

This research successfully designed and implemented an effective capacitor bank automation system for the improvement of power factors in household electrical installations.

- 1. Increased Power Factor ( $\cos \varphi$ ). The system successfully significantly increased the power factor from an average of 0.75-0.83 in pre-intervention conditions to 0.9-0.99 in post-intervention conditions. This proves that the system is capable of correcting the power factor close to the ideal value of 1.0.
- 2. Savings in Electrical Power Consumption (kWh). There is a significant decrease in electrical power consumption after the system is installed. This is shown by a decrease in average kWh consumption by 20-30% in Device 1 and 5-8% in Device 2.
- 3. Economic Benefits. Improved energy efficiency directly results in savings in electricity costs for consumers. The analysis showed that electricity costs decreased by an average of 35% in Device 1 and about 7% in Device 2.
- 4. Validity and Reliability. Validation and reliability testing using SPSS software confirms the reliability of the data. All validation and reliability values are above acceptable thresholds (above 0.8), with most approaching 1.0. This shows that the results of the measurement and analysis of the data have high validity and consistency, reinforcing the research findings that these systems work effectively and reliably. The varying success between Device 1 and Device 2 can be attributed to the difference in electrical load characteristics and usage profiles in each household.

## Acknowledgments

The researcher's acknowledments is addressed to all parties who support the compilation of this journal. The first thank you is addressed to the party who accommodated the research, namely the Electrical Engineering Undergraduate Study Program, the Faculty of Engineering, State University of Surabaya and one of R1 PLN's customers who has been willing to be used as the object of this research.

#### **REFERENCES**

- [1] T. W. Nugroho, I. Mustaqim, and A. Sandria Jaya Wardhana, 'Studi Kualitas Daya Listrik (Power Quality) Di Bangunan Gedung Xyz', J. Inform. dan Tek. Elektro Terap., vol. 13, no. 2, 2025, doi: 10.23960/jitet.v13i2.6563.
- [2] M. Mustamam, A. Lubis Rizky, A. Butar-Butar Hakim, and M. Affandi, Kualitas Daya Pada Sistem Tenaga Listrik Google Books. 2021. [Online]. Available: https://www.google.co.id/books/edition/Kualitas\_Daya\_Pada\_Sistem\_Tenaga\_Listrik/O2MWE AAAQBAJ?hl=id&gbpv=0
- [3] P.Sanjeevikumar, C.Sharmeela, J. B. Holm-Nielsen, and P.Sivaraman, Power Quality in Modern Power Systems. London: Academic Press, 2021.
- [4] Hikmayani Subur and Wahyu Muh Syata, 'Analisis Dampak Kenaikan Tarif Pajak Pertambahan Nilai (Ppn) Terhadap Masyarakat Dan Inflasi Di Indonesia', J. Rumpun Manaj. Dan Ekon., vol. 1, no. 5, pp. 205–210, 2024, doi: 10.61722/jrme.v1i5.3045.
- [5] D. A. Adove, U. I. Gunawan, and G. Pranajaksakti, 'Faktor-Faktor Yang Mempengaruhi Nilai Tukar Rupiah Terhadap Dollar Periode Tahun 1955-2022', Publ. Ris. Mhs. Akunt., vol. 6, no. 1, pp. 53–60, 2025, doi: 10.35957/prima.v6i1.11311.
- [6] M. Farkhan and Y. Muharni, 'Journal of Systems Engineering and Management Merancang Monitoring Perubahan Beban Akibat Perbaikan Faktor Daya Menggunakan', J. Syst. Eng. Manag., vol. 04, no. 01, pp. 31–36, 2025.
- [7] B. Ferdiansah, A. Margiantono, and F. Ahmad, 'Rancang Bangun Alat Monitoring Dan Proteksi Kapasitor Bank Berbasis Internet of Things', Jambura J. Electr. Electron. Eng., vol. 5, pp. 234–241, 2023.
- [8] D. Rizqy Zaputra, R. Monantun, and M. Subekti, 'Rancang Bangun Sistem Pendeteksi Api



- Berbasis IOT (Internet of Things)', J. Electr. Vocat. Educ. Technol., vol. 7, no. 2, pp. 75–86, 2024, doi: 10.21009/jevet.0072.02.
- [9] R. Ramadhan, Z. Saputra, and Surojo, 'Rancang Bangun Perbaikan Faktor Daya Menggunakan Kapasitor Bank Berbasis Mikrokontroler Untuk Beban Rumah Tangga Dengan Daya Maksimal 900 W', Pros. Semin. Nas. Inov. Teknol. Terap., pp. 287–293, 2021.
- [10] D. Corio, R. Maulana, P. Yunesti, and Z. Hendri, Perencanaan dan Operasi Sistem Tenaga Listrik. South Lampung: ITER PRESS, 2023.
- [11] Y. Suprihartini, Analisis Sistem Tenaga Listrik, 1st ed. Padang: Takaza Innovatix Labs, 2025.



**DOI:** 10.33019/jurnalecotipe.v12i2.4569

# Optimization of Spot Welding Performance Through Microcontroller- Solenoid Drive and Ultrasonic Sensing

Aldi Rahman<sup>1</sup>, Surfa Yondri<sup>2</sup>, Riza Widia<sup>3</sup>, Muhardika<sup>4</sup>, Yani Kamisa Putri<sup>5</sup>, Dedi Erawadi<sup>6</sup>, Tri Artono<sup>7</sup>, Muhammad Rizal Syauqii<sup>8</sup>

1,2,3,4,5,6,7,8 Electrical Engineering, Padang State Polytechnics, Jl.Kampus, Limau Manis, Padang 25164, Indonesia.

#### **ARTICLE INFO**

#### **Article historys:**

Received: 16/07/2025 Revised: 03/09/2025 Accepted: 30/10/2025

#### Keywords:

Arduino; Spot Welding; Solenoid; Ultra Sensing; Welding Process Automation

#### **ABSTRACT**

This research discusses the design and testing of an Arduino microcontroller-based spot welder control system with solenoid drive and ultrasonic sensor as the main input. The system is designed to improve efficiency, precision, and consistency of welding results by automating the electrode clamping process as well as voltage regulation according to material specifications. The combination of a relay and voltage regulator module allows the current to be optimally adjusted based on the thickness of the work plate, thereby reducing welding defects. Tests show that the system is capable of detecting objects within 10 cm, and a welding time setting of 3 seconds proves sufficient to produce an optimal weld point. On plates with a thickness of 1.44 mm, the best results were achieved at voltages of 4V and 6V; for thicknesses of 1.8 mm and 2.2 mm, the optimal voltage was 8V. The pressure from the solenoid proved to be sufficient in joining the materials well. These results show that the microcontroller-based welding system is effective in adaptively managing the welding time and voltage, and provides consistent and robust results. These findings support the potential application of the system in smarter and more automated production processes in accordance with industry 4.0 principles.



This work is licensed under a Creative Commons Attribution 4.0 International License

#### **Corresponding Author:**

Aldi Rahman

Electrical Engineering, Padang State Polytechnics, Jl.Kampus, Limau Manis, Padang 25164, Indonesia. Email: aldi rahman@pnp.ac.id

# 1. INTRODUCTION

In the era of the Industrial Revolution 4.0, the need for smart, automated and efficient manufacturing systems is increasing. One process that undergoes continuous innovation is welding, especially the resistance spot welding (RSW) method. This method utilizes heat from electrical resistance to join two or more metal plates together. The process is fast, energy-efficient and suitable for mass production, making it widely used in the automotive, electronics and light metal industries [1]. In the context of production technology development, spot welding continues to be refined to meet the quality and efficiency standards of modern production [2]. As highlighted by Chinn et al. [10], effective control strategies in resistance spot welding are crucial to ensure joint consistency and high-quality results, which emphasizes the importance of developing innovative control methods. In order for the spot welding process to produce strong and consistent joints, a fast and accurate control system is required. Pneumatic technology is still widely used as an electrode drive, but this system has several disadvantages such as large size, dependence on air pressure, and response that is not always precise. Therefore, this research proposes the use of linear solenoids as a replacement for pneumatic systems.

Homepage: https://ecotipe.ubb.ac.id/

Email: jurnalecotipe@ubb.ac.id

Solenoids are more compact, have a fast response time, and are capable of providing sufficient pressure for light metal welding [5].

This system is controlled by an Arduino microcontroller which is in charge of regulating the working logic and duration of the active solenoid. Arduino was chosen because it is flexible, easy to program, and has proven effective in various automation control projects [3]. To improve the system's work efficiency, an ultrasonic sensor is used as the initial detection input. This sensor is capable of detecting workpiece distances of up to 10 cm with high accuracy [4]. When the sensor detects the presence of a workpiece, it will send a signal to the Arduino which then triggers the activation of the relay to deliver electric current to the solenoid [6]. The use of a layered relay system allows the control of large currents to the solenoid to remain stable and safe. The MY2N 12V DC relay is used to activate the MY4-GS relay, which functions as a voltage regulator control module. This voltage can be set according to the thickness and type of material to be welded. With the right voltage setting, the welding results can be more optimal and minimal defects [9]. This welding process is fully controlled by a semi-automatic system, which combines sensors, microcontrollers, relays, and actuators in a single system.

Similar research has been conducted by M. A. Wahab who explained the importance of current and time parameters in determining weld quality [7]. In addition, a study from A. A. Al-Fadhli showed that the use of microcontrollers in welding systems provides increased accuracy and flexibility in welding control [8]. Research by M. A. M. Yusof also proved that the Arduino-based automatic welding system is able to improve time efficiency and joint quality [11]. Meanwhile, Hon et al. [12] emphasized that technological innovation such as rapid prototyping has accelerated advancements in manufacturing systems. This perspective supports the idea that integrating microcontrollers, solenoid drives, and ultrasonic sensors into spot welding is part of a broader trend toward smarter and more efficient production technologies. The methods to be used in this research include the design of mechanical and electronic systems of spot welding machines, integration of ultrasonic sensors for workpiece detection, programming Arduino microcontrollers to set the working time of the solenoid and logic control, testing welding performance on metal plates with varying thicknesses, and analyzing welding results based on the influence of voltage and time on weld quality. Through this approach, a semi-automatic spot welding system that is efficient, precise, and easy to implement in small to medium scale industries is expected to be created.

#### 2. RESEARCH METHOD

This This spot welding machine is designed using an Arduino microcontroller-based automatic control system interface. This system uses a linear solenoid as the main actuator to move the welding electrode vertically to the workpiece surface. Specifically, the solenoid used is a Solenoid Fuel Pump 1751, which operates at 12 VDC with a current of about 2-3 A. It is wound with enamel-coated copper wire (diameter  $\pm 0.35-0.40$  mm) and capable of producing a magnetic field of around 450-600 Gauss, with a stroke length of 10-15 mm and a pressing force of 15-20 N. These characteristics make it suitable to replace pneumatic drives in providing consistent pressure and precision movement during the welding process.

To detect the presence of the workpiece, an ultrasonic sensor is mounted at the bottom of the electrode. The system employs the HC-SR04 ultrasonic sensor, which operates at 5 VDC, with a measurement range of 2–400 cm and an accuracy of about 3 mm. In this design, the sensor is programmed to detect objects within 10 cm to ensure accurate electrode positioning before the welding process begins. The signal from the ultrasonic sensor is sent to the Arduino when the workpiece is within the programmed detection distance. After receiving the signal, the Arduino introduces a short delay to confirm the position and then activates the MY2N 12VDC relay, which works in parallel with a 12VDC automotive relay. The contacts on the MY2N relay are used to drive the MY4-GS relay, which is connected to the voltage regulator module.

The welding process lasts for 3 seconds, according to the programming on the Arduino, which has been adjusted based on the results of trials on various plate thicknesses (1.44 mm, 1.8 mm, and 2.2 mm) and voltage variations (4V to 8V). Once the duration is over, the system automatically cuts off the current to the solenoid and the electrodes return to their initial position. The entire system is

**DOI:** 10.33019/jurnalecotipe.v12i2.4569

designed to work repetitively with high precision, efficiently, and easily operated to support automation in spot welding processes on an industrial scale.

This research begins with the creation of an operation process flowchart developed to describe the system workflow from initialization to decision making and actions taken. Figure 1. The flowchart describes the process of controlling the system based on distance measurements using ultrasonic sensors. The process starts with the initialization of the ultrasonic sensor, LCD, and relay. After that, the ultrasonic sensor measures the distance of the workpiece.

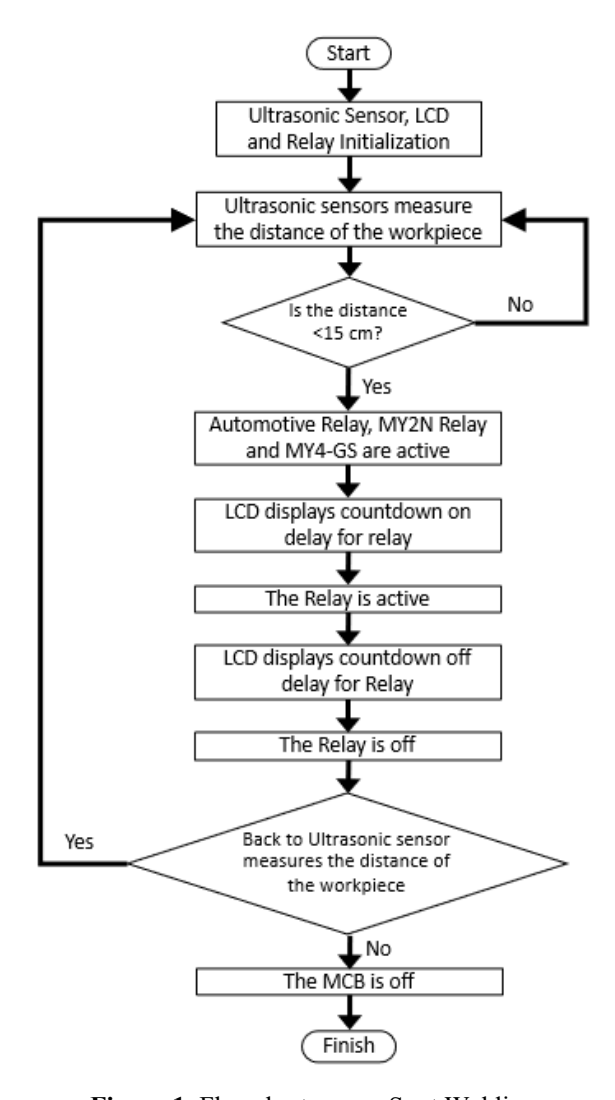


Figure 1. Flowchart proses Spot Welding

#### 2.1. Mechanical Design

The mechanical design of the tool includes structural design and arrangement of mechanical components to support the stability and efficiency of the tool. Figure 2 which is the front view shows the main arrangement such as the position of the electrode, solenoid, and ultrasonic sensor which are installed in line to maximize the accuracy of detecting the workpiece.

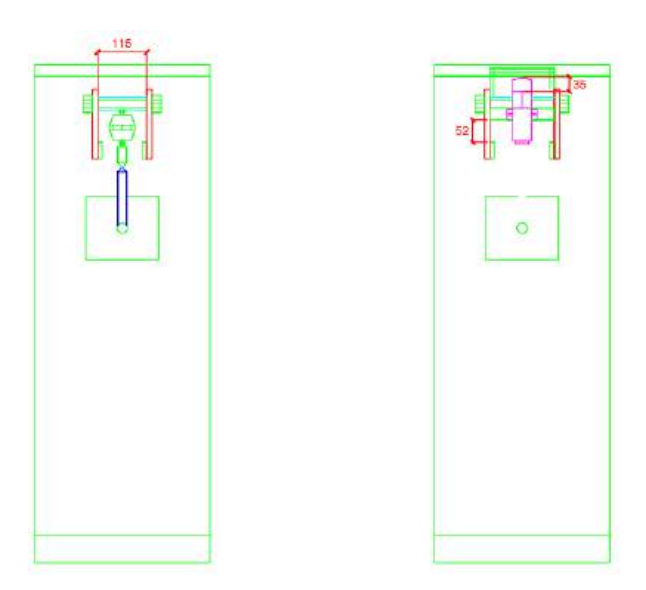


Figure 2. The Front View

While Figure 3, a side view, shows how the components are arranged vertically, including the swing arm mechanism and control system layout, to provide a clearer understanding of the direction of electrode movement during the welding process.

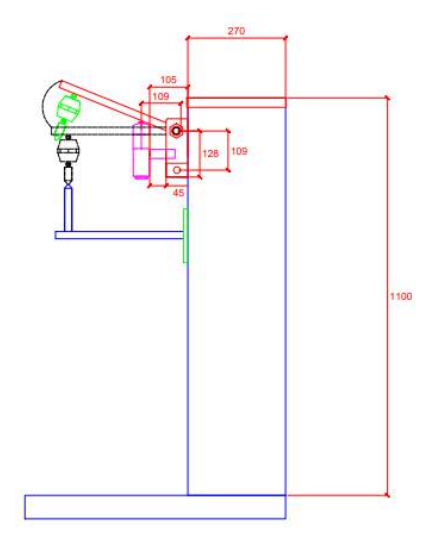


Figure 3. A Side View

Figure X shows the comparison of the spot welding machine before and after the integration of the microcontroller, solenoid actuator, and ultrasonic sensor. The initial design still relied on conventional control without precise automation, while the modified design demonstrates the application of Arduino-based control, Solenoid Fuel Pump 1751 as the electrode driver, and HC-SR04 ultrasonic sensor for accurate workpiece detection. This comparison highlights the improvement in automation and precision achieved through the proposed system.

**DOI:** 10.33019/jurnalecotipe.v12i2.4569



Figure 4. Before and After

The input component in this system is an ultrasonic sensor, which functions as a workpiece distance detector and sends signals to the Arduino. Arduino acts as the main processing and control center in this welding machine control system. Meanwhile, the output component consists of LCD and relay. In the relay output section, there are three relays connected to each other, where the third relay is connected to a potentio module that functions as a voltage regulator for the welding transformer. This stage is followed by the creation of an electronic circuit scheme that illustrates how all electronic components will be connected as shown in Figure 5.

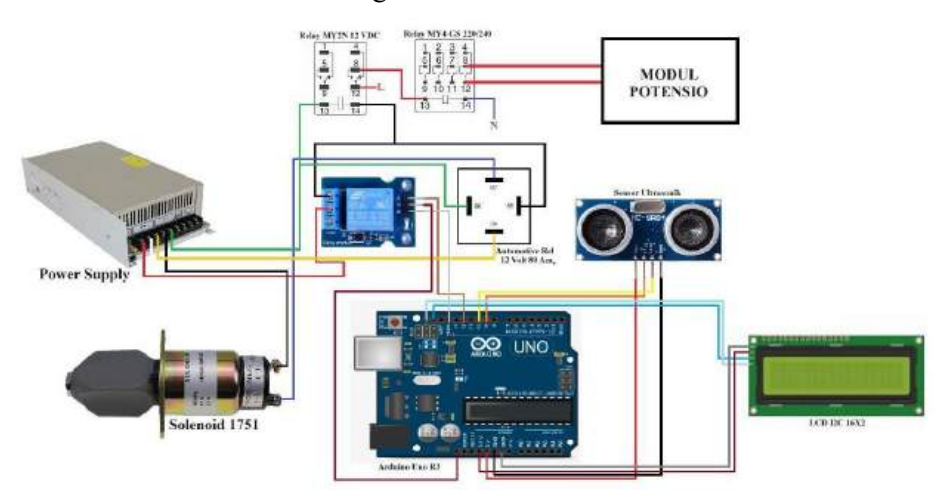


Figure 5. Component Circuit

# 2.2. Software Design

Software design includes the creation and development of software used to operate the tool. The program uses Arduino which is designed to control an automatic welding system based on ultrasonic sensors and relays. The ultrasonic sensor works by sending a signal through the trig pin and receiving its reflection through the echo pin, then calculating the distance of the workpiece based on the duration of the reflection. If the object is detected to be within a distance of less than or equal to 10 cm, the system will wait for 3 seconds to confirm the position, then activate the relay connected to the solenoid to press the electrode for 3 seconds. After that, the relay will be turned off automatically and the system returns to the initial state for the next cycle. The whole process is repeated periodically every 2 seconds, and displayed in real-time via Serial Monitor for debugging or monitoring distance

and relay status. This program is the core of a simple yet effective microcontroller-based spot welding control system.

#### 2.3. Hardware Design

Hardware design involves the creation of electronic circuits and the selection and arrangement of sensors, actuators and other components needed to function according to the device specifications. This stage begins with the creation of a system block diagram showing the main components and how they are interconnected. The system block diagram can be seen in Figure 6.

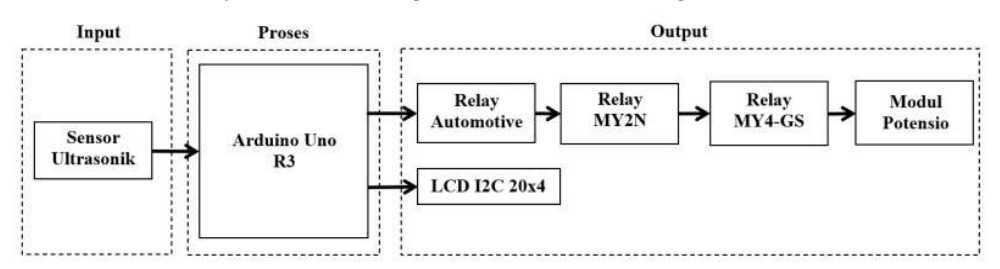


Figure 6. Blok diagram Hardware

The method of data collection in this study was carried out through the design and testing of a microcontroller-based spot welder welding system. This system consists of main components such as solenoid as electrode driver, Arduino as control center, and ultrasonic sensor as input to detect the presence of workpiece. In addition, a combination of 5V, 12V 80A relays, MY2N 12VDC relays, and MY4-GS relays are used to regulate the electric current to the solenoid and voltage regulator module. This voltage regulator module allows adjustment of the voltage level according to the type and thickness of the material being tested, so that welding defects can be minimized.

Testing is executed by operating the system in stages. The MCB is turned on first to activate the control and power circuits. Next, the switch on the voltage module is activated and the voltage is manually adjusted based on the test material. The test starts from the lowest voltage to prevent early damage to the material. Each change in voltage was tested on materials of different thicknesses, and the welding results were observed to assess the quality of the resulting weld points. This process is repeated to obtain accurate and consistent data.

During the test, the ultrasonic sensor detects the presence of a workpiece within a maximum distance of 15 cm from the electrode. When the workpiece is detected, the sensor sends a signal to the Arduino to activate the relay, which then flows current to the solenoid. The solenoid will pull the swing arm of the electrode to clamp the workpiece. Once the time is up, the relay cuts off the current and the solenoid returns to its original position. Each time this process is completed, data related to voltage, material thickness, and weld quality is recorded as part of data collection.

#### 3. RESULTS AND DISCUSSION

In the first experiment, a plate with a thickness of 1.4 mm was used. Experiments were carried out using varying voltages. Testing using a voltage of 2 and 4 volts the filter and plate stick very well, testing using a voltage of 6 volts the filter and plate stick but the filter is damaged, testing using tegangaan 8 and 10 volts the filter and plate do not stick and the filter is damaged.

In the second experiment, a plate with a thickness of 1.8 mm was used. Experiments were carried out using a voltage of 2 and 4 volts, the filter and plate did not stick, testing using a voltage of 6 and 8 volts, the filter and plate stuck well, testing using a voltage of 10 volts, the filter and plate stuck but the filter was damaged.

In the third experiment, a plate with a thickness of 2 mm was used. Experiments were carried out using voltages of 2, 4, and 6 filters and plates did not stick, testing using voltages of 8 and 10 volts filters and plates stuck well.

This test is carried out by welding on workpieces with plate thicknesses of 1.4mm, 1.8mm, and 2mm. The following data results taken from the welding results can be seen in Table 1.

**DOI:** 10.33019/jurnalecotipe.v12i2.4569

Table 1. Welding Testing

Thickness of Plate (mm)	(V)	(A)	(Watt)	(s)	Welding Result		
	2	55	110	3	Plate and filter are attached but not strong		
	4	354	1416	3	DI		
1,4	6	691	4146	3	Plate and filter are strong attached		
	8	1149	9192	3	The filter is attached to the plate, but the filter is slightly damaged		
	10	OL	OL	3	The filter is melted and there are holes in the plate		
	2	35	70	3	Plate and filter are not attached		
1,8	4	306	1224	3	Plate and filter are attached but not strong		
	6	535	3210	3	The filter is attached to the plate, but the filter is slightly damaged		
	8	850	6800	3	Plate and filter are strongly attached		
	10	1558	15580	3	Strainer melted but plate remains good		
	2	46	92	3	Plate and filter are strongly attached		
2,2	4	263	1052	3	Trace and finer are strongly attached		
	6	716	4296	3	Plate and filter are strongly attached		
	8	1005	8040	3	<u> </u>		
	10	1718	17180	3	The filter is still good but there is a hole in the plate		

The experiment can be seen in Figure 7, which presents the documentation evidence that supports the explanation and data shown in Table 1. The figure illustrates the actual implementation of the system under different voltage levels and plate thicknesses. This visual documentation validates the experimental setup and confirms the results summarized in the table, providing a clear comparison of welding outcomes based on the tested parameters.

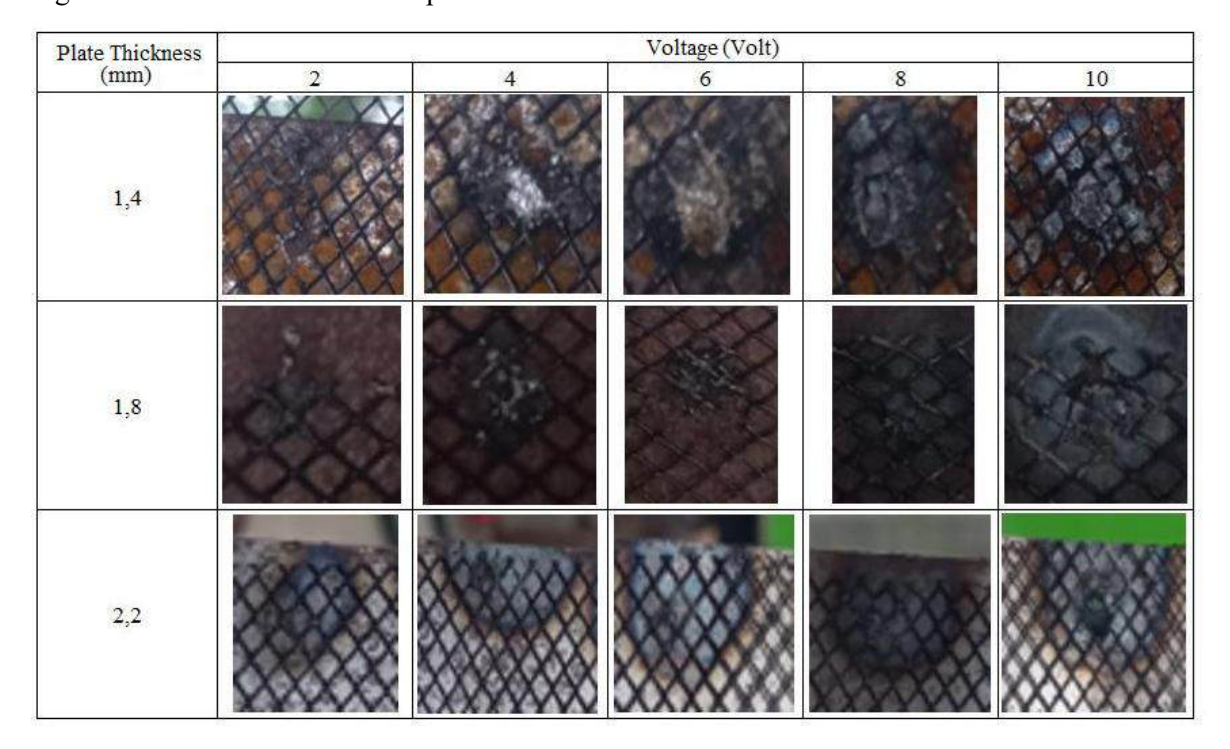


Figure 7. Spot Welding Test

#### 4. CONCLUSION

The experimental results show that welding efficiency is strongly influenced by the thickness of the material and the voltage used. For plates with a thickness of 1.44 mm, optimal results were achieved at a voltage of 4V-6V, while at thicknesses of 1.8 mm and 2.2 mm, efficient welding was obtained at a voltage of 8V. The microcontroller-based control system proved to be effective in managing sensors, relays, and solenoids, so as to regulate welding time and pressure precisely according to material characteristics. This modification improved welding quality, consistency, and efficiency. In addition, the automated system was able to detect material position, regulate pressure, and execute the welding process more reliably than the manual method. A series of independent trials were conducted prior to industrial deployment, and the results show that the system has great potential for wider application in a smart manufacturing environment in line with Industry 4.0 standards.

#### REFERENCES

- [1] Ma. Sahrevy, "Analisa Pengaruh Kuat Arus dan Waktu Las pada Proses Las Titik (Resistansi Spot Welding) terhadap Kekuatan Tarik pada Hasil Sambungan Las Pelat SS 400".L. Burlion, et al., "Keeping a ground point in the camera field of view of a landing UAV," *IEEE International Conference on Robotics and Automation, Vols 1*, pp. 5763-5768, 2013.
- [2] R. Siswanto and M. Eng, Buku Ajar Teknologi Pengelasan HMKB791, 2018.
- [3] S. Agus Setiawan and M. Hidayat, "Prototype Lampu Penerangan Jalan Otomatis Menggunakan Sensor LDR Berbasis Arduino Uno", [Online]. Available: <a href="https://www.offapedia.com/2021/04/pengertian-">https://www.offapedia.com/2021/04/pengertian-</a>
- [4] Galih Wsk, "Cara Kerja Sensor Ultrasonik: Teknologi Mendeteksi Jarak Akurat," wikielektronika.com. Accessed: Aug. 06, 2024. [Online]. Available: <a href="https://wikielektronika.com/cara-kerja-sensor-ultrasonik/">https://wikielektronika.com/cara-kerja-sensor-ultrasonik/</a>
- [5] Risky Abadi, "Solenoida: Pengertian, Fungsi, Cara Kerja, Penggunaan Sehari-Hari." Accessed: Aug. 12, 2024. [Online]. Available: https://thecityfoundry.com/solenoida/
- [6] Dickson Kho, "Pengertian Relay dan Fungsinya," *teknikelektronika.com*. Accessed: Aug. 12, 2024. [Online]. Available: <a href="https://teknikelektronika.com/pengertian-relay-fungsi-relay/">https://teknikelektronika.com/pengertian-relay-fungsi-relay/</a>
- [7] M. A. Wahab, *Welding: Principles and Applications*, 8th ed. Boston, MA: Cengage Learning, 2020.
- [8] A. A. Al-Fadhli and M. T. Abed, "Design and implementation of microcontroller-based resistance spot welding machine," *Int. J. Eng. Res. Technol. (IJERT)*, vol. 9, no. 2, pp. 213–218, Feb. 2020.
- [9] D. G. Chinn, R. A. Matula, and A. H. Titus, "Control strategies for resistance spot welding systems," *IEEE Trans. Ind. Appl.*, vol. 44, no. 6, pp. 1672–1678, Nov.–Dec. 2008.
- [10] D. G. Chinn, R. A. Matula, and A. H. Titus, "Control strategies for resistance spot welding systems," *IEEE Trans. Ind. Appl.*, vol. 44, no. 6, pp. 1672–1678, Nov.–Dec. 2008.
- [11] M. A. M. Yusof, M. F. Roslan, and R. A. Bakar, "Automated welding control system using Arduino microcontroller," in *Proc. 2018 IEEE Int. Conf. on Smart Instrumentation, Measurement and Applications (ICSIMA)*, Kuala Lumpur, Malaysia, 2018, pp. 1–5.
- [12] K. K. B. Hon, Y. Ma, and J. Y. H. Fuh, "An overview of rapid prototyping technologies in manufacturing," *Int. J. Adv. Manuf. Technol.*, vol. 15, no. 1, pp. 25–33, Jan. 1999.



**DOI:** 10.33019/jurnalecotipe.v12i2.4574

# A Comparative Study of Traditional PID Tuning Techniques and AI-Based Algorithmic Approaches Utilizing the Python Control Library

Purwadi Joko Widodo<sup>1</sup>, Heru Sukanto<sup>2</sup>, Budi Santoso<sup>3</sup>, Fitrian Imaduddin<sup>4</sup>, Lullus Lambang Govinda Hidayat<sup>5</sup>, Joko Triyono<sup>6</sup>, Iwan Instanto<sup>7</sup>, Rahman Wijaya<sup>8</sup>

1,2,3,4,5,6,7,8 Sebelas Maret University, Jl. Ir. Sutami Kentingan Surakarta, Indonesia

#### **ARTICLE INFO**

#### **Article historys:**

Received: 13/08/2025 Revised: 23/09/2025 Accepted: 30/10/2025

#### **Keywords:**

Artificial Intelligence; Genetic Algorithm; Particle Swarm Optimization; PID Parameter; Ziegler-Nichols; Python Control Library; Python Simulation

#### **ABSTRACT**

This study aims to compare PID parameter settings with conventional tuning methods and tune methods using AI (artificial intelligence) algorithms. This study was conducted by means of simulation using a computer program created in Python and utilizing AI libraries to solve the problem of determining PID (proportional-integral-derivative) parameters. Two AI algorithms used in this study, namely the Genetic Algorithm (GA) and Particle Swarm Optimization (PSO) methods, were compared with the conventional Ziegler-Nichols method. The study was conducted by applying the PID parameters obtained to a certain transfer function and then comparing them on several related aspects. The results of the study showed that the solution obtained using the AI method requires a longer execution time, more than 2 seconds for PSO and more than 3 seconds for GA, while ZN requires less than 1 second. However, the AI method can provide better solutions, as can be seen from the magnitude of the ITAE that occurs, where GA and PSO provide ITAE less than 1 while ZN is more than 22.



This work is licensed under a Creative Commons Attribution 4.0 International License

# **Corresponding Author:**

Purwadi Joko Widodo Sebelas Maret University, Jl. Ir. Sutami Surakarta, Jawa Tengah, Indonesia Email: purwadijokow@staff.uns.ac.id.

#### 1. INTRODUCTION

PID is one of the most widely applied methods in automation and control systems. This method can be applied to control parameters in a system, such as temperature, speed, position, pressure, and others. The PID controller minimizes the error between the setpoint value (the desired value) and the output value produced by the system. In PID, three actions are associated with the controller: proportional, integral, and derivative.

Proportional Component (P): This component is used to reduce errors by responding proportionally to the magnitude of the detected error. The larger the error, the greater the proportional response and reaction. Integral Component (I): This component is used to address errors that accumulate over time. This component is important for systems that experience small, continuous errors that cannot be addressed with the proportional component alone. Derivative Component (D): This component predicts future error trends based on the rate of error change. This component provides control to dampen rapid changes and avoid overshoot.



Volume 12, Issue 2, October 2025, pp. 234-244 ISSN <u>2355-5068</u>; e-ISSN <u>2622-4852</u>

**DOI:** 10.33019/jurnalecotipe.v12i2.4574

This method is quite simple, but determining the PID parameters, namely Kp, Ki, and Kd, which are specific to the conditions of the system in question, is quite a challenge. Mistakes in determining the Kp, Ki, and Kd parameters in a system may cause the system to become unstable or respond less than expected. For example, excessive overshoot or unacceptable stabilization time may occur[1]. Generally, PID parameter adjustment can be done through trial and error, which is, of course, time-consuming and results in less than optimal settings. Therefore, various more systematic methods such as grid search, genetic algorithms, or model-based optimization are used to help determine more precise parameters[2].

Classic methods such as Ziegler–Nichols (ZN) have long been used for PID tuning, but often result in high overshoot, long settling times, and steady-state errors that do not meet the needs of modern systems. To overcome these limitations, various artificial intelligence-based optimization methods, such as Particle Swarm Optimization (PSO) and Genetic Algorithm (GA) have begun to be used because they are able to produce PID parameters that are closer to design specifications, namely fast, stable, and precise responses.

The existence of computers and software and their development today are very important in this regard. Python, with its advantages, is also a choice in this regard. Python is a programming language that, in the last decade, has become a very popular computer programming language among engineers and researchers because of its ease of use and the variety of libraries available for numerical data processing, control analysis, and simulation. The main advantage of using Python in computer programming is its ability to integrate various libraries to handle complex technical aspects in a simple and intuitive way [3].

Python libraries were used in PID control implementation, including NumPy, SciPy, and Control. Numpy and scipy provide tools for performing fast numerical calculations, such as matrix operations, differentiation, and integration, which are crucial in managing dynamic systems [4]. The use of the matplotlib and plotly libraries enables the graphical visualization of simulation and experimental results, providing better insight into assessing system performance. The ability to visualize the system's response to changes in PID parameters or to external disturbances helps understand the behavior of more complex systems [5]. Python with the python-control library, as open-source software, offers a more affordable and flexible solution for teaching and research in the field of engineering control, covering the implementation of PID control in Python, including its use for simulation and analysis of control systems [6 - 8].

Implementation of PID control requires careful testing and parameter tuning, often performed directly on a physical system. However, simulation using computers and software allows users to achieve time and cost savings before physically implementing the control. Python allows users to do this. The use of Python allows faster experimentation with various parameter combinations to find optimal settings for P, I, and D parameters, which is not easily achieved with conventional methods [6,9].

Various advantages offered by Python are making more and more engineers, researchers, and developers turn to Python as a primary tool in managing PID control. Many articles have been written on the use of Python in the field of control, especially PID [10-11]. This shows Python's reliable performance in control system analysis.

This article uses Python to simulate and analyze PID control parameter settings using conventional methods and advanced methods utilizing AI algorithms. Using an AI algorithm to determine PID controller parameters, there are several popular and effective algorithms. Each algorithm has its advantages and disadvantages, and the selection of the best algorithm depends on the specific application context, such as system complexity, computational time, and required accuracy.

Several AI algorithms have been used for PID parameter optimization, including:

1. Genetic Algorithm (GA). This algorithm has advantages, suitable for optimization problems with many parameters and without explicit functions, can work well on large and non-linear parameter spaces, and does not require gradients or deep function information. The disadvantage is that this algorithm requires more iterations and a longer time for convergence compared to other algorithms, as a result, it can be expensive in computation if the population size or number of generations is too large[12].



**DOI:** 10.33019/jurnalecotipe.v12i2.4574

- 2. Particle Swarm Optimization (PSO). The PSO algorithm has several advantages, including being faster than GA for many optimization problems, being able to avoid overfitting well in large parameter spaces, and achieving faster convergence compared to GA. However, its drawback is that it is not as effective as GA for optimization with many local minimum points [13].
- 3. Simulated Annealing (SA). This algorithm has the advantage of being easy to implement and does not require a lot of computation. It can avoid getting stuck in local solutions and potentially find a global solution. However, its drawback is that the search process can be very slow, especially in large search spaces, and it is not always as effective as GA or PSO in terms of speed and accuracy on some problems [12].
- 4. Reinforcement Learning (RL) has the advantage of being able to continuously adjust based on environmental feedback, learning in real time, and adapting to changes in the system. One of the disadvantage is that this algorithm requires a lot of data for training and iteration.

GA and PSO are often used in PID parameter optimization because of their ability to explore a wide parameter space without requiring special assumptions about the form of the cost function[12].

#### 2. RESEARCH METHOD

# 2.1. Research Approach

This research uses a quantitative, experimental approach based on computer simulation. The objective is to assess the performance of a PID control system with parameters determined by an artificial intelligence (AI) algorithm, compared to conventionally determined PID parameters.

# 2.2. Research Design

The research design is carried out in several stages, as follows:

- 1. System Modeling. At this stage, a mathematical model of the controlled system is developed, such as a first- or second-order linear system (e.g., a heating system, a motor positioning system, etc.). The system model is then simulated using the Python programming language.
- 2. PID Control Design. The next stage is implementing PID control with initial parameters (the Ziegler-Nichols method can be used as a baseline), followed by developing the PID control function to be used in the simulation.
- 3. AI Development and Integration. The next stage is developing an AI algorithm to optimize the PID parameters (Kp, Ki, Kd). The algorithms used in this research are the Genetic Algorithm (GA) and Particle Swarm Optimization (PSO). The objective function in the optimization process is to minimize system errors, such as:
  - a. Integral of Time-weighted Absolute Error (ITAE)
  - b. Overshoot, settling time, rise time
- 4. Simulation and Data Collection: This stage runs simulations on two scenarios: a conventional PID with Ziegler-Nichols theory (baseline) and a PID with AI-optimized parameters, and then data is recorded on the system's response to disturbances or setpoint changes.
- 5. System Performance Evaluation: The next stage is to analyze system performance based on response graphs and performance metrics, namely rise time, settling time, overshoot, and steady-state error. The error value in this study uses the ITAE criterion.

The flowchart of the research is illustrated in Figure 1 and Table 1 shows parameters used in simulations Figure 1 shows this research begins with system modeling in the form of a transfer function. Next, a PID control design is carried out using the conventional Ziegler–Nichols method and its performance is evaluated through simulation. To improve system performance, PID parameters are then optimized with AI-based algorithms, Genetic Algorithm (GA) and Particle Swarm Optimization (PSO). The optimization results are simulated again to obtain system performance data which are then compared with the results of conventional methods. Based on the results of the comparative evaluation, an analysis is carried out and conclusions are drawn regarding the effectiveness of the optimization method compared to the classical approach.

# 2.3. Tools and Equipment

1. Programming Language: Python

Volume 12, Issue 2, October 2025, pp. 234-244 ISSN <u>2355-5068</u>; e-ISSN <u>2622-4852</u>

**DOI:** 10.33019/jurnalecotipe.v12i2.4574

2. The Python libraries used in this research are numpy, scipy, and matplotlib for numerical simulation and visualization, the control library for dynamic system models, and the Python library for AI.

# 2.4. Data Collection Techniques

Data is obtained from simulation results in the form of system response graphs and performance metric values for each scenario. The simulation is run several times to validate the results.

#### 2.5. Data Analysis Techniques

Analysis is conducted quantitatively by comparing simulation results between conventional PID and PID-AI, presented in the form of comparison tables and system performance graphs.

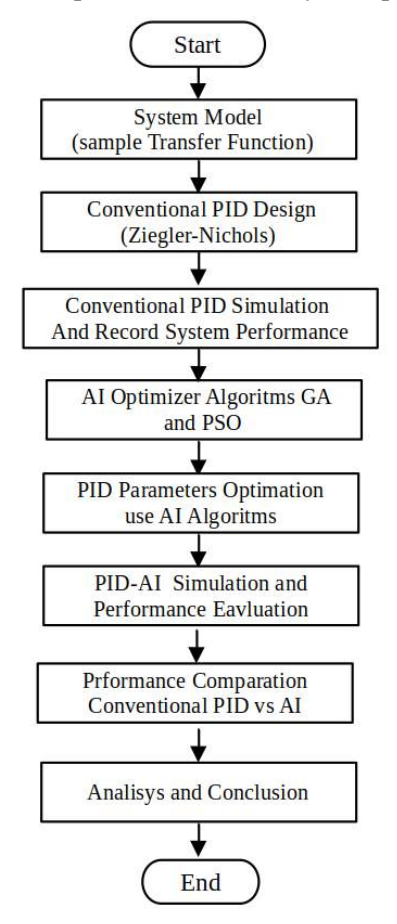


Figure 1. Flowchart of Research Method

# Pseudocode used for PID + AI Simulation,

```
# Step 1: System Model
def system_model(K, T, time):
    # return response of a transfer function (e.g., first order system)
    return control.TransferFunction([K], [T, 1])

# Step 2: PID Evaluation
def pid_simulation(Kp, Ki, Kd, system, t):
    # calculate system respons use PID control
    # use control.feedback and control.forced_response
    return output, error_metrics

# Step 3: Objectif Function for AI
def objective_function(params):
    Kp, Ki, Kd = params
    output, error = pid_simulation(Kp, Ki, Kd, system_model(...), t)
    # return ITAE
    return compute_ITAE(error, t)

# Step 4: Optimatiton with AI (PSO or GA)
best_params = run_ai_optimizer(objective_function)

# Step 5: Repeat Simulation with best Parameter
output_ai, error_ai = pid_simulation(*best_params, system_model(...), t)

# Step 6: Compare with Conventional PID method
output_std, error_std = pid_simulation(Kp_manual, Ki_manual, Kd_manual, system_model(...), t)
```

# Step 7: Visualisation and Analisys
plot\_comparison(output\_std, output\_ai)
report\_performance\_metrics(error\_std, error\_ai)

Table 1. Parameters Simulations

Algorithm	Parameters	Values (Default in code)			
GA (Genetic Algorithm)	Population Size (pop_size)	20			
	Maximum Generations (gen_max)	30			
	Mutation Rate (mutation_rate)	0.1			
	PID Parameter Bounds (bounds)	$Kp \in [0.5], Ki \in [0.5], Kd \in [0.2]$			
PSO (Particle Swarm Optimization)	Number of Particles (num_particles)	15			
	Maximum Iterations (max_iter)	30			
	Inertia Weight (w)	0.5			
	Learning Coefficient (c1, c2)	1.5, 1.5			
	PID Parameter Bounds (bounds)	Kp∈[0.5],Ki∈[0.5],Kd∈[0.2]			
ZN (Ziegler-Nichols)	Calculation based on gain margin (Ku) and ultimate period (Pu)	Calculation base on formula			
Aspect	Simulation Time (T_FINAL)	20 s			
	Number of Time Points (T_STEPS)	500			
	Time Range (T)	0 – 20 s			
	Plant	$G(s)=1/(s^2+6s+5)$			
	Input	Step input = 1			
	Evaluation Criteria	ITAE			
	Performance Analysis	Overshoot, Rise Time, Settling Time, Steady- State Error			

#### 3. RESULTS AND DISCUSSION

For observation and comparison in this study, a Python program was built using three selected methods, namely the Ziegler-Nichols method, representing the conventional method, and the GA and PSO methods, representing the AI method. The three methods produce a graph and several important data points related to the methods above. The developed Python code allows users to change the system's transfer function value, and generate PID parameter values, namely overshot, ITAE error, rise time, settling time, and the required execution time. Below is Python code for the simulation.

```
Kp, Ki, Kd = pid
C = tf([Kd, Kp, Ki], [1, 0])
TF = feedback(C * plant, 1)
t, y = step_response(TF, T)
overshoot = (np.max(y) - 1.0) * 100
ess = np.abs(1.0 - y[-1])
rise_time = t[np.where(y >= 0.9)[0][0]] if any(y >= 0.9) else None
settling_idx = np.where(np.abs(y - 1.0) > 0.05)[0]
settling_time = t[settling_idx[-1]] if len(settling_idx) > 0 else t[-1]
return overshoot, ess, rise_time, settling_time
 # === GA ===
def ga ptd(plant, pop_size=20, gen_max=30, mutation_rate=0.1, bounds=((0, 5), (0, 5), (0, 2))):
    def random_individual():
        return [random.uniform(*bounds[i]) for i in range(3)]
         def crossover(p1, p2):
                  alpha = random.random()
return [(1 - alpha) * p1[i] + alpha * p2[i] for i in range(3)]
         def mutate(ind):
    i = random.randint(0, 2)
                  ind[i] += random.uniform(-1, 1)
ind[i] = max(bounds[i][0], min(bounds[i][1], ind[i]))
return ind
         population = [random_individual() for _ in range(pop_size)]
for _ in range(gen_max):
    scores = [pid_itae(ind, plant) for ind in population]
    ranked = sorted(zip(scores, population), key=lambda x: x[0])
    population = [x[1] for x in ranked[:pop_size//2]]
                  children = []
while len(children) < pop_size - len(population):</pre>
                          p1, p2 = random.sample(population, 2)
child = crossover(p1, p2)
if random.random() < mutation_rate:
    child = mutate(child)
                           children.append(child)
         population += children
return ranked[0][1]
 w = 0.5
         c1 = 1.5
         c2 = 1.5
         dim = 3
         particles = np.random.uniform([b[0] for b in bounds], [b[1] for b in bounds], (num_particles, dim))
        particles = np.zeros_like(particles)
personal_best = particles.copy()
personal_best_scores = np.array([pid_itae(p, plant) for p in particles])
global_best = personal_best[np.argmin(personal_best_scores)]
         for _ in range(max_iter):
    for i in range(num_particles):
        r1, r2 = np.random.rand(dim), np.random.rand(dim)
                          w * velocities[i] = (
    w * velocities[i]
    + c1 * r1 * (personal_best[i] - particles[i])
    + c2 * r2 * (global_best - particles[i])
                           /
particles[i] += velocities[i]
particles[i] = np.clip(particles[i], [b[0] for b in bounds], [b[1] for b in bounds])
                           score = pid_itae(particles[i], plant)
if score < personal_best_scores[i]:
    personal_best[i] = particles[i].copy()
    personal_best_scores[i] = score</pre>
                  global_best = personal_best[np.argmin(personal_best_scores)]
         return global_best.tolist()
 # === Ziegler-Nichols Tuning ===
# === Ziegler-Nichols Tuning ===

def zn_pid(plant):
    K = 1.0
    C = tf([K], [1])
    loop = C * plant
    gm, pm, wg, wp = margin(loop)
    if gm == float("inf") or wp == 0 or np.isnan(gm) or np.isnan(wp):
        print("ZN: margin gagal dihitung, fallback ke PID default")
        return [1.0, 1.0, 0.0] # fallback
        Ku = gm

Pu = 2 * np.pi / wp

Kp = 0.6 * Ku

Ki = 1.2 * Ku / Pu

Kd = 0.075 * Ku * Pu

return [Kp, Ki, Kd]
# === Plot Comparation ===
def plot_comparison(pids, labels, plant):
   plt.figure()
   for pid, label in zip(pids, labels):
```

```
Kp, Ki, Kd = pid
C = tf([Kd, Kp, Ki], [1, 0])
TF = feedback(C * plant, 1)
t, y = step_response(TF, T)
plt.plot(t, y, label=label)
plt.title("Step Response Comparison")
plt.xlabel("Time (s)")
plt.ylabel("Output")
plt.grid(True)
      plt.grid(True)
plt.legend()
      plt.show()
# === Save Result as CSV ===
     itae = pid_itae(pid, plant)
os, ess, tr, ts = analyze_response(pid, plant)
writer.writerow([method] + pid + [itae, os, ess, tr, ts, elapsed])
    === Main ===
__name__ == "__main_
plant = get_plant()
       t0 = time.time()
      pid_zn = zn_pid(plant)
t_zn = time.time() - t
      t0 = time.time()
pid_ga = ga_pid(plant)
t_ga = time.time() - t
       t0 = time.time()
       pid_pso = pso_pid(plant)
t_pso = time.time() - t0
       methods = ["Ziegler-Nichols", "Genetic Algorithm", "Particle Swarm"]
pids = [pid_zn, pid_ga, pid_pso]
times = [t_zn, t_ga, t_pso]
       print("\nZiegler-Nichols PID:", pid_zn, f"(Waktu: {t_zn:.2f}s)")
print("GA PID:", pid_ga, f"(Waktu: {t_ga:.2f}s)")
print("PSO PID:", pid_pso, f"(Waktu: {t_pso:.2f}s)")
       for method, pid, elapsed in zip(methods, pids, times):
   os, ess, tr, ts = analyze_response(pid, plant)
   print(f"{method}: Overshoot = {os:.2f}%, ess = {ess:.4f}, Rise Time = {tr:.2f}s, Settling Time = {ts:.2f}s, \
                                Time = {elapsed:.2f}s")
      plot_comparison(pids, methods, plant)
save_results_to_csv("pid_comparison_results.csv", methods, pids, times, plant)
print("\nResult was saved at 'pid_comparison_results.csv'")
```

By taking a simple transfer function as shown in Figure 2 and the system transfer function as shown in equation (1), a simulation was then carried out with the Python Program Code that was created and the results were compared. A simple example is used in the simulation to simplify the simulation and comparisons performed.

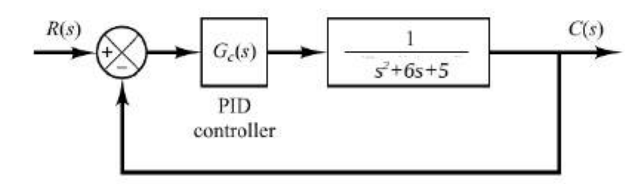


Figure 2. System block diagram used in simulations

$$FA = \frac{1}{s^2 + 6s + 5} \tag{1}$$

Figures 3 and 4 show the simulation results of the three methods being compared to observe the system's response to the step function test signal. Figure 3 is the first simulation, and Figure 4 is the second simulation to verify the result of the first simulation.

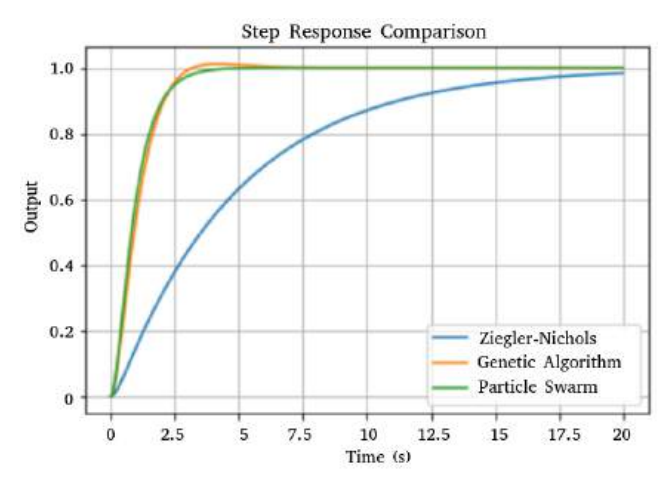


Figure 3. Simulation result 1

Ziegler-Nichols PID: [1.0, 1.0, 0.0] (Execution Time: 0.00s)
GA PID: [4.024979381891309, 4.887865592973621, 0.017178639320462367] (Execution Time: 3.97s)
PSO PID: [5.0, 5.0, 0.0] (Execution Time: 2.99s)
Ziegler-Nichols: Overshoot = -1.61%, ess = 0.0161, Rise Time = 11.26s, Settling Time = 14.55s, Time = 0.00s
Genetic Algorithm: Overshoot = 1.18%, ess = 0.0000, Rise Time = 2.08s, Settling Time = 2.40s, Time = 3.97s
Particle Swarm: Overshoot = -0.00%, ess = 0.0000, Rise Time = 2.04s, Settling Time = 2.48s, Time = 2.99s

**Table 2.** Numerical datas of PID parameters generated from the 1<sup>st</sup> simulation

Method	Кр	Ki	Kd	ITAE	Overshoot	Steady State Error	Rise Time	Settling Time	Execution Time (s)
Ziegler-Nichols	1.00000	1.00000	0.00000	22.08894	-1.60876	0.01609	11.26253	14.54910	0.00151
Genetic Algorithm	4.02498	4.88787	0.01718	0.92264	1.18237	0.00000	2.08417	2.40481	3.96686
Particle Swarm	5.00000	5.00000	0.00000	0.79987	0.00000	0.00000	2.04409	2.48497	2.99478

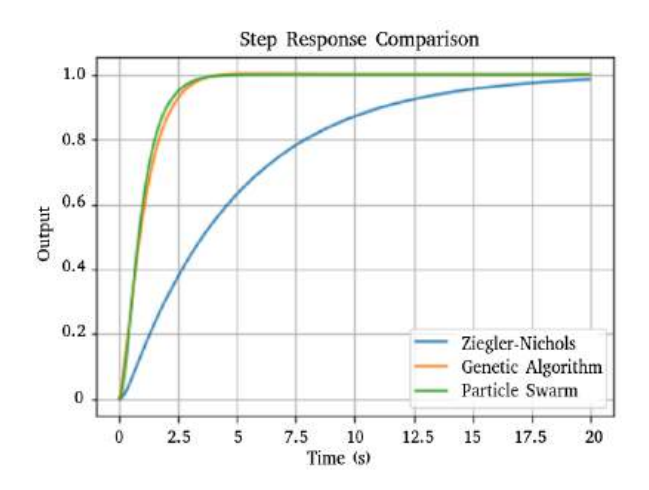


Figure 4. Simulation Result 2

Ziegler-Nichols PID: [1.0, 1.0, 0.0] (Execution Time: 0.00s)
GA PID: [4.587986891341883, 4.718672144798576, 0.33918189648143965] (Execution Time: 9.29s)
PSO PID: [5.0, 5.0, 0.0] (Execution Time: 6.80s)
Ziegler-Nichols: Overshoot = -1.61%, ess = 0.0161, Rise Time = 11.26s, Settling Time = 14.55s, Time = 0.00s
Genetic Algorithm: Overshoot = 0.20%, ess = 0.0000, Rise Time = 2.28s, Settling Time = 2.73s, Time = 9.29s
Particle Swarm: Overshoot = -0.00%, ess = 0.0000, Rise Time = 2.04s, Settling Time = 2.48s, Time = 6.80s

**Table 3.** Numerical datas of PID parameters generated from the 2<sup>nd</sup> simulation

			,	L	0				
Method	Кр	Ki	Kd	ITAE	Overshoot	Steady State Error	Rise Time	Settling Time	Execution Time (s)
Ziegler-Nichols	1.00000	1.00000	0.00000	22.08894	-1.60876	0.01609	11.26253	14.54910	0.00311
Genetic Algorithm	4.58799	4.71867	0.33918	0.94581	0.20224	0.00000	2.28457	2.72545	9.29095
Particle Swarm	5.00000	5.00000	0.00000	0.79987	0.00000	0.00000	2.04409	2.48497	6.80492

**DOI:** 10.33019/jurnalecotipe.v12i2.4574

The evaluation was conducted by analyzing system performance against step input signals and measuring several performance parameters, such as Integral Time-weighted Absolute Error (ITAE), overshoot, rise time, settling time, and steady-state error (SSE). The results of two tests showed a consistent performance pattern.

The Ziegler–Nichols method demonstrated a very stable system response with a very small overshoot value (~1.61%). However, the response speed was relatively slow, with a rise time of 11.26 seconds and a settling time that was not reached within the 20-second simulation duration, in this case ~14.55 seconds. The high ITAE value (22.08894) also indicates that the system's accumulated error is still large. This is consistent with the characteristics of the Ziegler–Nichols method, which was initially developed for heuristic initial PID tuning of continuous-time linear systems without regard for optimal performance [2].

In contrast, Genetic Algorithm method demonstrated significantly more responsive performance. With a rise time of less than 3 seconds and a settling time of approximately under 3 seconds, this method was able to quickly adjust the system to achieve stability. Although its overshoot was higher than PSO (approximately 1.18%–0.20%), GA remained superior in terms of speed and effectiveness in reducing error, as widely reported in the control optimization literature [14]. The lower ITAE value (~0.92–0.94) compared to ZN indicates that the GA tuning results were more efficient in reducing the total error over time.

The Particle Swarm Optimization method demonstrated the most balanced performance of the three. With a smaller overshoot (approximately  $\sim 0\%$ ) and rise and settling times nearly equivalent to GA, PSO provided excellent results in the context of a tradeoff between stability and speed. PSO is known to excel in exploring and exploiting global solution spaces without requiring many explicit parameters, as demonstrated in the literature 15,16]. The similar ITAE values to GA ( $\sim 0.79$ ) indicate that PSO is also capable of effectively minimizing errors.

In terms of steady-state error, both GA and PSO yielded the same final value (~0.0000), significantly lower than the ZN method. This indicates that both AI-based methods can provide more accurate and precise PID tuning, consistent with previous studies on artificial intelligence in system control [17].

Overall, intelligent optimization approaches such as GA and PSO have been shown to provide significantly superior PID tuning results compared to classical methods. GA is more suitable for systems requiring very fast response, albeit with slightly larger overshoot. Meanwhile, PSO is well-suited for systems requiring a compromise between stability and speed. On the other hand, the Ziegler–Nichols method still has practical value as an initial approach or rough reference for PID tuning, although its results are less than optimal in the context of modern dynamic performance.

The test results show that the Ziegler–Nichols (ZN) method provides the lowest performance, with high ITAE, significant overshoot, and long rise and settling times, despite its very short execution time. In contrast, artificial intelligence-based optimization methods, namely Genetic Algorithm (GA) and Particle Swarm Optimization (PSO), consistently produce much better performance. Both methods are able to reduce ITAE by more than 95%, eliminate steady-state error, and accelerate rise and settling times by more than 80% compared to ZN. PSO shows more stable performance with zero overshoot and relatively consistent results, while GA tends to vary but still produces significant improvements.

The application of GA and PSO in control systems provides practical advantages, they are more efficient, accurate, and adaptive PID tuning compared to classical methods such as Ziegler–Nichols. Both of them are capable for optimation performance in complex systems that are nonlinear or have variable parameters, for example in industrial temperature control, electric motors, and renewable energy systems. PSO is faster in convergence, while GA is more flexible in finding optimal solutions, so both can be selected according to needs. Although they require higher computational costs, modern hardware developments allow offline and online implementations, and Python with its various libraries provides an alternative for researcher and engineers to do so.

# 4. CONCLUSION

Based on the simulation results, it can be concluded that tune PID parameters, can be improve use artificial intelligence algorithms, intelligent optimization-based tuning methods such as the Genetic



Algorithm (GA) and Particle Swarm Optimization (PSO) significantly improve performance compared to the classical Ziegler-Nichols (ZN) method.

The Ziegler–Nichols method demonstrates good system stability with very small overshoot values(~1.61%). ZN system response tends to be slow and less efficient in reducing the total error over time, as reflected by the high ITAE value more than 22. This makes the ZN method more suitable as an initial tuning approach or for systems that do not allow any overshoot at all. On the other hand, the Genetic Algorithm method demonstrates very fast system response, both in terms of rise time (~2s) and settling time(~2s), and very small steady-state error(~0). However, this method produces relatively higher overshoot(~0.2) than PSO value (~0). The Particle Swarm Optimization method provides the most balanced performance, with lower overshoot than GA while maintaining excellent response speed and error efficiency. ITAE values produce by PSO (~0.7)are nearly equivalent to those of GA(~0.9), demonstrating its high effectiveness in PID tuning.

Considering all evaluation parameters, the PSO method can be considered an optimal approach for systems that require a balance between speed and stability. GA, on the other hand, excels in applications that prioritize response speed. So, the Ziegler–Nichols method remains relevant as a baseline or initial reference, although it is not as efficient as the two intelligent methods in complex dynamic control. Last but not least Python with its libraries, is quite reliable for solving control problems both conventionally and by applying AI algorithms. In the future, further exploration can be carried out on the use of Python as a freeware for various experiments, especially in the field of control engineering.

# Acknowledgments

LPPMP UNS through the Hibah Penguatan Kapasitas Group Riset (PKGR UNS) with Research Assignment Agreement Number 371/UN27.22/PT.01.03/2025.

# REFERENCES

- [1] K. Ogata, "Modern Control Engineering. in Instrumentation and Controls Series". Prentice Hall, 2010. [Online]. Available: https://books.google.co.id/books?id=Wu5GpNAelzkC
- [2] J. G. Ziegler and N. B. Nichols, "Optimum Settings for Automatic Controllers," Journal of Fluids Engineering, vol. 64, no. 8, pp. 759–765, Nov. 1942, doi: 10.1115/1.4019264.
- [3] G. van Rossum, "Python Programming Language," in USENIX Annual Technical Conference, 2007. [Online]. Available: https://api.semanticscholar.org/CorpusID:45594778
- [4] C. R. Harris et al., "Array programming with NumPy" Nature, vol. 585, no. 7825, pp. 357–362, Sept. 2020, doi: 10.1038/s41586-020-2649-2.
- [5] J. D. Hunter, "Matplotlib: A 2D Graphics Environment," Computing in Science & Engineering, vol. 9, no. 3, pp. 90–95, 2007, doi: 10.1109/MCSE.2007.55.
- [6] D. H. Kim, "Advanced Lecture for PID Controller of Nonlinear System in Python," IJRTE, vol. 9, no. 6, pp. 20–29, Mar. 2021, doi: 10.35940/ijrte.F5375.039621.
- [7] S. Fuller, B. Greiner, J. Moore, R. Murray, R. Van Paassen, and R. Yorke, "The Python Control Systems Library (python-control)," in 2021 60th IEEE Conference on Decision and Control (CDC), Austin, TX, USA: IEEE, Dec. 2021, pp. 4875–4881. doi: 10.1109/CDC45484.2021.9683368.
- [8] P. Saraf, M. Gupta, and A. M. Parimi, "A Comparative Study Between a Classical and Optimal Controller for a Quadrotor," Sept. 28, 2020, arXiv: arXiv:2009.13175. doi: 10.48550/arXiv.2009.13175.
- [9] B. Smith, "Building a Simulated PID Controller in Python," Medium. Accessed: July 31, 2025. [Online]. Available: https://medium.com/@bsmith4360/building-a-simulated-pid-controller-in-python-111b08ccae1a



Volume 12, Issue 2, October 2025, pp. 234-244 ISSN <u>2355-5068</u>; e-ISSN <u>2622-4852</u>

**DOI:** 10.33019/jurnalecotipe.v12i2.4574

- [10] D. H. Kim and H. Alemayehu, "A study on Teaching Method of Control Engineering by Using Python Based PID," International Advanced Research Journal in Science, Engineering and Technology, vol. 7, no. 9, pp. 1–9, Sept. 2020, doi: 10.17148/IARJSET.2020.7901. R. V. Petrosian, I. A. Pilkevych, and A. R. Petrosian, "Algorithm for optimizing a PID controller model based on a digital filter using a genetic algorithm," in doors, 2023. [Online]. Available: https://api.semanticscholar.org/CorpusID:259115656
- [11] A. A. Salem, M. A. Moustafa, and M. E. Ammar, "Tuning PID Controllers Using Artificial Intelligence Techniques.," 2014. [Online]. Available: https://api.semanticscholar.org/CorpusID:199020399
- [12] A. Taeib, A. Ltaeif, and A. Chaari, "A PSO Approach for Optimum Design of Multivariable PID Controller for nonlinear systems," June 26, 2013, arXiv: arXiv:1306.6194. doi: 10.48550/arXiv.1306.6194.
- [13] D. Goldberg, "Genetic Algorithm in Search, Optimization, and Machine Learning," Addison-Wesley, Reading, Massachusetts, vol. xiii, Jan. 1989.
- [14] J. Kennedy and R. Eberhart, "Particle swarm optimization," in Proceedings of ICNN'95 International Conference on Neural Networks, Nov. 1995, pp. 1942–1948 vol.4. doi: 10.1109/ICNN.1995.488968.
- [15] D. Oliva, A. Ramos Michel, M. Navarro, E. H. Haro, and A. Casas, "Particle Swarm Optimization," 2023, pp. 49–71. doi: 10.5281/zenodo.7537827.



# A New 12-Phase Toroidal Transformer Design to Improve Efficiency and Power Quality in Electric Vehicle Fast Charging Systems

Partaonan Harahap<sup>1</sup>, Muhammad Imran Hamid<sup>2</sup>, Ariadi Hazmi<sup>3</sup>

1.3 Department of Electrical Engineering, Faculty of Engineering, Universitas Muhammadiyah Sumatera Utara, Indonesia, 1.2 Department of Electrical Engineering, Faculty of Engineering, Universitas Andalas, Padang, Indonesia,

#### **ARTICLE INFO**

#### **Article historys:**

Received: 13/07/2025 Revised: 25/09/2025 Accepted: 30/10/2025

#### **Keywords:**

12-Phase Configuration; Electric Vehicle; Energy Efficiency; Fast Charging; Toroidal Transformer

#### **ABSTRACT**

Transformers are essential components in electric vehicle (EV) fast charging systems, particularly in ensuring high efficiency and maintaining power quality. This study introduces a new design and implementation of a 12-phase toroidal transformer integrated into a 50 kW fast charging system. The main contribution of this research lies in improving energy efficiency, thermal stability, and harmonic suppression, which are critical challenges in conventional transformer configurations. The proposed transformer was modeled and simulated using MATLAB/Simulink, followed by prototype fabrication and experimental validation. Simulation and test results demonstrated that the 12-phase toroidal transformer achieved an efficiency of 98.3%, representing a 2.2% improvement over a conventional 6-phase configuration. Furthermore, steady-state coil temperature decreased by 10°C, while DC voltage ripple was reduced from 6.7% to 3.2%. Harmonic performance also improved significantly, with Total Harmonic Distortion (THD) dropping from 7.8% to 4.5% at the AC side and from 4.2% to 2.1% after rectification. In terms of charging performance, the system successfully shortened the charging time for an 80% state of charge (SoC) battery from 32 minutes to 27 minutes, a reduction of 15.6%. These findings confirm that the 12-phase toroidal transformer provides a technically reliable and novel solution for nextgeneration EV fast charging infrastructure, delivering both high efficiency and improved power quality.



This work is licensed under a Creative Commons Attribution 4.0 International License

# **Corresponding Author:**

Partaonan Harahap

Department of Environmental Engineering, Faculty of Engineering, Muhammadiyah University of North Sumatra, Indonesia, Email: partaonanharahap@umsu.ac.id

# 1. INTRODUCTION

The development of electric vehicle (EV) technology has experienced rapid growth in recent years. This phenomenon is driven by the increasing awareness of the importance of transitioning to clean energy, reducing carbon emissions, and the need for efficient and sustainable transportation solutions. Electric vehicles have now become the main alternative to fossil fuel-powered vehicles because they have high efficiency, relatively low operational costs, and a smaller environmental impact. However, the success of mass adoption of electric vehicles heavily depends on the availability of adequate supporting infrastructure, particularly fast, reliable, and efficient charging systems[1],[2].

One of the vital components in the modern electric vehicle ecosystem is the fast charging system. The presence of high-power charging systems has a significant impact on battery charging time and user

**DOI:** 10.33019/jurnalecotipe.v12i2.4568

convenience. However, fast charging systems also face complex technical challenges, one of which is the emergence of harmonics due to the use of non-linear power conversion devices such as rectifiers. Harmonics can cause voltage distortion, increase power loss, and reduce the stability of the power system. Therefore, improving power quality and reducing harmonics are the main focuses in the development of fast charging systems[3],[4].

Transformers play a crucial role in this system, as they serve as a bridge between the AC voltage source and the DC rectifier system. Conventional transformers widely used today, whether in 3-phase or 6-phase configurations, often result in uneven current distribution, asymmetric magnetic flux distribution, and relatively high power losses. To address these issues, innovation in transformer design is needed, which is not only more energy-efficient but also has the capability to suppress harmonics and improve output power quality.

One innovative form of transformer that has proven to have good technical performance is the toroidal transformer. The toroidal core, which is ring-shaped, allows the magnetic flux to flow more evenly and symmetrically, which directly reduces core losses and improves power conversion efficiency. In addition, toroidal transformers have advantages in terms of more compact size, lighter weight, and lower electromagnetic interference. Unfortunately, the use of toroidal transformers in EV fast charging systems is still relatively limited, especially in multi-phase configurations that have potential for further development[5],[6]. Multi-phase configurations, particularly 12-phase, offer significant potential to enhance efficiency and power quality in fast charging systems. By arranging the secondary windings at a 30-degree phase angle, this system can produce a more balanced and smoother sinusoidal voltage. This is particularly ideal for use with a 12-pulse rectifier, which is known to significantly reduce the 5th and 7th order harmonics and decrease DC voltage ripple[7],[8],[9]Therefore, the development of a 12-phase toroidal transformer represents a promising innovative approach to enhance energy efficiency, improve harmonic profiles, and reduce electric vehicle battery charging time.

This research offers novelty in the design and implementation of a toroidal transformer with a 12-phase configuration for a 50 kW fast charging system. The innovations presented include the precise development of the physical design of the toroidal transformer with symmetric winding distribution, the use of interleaving techniques for thermal efficiency and hotspot reduction, and performance validation through MATLAB/Simulink simulations and physical prototype testing[10],[11]. This design is also directly applied in the charging system with the integration of a 12-pulse rectifier and a 50 kWh battery, thereby producing a realistic and applicable model for the next generation of fast charging systems[12]. The main objective of this research is to design and develop a 12-phase toroidal transformer prototype that can enhance the efficiency of EV fast charging systems. This objective is broken down into several focuses: first, designing a toroidal transformer with high energy efficiency and thermal stability; second, integrating it into a 12-pulse rectifier system; third, evaluating its performance through simulations and tests on efficiency, THD, temperature, and voltage ripple parameters; and fourth, comparing it with a conventional 6-phase transformer configuration as a basis for performance improvement[10],[3].

The problem formulation developed in this research includes the following aspects: (1) how to design a toroidal transformer with a 12-phase configuration that is efficient and thermally stable in a 50 kW fast charging system? (2) to what extent can a 12-phase toroidal transformer suppress harmonics and voltage ripple compared to a 6-phase transformer? (3) how does the use of a 12-phase transformer affect battery charging time and power quality? and (4) how do the simulation results align with the prototype testing results in evaluating the overall system performance.

By answering these questions, this research is expected to make a tangible contribution to the development of more efficient, reliable, and grid-friendly electric vehicle fast charging system technologies. In addition, the results of this research can also serve as a reference in the design of high-efficiency transformers that support the energy infrastructure needs of the future based on renewable energy[11],[12].

#### 2. RESEARCH METHOD

This research employs an experimental quantitative approach based on engineering techniques to design and test a toroidal transformer in a 50 kW electric vehicle fast charging system[3]. The research consists of three main stages: design and simulation, prototype fabrication, and performance testing.



# 2.1. Design and Simulation

The transformer design is carried out using MATLAB/Simulink software, with the following parameters:

Input: 3-phase voltage 400 V RMS, frequency 50 Hz.

Output: 12 phase outputs, each with a voltage of 230 V RMS.

Core: Toroidal core made of M6 silicon steel.

Phase configuration: 12 phases with a phase-to-phase angle of 30°, using phase shifting and interleaving techniques. Physical construction: The primary coils are arranged evenly for 3-phase input, and 12 secondary coils are formed in a circular manner following the toroidal structure. The simulation was conducted to observe the distribution of magnetic flux, power losses (core loss and copper loss), as well as the temperature and current distribution in each phase. A 12-pulse rectifier model was used to evaluate power quality and DC voltage ripple.

# 2.2. Prototype Development

The 50 kW capacity 12-phase toroidal transformer prototype is built using class H enamel wire and precisely wound using a toroidal winding machine. The ferromagnetic core is precisely shaped to maintain a homogeneous flux distribution.

# 2.3. Performance Testing

The testing was conducted under three load conditions: Load 25% (12.5 kW) 50% load (25 kW) Load 100% (50 kW)

# 2.4. Parameters that are measured include:

Energy efficiency (%)
Steady-state temperature of the coil
Output DC voltage ripple
Voltage and current of each secondary phase
Harmonic profile using FFT (Fast Fourier Transform)

# 3. RESULTS AND DISCUSSION

# 3.1. Result

The results of this study were obtained through simulations using MATLAB/Simulink and direct testing of a 12-phase toroidal transformer prototype. The main objective of this research was to evaluate system performance in terms of energy efficiency, power losses, thermal stability, power quality, and battery charging time. The 12-phase transformer was then compared with a conventional 6-phase transformer to highlight significant technical improvements[13],[14].

To strengthen the clarity of the findings, several supporting visuals have been added and explained in greater detail. The Simulink block diagram is presented with detailed descriptions of each subsystem, including the three-phase source, the 12-phase toroidal transformer, the rectifier, and the DC load. In addition, tables of design parameters and prototype specifications were included to provide a clearer technical reference. Graphs illustrating efficiency improvements, coil temperature reduction, harmonic distortion reduction, and decreased voltage ripple are also presented, thereby providing visual evidence of the comparative advantages of the 12-phase configuration over the 6-phase system. These improvements ensure that the research descriptions are more scientifically rigorous, systematic, and supported by adequate visualizations, allowing readers to more easily understand the significance of the results.

Simulation and experimental data showed that the 12-phase toroidal transformer demonstrated superior performance compared to the conventional 6-phase configuration. Under full load conditions (50 kW), the 6-phase system achieved an efficiency of 96.1%, whereas the 12-phase configuration improved efficiency to 98.3%. This 2.2% improvement was obtained from reductions in core losses, from 187 W to 129 W, and copper losses, from 315 W to 224 W[15].

**DOI:** 10.33019/jurnalecotipe.v12i2.4568

In terms of thermal performance, the steady-state coil temperature of the 12-phase transformer stabilized at 71°C, which is 10°C lower than the 81°C observed in the 6-phase system. This result indicates better heat distribution and improved thermal regulation[16],[17],[18].

Power quality also showed significant improvement. The DC-side voltage ripple decreased from 6.7% in the 6-phase system to only 3.2% in the 12-phase system. Meanwhile, Total Harmonic Distortion (THD) before rectification dropped from 7.8% to 4.5%, and after rectification decreased from 4.2% to 2.1% [19],[20].

These improvements confirm that the 12-phase configuration is more effective in suppressing harmonics while producing a smoother DC voltage profile. From the perspective of battery charging performance, the use of a 12-phase toroidal transformer enabled shorter charging times. To reach 80% state of charge (SoC), the 6-phase system required 32 minutes, whereas the 12-phase system required only 27 minutes. This reduction of 5 minutes, equivalent to 15.6%, provides tangible benefits for both users and fast-charging infrastructure providers .

Overall, the simulation and experimental results, supported by visualizations in the form of tables, graphs, and block diagrams, demonstrate that the 12-phase toroidal transformer can deliver improvements in energy efficiency, thermal stability, and power quality. Therefore, this technology represents a reliable and innovative solution to support the development of next-generation electric vehicle fast charging systems.

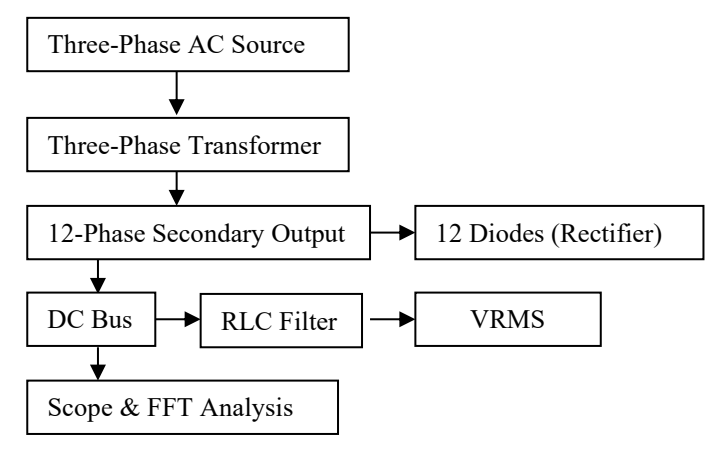


Figure 1. Simulink Block Structure

Explanation of the 12-Phase Subsystem

Input: 3-phase AC (A, B, C)

Output: 12 secondary phase voltages

Method: Phase-shifting coil, secondary phase angle =  $30^{\circ}$ 

Winding calculation:

$$Vsek=Vprimer \times Ns /Np$$
 (1)

Adjusted so that the output of each secondary phase = 230 V RMS.

# 1. Application of Resonant DC-DC Converter

One way to improve the efficiency of fast charging systems is by using a resonant-based DC-DC converter[21]. This converter can reduce power loss and enhance the overall efficiency of the charging system. The basic formula for calculating the efficiency of a resonant converter is:

$$\eta = \frac{P_{out}}{P_{In}} \times 100\% \tag{2}$$

2. The Use of Active Filters to Reduce Harmonic Distortion.

**DOI:** 10.33019/jurnalecotipe.v12i2.4568

Harmonic distortion often becomes a problem in fast charging systems due to the non-linear currents generated by converters. To address this, active filters can be used[22],[23]. The formula to calculate total harmonic distortion (THD) is:

$$THD = \frac{\sqrt{\Sigma_{n=2}^{N} I_n^2}}{I_n} \tag{3}$$

Where :  $I_n$  = the nth harmonic current and  $I_{I}$  = the fundamental current

#### 3. Optimization of Communication Protocol

Optimizing communication protocols between electric vehicles and charging stations is also important for improving charging efficiency. Protocols like ISO 15118 enable better two-way communication[18], facilitating more efficient power management during the charging process.

Function Component Three-Phase Voltage Source Three-phase AC voltage source (400 V, 50 Hz) Main Transformer Three-phase transformer (distribution model) Custom 12-Phase Transformer Subsystem Subsystem for 12-phase toroidal secondary winding Universal Bridge (Rectifier) 12-pulse rectifier using 12 diodes or thyristors **RLC Filter** Smooths DC ripple Load (Battery) 50 kWh battery model as charging load Powergui Simulink time-domain simulation environment Scope, FFT Analysis Monitoring THD, current, and voltage waveforms

**Table 1.** The Simulink model consists of the following main components

Table 2. Specifications

Table 2. Specifications							
Parameter	Value						
Transformer power (S)	50,000 VA						
Input voltage (primary)	3-phase, 400 V						
Output voltage per phase	48 V AC (12 phases)						
Frequency	50 Hz						
Target efficiency	≥ 96%						
Transformer type	Toroidal						
Power factor (pf)	0.85 (for current estimation)						
Phase voltage (line-to-neutral)	$400 \text{ V} / \sqrt{3} = 230 \text{ V}$						

# 3.2. Discussion

The results clearly demonstrate the superior performance of the 12-phase toroidal transformer in fast-charging applications for electric vehicles. The improvement in energy efficiency reflects better utilization of input power and a reduction in internal losses. The more uniform magnetic flux distribution in the toroidal core, combined with optimized secondary winding geometry, plays a crucial role in minimizing both core and copper losses. This contributes directly to a more energy-efficient and cost-effective system[24].

The enhanced thermal performance—evidenced by the lower coil temperatures—indicates improved heat management within the transformer. The toroidal design supports better airflow and balanced current distribution, reducing localized hotspots and increasing the longevity of insulation materials[25],[26]. This is especially important in high-power charging systems where thermal stress can severely impact reliability. Power quality improvements, particularly the reduction in DC ripple and harmonic distortion, confirm the effectiveness of using a 12-phase configuration in conjunction with a 12-pulse rectifier. These characteristics are vital for maintaining battery health, minimizing EMI issues, and ensuring regulatory compliance in grid-connected systems. Finally, the reduction in battery charging

**DOI:** 10.33019/jurnalecotipe.v12i2.4568

time directly enhances user experience and station throughput—two essential factors for the widespread adoption of EVs. The 12-phase toroidal transformer not only enables faster charging but does so without compromising efficiency or power quality. In summary, the data validate the feasibility and advantages of applying 12-phase toroidal transformer technology in 50 kW fast-charging systems. This innovation supports the goal of delivering sustainable, reliable, and high-performance EV infrastructure.

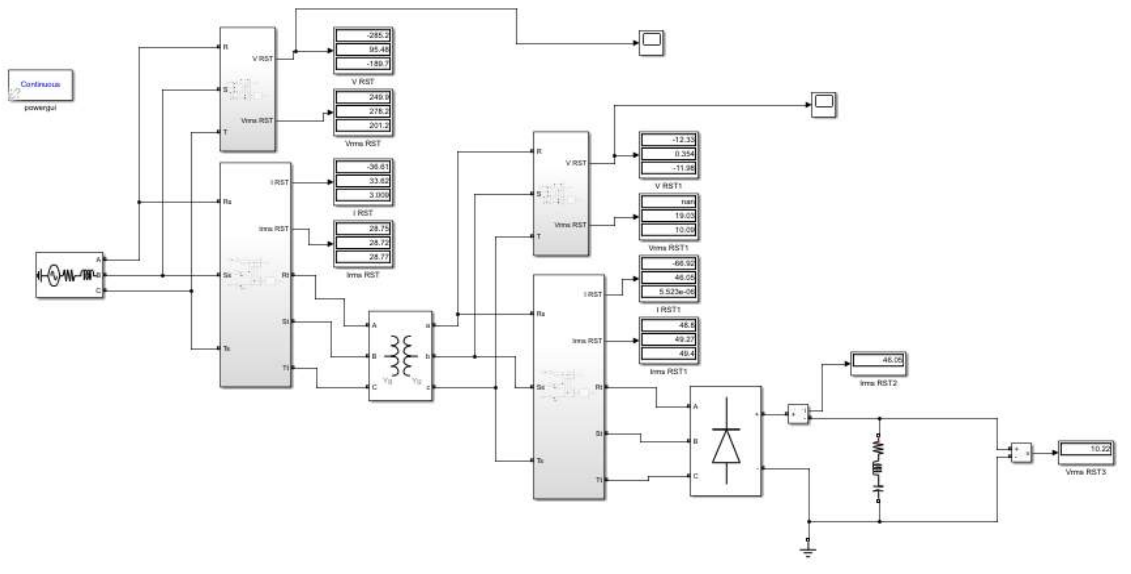


Figure 2. Simulink design

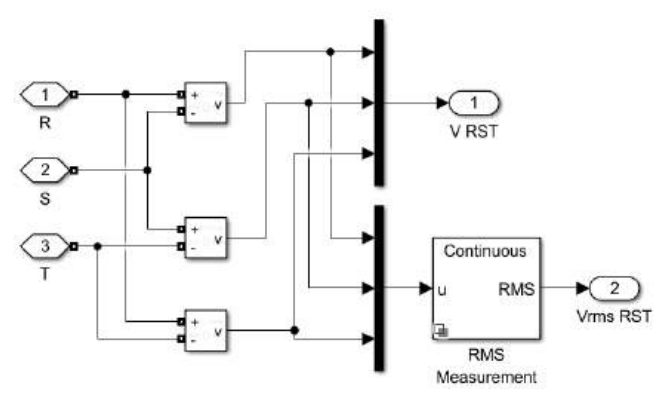


Figure 3. Block Diagram of Vrms Voltage

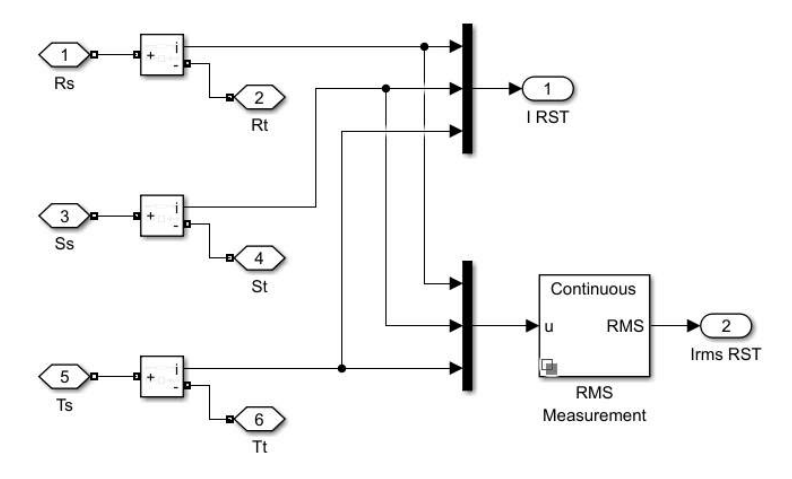


Figure 4. Block Diagram of Vrms Current



The Vrms Current Block DiagramSimulink image in this article presents a block diagram representation of a 12-phase toroidal transformer-based electric vehicle fast charging system. This model is built in the MATLAB/Simulink environment with the primary goal of simulating the performance of the transformer in delivering power from a three-phase source to a DC load in the form of an electric vehicle battery, through an efficient and high-quality power conversion process.

In the input section, the system starts with the Three-Phase Voltage Source block that simulates the AC voltage of the power grid (400 V, 50 Hz). This source is connected to the Three-Phase Transformer, which serves as the main power distribution transformer and the starting point for forming the secondary phases. After that, the energy is transmitted to the Custom 12-Phase Toroidal Transformer Subsystem, which is the main subsystem that regulates the formation of twelve phase outputs from three phase inputs with a 30° phase shift between each secondary phase. This is done to optimize harmonic cancellation and smooth the rectified voltage profile.

Each output from the secondary transformer is connected to the Universal Bridge, which acts as a 12-pulse rectifier. This block is designed using 12 diodes or thyristors configured to convert multi-phase AC voltage into DC voltage. The output from the rectifier is then filtered using an RLC Filter, which serves to reduce DC voltage ripple and produce a more stable voltage before reaching the load.

The load used in the simulation is a 50 kWh DC battery model, which represents the typical capacity of medium electric vehicles. The effect of load changes on current, voltage, and temperature is evaluated in various testing scenarios (25%, 50%, and 100% load). To analyze the system's performance, the Scope and FFT Analysis blocks are used, which record and display the current and voltage waveforms at various points in the system, as well as calculate the Total Harmonic Distortion (THD) of the generated signals. Additionally, the Powergui block is utilized to run time-domain simulations and support electrical analysis based on dynamic simulations.

Through this model, data related to energy efficiency, harmonic reduction, coil temperature, and battery charging time were obtained, which were subsequently used as a basis for comparison between the 6-phase and 12-phase transformer configurations. This Simulink diagram serves as an important visual aid in understanding how a multi-phase structure directly impacts the performance of the electric vehicle fast charging system.

### 4. CONCLUSION

This study presents the successful design, simulation, and implementation of a 12-phase toroidal transformer for a 50 kW electric vehicle fast charging system. Compared to a conventional 6-phase configuration, the proposed transformer demonstrated significant improvements across key performance metrics. Energy efficiency increased by 2.2%, while both core and copper losses were substantially reduced. Thermal stability was enhanced, with a 10°C reduction in steady-state coil temperature, indicating better heat management within the transformer. Moreover, the charging time required to reach 80% state of charge (SoC) was reduced from 32 minutes to 27 minutes. This time reduction directly improves user convenience and charging station throughput, both of which are critical to the broader adoption of electric vehicles. In conclusion, the integration of a 12-phase toroidal transformer into EV fast charging systems provides a practical and scalable solution to improve system efficiency, thermal reliability, and overall performance. The outcomes of this study contribute valuable insights for the development of sustainable, high-performance charging infrastructure for next-generation electric mobility.

# Acknowledgments

We would like to express our deepest gratitude to the University of Muhammadiyah North Sumatra (UMSU) and Andalas University (UNAND) for their invaluable support in facilitating this review research. The resources, guidance, and collaborative environment provided by both institutions played a crucial role in the successful completion of this research. This review is a testament to their commitment to advancing research in power electronics and renewable energy systems.

**DOI:** 10.33019/jurnalecotipe.v12i2.4568

# REFERENCES

- [1] S. Vishwakarma and S. K. Sonkar, "Total Harmonic Reduction by Multi Pulse Converters," vol. 9, no. 2, pp. 930–935, 2022.
- [2] A. Ahmad, Z. Qin, T. Wijekoon, and P. Bauer, "An Overview on Medium Voltage Grid Integration of Ultra-Fast Charging Stations: Current Status and Future Trends," *IEEE Open J. Ind. Electron. Soc.*, vol. 3, pp. 420–447, 2022, doi: 10.1109/OJIES.2022.3179743.
- [3] H. C. Park, S. S. Min, J. H. Lee, S. S. Park, S. H. Lee, and R. Y. Kim, "Design of Half-Bridge Switching Power Module Based on Parallel-Connected SiC MOSFETs for LLC Resonant Converter with Symmetrical Structure and Low Parasitic Inductance," *Electron.*, vol. 13, no. 5, 2024, doi: 10.3390/electronics13050937.
- [4] M. I. Fahmi, U. Baafai, A. Hazmi, and T. H. Nasution, "Harmonic reduction by using single-tuned passive filter in plastic processing industry," *IOP Conf. Ser. Mater. Sci. Eng.*, vol. 308, no. 1, 2024, doi: 10.1088/1757-899X/308/1/012035.
- [5] M. Shahjalal, T. Shams, M. N. Tasnim, M. R. Ahmed, M. Ahsan, and J. Haider, "A Critical Review on Charging Technologies of Electric Vehicles," *Energies*, vol. 15, no. 21, 2022, doi: 10.3390/en15218239.
- [6] S. Niu, Q. Jia, Y. Hu, C. Yang, and L. Jian, "Safety Management Technologies for Wireless Electric Vehicle Charging Systems: A Review," *Electron.*, vol. 14, no. 12, pp. 1–27, 2025, doi: 10.3390/electronics14122380.
- [7] A. M. N. Putra, A. Adrianti, and M. I. Hamid, "Review on Innovative DC-DC Converter Design for High Efficiency and High Voltage Gain Applications," *J. Ecotipe (Electronic, Control. Telecommun. Information, Power Eng.*, vol. 12, no. 1, pp. 87–94, 2025, doi: 10.33019/jurnalecotipe.v12i1.4533.
- [8] A. Hazmi, M. I. Hamid, R. Fernandez, H. Andre, R. W. Pratama, and M. M. Rahman, "Characteristics of lightning-rainfall in Padang tropical thunderstorm," *AIP Conf. Proc.*, vol. 2891, no. 1, pp. 12–14, 2024, doi: 10.1063/5.0200950.
- [9] Rimbawati, N. Ardiansyah, and Noorly Evalina, "Voltage Control System Design," *Semnastek Uisu*, vol. 1, pp. 14–20, 2019.
- [10] S. Panneerselvam, K. Kandasamy, and C. Perumal, "Modelling and simulation of sinusoidal pulse width modulation controller for solar photovoltaic inverter to minimize the switching losses and improving the system efficiency," *Arch. Electr. Eng.*, vol. 71, no. 3, pp. 615–626, 2022, doi: 10.24425/aee.2022.141674.
- [11] R. Abdollahi and G. Gharehpetian, "Inclusive Design and Implementation of Novel 40-Pulse AC–DC Converter for Retrofit Applications and Harmonic Mitigation," *IEEE Trans. Ind. Electron.*, vol. 63, pp. 667–677, 2016, doi: 10.1109/TIE.2015.2481364.
- [12] D. Challenges, D. Overview, C. Evaluation, J. W. Kolar, and J. Huber, "The Essence of Solid-State Transformers," 2023.
- [13] IEEE 519-2014 standard, "IEEE 519-2022 Review What has changed from the previous 2014 version?," pp. 1–5, 2022.
- [14] F. De León, S. Purushothaman, and L. Qaseer, "Leakage inductance design of toroidal transformers by sector winding," *IEEE Trans. Power Electron.*, vol. 29, no. 1, pp. 473–480, 2014, doi: 10.1109/TPEL.2013.2251429.
- [15] D. A. Crolla, Automotive engineering: powertrain, chasis system and vehicle body, no. 1. 2009.
- [16] R. Collin, Y. Miao, A. Yokochi, P. Enjeti, and A. Von Jouanne, "Advanced electric vehicle fast-charging technologies," *Energies*, vol. 12, no. 10, 2019, doi: 10.3390/en12101839.



- [17] Rimbawati, M. A. Siregar, Z. Siagian, J. Riandra, P. Harahap, and B. Oktrialdi, "Lightning Arrester Design as a Security System for Photovoltaic Systems in Pematang Johar Village," *Proceeding ELTICOM 2022 6th Int. Conf. Electr. Telecommun. Comput. Eng. 2022*, pp. 54–59, 2022, doi: 10.1109/ELTICOM57747.2022.10038261.
- [18] P. Harahap, F. I. Pasaribu, and M. Adam, "Prototype Measuring Device for Electric Load in Households Using the Pzem-004T Sensor," *Budapest Int. Res. Exact Sci. J.*, vol. 2, no. 3, pp. 347–361, 2020.
- [19] K. Gamit and K. Chaudhari, "Multi Pulse Rectifier Using Different Phase Shifting Transformers and Its THD Comparison for Power Quality Issues," *Int. Res. J. Eng. Technol.*, vol. 3, no. 1, pp. 1025–1033, 2019.
- [20] P. Nencioni, S. Gianfranceschi, M. C. Terzi, and G. Landgraf, "E Arthnet O Nline Xml F Ront E Nd," *Online*, pp. 1–28, 2003.
- [21] H. J. Bergveld, W. S. Kruijt, and P. H. L. Notten, *Battery Management Systems*. 2002. doi: 10.1007/978-94-017-0843-2.
- [22] H. D. Saputro, "Harmonic Analysis Of Current And Voltage Electricity In The Unnes Bptik Building And E11 Electrical Engineering," p. 88, 2019.
- [23] V. Ramakrishnan *et al.*, "A Comprehensive Review on Efficiency Enhancement of Wireless Charging System for the Electric Vehicles Applications," *IEEE Access*, vol. 12, no. April, pp. 46967–46994, 2024, doi: 10.1109/ACCESS.2024.3378303.
- [24] L. A. Ramos, R. F. Van Kan, M. Mezaroba, and A. L. Batschauer, "A Control Strategy to Smooth Power Ripple of a Single-Stage Bidirectional and Isolated AC-DC Converter for Electric Vehicles Chargers," *Electron.*, vol. 11, no. 4, 2022, doi: 10.3390/electronics11040650.
- [25] G. W. McLean, "Generators," *Newnes Electr. Power Eng. Handbook, Second Ed.*, vol. 11, no. 1, pp. 105–133, 2021, doi: 10.1016/B978-075066268-0/50005-6.
- [26] A. Hazmi, P. Emeraldi, M. I. Hamid, S. Melati, and N. Takagi, "Reconstruction of lightning channel based on acoustic radiation," *Int. J. Electr. Eng. Informatics*, vol. 11, no. 2, pp. 341–351, 2019, doi: 10.15676/ijeei.2019.11.2.8.



DOI: 10.33019/jurnalecotipe.v12i2.4575

# Adaptive PID-PD Hybrid Control for Precise Motion of ROVs in Dynamic Environments

# Hendi Purnata<sup>1</sup>, Hera Susanti<sup>2</sup>, Dwi Sahidin<sup>3</sup>, Galih Mustiko Aji<sup>4</sup>, Nanda Pranandita<sup>5</sup>

Mechatronics Engineering, Cilacap State of Polytechnic, Jl. Dr. Soetomo No. 1, Cilacap 53212, Indonesia
 <sup>2,4</sup>Electronics Engineering, Cilacap State of Polytechnic, Jl. Dr. Soetomo No. 1, Cilacap 53212, Indonesia
 <sup>3</sup>Electrical Engineering, Cilacap State of Polytechnic, Jl. Dr. Soetomo No. 1, Cilacap 53212, Indonesia
 <sup>5</sup>Mechanical Engineering and Manufacturing, Bangka Belitung State Polytechnic of Manufacturing, Kawasan Industri Airkantung, Sungailiat, Bangka, 33211, Indonesia

#### ARTICLE INFO

#### Article historys:

Received: 13/08/2025 Revised: 23/09/2025 Accepted: 30/10/2025

#### **Keywords:**

Dynamic Marine Conditions; Marine Robotics; PD Controller; PID Controller; Remotely Operated Vehicles; Rotation Control; ROV Position Control; Underwater Robotics

#### **ABSTRACT**

This study aims to develop and evaluate an Adaptive PID-PD Hybrid Control System to enhance the position and rotation control of a Remotely Operated Vehicle (ROV) in challenging sea conditions. In this study, two main stages were conducted. First, a dynamic model of the ROV was developed, encompassing translation for movement in three-dimensional space (x, y, z) and rotation for changes in orientation (roll, pitch, yaw). Second, the adaptive PID-PD hybrid controllers were implemented and evaluated on the ROV model to ensure stability and precision in motion control. Simulation results demonstrate that the proposed controller effectively maintains position with surge overshoot of 23.3%, sway of 1.67%, and heave of 47.17%. The settling time ranges from 41.53 to 107 seconds, indicating areas for further tuning. In terms of velocity response, surge velocity shows a high overshoot of 106.26%, while sway and heave velocities present smaller overshoots but require longer stabilization times. The integration of PID and PD in a hybrid adaptive framework yields improved inner-loop response and overall robustness. These findings highlight the potential of the adaptive hybrid controller to enhance stability, responsiveness, and operational effectiveness of ROVs in dynamic marine conditions.



This work is licensed under a Creative Commons Attribution 4.0 International License

#### **Corresponding Author:**

Hendi Purnata

Mechatronics Engineering, Cilacap State of Polytechnic, Jl. Dr. Soetomo No. 1, Cilacap 53212, Indonesia

Email: hendipurnanta@pnc.ac.id

#### 1. INTRODUCTION

Remotely Operated Vehicles (ROVs) have become an essential tool in the exploration and maintenance of underwater systems, such as oil drilling, marine ecosystem monitoring, and search and rescue operations [1]. With the advancement of technology and the increasing demand for operations in extreme deep-sea environments, the primary challenge in using ROVs is maintaining the stability of the vehicle's position and rotation in a dynamic marine environment. Factors such as ocean currents, waves, and pressure changes pose significant obstacles to the accurate and efficient operation of ROVs [[2], [3], [4].

Environmental constraints faced by ROVs during underwater operations include unique underwater challenges that affect positioning, navigation, and timing performance, as well as increased pressure at depth, leading to large physical systems with high operational costs [5], [6]. Technological

advancements in ROVs to address these challenges include the development of lighter and smaller ROVs through the use of hollow carbon fiber structural components and optical fiber microtethers, enhancing accessibility to the world's oceans. Additionally, the use of cost-effective DIY kits and adaptation to existing ROV platforms is expected to expand the reach of this technology, making ROVs more widely available[[7], [8], [9]

Several studies to overcome challenges in robotic systems involve regulating motors so that they can follow the desired set point, as in the study [10], [11] sing PID controller control to regulate speed so that it matches the desired position. Then, research from [11], [12], [13] utilizing a combination of PID control and neural networks to produce an appropriate control method. However, some of the above studies have not been applied to robotic systems such as ROVs, so it is a challenge to implement the control system into robotic systems.

To address these challenges, various innovations have been developed, including the creation of lighter and more compact ROVs using materials such as hollow carbon fiber, the use of optical fiber micro-tethers, and modular systems to facilitate maintenance and mission adaptation [14], [15]. However, the greatest challenge remains in maintaining position and rotation control under the influence of dynamic marine environments. Adaptive control systems are crucial for maintaining ROV stability. One widely used method is the PID (Proportional-Integral-Derivative) controller, which can provide quick responses to disturbances, although its settings must be optimized to remain stable under extreme conditions [[16], [17], [18] The integration of PID with Proportional–Derivative (PD) control in a hybrid adaptive framework offers promising improvements in system responsiveness and robustness.

Accordingly, this study aims to develop and evaluate an Adaptive PID-PD Hybrid Control System to enhance position and orientation stability of ROVs in dynamic marine environments, thereby improving operational effectiveness and minimizing the risk of instability-induced damage during underwater missions.

# 2. RESEARCH METHOD

This research is an experimental study employing simulation and control system analysis, with the aim of developing and evaluating an Adaptive PID–PD Hybrid Controller to maintain the position and orientation stability of an ROV under dynamic marine conditions. The study consists of two main stages. First, a dynamic model of the ROV was developed, incorporating translational motion in three-dimensional space (x, y, z) as well as rotational dynamics for orientation changes (roll, pitch, yaw). Second, the adaptive PID–PD hybrid controllers were implemented and evaluated on the ROV model. Simulations were carried out to assess performance under environmental disturbances such as currents, waves, and hydrodynamic drag forces, with the objective of improving the ROV's stability, responsiveness, and control accuracy. The simulations were conducted using MATLAB/Simulink, which is widely used for control system analysis and simulation of dynamic models. SolidWorks was utilized for modeling the ROV geometry.

# 2.1. ROV Model

The ROV used in this study is equipped with eight actuators or octarotors, as shown in Figure 1. The dynamic model of the ROV can be divided into two main parts: translation equations for movement in three-dimensional space (x, y, z), and rotation equations for changes in orientation (roll, pitch, yaw).

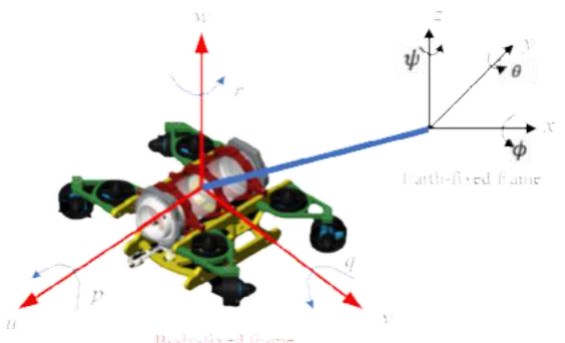


Figure 1. ROV Model Body-fixed coordinate frame and Earth-fixed coordinate frame

**DOI:** 10.33019/jurnalecotipe.v12i2.4575

Figure 1 shows the geometric model of the ROV modeled by SolidWorksTM. The ROV model is powered by eight brushless DC thrusters (T1–T8) for *surge, sway, heave, roll, pitch, and yaw* movements. Mechanical properties such as mass, moment of inertia, center of gravity, and buoyancy of the ROV were obtained, with a The mass of the ROV was assumed to be 30 kg in air, with buoyancy forces calculated based on the dimensions and material properties of the ROV. The model assumes a water density of  $1000 \text{ kg/m}^3$ , and the effects of ocean currents and drag forces were simulated based on typical deep-sea conditions. The initial conditions for the position and velocity of the ROV were set to zero, a weight of 392.4 N, and a buoyancy force of 615.5 N, with overall dimensions of 420 mm (length)  $\times 596.57 \text{ mm}$  (width)  $\times 250 \text{ mm}$  (height). The equations of motion for the ROV are given in equation (1).

$$M_{\mathcal{V}} + C(v) v + D(v) + G_f(\eta) = \tau \tag{1}$$

In this equation,  $M_{\mathcal{V}}$  represents the inertial mass matrix, C(v) is the Coriolis matrix, and D (us the damping force matrix, while  $G_f$  is the gravitational force vector. These components describe the ROV's translational and rotational motion dynamics. the body frame and Earth in Figure 1, the position and orientation are defined in the Earth-fixed frame as shown in Equation (2). Additionally, the linear velocity and angular velocity of the ROV are presented in the body-fixed frame (2) as shown in Equation (3).

$$\eta = \left[ x \, y \, z \, \phi \, \theta \, \psi \, \right] \tag{2}$$

$$v = [v w]^T = [u v w p q r]^2$$
(3)

The vector  $\eta$  represents the ROV's position and orientation in space, with x,y,z denoting the linear positions and  $\varphi$ ,  $\theta$ ,  $\psi$  the roll, pitch, and yaw angles, respectively. The velocity in the Earth-fixed frame can be obtained from the ROV velocity in the body-fixed frame through the following transformation.

$$\dot{\eta} = J(\eta)v \tag{4}$$

The sum of the inertial mass and the fluid inertia matrix can be written as M = MRB + MA where the inertial mass of the body and the mass can be rewritten as:

$$M_{RB} = \begin{bmatrix} m & 0 & 0 & 0 & mz_G & -my_G \\ 0 & m & 0 & -mz_G & 0 & mx_G \\ 0 & 0 & m & my_G & -mz_G & 0 \\ 0 & -mz_G 0 & my_G & l_x & -l_{xy} & -l_x \\ mz_G & mx_G & -mx_G 0 & -l_x & l_y & -l_z \\ -my_G & & & -l_x & -l_{zy} & l_z \end{bmatrix}$$

$$(5)$$

$$\mathbf{M}_{\mathbf{A}} = \begin{bmatrix} X_{ii} & X_{iv} & X_{w} & X_{pi} & X_{qi} & X_{pi} \\ Y_{ii} & Y_{iv} & Y_{wi} & I_{fi} & I_{fd} & Y_{pi} \\ Z_{ii} & Z_{iv} & Z_{wi} & Z_{pi} & Z_{qi} & Z_{pi} \\ K_{ii} & K_{iv} & K_{wi} & K_{pi} & K_{qi} & K_{ri} \\ M_{ii} & M_{iv} & M_{wi} & M_{pi} & M_{qi} & M_{ri} \\ N_{ii} & N_{iv} & N_{w} & N_{vi} & N_{di} & N_{ri} \end{bmatrix}$$

$$(6)$$

with  $\Lambda_{*} = \frac{1}{16} \Lambda_{*}$  and so on hydrodynamic Damping Force Matrix.

$$D_L = -diag \{X_{\mathcal{U}}, Y_{\mathcal{V}}, Z_{\mathcal{W}}, K_{\mathcal{D}}, M_{\mathcal{Q}}, N_{\mathcal{T}}\}$$

$$\tag{7}$$

$$D_{q} = -diag \{X_{u|u|}, Y_{v|v|}, Z_{w|w|}, K_{p|p|}, M_{q|q|}, N_{r|r|}\}$$
(8)

The thrust generated by the ROV is represented by the propeller configuration matrix, **T**. The input forces and moments are calculated for six degrees of freedom (DOF). The forces and moments for the open-loop configuration are as follows:

 $τ_X = u_3 \cos \cos \alpha + u_4 \cos \cos \alpha + u_7 \cos \cos \alpha + u_8 \cos \cos \alpha$   $τ_Y = -u_1 \cos \cos \beta + u_2 \cos \cos \beta + u_3 \sin \sin \alpha - u_4 \sin \sin \alpha + u_7 \sin \sin \alpha - u_8$   $\sin \sin \alpha$   $τ_Z = u_1 \cos \cos \beta + u_2 \cos \cos \beta + u_5 + u_6 + u_7 + u_8$   $τ_Φ = 0.155u_1 \cos \cos \beta - 0.155u_2 \cos \cos \beta - 0.275u_5 + 0.275u_6 + 0.155u_7$   $\cos \cos \beta - 0.155u_8 \cos \beta$   $τ_Φ = 0.3945u_1 \cos \cos \beta + 0.3945u_2 \cos \cos \beta + 0.4305u_3 \cos \cos \beta + 0.4305u_4$   $\cos \cos \beta - 0.0355u_5 - 0.0355u_5 - 0.0355u_6 + 0.3945u_7 \cos \cos \beta + 0.3945u_8 \cos \beta$   $τ_Ψ = -0.3945u_1 \sin \sin \beta + 0.3945u_2 \sin \sin \beta - 0.6605u_3 \sin \sin \beta + 0.6605u_4$   $\sin \sin \beta - 0.3945u_7 \sin \sin \beta + 0.3945u_8 \sin \sin \beta$ 

The propulsion configuration matrix **T** based on the propulsion layout on the ROV platform is defined as follows:

$$T = \begin{bmatrix} \cos \alpha & \cos \alpha & 0 & 0 & 0 & \cos \alpha & \cos \alpha \\ -\cos \beta & \cos \beta & \sin \alpha & -\sin \alpha & 0 & 0 & \sin \alpha & -\sin \alpha \\ \cos \beta & \cos \beta & 0 & 0 & 1 & 0 & 1 & 1 \\ 0.155\cos \beta & -0.155\cos \beta & 0 & 0 & -0.275 & 0.275 & 0.155\cos \beta & -0.155\cos \beta \\ 0.3945\cos \beta & 0.3945\cos \beta & 0.4305\cos \beta & 0.4305\cos \beta & -0.0355 & -0.0355 & 0.3945\cos \beta & 0.3945\cos \beta \\ -0.3945\sin \beta & 0.3945\sin \beta & -0.6605\sin \beta & 0.6605\sin \beta & 0 & 0 & -0.3945\sin \beta & 0.3945\sin \beta \end{bmatrix}$$
(10)

# 2.2. PID Control System

Most existing ROV systems use a series of single-input single-output (SISO) PID controllers, where each controller is designed for one degree of freedom (DOF).

$$u = \left( K_p e(t) + K_d e(t) + K \qquad \int_0^t e(t) dt \right)$$
(11)

Where there are inner and outer PID controllers, and their gains can be adjusted or tuned according to the desired output, the following are the outer PID controller values used for six degrees of freedom (DOF). The inner and outer PID loop gains can be seen in this table:

Table 1. Adaptive PID-PD Hybrid Gain Tuning

Outer Loop (PID)  - Position/Angle	Outer Kp	Outer Ki	Outer Kd	Inner Kp	Inner Kd
Surge (position)	4	0.2	2	3	0.001
Sway (position)	4	0	2	9	0.001
Heave (position)	4	0	2	10	0.001
Roll (angle)	4	0	2	10	0.001
Pitch (angle)	4	0.2	2	10	0.001
Yaw (angle)	4	0.2	2	10	0.001

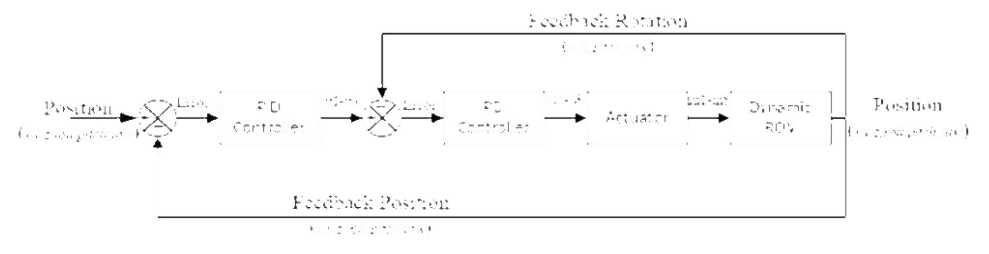


Figure 2. Adaptive PID-PD hybrid gain tuning controller block diagram of ROV

**DOI:** 10.33019/jurnalecotipe.v12i2.4575

# 3. RESULTS AND DISCUSSION

In this study, an analysis was conducted on the response of the control system of an ROV operating under the influence of a dynamic marine environment. The primary objective was to evaluate the stability of the position and rotation of the ROV controlled by a Adaptive PID–PD Hybrid Gain Tuning. The simulations were performed using MATLAB/Simulink to model the dynamic ROV behavior and implement the Adaptive PID–PD Hybrid Gain Tuning. This allowed for precise control system analysis under various marine conditions. The response results showed the control system time for the 6 degrees of freedom (DOF) of the ROV: Surge, Sway, Heave, Roll, Pitch, and Yaw.

# 3.1. Position Response

In this study, an analysis was conducted on the surge position (x) response of the ROV with a set point depth of 5 meters. Figure 3 shows the control system response time for the surge position.

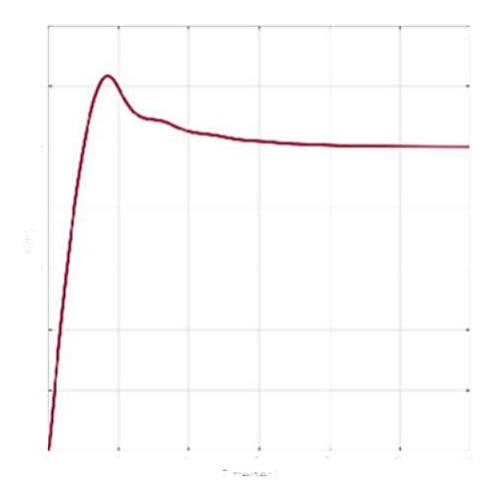


Figure 3. Surge Response (x)

For the Surge channel (x), the analysis results show that the final position reached approximately 5.006 meters, very close to the desired set point value, with an overshoot of 23.3%. This indicates that although the ROV successfully reached the target position, there was a slight excessive movement that exceeded the set point value initially. The rise time was recorded at approximately 7.59 seconds, indicating a relatively fast response toward the target position. However, the system required a settling time of approximately 57.9 seconds to stabilize at the final position. Overall, this surge response can be considered a fairly fast *step response* with some overshoot and moderate settling time, although further optimization of the PID controller is needed to reduce overshoot and accelerate stabilization time.

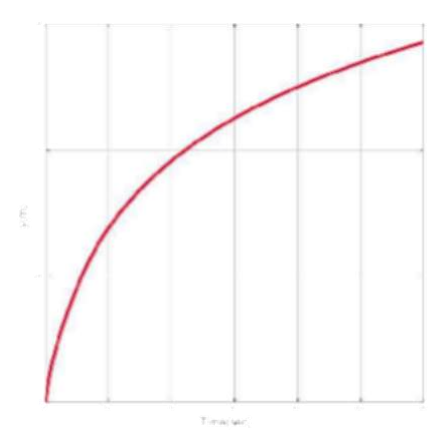


Figure 4. Sway Position

Figure 4 shows the Sway channel (y). The analysis results indicate that the final position is approximately 1.403 meters, very close to the desired set point. The overshoot is very small, only about 1.67%, indicating that the sway position control successfully avoided excessive movement at the beginning. However, the rise time to reach the target position is relatively slow, at approximately 80.8 seconds, indicating a slower response compared to the surge channel. Additionally, the settling time required is quite long, at 107 seconds, indicating that although the ROV eventually stabilizes at the desired position, the time required to achieve stability requires further attention.

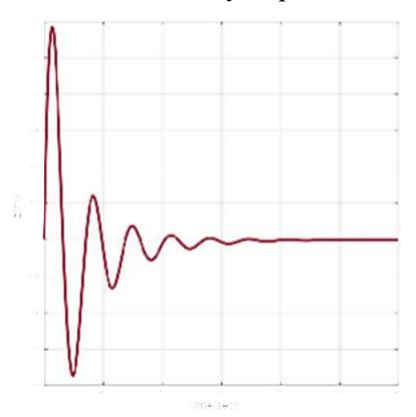
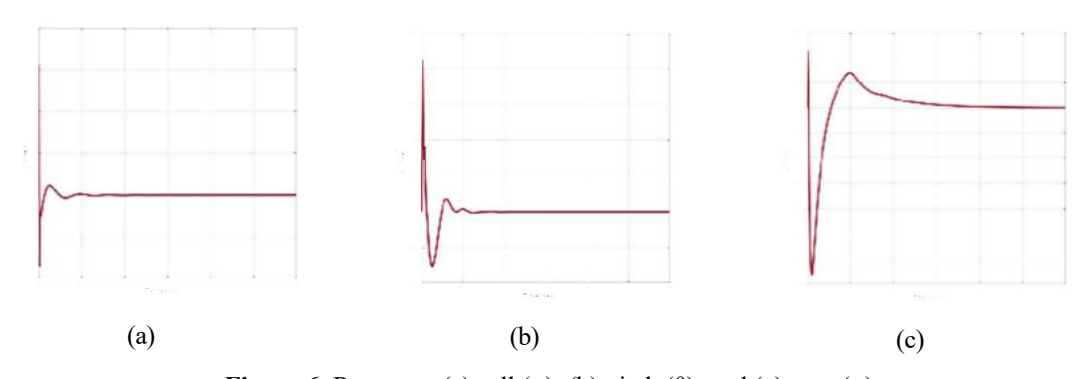


Figure 5. Heave Position

Figure 5. Shows the Heave channel (z), with the final position recorded at approximately -6.0e-5 meters, very close to zero, indicating that the system successfully returned the position to a stable value. The peak deviation was recorded at approximately 0.117 meters at 2.74 seconds, indicating initial oscillations before reaching a stable value. Following this oscillation, the settling time required was 52.3 seconds, indicating that although the system eventually stabilized at the desired value, it took a significant amount of time to come to a complete stop. Overall, this response demonstrates the presence of initial damped oscillations, which eventually settle at a stable position near zero meters, but require a prolonged stabilization period.



**Figure 6**. Response (a) roll ( $\varphi$ ), (b) pitch ( $\theta$ ), and (c) yaw ( $\psi$ )

Figure 6 shows the response graph for roll  $(\varphi)$ , pitch  $(\theta)$ , and yaw  $(\psi)$ , indicating that the control of roll and pitch successfully damped quickly to very small final values,  $-3.65e-6^{\circ}$  and  $-4.0e-7^{\circ}$ , respectively, with relatively small peak deviations and fast settling times (approximately 13.37 seconds for roll and 15.45 seconds for pitch). This indicates that both rotation channels are sufficiently stable with short stabilization times. However, for yaw, although the final value is very small  $(3.29e-5^{\circ})$ , there is a larger overshoot with a peak deviation of  $0.03312^{\circ}$  at 2.16 seconds, and a much longer settling time of approximately 57.31 seconds, indicating larger initial oscillations and longer settling times. This indicates that the control settings for yaw may require further adjustment to reduce overshoot and accelerate the stabilization time.

The surge position (x) showed a final position of approximately 5.006 meters, with a 23.3% overshoot. This result, although close to the desired set point, indicates that while the ROV successfully

**DOI:** 10.33019/jurnalecotipe.v12i2.4575

reached the target position, there was initial excessive movement. The sway position (y) demonstrated excellent stability, with only a 1.67% overshoot, though the response time was slower, with a rise time of 80.8 seconds. Heave position (z) returned to a stable value near zero after experiencing a peak deviation of 0.117 meters at 2.74 seconds, and the system required 52.3 seconds to stabilize. The roll, pitch, and yaw angles all exhibited fast stabilization times, with roll and pitch showing excellent damping, while yaw required longer settling times due to higher overshoot and initial oscillations.

### 3.2. Velocity Response

In this section, we will analyze the velocity response of the ROV with a desired set point for a speed of approximately 0 m/s. The figure shows the velocity response of the ROV controlled by the Adaptive PID–PD Hybrid Gain Tuning.

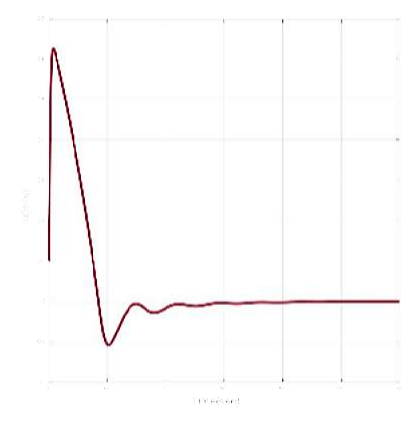


Figure 7. Surge Velocity Response

Figure 7 shows the surge velocity (u) channel, with a final value recorded at approximately -3.09e-4 m/s, indicating a slight deviation from zero. The peak deviation was recorded at approximately 0.6256 m/s at 1.56 seconds, indicating a large overshoot at the beginning. After that, the system underwent a settling process with a time of approximately 40.94 seconds, indicating that although the ROV eventually reached a more stable velocity value, the system required a considerable amount of time to fully stabilize. The rise time was recorded at approximately 1.52 seconds, indicating that the system is sufficiently responsive in reaching the final value, but with a significant overshoot (approximately 106.26%), suggesting that the PID controller settings may require further adjustment, particularly to reduce overshoot and accelerate the stabilization process.

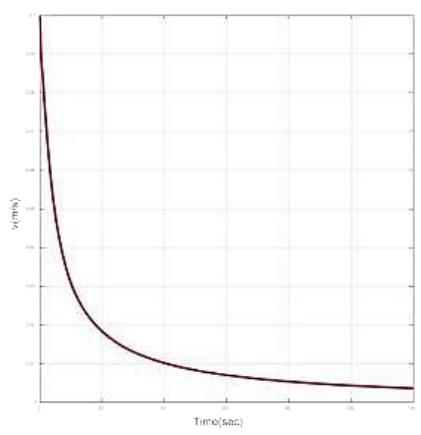


Figure 8. Sway Velocity Response

Figure 8 shows the sway velocity (v) channel, with a final value recorded at approximately 3.87e–3 m/s, with very little overshoot, only 0.20%. This indicates that although the system control has avoided excessive movement, the recorded rise time is 28.50 seconds, which is very slow. This indicates that the system requires a long time to respond and reach a stable position. Additionally, the long settling time

**DOI:** 10.33019/jurnalecotipe.v12i2.4575

(74.51 seconds) indicates significant drift in the sway position, which may be caused by insufficiently aggressive inner-loop tuning or asymmetry in the drag forces. Overall, this sway response requires an increase in inner-loop gain to accelerate response time and reduce the drift occurring.

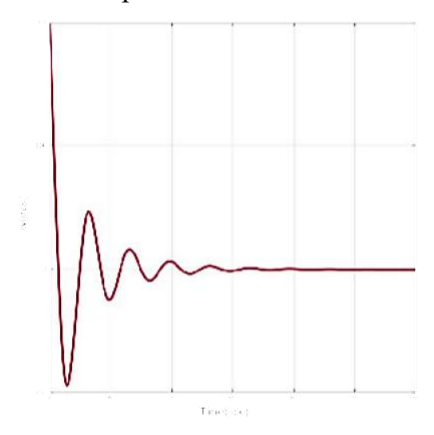


Figure 9. Heave Velocity Response

Figure 9. This is the heave velocity (w) channel, with a final value recorded at approximately 4.19e-7 m/s, which is very close to zero, indicating that the control system successfully returned the position to a stable state near zero. The overshoot is 47.17% smaller than the surge, but still indicates excessive movement before finally stabilizing. The rise time is recorded at 2.21 seconds, which is faster than some other channels, indicating that the system can respond quickly. However, the relatively long settling time (41.53 seconds) indicates that although the heave was successfully stabilized, the stabilization process took longer. This suggests that while the rise time control is adequate, the PID settings in the inner loop need to be adjusted to accelerate the stabilization process without compromising stability.

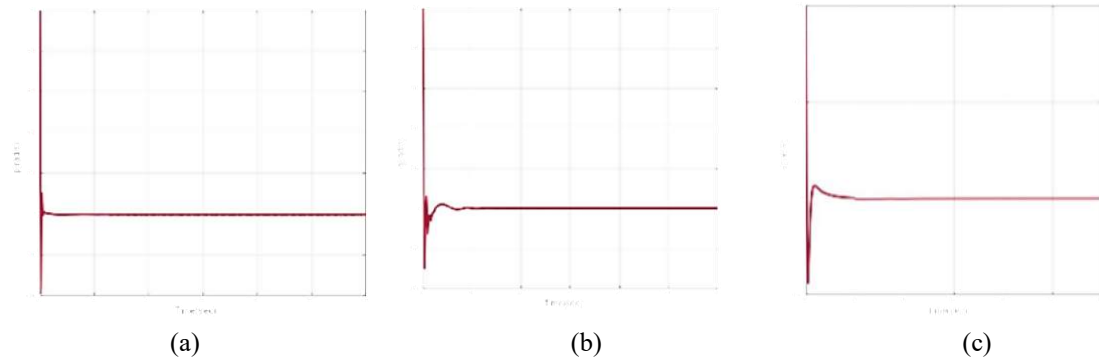


Figure 10. Roll rate (p), Pitch rate (q), and Yaw rate (r) response

Figure 10 shows the analysis of roll rate (p), pitch rate (q), and yaw rate (r). The graph indicates that the roll rate can return to a stable position very quickly, with a final value recorded at -1.70e-5 deg/s. The overshoot in the roll rate of 39.29% indicates an initial swing, but the very fast rise time (0.078 seconds) and settling time of only 0.98 seconds show that the system responds very well and stabilizes quickly. For the pitch rate, the final value is very small (3.04e-9 deg/s), but the overshoot is higher (30.09%) and the settling time is longer (8.87 seconds), indicating a slightly slower response and requiring more time to stabilize. For yaw rate, although the rise time is fast (0.199 seconds), the overshoot is 43.87% and the settling time is quite long (9.75 seconds), indicating a large initial swing and a longer stabilization time.

The analysis of velocity responses revealed similar trends. Surge velocity experienced a large overshoot (106.26%), highlighting the need for further optimization in the inner-loop control. On the other hand, the sway velocity showed minimal overshoot (0.20%) but exhibited slower stabilization, taking 74.51 seconds to reach a stable value. Heave velocity had a 47.17% overshoot, with the system

**DOI:** 10.33019/jurnalecotipe.v12i2.4575

requiring 41.53 seconds for stabilization, suggesting that adjustments to the PID settings are needed for faster stabilization.

Overall, the roll rate demonstrates highly responsive and stable control, with moderate overshoot and very fast settling time. The pitch rate has slightly higher overshoot and requires a longer stabilization time, while the yaw rate shows significant overshoot and the longest settling time. This indicates that for the yaw rate, control settings need to be adjusted to reduce overshoot and accelerate the stabilization process, while for roll and pitch, control settings are already adequate although slight adjustments to the gain are needed to speed up the response.

#### 4. CONCLUSION

This study successfully developed and evaluated an Adaptive PID-PD Hybrid Controller to improve the position and rotation control of a Remotely Operated Vehicle (ROV) in a dynamic marine environment. Simulation results showed that the Cascade PID controller successfully maintained the ROV's position with surge overshoot reaching 23.3%, sway only 1.67%, and heave around 47.17%. The settling time required for stabilization ranged from 41.53 to 107 seconds, with rise times varying from 1.52 seconds (surge velocity) to 28.50 seconds (sway velocity). In terms of velocity, the surge velocity experienced a large overshoot of 106.26%, while the sway velocity and heave velocity had smaller overshoots with longer stabilization times. Overall, the adaptive PID-PD hybrid framework proved effective in maintaining the stability of the ROV's position and rotation; however, further optimization of the inner-loop gain is required to reduce overshoot and accelerate stabilization time, particularly in the sway and yaw channels. Additional adjustments to the PID gain are expected to enhance system responsiveness, reduce drift, and improve the ROV's speed and position stabilization in dynamic sea conditions. Moving forward, future research should explore adaptive control to enable real-time adjustments to system parameters based on changing environmental conditions, such as fluctuating currents and wave heights. Additionally, integrating machine learning could allow ROVs to autonomously optimize control parameters, making them more resilient and responsive in dynamic conditions. These advancements would position this study as a significant step forward in autonomous underwater systems and pave the way for further innovations in marine robotics.

# Acknowledgments

This research was supported by the Research and Community Service Center (P3M) of the Cilacap State Polytechnic and DPPM Kemendiktisaintek. We would like to thank all those who have provided support and contributed to the implementation of this research. The support we received was very meaningful in realizing the technological development that we are studying.

# **REFERENCES**

- [1] Y. Chen, H. Zhang, W. Zou, H. Zhang, B. Zhou, and D. Xu, "Dynamic modeling and learning based path tracking control for ROV-based deep-sea mining vehicle," *Expert Syst. Appl.*, vol. 262, p. 125612, 2024, <a href="https://doi.org/10.1016/j.eswa.2024.125612">https://doi.org/10.1016/j.eswa.2024.125612</a>
- [2] Tran, N.-H., Le, M.-C., Ton, T., Le, T.-C., & Tran, T. (2020). ROV Stabilization Using an Adaptive Nonlinear Feedback Controller. In *Lecture Notes in Computer Science*, 144–155. <a href="https://doi.org/10.1007/978-3-030-62324-1\_13">https://doi.org/10.1007/978-3-030-62324-1\_13</a>.
- [3] Sahili, J., Hamoud, A., & Jammoul, A. (2018). ROV Design Optimization: Effect on Stability and Drag Force. In 2018 6th RSI International Conference on Robotics and Mechatronics (IcRoM), 413–417. https://doi.org/10.1109/ICROM.2018.8657510
- [4] Yang, Y., Yang, R., Qin, H., Li, R., & Ye, W. (2024). Research on Vision-Based ROV Underwater Positioning Method. In *Proceedings of the 2024 5th International Conference on Geology, Mapping, and Remote Sensing (ICGMRS)*, 131–137. https://doi.org/10.1109/ICGMRS62107.2024.10581261
- [5] Diamanti, E., Mentogiannis, V., Ødegård, Ø., & Koutsouflakis, G. (2025). Underwater drones as

Volume 12, Issue 2, October 2025, pp. 254-263 ISSN 2355-5068; e-ISSN 2622-4852 **DOI:** 10.33019/jurnalecotipe.v12i2.4575

- a low-cost, yet powerful tool for underwater archaeological mapping: Case studies from the Mediterranean. *Journal of Computer Applications in Archaeology*, 8(1), 10–24. <a href="https://doi.org/10.5334/jcaa.184">https://doi.org/10.5334/jcaa.184</a>
- [6] Salah, S., et al. (2021). Design of lightweight, low-cost remotely operated underwater vehicle. In *Proceedings of the ASME Design Engineering Technical Conference*. https://doi.org/10.1115/DETC2021-70555.
- [7] McCulley, R. (2009). Almost disposable ROVs earning respect offshore. *Offshore Engineer*, 34(5). Retrieved from <a href="https://www.scopus.com/inward/record.uri?eid=2-s2.0-67650723276&partnerID=40&md5=74848ea67f12dfc35ffe54ce9c7dae59">https://www.scopus.com/inward/record.uri?eid=2-s2.0-67650723276&partnerID=40&md5=74848ea67f12dfc35ffe54ce9c7dae59</a>
- [8] Poretti, M., Benson, B., & Rauch, C. (2013). Design of modular camera tool for mini underwater ROVs. In OCEANS 2013 MTS/IEEE San Diego: An Ocean in Common. <a href="https://www.scopus.com/inward/record.uri?eid=2-s2.0-84896368489&partnerID=40&md5=448b0974ee92f9e06c8ba20cd8641d6a">https://www.scopus.com/inward/record.uri?eid=2-s2.0-84896368489&partnerID=40&md5=448b0974ee92f9e06c8ba20cd8641d6a</a>
- [9] Ravichandran, S., et al. (2022). Accelerated testing and results of underwater electric thrusters for mini observation class ROVs. In *Oceans Conference Record (IEEE)*. https://doi.org/10.1109/OCEANSChennai45887.2022.9775357.
- [10] Mansoor, A., Salih, T., & Abdullah, F. (2022). Speed Control of Separately Excited D.C. Motor using Self-Tuned Parameters of PID Controller. *Tikrit Journal of Engineering Sciences*, 20(1), 1–8. <a href="https://doi.org/10.25130/tjes.20.1.01">https://doi.org/10.25130/tjes.20.1.01</a>.
- [11] Wu, X.-G., Wang, X.-D., Yu, T.-W., & Xie, X.-P. (2007). PID control on the current of electromagnetic clutch tuned by neural network. *Dianji yu Kongzhi Xuebao/Electric Machines and Control*, 11(4), 335–339. <a href="https://www.scopus.com/inward/record.uri?eid=2-s2.0-34547976761&partnerID=40&md5=b16f8f07ba1451e7972865fb176f4e5e">https://www.scopus.com/inward/record.uri?eid=2-s2.0-34547976761&partnerID=40&md5=b16f8f07ba1451e7972865fb176f4e5e</a>
- [12] Li, J., Zhang, L., Huang, X., Zhang, Q., & Wang, G. (2022). Cascade PID control algorithm for wind turbine blade mold temperature based on improved RBF neural network. *Taiyangneng Xuebao/Acta Energiae Solaris Sinica*, 43(3), 330–335. <a href="https://doi.org/10.19912/j.0254-0096.tynxb.2020-0640">https://doi.org/10.19912/j.0254-0096.tynxb.2020-0640</a>.
- [13] He, D., Shi, F., Tan, S., & Deng, Q. (2020). Research on inverse kinematics algorithm of 6-DOF industrial robot based on RBF-PID. *Journal of Physics: Conference Series*, 1624, 042017. https://doi.org/10.1088/1742-6596/1624/4/042017.
- [14] Qafko, T., et al. (2024). Design and control of an underwater remotely operated vehicle using thrust force vectors. In *URTC 2024 2024 IEEE MIT Undergraduate Research Technology Conference*, Proceedings. <a href="https://doi.org/10.1109/URTC65039.2024.10937653">https://doi.org/10.1109/URTC65039.2024.10937653</a>.
- [15] Ali, F. A., Aras, M. S. M., Azis, F. A., Sulaima, M. F., & Jaaffar, I. (2014). Design and development of auto depth control of Remotely Operated Vehicle using thruster system. *Journal of Mechanical Engineering and Sciences*, 7(1), 1141–1149. <a href="https://doi.org/10.15282/jmes.7.2014.13.0111">https://doi.org/10.15282/jmes.7.2014.13.0111</a>.
- [16] Jayasundere, N. D., & Gunawickrama, S. (2016). Underwater ROV with fuzzy logic motion control. In 2016 IEEE International Conference on Information and Automation for Sustainability (ICIAfS), 1–6. https://doi.org/10.1109/ICIAFS.2016.7946564.
- [17] Xia, P., Zhou, T., Ye, Y., & Du, J. (2024). Human autonomy teaming for ROV shared control. *Journal of Computing in Civil Engineering*, 38, CPENG-5756. https://doi.org/10.1061/jccee5.cpeng-5756.
- [18] Tan, Y. H., Liu, X., & Chen, B. M. (2018). Hardware adaptation of a small commercial ROV for autonomous use. In 2017 Asian Control Conference, ASCC 2017, 1252–1257. https://doi.org/10.1109/ASCC.2017.8287350.



**DOI:** 10.33019/jurnalecotipe.v12i2.4578

# Least Square-Based Modelling of 0.5 HP Single-Phase Induction Motor

Abdul Hadi<sup>1</sup>, Rindilla Antika<sup>2</sup>, M. Farhan<sup>3</sup>, Akmal Arif Ridhi Putra<sup>4</sup>, Diva Ramadhan<sup>5</sup>

1.2,3,4,5 Politeknik Negeri Bengkalis, Jl. Bathin Alam, Sungai Alam, Bengkalis-28714, Riau, Indonesia

#### **ARTICLE INFO**

#### Article historys:

Received: 22/08/2025 Revised: 05/09/2025 Accepted: 30/10/2025

#### **Keywords:**

Induction Motor; Least Squares; Modeling and Parameter Estimation

#### **ABSTRACT**

A single-phase induction motor is a cost-effective device for converting electrical energy into mechanical energy, making it widely used by small medium-sized enterprises (SMEs). Understanding motor characteristics and analyzing control system performance requires precise mathematical modelling. Nevertheless, it is difficult to derive models from physical laws, and frequently overlooks fundamental elements like usage duration and environmental conditions. This study proposes using the Least Squares method to model a 0.5 HP single-phase induction motor. With an MSE of 0.0307 and an RMSE of 0.1753, the results demonstrate that the estimated model closely resembles the real system, with only minor errors. Simulink simulations demonstrate consistent delay time and settling time values across different input variations in both open and closed-loop tests. In closed-loop conditions, rise time was nonlinear, with the slowest response occurring at 220 V and the fastest at 190 V. In open-loop conditions, rise time increased linearly with input reference. These results demonstrate that, without requiring in-depth knowledge of the physical system, the Least Squares method offers a productive and useful way to create precise mathematical models of single-phase induction motors.



This work is licensed under a Creative Commons Attribution 4.0 International License

#### **Corresponding Author:**

Abdul Hadi

Politeknik Negeri Bengkalis, Jl. Bathin Alam, Sungai Alam, Bengkalis-28714, Riau, Indonesia Email: abdulhadi@polbeng.ac.id.

#### 1. INTRODUCTION

An induction motor is a device that converts electrical energy into mechanical energy. Induction motors are widely used for system devices that are controlled in the industry. The use of many induction motors as an actuator device in the control system. In a control system, the application of mechanical systems has a motion dynamic. The motion dynamics of a mechanical device will display the characteristics of how the system looks. The exact information on the characteristics of the dynamic system will result in the design of the relevant control system.

The characteristics of the system can be described from the response graph simulated through the device (tools) software such as Matrix Laboratory (Matlab) [1]. It requires a mathematical model of the controlled system in using MatLab. Therefore, the importance of mathematical models is to identify and gain the characteristics of a controlled system. Then, this model also used to support the engineer in designing PID controls more easily. It is known that PID control is the most widely used control method in the industry. The process of obtaining a mathematical model of a controlled system is also called system identification.

Volume 12, Issue 1, October 2025, pp. 264-274 ISSN 2355-5068; e-ISSN 2622-4852 **DOI:** 10.33019/jurnalecotipe.v12i2.4578

The process of obtaining a mathematical model of a controlled mechanical system requires several methods. The most common method is the method of degradation of the laws of chemical physics of the system. The model produced by this system requires special expertise related to physical science and chemistry. In addition, some physical conditions, such as service life, measurements of inductant parameters, and capacitation, are not known with certainty and accuracy, which causes the results of the resulting model to be irrelevant for the physical system used at that time. Therefore, this study identifies mathematical modeling of induction motors using the Least Squares method. This method is a practical solution in finding mathematical models that use input and output processes in the system.

The study aims to identify the mathematical model of the single-phase induction motor based on data from an experiment using the Least Squares method. It is also aimed to evaluate the accuracy of the identification model by comparing it to actual data. Furthermore, it also to obtain a mathematical model of a high-accuracy induction motor with minimal error using the Mean Squared Error (MSE). Mathematical models are produced in the form of a transfer function which functions as the relationship between the transformation of the Input Laplace with the Transformation of the Output Laplace.

The limitation of this research is using single-phase induction motor of 1 phase, 0.5 HP, 1400 RPM. Data input-output process is in the form of voltage as input and current in output, the model obtained is a low-order model, and the method of getting a model using Least Squares. The data used in this study uses real system data, namely single-phase induction motors that are directly connected to the current sensor and PZEM voltage on the input side of the single-phase induction motor.

Research on induction motor modeling can be seen in the work of Marina Konuhova, who developed motor models with and without considering current. The study showed that the model with current consideration produced faster starting current amplitude and steady-state transition [2]. Another study by Siyu Sao focused on fault diagnosis in motor modeling. The results demonstrated that the model achieved higher accuracy and could be effectively applied to induction motors [3]. However, the models in these studies overlooked variations in physical parameters, which may change over time due to continuous operation.

A good model should accurately represent system characteristics and closely approximate the physical system. The Least Squares method has been widely employed for parameter identification [4]–[9], including applications in battery monitoring, robotic arms, and large-scale systems.

From existing studies, [1]–[9], an estimated parameter of 0.5 HP single-phase induction motors is not yet available, as only research [1] is for modeling motors, but DC motors. The data used is online data from Simulink, not real data. The Least Squares method is already used for modeling but is not yet available for the 0.5 HP single-phase induction motor. Therefore, this study proposes the modeling of a single-phase induction motor using Least Squares Estimation.

### 2. RESEARCH METHOD

#### 2.1. Modelling Control System

A control system is a system designed to regulate or control certain parameters of a process or physical system in order to work as expected. In the context of the technique, the control system is widely used to regulate the speed of the motor, temperature, pressure, position, current, voltage, and so on.

The control system is divided into two main types: an open-loop control system and a closed-loop control system. The open system has no feedback mechanism, whereas a closed system has feedback to correct errors between the actual output and the desired output.

System modeling is a mathematical process for representing the dynamic behavior of a physical system in the form of a mathematical model. The goal is for the system to be analyzed, simulated, or systematically controlled.

Mathematical models of the control system usually consist of several forms, namely in the form of:

- 1. Differential equation (for the continuous system)
- 2. Different equations (for discrete systems)
- 3. Transfer function

**DOI:** 10.33019/jurnalecotipe.v12i2.4578

# 4. State-space Model

## 5. Black Box Model

In modeling physical systems such as electric motors, models are often obtained through several ways, namely, first, theoretical approaches: based on the laws of physics (e.g., Kirchhoff's law, Newton's law). The second, with an empirical approach or system identification, based on input-output data from experiments [10], [11].

Single-phase induction motors are usually modeled using resistance, inductance, and capacitance parameters for identification based on physical laws. However, because of wear and use, these parameters might change over time. Furthermore, using physical law-based approaches necessitates precise parameter measurement and specific knowledge. Under some circumstances, a number of variables that are frequently overlooked in physical systems, such as vibration and ambient temperature, can also result in inaccurate models.

# 2.2. Identification System with the Least Squares Method

System identification is the process of determining a mathematical model of a system based on input—output data obtained through experiments. This process is crucial when the physical model of a system is too complex for theoretical analysis or when the system parameters are not precisely known [12]. System identification is a branch of systems engineering and is widely applied in control, prediction, and simulation of dynamic systems such as electric motors, hydraulic systems, thermal systems, and others.

A single-phase electric motor is an actuator commonly used in both industrial and household applications. This motor exhibits dynamic behavior, as its outputs (e.g., speed or current) vary over time in response to changes in its inputs (e.g., supply voltage). The behavior of such a motor can be represented as a low-order system (first- or second-order), depending on the level of complexity and the modeling objectives. Since many of its physical parameters are not precisely known, system identification offers a practical solution for modeling and analysis.

The Least Squares (LS) method is a widely used parameter estimation technique in linear system identification. Its primary objective is to minimize the sum of squared errors between the actual system output and the estimated model output [4]–[9].

In system modelling, several common representations can be expressed in both the time and frequency domains, including transfer function models, state-space models, and discrete models. A transfer function is defined as the ratio of the Laplace transform of the output to the Laplace transform of the input, assuming all initial conditions are zero. This representation is particularly suitable for linear time-invariant (LTI) systems. The general form of the transfer function, where G(s) denotes the transfer function, Y(s) the output, and U(s) the input, can be expressed as equation (1) follows:

$$G(s) = \frac{Y(s)}{U(s)} \tag{1}$$

Representation of the second system model is the state space model (state space), where x(t) is a state matrix, A is the matrix of the state system, B is the input matrix, and C is the output matrix with the shape of the vector matrix of the following state.

$$x \cdot (t) = Ax(s) + Bu(s) \tag{2}$$

$$y(t) = Cx(s) + Du(s)$$
(3)

Representation of the Discrete model can be seen in digital or real-time systems, where discrete models are used, for example:

$$y(k) = -a_1 y(k-1) - a_2 y(k-2) + b_1 u(k-1) + b_2 u(k-2)$$
 (4)

where:

y(k) : system output (e.g., speed or motor current) at the time

of k u(k) : system input (e.g., voltage) at time k

 $a_1, a_2, b_1, b_2$ : the parameters of the model to be estimated

e(k) : noise or interference

**DOI:** 10.33019/jurnalecotipe.v12i2.4578

Mathematically, a linear model of a discrete system can be written as a linear regression model, such as equation (4) above, to form an equation connecting the output with the input. The input and output equations can be written in the form of equivalent matrix notation, which is written in equation (5) as follows.

$$Y = \varphi \theta + E \tag{5}$$

With the definition of each notation, namely:

$$Y = \begin{bmatrix} y(3) \\ y(4) \\ \vdots \\ y(N) \end{bmatrix} \tag{6}$$

$$\varphi = \begin{bmatrix} -y(2) & -y(1) & u(2) & u(1) \\ -y(3) & -y(2) & u(3) & u(2) \\ \vdots & \vdots & \vdots & \vdots \\ -y(N-1) & -y(N) & u(N-1) & u(N-2) \end{bmatrix}$$
(7)

$$\theta = \begin{bmatrix} a_2 \\ b_1 \\ b_2 \end{bmatrix} \tag{8}$$

where E = vector error.

The solution is obtained by  $\theta$ 

$$\hat{\boldsymbol{\theta}} = (\boldsymbol{\varphi}^T \boldsymbol{\varphi})^{-1} \boldsymbol{\varphi}^T Y \tag{9}$$

Equation (9) is the Least Squares Estimation (LSE) parameter estimation.

The identification of this parameter is carried out with some process test data. After obtaining the estimation parameters, the model's accuracy is evaluated by looking for errors using Mean Squared Error (MSE). The smallest error value is found from multiple test data. The most minor error from several tests of the test data that will be used as research results.

Error values are searched with the following equation:

$$e(i) = yi - yp \tag{10}$$

Where e(i) is the error value sought, yi is the actual output of the observation process data, and yp is the prediction output or the output of the model resulting from the estimate. MSE and RMSE is obtained from equations (11.a) and (11.b).

$$MSE = \sum_{n=1}^{1} (yi - yp)^{2}$$
 (11a)

$$RMSE = \sqrt{\frac{1}{n} \sum_{i=1}^{n} (yi - yp)^{2}}$$
(11b)

where n is the amount of data used to make predictions.

R-squared is a way to assess how well a mathematical or statistical model describes the observed data. The goal is to find out whether the model we create fits with real data, or how accurate the model's prediction is compared to the real data. Thus, R Square functions to see the accuracy of the model, how representative the model is of real data, and how much error there is between prediction and observation. The R-squared can be obtained from the following equation.

$$R^{2}=1-\frac{\sum (yi-yp)^{2}}{\sum (yi-yp)^{2}}$$
(12)

**DOI:** 10.33019/jurnalecotipe.v12i2.4578

The accuracy of the model's prediction is between 0 and 1. If the value is 0, then the model does not explain the data. Furthermore, the prediction is considered perfect if the value is 1. The R-squared can be negative, which is considered a worse model than the data average.

## 3. RESULTS AND DISCUSSION

# 3.1. Transfer Function of 0.5 HP Single-phase Induction Motor Modeling

The experiment used process operation data, namely input data in the form of voltage and output data in the form of current on the motor. From the calculation of parameter estimation with a first-order approach, the following parameters in Equations (13) and (14) are obtained.

$$a_1 = -0.8014$$
 (13)

$$b_1 = 0.0033$$
 (14)

So that it can be arranged in equation (15) of the discrete model representation, namely:

$$y(k) = -0.8014 \ y(k-1) + 0.0033 \ u(k-1)$$
 (15)

From the acquisition of the above estimation parameters, the data error level is obtained from 2 equations, namely Mean Squared Error (MSE) and Root Mean Square Error (RMSE). The results of the estimates are obtained in equations (16) and (17) below.

$$MSE=0.0307$$
 (16)

$$RMSE=0,1753$$
 (17)

In addition to the representation of the model in discrete equations, it can also be described in the form of Discrete Transfer Functions as follows in equation (18).

$$G_Z = \frac{0.003271}{z - 0.8014} \tag{18}$$

By performing several transformation methods from Discrete Transfer Functions to Continuous Transfer Functions, equations (19) to equations (22) are obtained.

$$G_{(s)} = \frac{0.3646}{s + 22.14} \tag{19}$$

$$G_{(s)} = \frac{-0,00189s + 0,3646}{s + 22,14} \tag{20}$$

$$G_{(s)} = \frac{-0,001816s + 0,3631}{s + 22,05} \tag{21}$$

$$G_{(s)} = \frac{0.3646}{s + 22,14} \tag{22}$$

The method of transforming the discrete transfer function to a continuous transfer function from the 4 equations above, respectively, namely Zero Order Hold, First Order Hold, Bilinear/Tustin, and Pole-Zero Matching. From Equations (17) to (20) above, equations (17) and equations (20) have the same value. Therefore, the next research will be discussed using the transfer function.

The results of the graph plot are obtained with input and output graph images as shown in Figure 1 below.

**DOI:** 10.33019/jurnalecotipe.v12i2.4578

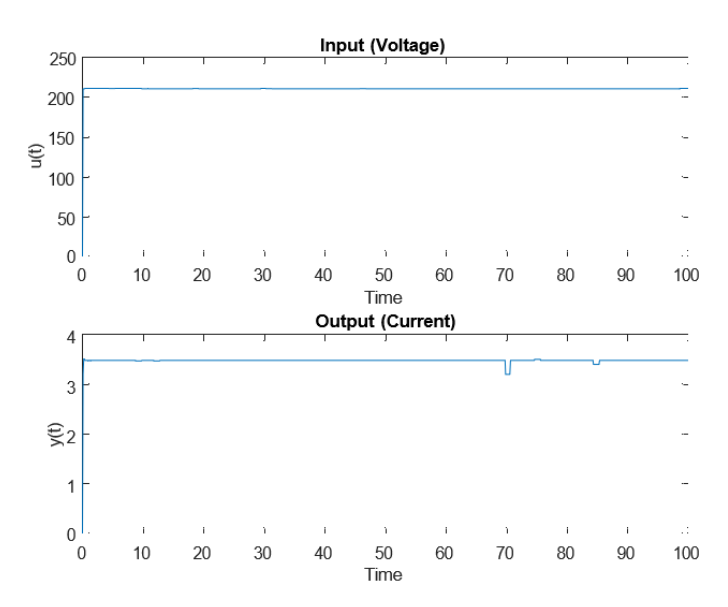


Figure 1. Graph of input and output data

From Figure 1 above, the input and output data of the induction motor system are stable. The output also fluctuates slightly at 70 and 86 seconds.

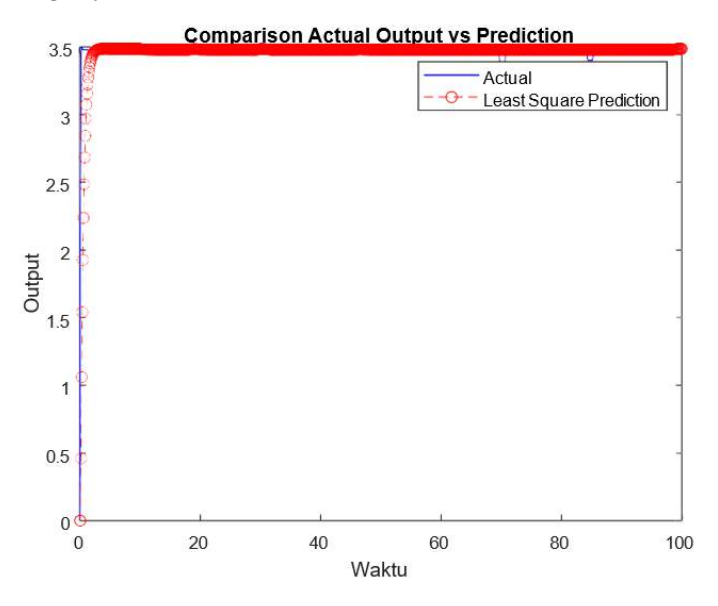


Figure 2. Comparison of Actual Output with Prediction

Figure 2 above shows that the prediction can follow the actual output with a pattern that the graph follows the desired actual output. The blue graph represents the actual output, and the red graph illustrates the predicted output.

After viewing the actual comparison graph with the prediction, the prediction error is also depicted in the form of the Prediction Output Result graph in Figure 3 below.

**DOI:** 10.33019/jurnalecotipe.v12i2.4578

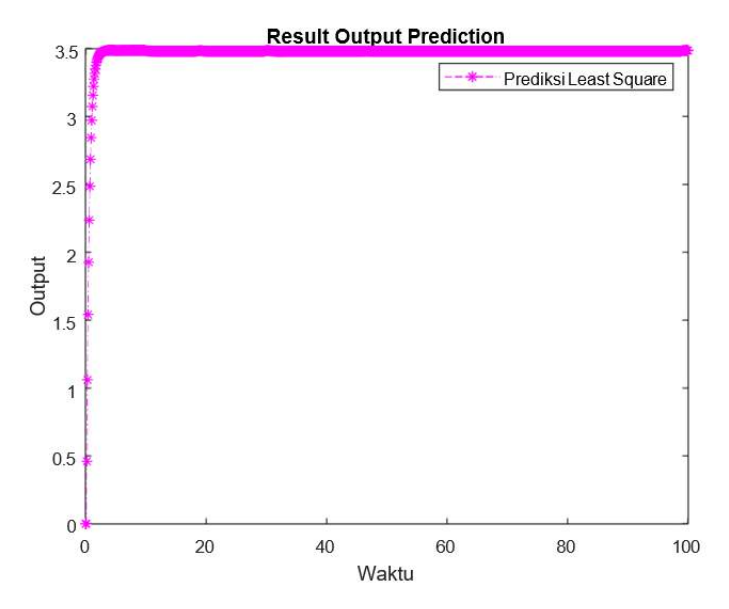


Figure 3. Prediction Output Results

The prediction output results in Figure 3 show that the response can be steady and stable at setpoint 3.5. This means that it corresponds to the actual output.

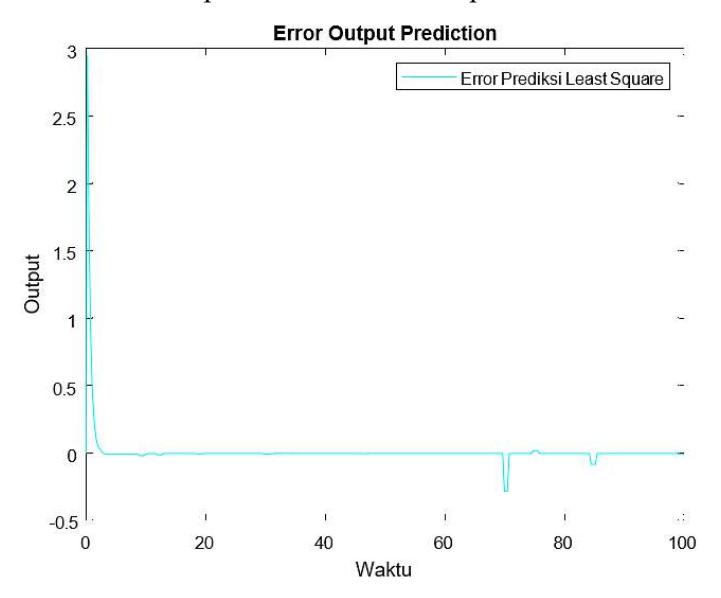


Figure 4. Prediction Output Error

From the results of the calculation of parameter estimation, the prediction output error was obtained as shown in Figure 4 above. From Figure 4, it can be seen that the prediction error is stable at Zero. This means that the parameters of the estimated results show the right value. Apart from the graph in Figure 4 above, the results of the MSE and RMSE error calculations in Equations (16) and (17) are relatively small. This points to the accuracy of the resulting model. The estimation parameter using the Least Squares method, Equations (19) to (22), is obtained, and then the Transfer Function Equation is determined to see its characteristics using Equations (19) and (22). The experiment to determine the system characteristics was carried out through open-loop and closed-loop simulations, using step input variations ranging from 180 V to 230 V. Equations (19) and (22) are changed to equation (23) below.

$$G_{(s)} = \frac{0.016}{0.045s + 1} \tag{23}$$

Volume 12, Issue 1, October 2025, pp. 264-274 ISSN 2355-5068; e-ISSN 2622-4852 **DOI:** 10.33019/jurnalecotipe.v12i2.4578

Equation (23) above is a single-phase Induction Motor mathematical model estimated using the Least Squares Method. An experiment was carried out using Simulink with an input step to obtain the characteristics of this single-phase Induction Motor.

# 3.2. Open-Loop Response Characteristics

The 0.5 HP single-phase induction motor is widely used in household industries and small to medium-sized enterprises (SMEs). The purpose of the testing is to observe and analyze the system characteristics of this motor. The experiments were carried out by applying step input voltages ranging from 180 V to 230 V. The open-loop test results are presented in Figure 5 below. An experimental image can be seen in the following Figure 5.

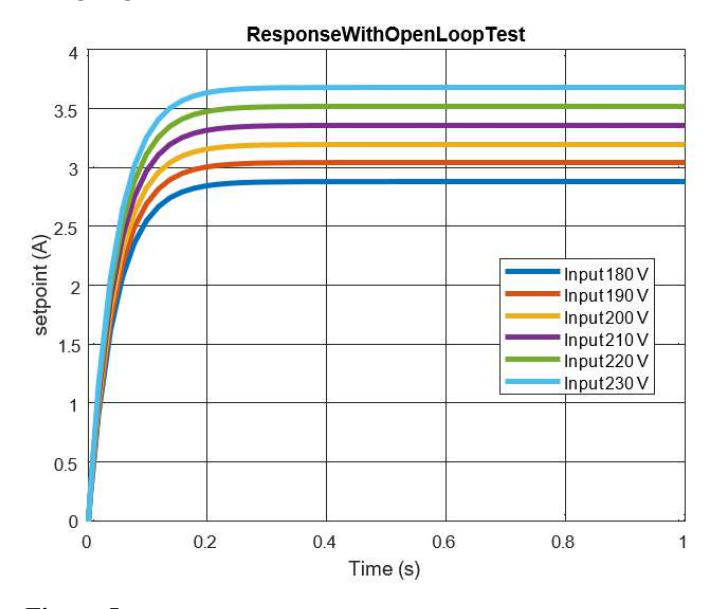


Figure 5. System Response Graph Obtained from Open-Loop Testing

The transient response analysis produced a number of important parameters, including delay time, rise time, 2% settling time, and 5% settling time, as shown in Figure 5. Table 1 presents these findings for comparison and clarity.

Input (Voltage)	Setpoint (Ampere)	Delay Time (s)	Rise Time (s)	Settling Time 2% (s)	Settling Time 5% (s)
180	2.880	0.046	0.391	0.176	0.135
190	3.040	0.046	0.393	0.176	0.135
200	3.200	0.046	0.395	0.176	0.135
210	3.360	0.046	0.397	0.176	0.135
220	3.520	0.046	0.399	0.176	0.135
230	3.680	0.046	0.402	0.176	0.135

Table 1. Open-Loop Testing Parameters Response

Table 1 provides a summary of the system response analysis's findings. All input variations result in the same delay time, 2% settling time, and 5% settling time. This consistency shows that, independent of the applied input, the single-phase induction motor's transfer function model is stable and does not significantly alter these three parameters. This stability demonstrates how well the model captures the basic dynamic properties of the motor.

On the other hand, the rise time parameter varies in response to changes in the input. In particular, the rise time slows down as the input voltage rises. At 190 V, the rise time was the fastest, and at 220 V, the slowest. In closed-loop testing, this shows a nonlinear relationship between input voltage and rise time, whereas in open-loop conditions, the rise time grows linearly with the input reference. These

**DOI:** 10.33019/jurnalecotipe.v12i2.4578

results imply that while the Least Squares Estimation (LSE) approach effectively captures the fundamental motor dynamics, further improvements might be required to handle nonlinearities at higher input levels.

# 3.3. Closed-Loop Response Characteristics

Closed-loop testing was done on the single-phase induction motor's mathematical model, which is represented by equation (23). Figure 6 shows the obtained system response. Input variations ranging from 180 V to 230 V were used in the test.

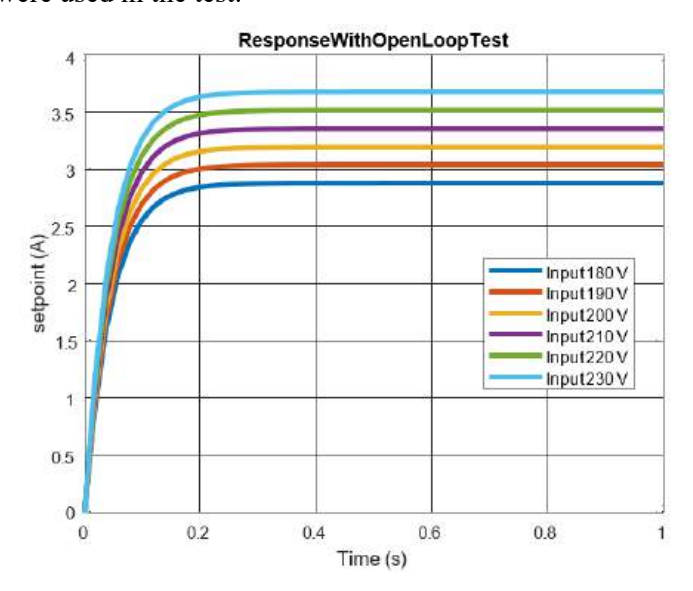


Figure 6. System Response Graph Obtained from Closed-Loop Testing

From Figure 6, the delay time, rise time, 2% settling time, and 5% settling time were obtained by observing the response graph. These parameters are summarized in Table 2, which presents the results of the closed-loop testing.

Input (Voltage)	Setpoint (Ampere)	Delay Time (s)	Rise Time (s)	Settling Time 2% (s)	Settling Time 5% (s)
180	2.835	0.045	0.438	0.174	0.133
190	2.992	0.045	0.376	0.174	0.133
200	3.150	0.045	0.457	0.174	0.133
210	3.307	0.045	0.384	0.174	0.133
220	3.465	0.045	0.482	0.174	0.133
230	3.622	0.045	0.391	0.174	0.133

Table 2. Closed-Loop Testing Parameter Response

The parameters of delay time, 2% settling time, and 5% settling time are shown in Table 2 and are unaffected by changes in the input. Regardless of whether the testing is done in a closed-loop or open-loop setting, this result shows that the single-phase induction motor remains stable with regard to these three parameters. In contrast to the closed-loop test, the open-loop test required a little more time to reach the delay time, 2% settling time, and 5% settling time.

With a value of 0.376 seconds, the fastest response was recorded for the rise time parameter at an input of 190 V, while the slowest rise time was recorded at 220 V. This suggests that rise time is dependent on input levels. The closed-loop test revealed a nonlinear relationship between input variations and rise time, in contrast to the open-loop test, which showed that rise time increased linearly with input magnitude (larger input resulted in slower rise time).

The properties of the single-phase induction motor can be examined by calculating the transfer function in equation (23), as shown in Figures 5 and 6. Equation (23) can be used to design a

Volume 12, Issue 1, October 2025, pp. 264-274 ISSN 2355-5068; e-ISSN 2622-4852 **DOI:** 10.33019/jurnalecotipe.v12i2.4578

proportional-integral-derivative (PID) control system in addition to determining system characteristics. Determining the parameters Kp is necessary for the design of a PID controller requires the determination of the parameters Kp, Ki dan Kd. Then. Numerous techniques, including gain analysis [13], Ziegler–Nichols tuning [14], and trial and error, can be used to determine these parameters. However, only the gain analysis method can be used for the transfer function that was derived from Equation (23).

An accurate model is produced when the 0.5 HP single-phase induction motor's parameters are estimated using the Least Squares method. The MSE and RMSE values shown in Equations (16) and (17) support this, showing a high degree of agreement between the model output and the real system response. Additionally, because the Least Squares approach only uses experimental data, it makes it easier to create a mathematical model of the single-phase induction motor.

The Least Squares method's capacity to produce models that accurately depict real-world operating conditions is another benefit. This is due to the fact that the approach makes use of input- output process data, which permits it to disregard physical parameters like capacitance, resistance, and inductance that are not measurable or change over time. Furthermore, this method yields a fairly simple mathematical model that can be approximated by models of different orders based on the design requirements. A first-order model was used in this study to approximate the motor system.

#### 4. CONCLUSION

The estimated parameters from the experiment on using the Least Squares method to model a 0.5 HP single-phase induction motor were found to have relatively small error values and to closely resemble the actual system. The Root Mean Squared Error (RMSE) of 0.1753 and the Mean Squared Error (MSE) of 0.0307 both demonstrate this accuracy. The resulting continuous transfer function is:  $G_{(s)} = \frac{0.016}{0.045s+1}$ . In both open-loop and closed-loop testing, the delay time, 2% settling time, and 5% settling time remained comparatively constant, according to the transient response analysis from the Simulink experiments with various input variations. The rise time in the open-loop setup rose linearly as the input reference values increased. The rise time, on the other hand, showed nonlinear behavior in the closed-loop configuration, with the slowest rise time occurring at 220 V and the fastest at 190 V. Without requiring in-depth knowledge of the physical system, the Least Squares approach was successful in producing a mathematical model. Future studies could incorporate the ARMAX method to further develop the Least Squares modeling approach for real-time online systems.

# Acknowledgments

The authors gratefully acknowledge the support of Politeknik Negeri Bengkalis, especially the Center for Research and Community Service (P3M), for providing the funding and facilities that enabled the successful completion of this research.

# REFERENCES

- [1] N. Donjaroennon, S. Nuchkum, and U. Leeton, "Mathematical model construction of DC Motor by closed-loop system Identification technique Using Matlab/Simulink," in *Proceeding of the 2021 9th International Electrical Engineering Congress, iEECON 2021*, 2021, pp. 289–292. doi: 10.1109/iEECON51072.2021.9440305.
- [2] M. Konuhova, "Modeling of Induction Motor Direct Starting with and without Considering Current Displacement in Slot," *Appl. Sci.*, vol. 14, no. 20, 2024, doi: 10.3390/app14209230.
- [3] S. Shao, R. Yan, Y. Lu, P. Wang, and R. X. Gao, "DCNN-Based multi-signal induction motor fault diagnosis," *IEEE Trans. Instrum. Meas.*, vol. 69, no. 6, pp. 2658–2669, 2020, doi: 10.1109/TIM.2019.2925247.
- [4] F. Naseri, E. Schaltz, D. I. Stroe, A. Gismero, and E. Farjah, "An Enhanced Equivalent Circuit Model with Real-Time Parameter Identification for Battery State-of-Charge Estimation," *IEEE Trans. Ind. Electron.*, vol. 69, no. 4, pp. 3743–3751, 2022, doi: 10.1109/TIE.2021.3071679.

**DOI:** 10.33019/jurnalecotipe.v12i2.4578

- [5] Z. Li, S. Li, and X. Luo, "An overview of calibration technology of industrial robots," *IEEE/CAA J. Autom. Sin.*, vol. 8, no. 1, pp. 23–36, 2021, doi: 10.1109/JAS.2020.1003381.
- [6] Y. Ji and L. Lv, "M-Decomposed Least Squares and Recursive Least Squares Identification Algorithms for Large-Scale Systems," *IEEE Access*, vol. 9, pp. 139466–139472, 2021, doi: 10.1109/ACCESS.2021.3113707.
- [7] T. Zhang, S. Wang, X. Huang, and L. Jia, "Kernel Recursive Least Squares Algorithm Based on the Nystr" om Method With k-Means Sampling," *IEEE Signal Process. Lett.*, vol. 27, no. 1, pp. 361–365, 2020, doi: 10.1109/LSP.2020.2972164.
- [8] K. Komatsu, Y. Miyaji, and H. Uehara, "Weighted Least Squares with Orthonormal Polynomials and Numerical Integration for Estimation of Memoryless Nonlinearity," *IEEE Wirel. Commun. Lett.*, vol. 9, no. 12, pp. 2197–2201, 2020, doi: 10.1109/LWC.2020.3017807.
- [9] Z. Zhao, P. Davari, W. Lu, H. Wang, and F. Blaabjerg, "An Overview of Condition Monitoring Techniques for Capacitors in DC-Link Applications," *IEEE Trans. Power Electron.*, vol. 36, no. 4, pp. 3692–3716, 2021, doi: 10.1109/TPEL.2020.3023469.
- [10] Katsuhiko Ogata, Modern Control Engineering, 3rd ed. 1997.
- [11] Katsuhiko Ogata, Discrete-Time Control Systems, 2nd ed. 1995.
- [12] L. Ljung, System Identification-Theory for the user, vol. 25, no. 3. 1987. doi: 10.1016/0005-1098(89)90019-8.
- [13] Abdul Hadi, "Perbandingan Tuning Parameter Kontroler PD Menggunakan Metode Trial and Error dengan Analisa Gain pada Motor Servo AC," *INOVTEK Politek. Negeri Bengkalis*, vol. d, pp. 1–23, 2016.
- [14] P. D. Lestari and Abdul Hadi, "Desain PI Controller menggunakan Ziegler Nichols Tuning pada Proses Nonlinier Multivariabel," *Semin. Nas. Teknol. Inf. Komun. dan Ind. 4*, pp. 439–446, 2012.



Volume 12, Issue 2, October 2025

ISSN 2355-5068 e-ISSN 2622-4852

#### Publisher Address :

Electrical Engineering Department
Faculty of Science and Engineering - Bangka Belitung University
Balunijuk, Kab. Bangka, Prov. Kep. Bangka Belitung
University Phone: (0717) 422145, 422965 Fax. (0717) 421303
Faculty Phone: (0717) 4260033 ext. 2122, 2124
Website: https://ecotipe.ubb.ac.id/index.php/ecotipe
E-mail: jurnalecotipe@ubb.ac.id / jurnal.ecotipe@yahoo.com